PHYSICS LETTERS

VOLUME 68B, 1977

NORTH-HOLLAND PUBLISHING COMPANY

AMSTERDAM

NEW PARTICLE SEARCHES AND DISCOVERIES

A Supplement to the 1976 Edition of "Review of Particle Properties"

Particle Data Group

Thomas G. TRIPPE, Angela BARBARO-GALTIERI, Charles P. HORNE,
Robert L. KELLY, Alan RITTENBERG, Arthur H. ROSENFELD, George P. YOST
Lawrence Berkeley Laboratory[1], *University of California, Berkeley, California 94720, USA*

Naomi BARASH-SCHMIDT
Brandeis University, Waltham, Massachusetts 02154, USA

Claude BRICMAN, Richard J. HEMINGWAY, Michael J. LOSTY
CERN, CH-1211 Genève 23, Switzerland

Matts ROOS
Department of Nuclear Physics, University of Helsinki, Helsinki 17, Finland

Vladimir CHALOUPKA
Stanford Linear Accelerator Center, Stanford, California 94305, USA

and

Betty ARMSTRONG (*Technical Associate*)
Lawrence Berkeley Laboratory[1], *University of California, Berkeley, California 94720, USA*

Received 24 March 1977

This supplement to the 1976 edition of "Review of particle properties", Particle Data Group [Rev. Mod. Phys. 48, No. 2, Part II (1976)], contains tabulations of experimental data bearing on the "new particles" and related topics; categories covered include charmed particles, ψ's and their decay products, and heavy leptons. Errata to the previous edition are also given.

As in 1975, we have decided this year to publish only a supplement to the previous edition of the "Review of Particle Properties", rather than a complete update; the latter will appear instead in April 1978 in Physics Letters B.

[1] The Berkeley Particle Data Center is jointly supported by the U.S. Energy Research and Development Administration, the Office of Standard Reference Data of the National Bureau of Standards, and the National Science Foundation.

This supplement consists primarily of a *Table* and *Data card listings* giving results relating to charmed particles, ψ's and their decay products, heavy leptons, quarks, magnetic monopoles, intermediate bosons, and other proposed states. Several mini-reviews in the *Listings* discuss various aspects of these particles. Also presented are some cross section plots for e^+e^- and νN scattering, which were not included in the 1976 edition. Finally, errata to the 1976 edition are given.

Charmed Particle Table

April 1977
(Approximate closing date for data: February 1, 1977)

Our normal policy to include only well established results in the Tables has been temporarily relaxed for the Charmed Particle Table. This is because many important results are preliminary or unconfirmed. We have put some such results into the Table but have parenthesized them. The more speculative results have not been included in the Table at all, but are described in the Data Card Listings which follow. The charmonium results, on the other hand, are not as new and are treated in the Charmonium Table in the traditional manner.

				Partial Decay Mode		
Particle	$I(J^P)$	Mass (MeV)	Full width (MeV)	Mode	Fraction (%)	p or p_{max}[a] (MeV/c)
CHARMED MESONS[b]						
$D^+(1870)$	$\frac{1}{2}(\ \ )$[c]	1876 ± 15	< 40	weak decay: $K^-\pi^+\pi^+$		849
$D^o(1870)$	$\frac{1}{2}(\ \ )$[c]	1865 ± 12[d]	< 2.4	$K^-\pi^+$		861
				$K^-\pi^+\pi^+\pi^-$		813
				$(K_S^o\pi^+\pi^-)$[e]		842
		$\frac{\Gamma(D^o \to \bar{D}^o \to K^+\pi^-)}{\Gamma(D^o \to K\pi)}$	< 0.16			
$D^{*+}(2010)$	$(\ \ )$[c]	2010 ± 12	< 2.4	$D^o\pi^+$		~ 39[f]
				$(D^+\gamma)$[e]		~ 130[f]
	$m_{D^{*+}} - m_{D^o} = 145.3 \pm 0.5$ MeV					
$D^{*o}(2010)$	$(\ \ )$[c]	(2005 ± 3)[e]	(< 5)[e]	$(D^o\pi^o)$[e]	$(\sim 55\text{-}65)$[e]	~ 39[f]
				$(D^o\gamma)$[e]	$(\sim 45\text{-}35)$[e]	~ 136[f]
	$(m_{D^{*o}} - m_{D^o} = 141 \pm 5$ MeV$)$[e]					
CHARMED BARYONS[b] (TENTATIVE ENTRY – SEE DISCUSSION IN REVIEW BELOW)						
$\Lambda_c^+(2260)$	$(\ \ )$[c]	2260 ± 10	< 75	$\Lambda\pi^+\pi^+\pi^-$		789
	Λ_c^+ and $\bar{\Lambda}_c^-$ states observed					
$\Sigma_c(2430)$	$(\ \ )$[c]	2426 ± 12		$\Lambda_c^+\pi$		~ 87[f]
	Σ_c^{++} and $\bar{\Sigma}_c^o$ states observed. $\Sigma_c^{++,+,o}$ expected from SU(4).					

[a] For single decays into more than two particles, p_{max} is the maximum momentum that any particle can have.

[b] For antiparticle, charge conjugate all particles; e.g., $D^o \to K^-\pi^+$ becomes $\bar{D}^o \to K^+\pi^-$.

[c] The quantum numbers expected from charm are: $I(J^P) = \frac{1}{2}(0^-)$ for D states, $\frac{1}{2}(1^-)$ for D* states, $0(\frac{1}{2}^+)$ for Λ_c^+, and $1(\frac{1}{2}^+)$ for Σ_c.

[d] A more precise but preliminary result is given in the Data Card Listings.

[e] Parentheses indicate a preliminary result.

[f] These decay momenta are sensitive to the mass differences.

Charmonium Table

April 1977
(Approximate closing date for data: February 1, 1977)

Particle	$I^G(J^P)C_n$ estab.	Mass (MeV)	Full width (MeV)	Mode (Partial Decay Mode)	Fraction (%)	p or p_{max}‡ (MeV/c)
→						
J/ψ(3100)	$\underline{0^-(1^-)-}$	3098 ± 3	0.067 ± 0.012	e^+e^-	7 ± 1	1549
				$\mu^+\mu^-$	7 ± 1	1545
				hadrons	86 ± 2	
				†[identified hadron modes	~15] ¶	
				†[identified radiative modes	~0.4] ¶	
χ(3415)	$\underline{0^+}(0^+)\underline{+}$	3413 ± 5		ππ		1701
				$K\bar{K}$		1634
				4π (including ππρ)	¶	1678
				6π		
				$\pi\pi K\bar{K}$ (incl. $\pi K\bar{K}^*$)		1579
				γ J/ψ(3100)		300
→						
P_c or χ(3510)	$\underline{0^+}(A)\underline{+}$ J > 0	3510 ± 4		4π (incl. ππρ)		1727
				6π	¶	
				$\pi\pi K\bar{K}$ (incl. $\pi K\bar{K}^*$)		1632
				γ J/ψ(3100)	dominant	388
χ(3550)	$\underline{0^+}(N)\underline{+}$ J > 0	3554 ± 5		ππ		1772
				$K\bar{K}$		1707
				4π (incl. ππρ)	¶	1750
				6π		
				$\pi\pi K\bar{K}$ (incl. $\pi K\bar{K}^*$)		1655
ψ(3685)	$\underline{0^-(1^-)-}$	3684 ± 4	0.228 ± 0.056	e^+e^-	0.9 ± 0.2	1842
				$\mu^+\mu^-$	0.8 ± 0.2	1839
				hadrons	98.1 ± 0.3	
				†[J/ψ $\pi^+\pi^-$	33 ± 3]	474
				†[J/ψ $\pi^o\pi^o$	17 ± 3]	478
				†[J/ψ η	4.2 ± 0.7]	189
				†[other identified hadron modes	~0.6] ¶	
				†[γ χ(3415)	7 ± 2]	261
				†[γ χ(3510)	7 ± 2]	170
				†[γ χ(3550)	7 ± 2]	128
→						
ψ(4415)	$\underline{(1^-)-}$	4414 ± 7	33 ± 10	e^+e^-	0.0013 ± 0.0003	2207
				hadrons	dominant	

→ Indicates entries in the Charmonium Data Card Listings [X(2830), X(3455), and ψ(4030)] omitted from this Table. We do not regard these as established resonances.

¶ See Charmonium Data Card Listings.

† Square brackets indicate a subreaction of the previous (unbracketed) decay mode(s).

‡ For decays into more than two particles, p_{max} is the maximum momentum that any particle can have.

CHARMED PARTICLES

A prime motivation for the publication of this supplement has been the discovery of charm in May 1976 (GOLDHABER 76 in the D^o section of the Data Card Listings) shortly after the regular biannual editon of the "Review of Particle Properties" was published in April 1976. The analogous situation occurred two years earlier with the discovery of the J/ψ (AUBERT 74 and AUGUSTIN 74 in the Charmonium section). We plan to continue our biannual publication policy with the next regular edition scheduled for April 1978.

This charm review and the Table and Data Card Listings on the D, D^*, Λ_c^+, and Σ_c and on charm searches are intended to summarize the experimental evidence on charmed particles. There are many excellent reviews of charm, a few of which are listed in references 1 and 2. Others, related to specific particles or searches, are listed in the appropriate reference sections below.

In the discussions of charm expectations which follow, we mean charm as in the standard GIM model[3] with four spin-1/2, fractionally-charged, baryon number $B = 1/3$ quarks with quantum number assignments as follows:

Symbol	Q	I_3	S	C
u	2/3	1/2	0	0
d	-1/3	-1/2	0	0
s	-1/3	0	-1	0
c	2/3	0	0	1

where the charge is related to the third component of the isospin, baryon number, strangeness, and charm by

$$Q = I_3 + \tfrac{1}{2}(B + S + C) .$$

The conventional model for describing the weak interactions involving these quarks and leptons is a Weinberg-Salam theory[4] with left-handed weak isodoublets

$$\begin{pmatrix} \nu_e \\ e^- \end{pmatrix} \quad \begin{pmatrix} \nu_\mu \\ \mu^- \end{pmatrix} \quad \begin{pmatrix} u \\ d' \end{pmatrix} \quad \begin{pmatrix} c \\ s' \end{pmatrix}$$

and right-handed weak isosinglets. Here

$$d' = d\cos\theta + s\sin\theta$$
$$s' = s\cos\theta - d\sin\theta,$$

where θ is the Cabibbo mixing angle ($\sin^2\theta \cong 0.055$).

Then, following Jackson's (ref. 1) shorthand notation, the weak interaction has a current-current structure

$$H_W = \frac{G}{\sqrt{2}} J J^\dagger \text{ with } J = J_C + J_N \quad ,$$

where the charged and neutral currents are

$$J_C = \bar{\nu}_e e + \bar{\nu}_\mu \mu + \bar{u}\,(d\cos\theta + s\sin\theta) + \bar{c}\,(s\cos\theta - d\sin\theta)$$

$$J_N = \bar{\nu}_e\nu_e + \bar{\nu}_\mu\nu_\mu - \bar{e}e - \bar{\mu}\mu + \bar{u}u + \bar{c}c - \bar{d}d - \bar{s}s$$

ignoring the Lorentz group structure. Thus only the charged current has terms which change charm, and the Cabibbo-favored transition is to a strange quark ($c\to s$), giving $\Delta C = \Delta S$.

The experiments related to charm are divided below into four sections:

1) Charmed Mesons — the D and D* states.
2) Charmed Baryons — the Λ_c and Σ_c states.
3) Charm Searches and Evidence — charm information not relatable to a given state.
4) Charmonium — the J/ψ states.

References

1. Proceedings of Summer Institute on Particle Physics, Aug. 2-13, 1976, Report No. SLAC-198 (Nov. 1976), especially: J.D. Bjorken, p.1; S.G. Wojcicki, p. 43; J.D. Jackson, p. 147 (also available separately as LBL-5500); D. Hitlin, p. 203; G. Goldhaber, p. 379 (also available separately as LBL-5534); S.L. Glashow, p. 473; A. De Rujula (a pictorial review), p. 483; also F.J. Gilman, 1976 Particles and Fields Conference at Brookhaven National Lab, SLAC-PUB-1833, Nov. 1976.
2. M.K. Gaillard, B.W. Lee, and J.L. Rosner, Rev. Mod. Phys. 47, 277 (1975).

3. S.L. Glashow, J.Iliopoulos, and L. Maiani, Phys. Rev. D2, 1285 (1970); also B.J. Bjorken and S.L. Glashow, Phys. Lett. 11, 255 (1964).
4. S. Weinberg, Phys. Rev. Lett. 19, 1264 (1967) and A. Salam, in Elementary Particle Theory, ed. N. Svartholm (Almqvist and Wiksell, Stockholm, 1968), p. 367.

CHARMED MESONS

Note that D and D^* are used throughout this review to mean the apparently charmed states at ~1870 MeV and ~2010 MeV, respectively, and should not be confused with the uncharmed D(1285) meson.

There is very strong evidence for the charm interpretation of the narrow $K\pi$, $K2\pi$, $K3\pi$ states observed in e^+e^- collisions at SPEAR. In agreement with the expectations for charmed mesons,[1-3] the following are observed (GOLDHABER 76, PERUZZI 76, WISS 76, GOLDHABER2 76, FELDMAN 77, and GOLDHABER 77 - see data cards and comments in the D and D* sections below):

a) The D state appears to be produced only in association with equal (~1870 MeV) or higher mass states. Electromagnetic production of charm via a massive virtual photon would produce charm-anticharm pairs.

b) The D^+ decays via the exotic charge mode $K^-\pi^+\pi^+$ and not $K^+\pi^+\pi^-$. A charmed charge-plus $(c\bar{d})$ meson decays weakly to an uncharmed negative strangeness state as expected for $\Delta C=\Delta S$.

c) The observed decay modes of the D are Cabibbo-favored (strange). The Cabibbo-suppressed modes ($c\to d$, $\Delta S=0$) are not observed within present statistics.

d) An excited state appears at ~2010 MeV in agreement with mass predictions.[4]

e) The masses suggest that the D states and D^* states are isospin multiplets. There are two distinct neutral states as is known from the D^0-$\bar{D}^0$ mixing studies (see D^0 branching ratio R5 section), suggesting the isodoublet structure (D^+, D^0) and $(D^-, \bar{D}^0)$ as expected for charmed nonstrange mesons $(c\bar{d}, c\bar{u})$ and $(\bar{c}d, \bar{c}u)$.

f) Parity violation indicates that the ground state decays weakly. Charm conservation prevents strong decay.

g) There is evidence that semileptonic decay modes exist as would be expected from elementary processes such as $c\to se^+\nu_e$. In e^+e^- collisions at DESY, BRAUNSCHWEIG 76 (DASP) see single electrons with hadrons and BURMESTER 76 (PLUTO) see a correlated $e^+K_S^0$ signal (see Charm Searches and Evidence section of the Data Card Listings, subsection CE, below). Identification with a particular charm state is not possible, but the threshold and cross section are compatible with D production.

There is evidence for the existence of the D^0 state outside e^+e^- collisions. KNAPP 76 report a weak signal in $K_S^0\pi^+\pi^-\pi^+\pi^-$ in Fermilab photoproduction data at the D^0 mass. Their current experiment with better acceptance should be able to make a more definitive statement.

The data are listed in the Data Card Listings and summarized in the Table at the beginning of this report. Preliminary results of which we are aware are included but are parenthesized.

References

1. M.K. Gaillard, B.W. Lee, and J.L. Rosner, Rev. Mod. Phys. 47, 277 (1975).
2. M.B. Einhorn and C. Quigg, Phys. Rev. D12, 2015 (1975).
3. A. De Rujula, H. Georgi, and S.L. Glashow, Phys. Rev. Lett. 37, 398 (1976).
4. A. De Rujula, H. Georgi, and S.L. Glashow, Phys. Rev. D12, 147 (1975).

$D^{\pm}(1870)$, $D^{0}(1870)$, $D^{*\pm}(2010)$, $D^{*0}(2010)$

Data Card Listings

Please note that the meaning of the columns and the various abbreviations appearing below can be found in the 1976 edition of the Review [Rev. Mod. Phys. 48, No. 2, Part II (1976)].

```
CODE EVENTS QUANTITY ERROR+  ERROR-  REFERENCE YR TECN SIGN COMMENTS     DATE
     ABOVE                                                              PUNCHED
     BACKGROUND
****** ********* ********* ********* ********* ********* ********* ********
```

$D^{\pm}(1870)$

```
31  CHARGED D(1870,JP=  )
------ --------- --------- --------- --------- --------- --------- --------

                  31  CHARGED D MASS (MEV)

M       50 1876.      15.             PERUZZI   76 SMAG +-  K+-PI+-PI+-     1/77*

------ --------- --------- --------- --------- --------- --------- --------

                  31  CHARGED D WIDTH FROM MASS SPECTRUM (MEV)

W    P  50  40.   OR LESS  CL=.90   PERUZZI   76 SMAG +- K-+PI+-PI+-       1/77*
W    P  PERUZZI 76 WIDTH IS CONSISTENT WITH THEIR EXPERIMENTAL RESOLUTION.  1/77*

------ --------- --------- --------- --------- --------- --------- --------

                  31  EVIDENCE FOR WEAK DECAY OF D

WK      70                           WISS      76                           1/77*
WK      WISS 76, USING A SAMPLE OF ABOUT 70 D+- --> K-+ PI+- PI+-           1/77*
WK      EVENTS WHICH INCLUDE THE PERUZZI 76 EVENTS, FINDS THAT THIS FINAL   1/77*
WK      STATE IS INCOMPATIBLE WITH NATURAL SPIN AND PARITY.  THE NATURAL    1/77*
WK      SPIN PARITY FINAL STATE IN DO --> K- PI+ (GOLDHABER 76) INDICATES   1/77*
WK      PARITY VIOLATION IN THE D+- AND DO DECAYS IF BOTH ARE MEMBERS OF    1/77*
WK      THE SAME ISOMULTIPLET AS SUGGESTED BY THEIR SIMILAR MASSES.         1/77*
WK      THIS SUGGESTS A WEAK DECAY AND CONSEQUENTLY A NARROW WIDTH OF ORDER 1/77*
WK      10**13 SEC-1 OR 10**-8 MEV.                                         1/77*

------ --------- --------- --------- --------- --------- --------- --------

                  31  CHARGED D  PARTIAL DECAY MODES

                                                      DECAY MASSES
P1      D+- INTO K+- PI+- PI+-                      493+ 139+ 139

****** ********* ********* ********* ********* ********* ********* ********

                        REFERENCES FOR CHARGED D

GOLCHABE 76 PRL 37 255      GOLDHABER,PIERRE,ABRAMS,ALAM+      (LBL+SLAC)
PERUZZI  76 PRL 37 569      +PICCOLO,FELDMAN,NGUYEN,WISS+      (SLAC+LBL)
WISS     76 PRL 37 1531     +GOLDHABER,ABRAMS,ALAM,BOYARSKI+   (LBL+SLAC)

****** ********* ********* ********* ********* ********* ********* ********
****** ********* ********* ********* ********* ********* ********* ********
```

$D^{0}(1870)$

```
32  NEUTRAL D(1870,JP=  )
------ --------- --------- --------- --------- --------- --------- --------

                  32  NEUTRAL D MASS (MEV)

M       234 1865.      15.          GOLDHABER 76 SMAG CHGD K PI AND K 3PI  1/77*
M          (1864.)    (5.4)         GOLDHAB2  76 SMAG K+PI-/ RECOIL INFO   3/77*
M             . . . . . . . . . .
M    FIT    1865.      12.      FROM FIT (ERROR INCLUDES SCALE FACTOR OF 1.0)  4/77*

------ --------- --------- --------- --------- --------- --------- --------

                  32  NEUTRAL D WIDTH FROM MASS SPECTRUM (MEV)

W       234   40.    OR LESS        GOLDHABER 76 SMAG CHGD K PI AND K 3PI  1/77*
W            (5.)    OR LESS        GOLDHAB2  76 SMAG K+PI-/ RECOIL INFO   3/77*
W        30    2.4   OR LESS        FELDMAN   77 SMAG D*+ TO DO PI+        3/77*
W        WIDTHS ARE CONSISTENT WITH EXPERIMENTAL RESOLUTION. SEE NOTE ON   3/77*
W        WEAK DECAY IN CHARGED D SECTION ABOVE.                            3/77*

------ --------- --------- --------- --------- --------- --------- --------

                  32  NEUTRAL D PARTIAL DECAY MODES

                                                      DECAY MASSES
P1      DO INTO K- PI+                              493+ 139
P2      DO INTO K- PI+ PI+ PI-                      493+ 139+ 139+ 139
P3      DO INTO KS PI+ PI-                          497+ 139+ 139
P4      DO INTO KS PI+ PI- PI+ PI-
P5      DO INTO PI- PI+                             139+ 139
P6      DO INTO K+ PI- (VIA DOBAR)                  493+ 139

        DOBAR MODES ARE CHARGE CONJUGATES OF ABOVE MODES

------ --------- --------- --------- --------- --------- --------- --------

                  32 NEUTRAL D BRANCHING RATIOS

R1      DO INTO (K- PI+)/TOTAL                         (P1)
R1      110 SEEN                    GOLDHABER 76 SMAG   E+E- 3.9-4.6 GEV  3/77*

R2      DO INTO (K- PI+ PI+ PI-)/TOTAL                 (P2)
R2      124 SEEN                    GOLDHABER 76 SMAG   E+E- 3.9-4.6 GEV  3/77*

R3      DO INTO  (PI- PI+)/(K- PI+)                    (P5)/(P1)
R3       24   (0.065)  (0.04)       GOLDHAB2  76 SMAG   CONSIS.WITH ZERO  3/77*

R4      DO INTO (KS PI+ PI-)/TOTAL                     (P3)
R4          SEEN                    SCHWITTER 76 SMAG   E+E- 4.03GEV ECM  3/77*

R5      DO INTO (KS PI+ PI- PI+ PI-)/TOTAL             (P4)
R5          POSSIBLY SEEN           KNAPP     76 SPEC   PHOTOPRODUCTION   3/77*

R6      DO INTO (K+ PI- VIA DOBAR)/(K PI)              (P5)/(P1+P5)
R6       THIS IS THE DO-DOBAR MIXING LIMIT
R6            (0.17) OR LESS  CL=.90  GOLDHABER 77 SMAG                    3/77*
R6             0.16  OR LESS  CL=.90  FELDMAN   77 SMAG   D*+ TO DO PI+    3/77*

****** ********* ********* ********* ********* ********* ********* ********

                        REFERENCES FOR NEUTRAL D

GOLDHABE 76 PRL 37 255       GOLDHABER,PIERRE,ABRAMS,ALAM+      (LBL+SLAC)
GOLDHAB2 76 SLAC CONF. 379   G.GOLDHABER (AVAIL. AS LBL-5534) (LBL+SLAC)
KNAPP    76 BNL CONF.        B.KNAPP                                (COLU)
SCHWITTE 76 BNL CONF.        R.F.SCHWITTERS (SLAC-PUB-1871,1977)    (SLAC)
FELDMAN  77 SUBMITTED TO PRL +PERUZZI,PICCOLO,ABRAMS,ALAM+      (SLAC+LBL)
GOLDHABE 77 CHICAGO APS      G.GOLDHABER                        (LBL+SLAC)

****** ********* ********* ********* ********* ********* ********* ********
****** ********* ********* ********* ********* ********* ********* ********
```

$D^{*\pm}(2010)$

```
62 CHARGED D*(2010,JP=  )
------ --------- --------- --------- --------- --------- --------- --------

                  62  CHARGED D*(2010) MASS (MEV)

M       18 2010.      20.            PERUZZI   76 SMAG +- E+E- RECOIL      1/77*
M    F  30(2010.)    (15.)           FELDMAN   77 SMAG +- E+E- DIRECT DEC  3/77*
M    F  FELDMAN 77 MASS IS NOT INDEPENDENT OF MASS DIFFERENCE BELOW AND THE 3/77*
M    F  GOLDHABER 76 DO MASS.                                              3/77*
M          . . . . . . . . . .
M    FIT   2010.      12.      FROM FIT (ERROR INCLUDES SCALE FACTOR OF 1.0)  4/77*

------ --------- --------- --------- --------- --------- --------- --------

                  62 (D*+) - (DO) MASS DIFFERENCE (MEV)

DM      30  145.3      0.5           FELDMAN   77 SMAG    D*+ TO DO PI+    3/77*
DM         . . . . . . . . . .
DM   FIT    145.3      0.5     FROM FIT (ERROR INCLUDES SCALE FACTOR OF 1.0)  4/77*

------ --------- --------- --------- --------- --------- --------- --------

                  62  CHARGED D*(2010) WIDTH (MEV)

W       18  (20.0)  OR LESS          PERUZZI   76 SMAG +- E+E-,PSI(4030)   1/77*
W       30    2.4   OR LESS          FELDMAN   77 SMAG    D*+ TO DO PI+    3/77*

------ --------- --------- --------- --------- --------- --------- --------

                  62  CHARGED D*(2010) DECAY MODES

                                                      DECAY MASSES
P1      D*+(2010) INTO DO PI+                      1865+ 139
P2      D*+(2010) INTO D+ GAMMA                    1876+   0

        D*-(2010) MODES ARE CHARGE CONJUGATES OF ABOVE MODES

------ --------- --------- --------- --------- --------- --------- --------

                  62  CHARGED D*(2010) BRANCHING RATIOS

R1      D*+(2010) INTO (DO PI+)/TOTAL                  (P1)
R1       30 SEEN                     FELDMAN   77 SMAG    DIRECT DECAY     3/77*

R2      D*+(2010) INTO (D+ GAMMA)/TOTAL                (P2)
R2          SEEN                     GOLDHABER 77 SMAG    RECOIL SPEC      4/77*

****** ********* ********* ********* ********* ********* ********* ********

                        REFERENCES FOR CHARGED D*(2010)

PERUZZI  76 PRL 37 569       +PICCOLO,FELDMAN,NGUYEN,WISS,+     (SLAC+LBL)
FELDMAN  77 SUBMITTED TO PRL +PERUZZI,PICCOLO,ABRAMS,ALAM+      (SLAC+LBL)
GOLDHABE 77 CHICAGO APS      G.GOLDHABER                        (LBL+SLAC)

****** ********* ********* ********* ********* ********* ********* ********
****** ********* ********* ********* ********* ********* ********* ********
```

$D^{*0}(2010)$

```
63  NEUTRAL D*(2010,JP=  )
------ --------- --------- --------- --------- --------- --------- --------

                  63  NEUTRAL D*(2010) MASS

M          (2005.)     (3.)          GOLDHAB2  76 SMAG    E+E- TO D*D*     3/77*

------ --------- --------- --------- --------- --------- --------- --------

                  63 (D*0) - (DO) MASS DIFFERENCE

DM   G      (141.)     (5.1)         GOLDHAB2  76 SMAG    E+E- TO D*D*,D*D 3/77*
DM   G  NOT INDEPENDENT OF GOLDHABER2 76 D*0 AND DO MASS VALUES.           3/77*

------ --------- --------- --------- --------- --------- --------- --------

                  63  NEUTRAL D*(2010) WIDTH (MEV)

W              (5.)   OR LESS        GOLDHAB2  76 SMAG    E+E- TO D*D*     3/77*

------ --------- --------- --------- --------- --------- --------- --------

                  63  NEUTRAL D*(2010) PARTIAL DECAY MODES

                                                      DECAY MASSES
P1      D*0(2010) INTO DO PIO                      1865+ 134
P2      D*0(2010) INTO DO GAMMA                    1865+   0

        D*0(2010)BAR MODES ARE CHARGE CONJUGATES OF ABOVE MODES

------ --------- --------- --------- --------- --------- --------- --------

                  63  NEUTRAL D*(2010) BRANCHING RATIOS

R1      D*0(2010) INTO (DO GAMMA)/(DO PIO + DO GAMMA)     (P2)/(P1+P2)
R1            (APPROX. 35 TO 45 PERCENT) GOLDHAB2  76 SMAG E+E- TO D*D*,D*D 3/77*

****** ********* ********* ********* ********* ********* ********* ********

                        REFERENCES FOR NEUTRAL D*(2010)

GOLDHAB2 76 SLAC CONF. 379   G.GOLDHABER (AVAIL. AS LBL-5534) (LBL+SLAC)

****** ********* ********* ********* ********* ********* ********* ********
****** ********* ********* ********* ********* ********* ********* ********
```

CHARMED BARYONS

The evidence for the observation of charmed baryons, though not as strong as for charmed mesons, is quite consistent with the charmed baryon picture.[1,2] A single event, identified with high probability as $\nu p \to \mu^- \Lambda \pi^+\pi^+\pi^+\pi^-$ observed at BNL (CAZZOLI 75 in Λ_c^+, Σ_c Data Card Listings below) has $\Delta S=-1$ and $\Delta Q=+1$ for the hadrons. For this event, rate arguments indicate a $\Delta S=-\Delta Q$ strength comparable to $\Delta S=\Delta Q$. For non-charmed particles, no $\Delta S=-\Delta Q$ semileptonic processes have been observed, and limits on such rates are a few percent of $\Delta S=\Delta Q$ rates. With charm, such events are expected at rates comparable to $\Delta S=\Delta Q$ rates. Production can occur via the Cabibbo-suppressed transition $\nu d \to \mu^- c$ ($\Delta Q=+1$, $\Delta S=0$), while the Cabibbo-favored nonleptonic decay involves the transition $c \to su\bar{d}$ ($\Delta Q=0$, $\Delta S=-1$) resulting in $\Delta Q=+1$, $\Delta S=-1$ as observed. Thus charm provides a natural explanation for this event. The $(\Lambda 4\pi)^{++}$ mass and one of the $(\Lambda 3\pi)^+$ mass combinations are in good agreement with charm predictions[3] for the lowest lying charmed baryon states with charge +2 and +1 and $J^P=1/2^+$, the $\Sigma_c^{++}(2430)$ and the Λ_c^+ (2260).

CAZZOLI 75 state that the most likely alternative to charm for this event is associated production of a missing K_L^0 with a probability of $\simeq 3\times 10^{-5}$.

We adopt the names Λ_c and Σ_c used by CAZZOLI 75. The name Λ or Σ indicates the isospin (u,d quark) structure, while the subscript c indicates that the strange quark in an uncharmed Λ or Σ has been replaced by a charmed quark giving $c(ud)_{I=0}$ for Λ_c^+ and $c(ud)_{I=1}$ for Σ_c. Alternative names to Λ_c and Σ_c are C_0 and C_1, used e.g. in ref. 1 and ref. 2.

Additional charmed baryon evidence comes from Fermilab photoproduction data (KNAPP 76) on the reaction

$$\gamma + \mathrm{Be} \to \bar{\Lambda} + \mathrm{pions}\ .$$

A narrow peak is observed in $\bar{\Lambda}\,\pi^-\pi^-\pi^+$ at 2.26 GeV and not in $\bar{\Lambda}\,\pi^+\pi^+\pi^-$. A higher mass (~2.5 GeV) peak in $(\bar{\Lambda}4\pi)^0$ is seen to cascade into this state. Their results are consistent with being

$$\left\{\begin{array}{l} \bar{\Sigma}_c^0\ (2430,\ J^P=1/2^+) \\ \bar{\Sigma}_c^0\ (2480,\ J^P=3/2^+) \end{array}\right\} \longrightarrow \bar{\Lambda}_c^-\ (2260)\pi^+,\quad \bar{\Lambda}_c^- \longrightarrow \bar{\Lambda}\pi^-\pi^-\pi^+$$

in striking agreement with the CAZZOLI 75 event.

Uncharmed Σ states are known to exist[4] in the neighborhood of the observed states. However, the narrow width of the $\bar{\Lambda}\pi^-\pi^-\pi^+$ peak and the absence of the opposite-charge state tend to favor the charm interpretation. One disturbing feature of the KNAPP 76 data which is contrary to charm expectations is the absence of a signal in the $\bar{\Lambda}\pi^+\pi^+\pi^-$ state.

BARISH 77 in an ANL deuterium exposure find one neutrino dilepton candidate, which they identify as

$$\nu_\mu d \to \mu^- p\pi^+\pi^-\pi^0 e^+\nu_e(n_s)\ ,$$

where the π^0 is inferred from the observation of a single converted photon, and the neutrino and spectator neutron are not seen. This event has a possible, but highly speculative interpretation as a semileptonic decay of a charmed baryon:

$$\nu_\mu d \to \mu^-\Sigma_c^{++}(2430)(n_s),\quad \Sigma_c^{++} \longrightarrow p\pi^+\pi^-\pi^0 e^+\nu_e$$

or

$$\Sigma_c^{++} \longrightarrow p\pi^+\pi^-\pi^0\bar{K}^0 e^+\nu_e\ ,$$

where the $\bar{K}^0$ escaped detection. With the second interpretation and the charm expectation that $\Sigma_c^{++}(2430)\to\Lambda_c\pi^+$, they speculate that they may have observed the semileptonic decay

$$\Lambda_c^+ \to p\pi^-\pi^0\bar{K}^0 e^+\nu_e\ .$$

This interpretation would require that mass$(\Sigma_c^{++}) > 2439$ MeV and mass$(\Lambda_c^+) > 2248$ MeV, limits consistent within errors with the CAZZOLI 75 mass values. It would also require a fairly unlikely spectator neutron momentum of 260 MeV. Other interpretations exist for this event including a lighter mass, ~2 GeV charmed baryon or a background non-dilepton event.

We put the Λ_c^+ and Σ_c into the table but consider these entries preliminary.

References

1. M.K. Gaillard, B.W. Lee, and J.L. Rosner, Rev. Mod. Phys. 47, 277 (1975).
2. B.W. Lee, C. Quigg, and J.L. Rosner, Phys. Rev. D15, 157 (1977).
3. A. De Rujula, H. Georgi, and S.L. Glashow, Phys. Rev. D12, 147 (1975).
4. A. de Bellefon and A. Berthon, Nucl. Phys. B109, 129 (1976) and Particle Data Group, Rev. Mod. Phys. 48, S232 (1976).

$\Lambda_c^+(2260)$

```
33  LAMBDA/C+(2260,JP=  )
------ --------- --------- --------- --------- --------- --------- --------

                 33  LAMBDA/C+ MASS (MEV)

M    C   1 2260.     20.             CAZZOLI   75 HBC  +  LAMBDA 2PI+ PI-   3/77*
M   S    1(2360.)   (590.)           SUGIMOTO  75 EMUL    INTO SIGMA PIO    3/77*
M   S    1(2230.)   (560.)           SUGIMOTO  75 EMUL    INTO SIGMA ETAO   3/77*
M    K  60 2260.     (10.)           KNAPP     76 SPEC -  ANTILAM 2PI- PI+  3/77*
M   B    1(2248.)   OR MORE          BARISH    77 DBC     MODE P4 BELOW     3/77*
M    C  CAZZOLI 75 IS BNL EXPT.  SEES (NEUTRINO P --> MU- LAMBDA 3PI+ PI-)   3/77*
M    C  EVENT WITH M(LAMBDA 4PI)=2426+-12MEV.  LARGE DS=-DQ RATE (SAME AS    3/77*
M    C  DS=DQ) SUGGESTS CHARM.  DERUJULA 75 PREDICTS 2 STATES NEAR THIS      3/77*
M    C  MASS WHICH DECAY STRONGLY BY PI+ EMISSION (MASS DIFF 160 AND 220MEV  3/77*
M    C  FOR THE TWO STATES) TO THE LOWEST MASS CHARMED BARYON.  THE THREE    3/77*
M    C  POSSIBLE PI+ EMISSION MASS DIFFS FOR THIS EVT ARE 338+-12, 327+-12   3/77*
M    C  AND 166+-15MEV.  WE USE THE LATTER FOR THE ABOVE QUOTED MASS.        3/77*
M   S   SUGIMOTO 75 VALUES ASSUME DECAY TRACK IDENTIFICATION AS SIGMA+-.     3/77*
M   S   VALUES TAKEN FROM GAISSER 76 TABLE 3. VERY SPECULATIVE INTERP.       3/77*
M    K  KNAPP 76 IS FNAL WIDE BAND PHOTON BEAM CN BE TARG. THEY SEE PEAK IN  3/77*
M    K  ANTILAM 2PI- PI+ BUT NOT IN ANTILAM 2PI+ PI-.  THEY ALSO SEE AN      3/77*
M    K  ANTILAM  2PI+ 2PI- STATE AT 2.5GEV CASCADING VIA PI- EMISSION TO     3/77*
M    K  THE 2.26 GEV STATE.                                                  3/77*
M   B   BARISH 77 IS ANL EXPT.  SEES ONE DILEPTON EVENT WHICH IS CONSISTENT  3/77*
M   B   WITH NEU P --> MU- SIGMA/C++, SIGMA/C++ --> LAMBDA/C+ PI+  AND       3/77*
M   B   LAMBDA/C+ --> P PI- PIO KOBAR E+ NEU.  THIS INTERPRETATION GIVES     3/77*
M   B   ABOVE MASS LIMIT. IT IS A VERY SPECULATIVE INTERPRETATION.           3/77*

------ --------- --------- --------- --------- --------- --------- --------

                 33  LAMBDA/C+ MEAN LIFE (UNITS 10**-12 SEC)
T   S    1   (4.5)                   SUGIMOTO  75 EMUL    INTO SIGMA PIO    3/77*
T   S    1   (0.68)                  SUGIMOTO  75 EMUL    INTO SIGMA ETAO   3/77*
T   S   SUGIMOTO 75 VALUES ASSUME DECAY TRACK IDENTIFICATION AS SIGMA+-.     3/77*
T   S   VALUES TAKEN FROM GAISSER 76 TABLE 3.  VERY SPECULATIVE.             3/77*

------ --------- --------- --------- --------- --------- --------- --------

                 33  LAMBDA/C+ WIDTH FROM MASS SPECTRUM

W    C  60   75.    OR LESS          KNAPP     76 SPEC -  ANTILAM 2PI- PI+  3/77*
W    C  KNAPP 76 MEASURES WIDTH 40+-20MEV CONSISTENT WITH THEIR EXPT         3/77*
W    C  RESOLUTION (30MEV) FOR A ZERO WIDTH STATE.                           3/77*

------ --------- --------- --------- --------- --------- --------- --------

                 33  LAMBDA/C+ PARTIAL DECAY MODES

                                                        DECAY MASSES
P1      LAMBDA/C+ INTO LAMBDA PI+ PI+ PI-              1115+ 139+ 139+ 139
P2      LAMBDA/C+ INTO SIGMA+ PIO                      1189+ 134
P3      LAMBDA/C+ INTO SIGMA+ ETA                      1189+ 548
P4      LAMBDA/C+ INTO P PI- PIO KO E+ NEU

------ --------- --------- --------- --------- --------- --------- --------

N       NOTE ON VERY TENTATIVE MODES P2, P3, AND P4                          3/77*
N        THESE MODES ARE VERY TENTATIVE.  P2 AND P3 ARE FROM SUGIMOTO 75     3/77*
N        (SEE GAISSER 76 REVIEW) AND P4 IS FROM BARISH 77.  EACH IS FROM A   3/77*
N        SINGLE EVENT.  SEE DETAILS IN TYPED REVIEW ABOVE.                   3/77*

****** ********* ********* ********* ********* ********* ********* ********

                          REFERENCES FOR LAMBDA/C+

CAZZOLI  75 PRL 34 1125       +CNOPS,CONNOLY,LOUTTIT,MURTAGH+        (BNL)
SUGIMOTO 75 PTP 53 1540       +SATO,SAITO                     (WASEDA+TOKY)
KNAPP    76 PRL 37 882        +LEE,LEUNG,SMITH +      (COLU+HAWA+ILL+FNAL)
BARISH   77 PR D15 1          +DERRICK,DOMBECK,MUSGRAVE +       (ANL+PURD)

                          THEORY AND REVIEW

DERUJULA 75 PR D12 147        +GEORGI,GLASHOW                        (HARV)
GAISSER  76 PR D14 3153       T.K.GAISSER,F.HALZEN            (BARTOL+WISC)
LEE      77 PR D15 157        +QUIGG,ROSNER                          (FNAL)

****** ********* ********* ********* ********* ********* ********* ********
****** ********* ********* ********* ********* ********* ********* ********
```

$\Sigma_c(2430)$

```
104  SIGMA/C(2430,JP=  )
------ --------- --------- --------- --------- --------- --------- --------

                 104  SIGMA/C MASS

M    C   1 2426.      12.            CAZZOLI   75 HBC  ++ LAMBDA/C+ PI+     3/77*
M   KC   9(2500.)                    KNAPP     76 SPEC 0  ANTILAMBDA/C-PI+  3/77*
M    C   1(2439.)   OR MORE          BARISH    77 DBC  ++ LAMBDA/C+ PI+     3/77*
M    C  SEE NOTES IN LAMBDA/C+ MASS SECTION ABOVE.                           3/77*
M   K   KNAPP 76 MAY NOT BE THE SAME STATE AS CAZZOLI 75.  DERUJULA 75       3/77*
M   K   PREDICT TWO SIGMA/C STATES AROUND 2.4-2.5 GEV.  THIS COULD BE BOTH.  3/77*

------ --------- --------- --------- --------- --------- --------- --------

                 104  SIGMA/C(2430) PARTIAL DECAY MODES

                                                        DECAY MASSES
P1      SIGMA/C(2430) INTO LAMBDA/C+ PI                2260+ 139

****** ********* ********* ********* ********* ********* ********* ********

                          REFERENCES FOR SIGMA/C(2430)

CAZZOLI  75 PRL 34 1125       +CNOPS,CONNOLY,LOUTTIT,MURTAGH+        (BNL)
KNAPP    76 PRL 37 882        +LEE,LEUNG,SMITH +      (COLU+HAWA+ILL+FNAL)
BARISH   77 PR D15 1          +DERRICK,DOMBECK,MUSGRAVE +       (ANL+PURD)

                          THEORY AND REVIEW

DERUJULA 75 PR D12 147        +GEORGI,GLASHOW                        (HARV)
LEE      77 PR D15 157        +QUIGG,ROSNER                          (FNAL)

****** ********* ********* ********* ********* ********* ********* ********
****** ********* ********* ********* ********* ********* ********* ********
```

CHARM SEARCHES AND EVIDENCE

Evidence for charm not directly relatable to a given state is listed in this section. Neutrino-induced dilepton events and the high-y anomaly in neutrino and antineutrino interactions are discussed. Short-lived tracks in emulsions are also dealt with, as are cross-section upper limits for charm searches. Direct lepton production in pN collisions is discussed in the Other New Particle Searches section below rather than in this section, because recent results favor other interpretations than charm.

For a more thorough treatment of some of the above topics, we refer the reader to other recent reviews of which we are aware (refs. 1-8).

Neutrino-induced Dilepton Events

The Harvard-Penn-Wisconsin-Fermilab collaboration (BENVENUTI 75) and the Caltech-Fermilab group (BARISH 76) have observed neutrino events with two muons in the final state. Most of these events have opposite-charge muons.

Bubble chamber experiments have observed neutrino-induced $\mu^- e^+$ events, many associated with strange particle production in the reaction

$$\nu N \to \mu^- e^+ K^0 (\text{or } \Lambda) + \text{anything}$$

(see DEDEN 75, BLIETSCHAU 75, VON KROGH 76, BARISH 77 in the Data Card Listings and the BARISH 77 discussion in the charmed baryon section above).

Data Card Listings

CHARM SEARCHES

Dilepton events have no conventional explanation. Production of charmed hadrons, heavy leptons, and intermediate bosons have been proposed as potential explanations. Production of charmed particles (C) in neutrino interactions would be expected to give rise to such events via the mechanism

$$\nu_\mu N \to \mu^- C + \text{hadrons}$$
$$\qquad\qquad\qquad \hookrightarrow \ell^+ \nu_\ell + \text{hadrons},$$

where the Cabibbo-favored transition would predict a strange particle among the hadrons. Thus the appearance of neutrino-induced dimuon events, $\mu^- e^+$ events, and associated strange particles can be understood via the charm mechanism.

The "High-y Anomaly"

In the naive quark-parton model one may write the double differential cross section for charged-current neutrino and antineutrino nucleon scattering as

$$\frac{d^2\sigma^\nu}{dxdy} = \frac{G^2 ME_\nu}{\pi}\left[q(x) + \bar{q}(x)(1-y)^2\right]$$

$$\frac{d^2\sigma^{\bar\nu}}{dxdy} = \frac{G^2 ME_{\bar\nu}}{\pi}\left[q(x)(1-y)^2 + \bar{q}(x)\right] .$$

Here $x = Q^2/2ME_h$ and $y = E_h/E_{\nu,\bar\nu}$ are scaling variables, M is the nucleon mass, E_h is the energy transferred to the final-state hadrons, $E_{\nu,\bar\nu}$ is the beam energy, both in the laboratory frame, $-Q^2$ is the square of the four-momentum transferred from incident neutrino to final-state μ (assuming muon neutrinos), and $G^2ME_\nu = 1.56 \times 10^{-38}$ cm^2/GeV. In these relations, valid for isoscalar nuclei (a reasonable approximation for real targets), $\frac{1}{x}q(x)dx$ and $\frac{1}{x}\bar{q}(x)dx$ are the probabilities of quarks and antiquarks being involved in the interaction while carrying a fraction x (evaluated in the infinite-momentum frame) of the target momentum. One frequently rewrites these in terms of $B(x) = 1 - 2\bar{q}(x)/[q(x) + \bar{q}(x)]$. Integrating over x,

$$\frac{d\sigma^{\nu,\bar\nu}}{dy} \propto E_{\nu,\bar\nu}\left[(1 - y + \frac{y^2}{2}) \pm By(1 - \frac{y}{2})\right]$$

where B here is a weighted average of B(x) over all x. Then (1-B)/2 is interpreted as the contribution of the antiquark fraction in the nucleon to the scattering. B near 1.0 means the antiquark contribution to the nucleon is small. In this case the above equations reduce to $d\sigma^\nu/dy \propto E_\nu$ and $d\sigma^{\bar\nu}/dy \propto E_{\bar\nu}(1-y)^2$.

B may be most easily measured from $d\sigma/dy$ for antineutrino beams, which is more sensitive to B than its counterpart for incident neutrinos. At low energies, the antiquark component seems to be small, and is confined to small x, as one might expect from a quark-antiquark "sea" in the nucleon, according to the conventional three-quark model (see, for example, review papers by Roe,[6] Perkins,[7] Steinberger,[8] and Wojcicki[4]). Recent experimental data at very high energies indicate an increasingly flat antineutrino y distribution (see for example, Barish et al.[9] and Benvenuti et al.,[10] and also the review papers above). That is, B apparently is increasing, at least in $\bar\nu$ reactions.

Both experiments which report this effect (sometimes called the "high-y anomaly" — an anomaly may be defined as something unaccounted for by conventional three-quark models) utilize electronic detectors with acceptances which are poor in various parts of the kinematical region, and both report rather large error bars for their determinations of B (collected and illustrated by Nezrick[11] and Roe[6]). Linear fits to the world's data on B as a function of energy, over the full energy range (Nezrick,[11] Roe[6]), yield slopes that are about 2-3 standard deviations from zero. Taken by themselves, the data for $E_{\bar\nu} < 70$ GeV are perfectly consistent with no energy dependence for B, with a value of about 0.8 or 0.9; hence there may be a threshold for a new effect at ~70 GeV (in which case a linear fit over all energies would not be appropriate). The strongest evidence for an anomaly comes from the HPWF experiment (for example, Benvenuti[10]), which finds under certain assumptions, $B^{\bar\nu} = 0.94 \pm 0.09$ averaged over the 10-30 GeV incident energy range, and 0.41 ± 0.13 for $E_{\bar\nu} > 70$ GeV. These experimenters also report B^ν different from $B^{\bar\nu}$, in this energy range, at the two standard deviation level.

Note from the above formulas that $B^{\bar{\nu}}$ decreasing with energy implies a rising ratio of antineutrino-to-neutrino charged-current cross sections. The accompanying figure shows current data for $E_{\nu,\bar{\nu}} > 40$ GeV. A rising trend may be present, although there is a single low point at 110 GeV (which represents only 11 events however).

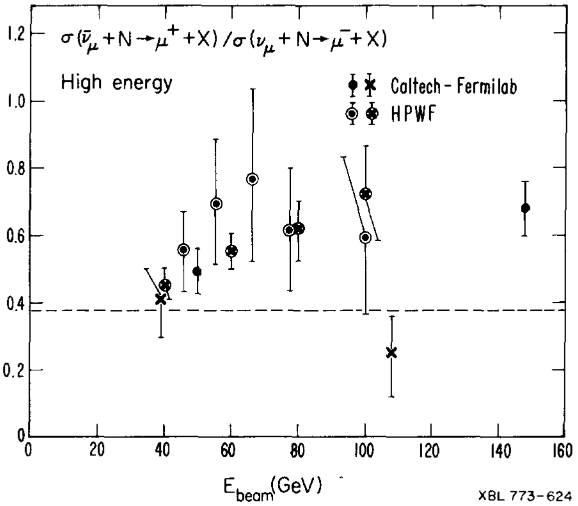

Ratio of $\bar{\nu}_\mu$ to ν_μ charged-current cross sections at incident energies above 40 GeV. For lower energies, the ratio is approximately 0.38 (dashed line). Encircled points: Harvard-Penn-Wisconsin-Fermilab collaboration [A. Benvenuti et al., Phys. Rev. Lett. 37, 189 (1976)]; non-circled points: Caltech-Fermilab collaboration [B.C. Barish et al., preprint CALT 68-560 (1976)]. Points denoted by X depend upon knowledge of the flux; solid points are a flux-independent (but model-dependent) determination.

A high-y anomaly of the magnitude reported by the HPWF group appears to be inconsistent with the conventional three-quark model. It may also be too large to be accommodated even with the addition of a fourth, charmed quark in the GIM picture. Hence, much work is being done concerning the possibility of additional (more than 4) quarks. These quarks are usually massive, to force an energy threshold, and right-handed, to force a $\bar{\nu}$ y anomaly (see, e.g., Barnett[12]). For example, Barish et al.[9] find a good fit to their data with a right-handed "b" quark of mass 5.1 GeV.

In conclusion, there is growing experimental evidence for an anomaly in the y-distribution for $\bar{\nu}$-induced events. This anomaly takes the form of a flattening of the $d\sigma/dy$ distribution relative to that expected from three-quark models with a $q-\bar{q}$ "sea", and occurs only at high energies. The relationship between this effect and the observation of prompt dileptons in ν and $\bar{\nu}$ production is unclear, but the high-y effect may have a higher energy threshold.

Short-lived tracks in emulsions

The mean life of a weakly decaying charmed meson or baryon of mass M (in GeV) is expected to be in the range[13]

$$\tau = (10^{-11} \text{ to } 10^{-13} \text{ sec}) \times \frac{1}{M^5}$$

with a corresponding mean path length for lab momentum p (in GeV/c) of

$$\ell = \frac{pc\tau}{M} = (1\mu \text{ to } 100\mu) \times p$$

Thus even at Fermilab energies, these would be hard to see as tracks in bubble chambers.

A number of cosmic ray experiments (e.g., NIU 71, TASAKA 73, and SUGIMOTO 75) have seen short-lived charged tracks which decay into a charged track and a π^0 or η. Charged-particle identification problems preclude unique determinations of masses and lifetimes. Table III of Gaisser and Halzen's review[5] of these events gives values in the range 1.5 GeV < M < 3.0 GeV and 2×10^{-14} sec < τ < 3×10^{-12} sec for the three strongest charm candidates (they involve possible pair production). Of these, one event (SUGIMOTO 75) is consistent with production of a $\Lambda_c^+\bar{\Lambda}_c^-$ pair with subsequent decays to $\Sigma^+\eta$ and $\bar{\Sigma}^-\pi^0$. None are consistent with $D^\pm$ production. Accelerator events with lifetimes $\sim 10^{-13}$ sec (KOMAR 75) and 6×10^{-13} sec (BURHOP 76) have also been reported.

Charm Searches

We list cross-section upper limits for the many unsuccessful charm searches. In cases where limits are given for many channels and mass ranges, we list only a range or a few likely channels and indicate in the comment cards the extent and location of the tables of data included in the paper.

Data Card Listings

CHARM SEARCHES

References

1. D. Cline, "Multilepton Production by Neutrinos and Antineutrincs: Charm, Charm-Changing Neutral Currents and New Flavors," Invited talk given at the APS Meeting, Division of Particles and Fields, BNL, October 1976, Wisconsin preprint (1976).
2. K.C. Stanfield, "Charm Searches in Hadron-Induced Interactions," Rapporteur talk given at the APS Meeting, Division of Particles and Fields, BNL, October 1976, Purdue preprint COO-1428-439.
3. S.P. Denisov, "Dilepton Production and Search for New Particles in Hadron-Hadron Collisions and Photoproduction," Rapporteur talk given at the XVIII International Conference on High Energy Physics, Tbilisi, 1976, IHEP preprint 76-154.
4. S.G. Wojcicki, "Weak Interactions at High Energy," Proceedings of Summer Institute on Particle Physics, August 2-13, 1976, SLAC Report No. 198 (November 1976).
5. T.K. Gaisser and F. Halzen, Phys. Rev. D14, 3153 (1976),
6. B. Roe, "New Results in High Energy Neutrino Physics," Invited talk presented at the APS Meeting, Division of Particles and Fields, BNL, October 1976, Wisconsin preprint (1976).
7. D.H. Perkins, "Topics in Lepton-Hadron Interactions," ANL-HEP-PR-76-54 (1976).
8. J. Steinberger, "High Energy Neutrino Experiments," in Proceedings of the 1976 CERN School of Physics, p.57 (1976).
9. B.C. Barish, et al., Phys. Rev. Lett. 38, 314 (1977).
10. A. Benvenuti, et al., Phys. Rev. Lett. 36, 1478 (1976).
11. F.A. Nezrick, "Search for New Particles Produced in $\bar{\nu}_\mu$ Nucleon Interactions in the 15-foot Bubble Chamber," Proceedings of the SLAC Summer Institute on Particle Physics, p.347; also Fermilab-Conf-76/90 EXP (1976).
12. R. Michael Barnett, Phys. Rev. Lett. 36, 1163 (1976).
13. M.K. Gaillard, B.W. Lee, and J.L. Rosner, Rev. Mod. Phys. 47, 277 (1975).


```
CE      CHARMED HADRON PRODUCTION CROSS SECTION(E+ E-) (UNITS 10**-35 CM**2)
CE      THESE VALUES ARE (CROSS SECTION)X(BR. RATIO TO MODE INDICATED)
CE   B   0   18.    OR LESS  CL=.90   BOYARSKI   75 SMAG K- PI+, K+ PI-       2/76
CE   B   0   40.    OR LESS  CL=.90   BOYARSKI   75 SMAG KOS PI+ PI-          2/76
CE   B   0   13.    OR LESS  CL=.90   BOYARSKI   75 SMAG PI+ PI-              2/76
CE   B   0   12.    OR LESS  CL=.90   BOYARSKI   75 SMAG K+ K-                2/76
CE   B   0   49.    OR LESS  CL=.90   BOYARSKI   75 SMAG K-PI+PI+, K+PI-PI-   2/76
CE   B   0   27.    OR LESS  CL=.90   BOYARSKI   75 SMAG KOS PI+, KOS PI-     2/76
CE   B   0   33.    OR LESS  CL=.90   BOYARSKI   75 SMAG KOS K+, KOS K-       2/76
CE   B   0   38.    OR LESS  CL=.90   BOYARSKI   75 SMAG PI+PI-PI+,PI+PI-PI-  2/76
CE   B   0   90.    OR LESS  CL=.90   BOYARSKI   75 SMAG K+PI-,KOPI+PI- + CC  2/76
CE   B   0   16.    OR LESS  CL=.90   BOYARSKI   75 SMAG K+ K-, PI+ PI-       2/76
CE   B   0   51.    OR LESS  CL=.90   BOYARSKI   75 SMAG K+PI-PI-,KOPI+ + CC  2/76
CE   B   0   76.    OR LESS  CL=.90   BOYARSKI   75 SMAG KOK+,PI+PI+PI- + CC  2/76
CE  P   64  (1.9)    (0.5)            PERL       75 SMAG    E(OR MU) NEUTRI.  2/76
CE   R  28   50.    OR MORE           BRAUNSCHW  76 DASP    E+- +HADRONS      3/77*
CE   U      300.     300.             BURMESTER  76 PLUT    KO E+- +ANYTHING  3/77*
CE   G 110   20.       5.0            GOLDHABER  76 SMAG    K-+PI+-           1/77*
CE   G 124   67.      11.0            GOLDHABER  76 SMAG    K-+PI+-PI+PI-     1/77*
CE   E  50   30.      15.             PERUZZI    76 SMAG    K-+PI+-PI+-       1/77*
CE   F 246   25.      10.             FELDMAN    77 SMAG    MUON .GE.3PRONG   3/77*
CE   B  BOYARSKI 75 IS SLAC(SPEAR) EXPT.  LOOKED FOR E+E- --> D ANYTHING      2/76
CE   B  AT ECM=4.8 GEV WHERE CHARMED MESON D DECAYED VIA CHANNELS SHOWN.      2/76
CE   B  ABOVE VALUES ARE FOR D MASS=1.85-2.40 GEV.  SIMILAR LIMITS ARE        2/76
CE   B  GIVEN FOR MASS=1.50-1.85, 2.40-4.00 GEV IN THEIR TABLE 1.             2/76
CE  P   PERL 75 IS SLAC(SPEAR) EXPT .  EVENTS ARE E+E- TO E+-MU-+ AND 2 OR    2/76
CE  P   MORE MISSING PARTICLES.  CS IS FOR ECM=4.8 GEV AND THETA=50-130DEG.   2/76
CE  P   CROSS SECTION RISES FROM 5X10**-36 AT E=4 TO ABOVE MAX. THEN DROPS    2/76
CE  P   TO 6E-36  AT E=7.5.   AUTHORS SAY THESE EVENTS HAVE NO CONVENTIONAL   2/76
CE  P   EXPLANATION.  SUGGEST HEAVY LEPTON OR CHARMED HADRON, M=1.6-2.0GEV.   2/76
CE  P   NOT CORRECTED FOR DETECTOR ACCEPTANCE.
CE   R  BRAUNSCHWEIG 76 SEES SINGLE ELECTRONS IN E+E- COLLISIONS AT DORIS.    3/77*
CE   R  ESTIMATED 2*CS*BR TO(E + HADRONS) IS 1 NB. MASS BETW 1.8 AND 2.1GEV   3/77*
CE   R  INFERRED FROM PROD THRESHOLD BEING BETW 3.7 AND 4.0 GEV.  E+-         3/77*
CE   R  MOMENTUM SPECTRUM AND OBSERVED MULTIPLICITY ARE INCONSISTENT WITH     3/77*
CE   R  HEAVY LEPTON HYPOTHESIS.                                              3/77*
CE   U  BURMESTER 76 IS A DORIS E+E- EXPT. THEY SEE KOS+PROMPT ELECTRONS AT   3/77*
CE   U  ECM=4.0-4.1 GEV. SUGGESTS PAIR PROD OF CHARMED PARTICLE OF MASS       3/77*
CE   U  1.8 TO 2.0 GEV.                                                       3/77*
CE   G  GOLDHABER 76 IS A SPEAR E+E- EXPT WITH ECM=3.9 TO 4.6 GEV. THEY SEE   1/77*
CE   G  PEAK AT 1865+-15 MEV, WIDTH LT 40 MEV. PROBABLY NEUTRAL STATE OF      1/77*
CE   G  SAME PARTICLE SEEN IN PERUZZI 76.  A PEAK IS ALSO OBSERVED IN THE     1/77*
CE   G  MASS SPECTRUM RECOILING AGAINST THESE STATES WITH MASS 1.96-2.2GEV.   1/77*
CE   E  PERUZZI 76 IS SPEAR E+E- EXPT AT 4.03 GEV. THEY SEE EXOTIC PEAK AT    1/77*
CE   E  M=1876+-15, WIDTH LT 40 MEV. NO STRUCTURE SEEN IN KPI+PI- CHANNEL.    1/77*
CE   F  FELDMAN 77 IS A CONTINUATION OF PERL 75.  ABOVE DATA IS FOR           3/77*
CE   F  ECM=5.8-7.8 GEV.  HEAVY LEPTONS COULD ACCOUNT FOR ONLY 20 PERCENT     3/77*
CE   F  OF THIS CS.  THEY SUGGEST EXCESS IS FROM WK. DECAYS OF NEW HADRONS.   3/77*

CG      CHARMED HADRON PRODUCTION CROSS SEC (GAMMA NUCLEON)  (CM**2)
CG   K  60 EVENTS                      KNAPP      76 SPEC LAMBDABAR PI-PI-PI+  2/77*
CG   Q   0  1.1E-29 OR LESS  CL=.95   QUINN      76 HBC      B++ M-           2/77*
CG   Q   0  1.2E-29 OR LESS  CL=.95   QUINN      76 HBC      B+ MO            2/77*
CG   K  KNAPP 76 SEES A PEAK AT M=2.26+-0.01 GEV/C**2. WIDTH IS 40+-20 MEV,   2/77*
CG   K  CONSISTENT WITH ZERO WIDTH STATE (RESOLUTION=30 MEV). NO PEAK SEEN    2/77*
CG   K  IN LAMBDABAR PI+ PI+ PI-. THEY ALSO SEE A LAMBDABAR (4PI)0 PEAK AT    2/77*
CG   K  2.5 GEV CASCADING DOWN TO THE PEAK AT 2.26. EXPT USED WIDE-BAND       2/77*
CG   K  PHOTON BEAM AT FNAL.                                                  2/77*
CG   Q  QUINN 76 USED A 9.3 GEV PHOTON BEAM AT SLAC. SEE TABLES 1 AND 3 FOR   2/77*
CG   Q  INDIVIDUAL CHANNELS. ABOVE LIMITS ARE FOR ALL CHANNELS WITH ONE OR    2/77*
CG   Q  NO MISSING NEUTRALS.                                                  2/77*

CPI     CHARMED HADRON PRODUCTION CROSS SECTION (PI NUCLEON)   (CM**2)
CPI  B   0 1.5 TO 3.7 E-30 OR LESS    BALTAY     75 HBC      15 GEV PI+P      7/76*
CPI  B   0 0.2 TO 35  E-30 OR LESS    BALTAY     75 HBC      15 GEV PI+P      7/76*
CPI  U   0 0.5 TO 15 E-30 OR LESS     BUNNELL    76 STRC     CL=.97           1/77*
CPI  C   0  1. TO 8. E-31  OR LESS    CESTER     76 SPEC     15 GEV/C PI-     2/77*
CPI  K   0  4.8E-32 OR LESS           COOK       76 STRC     225 GEV/C PI-    3/77*
CPI  G   0  4. TO 8. E-32  OR LESS    GHIDINI    76 SPEC     19 GEV/C PI P    2/77*
CPI  H   0  4. E-30 OR LESS  CL=.95   HAGOPIAN   76 DBC  SHORT LIVED 2-5GEV   2/76
CPI  H   1  7. E-31 OR LESS  CL=.95   HAGOPIAN   76 DBC  LONG LIVED 1.9-2GEV  2/76
CPI  H   0  3. E-31 OR LESS  CL=.95   HAGOPIAN   76 DBC  LONG LIVED1-1.9,2-5  2/76
CPI  A   0  3.8E-31 OR LESS  CL=.95   BLANAR     77 SPEC     200 GEV/C PI+    4/77*
CPI  B  BALTAY 75 SENSITIVE TO CHARMED PARTICLES WITH M=1.5 TO 4.0 GEV AND    7/76*
CPI  B  TAU LT 10**-11 WHICH THEN DECAY INTO STRANGE PARTICLES.               7/76*
CPI  B  THE FIRST VALUE ABOVE IS FOR ASSOC PROD OF CHARMED PARTICLES.         7/76*
CPI  B  SEE HIS TABLE 1 FOR SPECIFIC DECAY MODES.  THE SECOND RANGE OF        7/76*
CPI  B  VALUES IS FOR INCLUSIVE PROD OF CHARMED MESONS AND BARYONS WITH       7/76*
CPI  B  CHARGES -2 TO +2. SEE HIS TABLE 2 FOR SPECIFIC DECAY MODES.           7/76*
CPI  U  BUNNELL 76 IS A SLAC 15.5 PI+P EXPT. ALL POSSIBLE 2 TO 5-BODY MASS    1/77*
CPI  U  COMBINATIONS WERE STUDIED FOR NARROW RESONANCES PRODUCED IN COINC     1/77*
CPI  U  WITH SINGLE MUONS. MASS RANGE STUDIED WAS UP TO 3.1 GEV. SEE TABLE    1/77*
CPI  U  1 ON PG 87 FOR DETAILED RESULTS OF INDIVIDUAL CHANNELS.               1/77*
CPI  C  CESTER 76 LOOKS AT MASS RANGE 1.8 TO 2.5 GEV. SEE TABLE 1 FOR         2/77*
CPI  C  INDIVIDUAL CHANNELS. VALUES GIVEN ARE CROSS-SEC/NUCLEON ON CARBON.    2/77*
CPI  K  COOK 76 USES 225 GEV PI- BEAM. LOOKS FOR CORRELATION BETW VOS AND     3/77*
CPI  K  PROMPT MUONS TO SIGNAL DECAY OF CHARMED PARTICLE. LIMIT FOR M=2GEV.   3/77*
CPI  G  GHIDINI 76 LOOKED FOR CHARMED MESONS OF MASS GT 1.5 GEV AND BARYONS   2/77*
CPI  G  OF MASS GT 2.0 GEV. LIMITS ARE CL=.95. LIMITS FOR MOST CHANNELS LIE   2/77*
CPI  G  IN THE ABOVE RANGE.  SEE TABLE 2 FOR INDIVIDUAL CHANNELS.             2/77*
CPI  H  HAGOPIAN 76 IS A SLAC 15GEV PI+ D EXPT.  ALL POSSIBLE TWO AND THREE   2/76
CPI  H  BODY MASS COMBINATIONS WERE STUDIED FOR NARROW RESONANCES WITH MASS   2/76
CPI  H  1.5-5GEV FOR MESONS AND 2-5GEV FOR BARYONS.  INDIVIDUAL LIMITS FOR    2/76
CPI  H  TWO AND THREE BODY DECAY FROM MANY REACTIONS ARE GIVEN.               2/76
CPI  H  VEES WERE STUDIED FOR THE POSSIBILITY OF A NEW LONG LIVED (MEAN       2/76
CPI  H  LIFE 1E-11 SEC. OR MORE) NEUTRAL PARTICLE.  ONE CANDIDATE WITH MASS   2/76
CPI  H  1.9-2 GEV WAS FOUND.  SECOND LONG LIVED LIMIT FOR M=1-1.9, 2-5 GEV.   2/76
CPI  A  BLANAR 77 IS FNAL EXPT.  LIMIT IS FOR CS*BR TO MUONS.  ASSUMES        4/77*
CPI  A  DIFFRACTIVE CHARMED 2GEV MESON PAIR PRODUCTION.  OTHER LIMITS FOR     4/77*
CPI  A  PI AND P BEAMS GIVEN IN TABLE 1.                                      4/77*

CP      CHARMED HADRON PRODUCTION CROSS SECTION (P NUCLEON)   (CM**2)
CP   A   0  1. E-33 OR LESS              AUBERT     75 SPEC    PI+ K-           2/76
CP   A   0  4. E-33 OR LESS              AUBERT     75 SPEC    K+ PI-           2/76
CP   A   0  1. E-33 OR LESS              AUBERT     75 SPEC    K+ K-            2/76
CP   A   0  8. E-33 OR LESS              AUBERT     75 SPEC    PI+ PI-          2/76
CP   A   0  7. E-33 OR LESS              AUBERT     75 SPEC    P K-             2/76
CP   A   0  2. E-33 OR LESS              AUBERT     75 SPEC    K+ PBAR          2/76
CP   A   0  4. E-32 OR LESS              AUBERT     75 SPEC    P PI-            2/76
CP   A   0  2. E-33 OR LESS              AUBERT     75 SPEC    PI+ PBAR         2/76
CP   H   0  5. TO 20. E-30    OR LESS    AAHLIN     76 HBC     BARYON,M LT 2GEV 2/77*
CP   H   0 15. TO 100.E-30    OR LESS    AAHLIN     76 HBC     BARYON,M 2-3 GEV 2/77*
CP   H   0 10. TO 35. E-30    OR LESS    AAHLIN     76 HBC     MESON, M 1-2 GEV 2/77*
CP   G 0-2 SEE COMMENT G BELOW           BINKLEY    76 SPEC                     1/77*
CP   B   0  2. E-30 OR LESS              BINTINGER 76 SPEC     M=2 GEV/C**2     1/77*
CP   B   0  5. E-32 OR LESS              BINTINGER 76 SPEC     M=4 GEV/C**2     1/77*
CP   A  AUBERT 75 IS A BNL 30 GEV EXPT.  LOOKS FOR P BE --> JPRIME ANYTHING  2/76
CP   A  WHERE JPRIME DECAYED VIA THE CHANNEL SHOWN.  ABOVE VALUES ARE        2/76
CP   A  FOR M=2.25GEV AND ASSUME A WIDTH SMALL COMPARED TO THE RESOLUTION.   2/76
CP   A  UPPER LIMITS ARE ALSO GIVEN FOR THE ABOVE CHANNELS AND P PBAR FOR    2/76
CP   A  M=3.1 AND 3.7 GEV.  THOSE LIMITS RANGE FROM 7E-36 TO 4E-33.          2/76
CP   A  MA 77 SAYS AUBERT 75 LIMITS SHOULD BE AN ORDER OF MAG. LARGER.       2/77*
```

CHARM SEARCHES, CHARMONIUM STATES

Data Card Listings

```
CP   H  AAHLIN 76 IS A 19 GEV/C P-P EXPT AT CERN. VALUES GIVEN ARE CL=.975.  2/77*
CP   H  SEE TABLE 28, PG 479 FOR INDIVIDUAL LAMBDA (OR KS) +PIONS CHANNELS.  2/77*
CP   G  BINKLEY 76 MEASURES BR(C TO MU + OTHERS)*R WHERE R IS THE RATIO OF   1/77*
CP   G  THE CROSS-SEC FOR PRODUCING THE J/PSI TOGETHER WITH A C-CBAR PAIR    1/77*
CP   G  TO THE TOTAL CROSS-SEC FOR PRODUCING THE J/PSI AT THIS ENERGY. THE   1/77*
CP   G  EXPT WAS A 300 GEV/C FNAL RUN, AND SAW 2 TRI-MUON EVENTS. THIS GAVE  1/77*
CP   G  A .90 CL UPPER LIMIT OF .003 FOR THE MEASURED QUANTITY DESCRIBED     1/77*
CP   G  ABOVE.                                                               1/77*
CP   B  BINTINGER 76 IS CROSS-SEC TIMES BR INTO K- PI+.  WE SHOW TWO VALUES  1/77*
CP   B  FROM THEIR FIG.4 WHICH COVERS MASS RANGE 1.7-4 GEV.  SIMILAR LIMITS  1/77*
CP   B  ARE GIVEN FOR K+ PI- AND PI+ PI- CHANNELS.  LIMITS ARE PROPORTIONAL  1/77*
CP   B  TO CS*BR FOR J/PSI INTO MU+ MU-, TAKEN=10NB FOR ABOVE VALUES.        1/77*

CN     CHARMED HADRON PRODUCTION CROSS SECTION (N NUCLEON)  (CM**2)
CN   B   0  1.9E-31 OR LESS             BLESER    75 SPEC K+PI-, M=1.8 GEV   2/77*
CN   B   0  1.0E-31 OR LESS             BLESER    75 SPEC K+PI-, M=2.5 GEV   2/77*
CN   B   0  1.0E-31 OR LESS             BLESER    75 SPEC K- P , M=2.5 GEV   2/77*
CN   W   0  2.5E-29 OR LESS  CL=.975    WARD      75 HBC     KS PI+ PI-      1/77*
CN   A   0  6. E-32 OR LESS             ABOLINS   76 SPEC    PI+ PI-         1/77*
CN   A   0  7. E-32 OR LESS             ABOLINS   76 SPEC    PBAR P          1/77*
CN   A   0  4. E-32 OR LESS             ABOLINS   76 SPEC    K- PI+          1/77*
CN   A   0  6. E-32 OR LESS             ABOLINS   76 SPEC    K- P            1/77*
CN   B  BLESER 75 USES NEUTRONS UP TO 300 GEV/C, BE TARGET. EXAMINES MASS    2/77*
CN   B  RANGE UP TO 3.5 FOR KPI, UP TO 4.0 FOR KP. VALUES ARE CROSS-SEC/NUC  2/77*
CN   W  WARD 75 IS N-P EXPT WITH MOM UP TO 24 GEV/C. THIS VALUE IS FOR MASS  1/77*
CN   W  RANGE 1.5-2.5 GEV.  SEE TABLE 1 PG 31 FOR UPPER LIMITS ON C++,C+,    1/77*
CN   W  CO,D+,DO,D- DECAYS INTO VARIOUS FINALSTATES IN MASS RANGE 1.5-5GEV.  1/77*
CN   W  UPPER LIMIT FOR SEEING DECAY OF CHGD CHARMED PARTICLE INTO VO FOR    1/77*
CN   W  TAU GT 10**-11 SEC GIVEN AS 1.5*EXP(T) FOR VO =LAMBDA OR SIGMA, AND  1/77*
CN   W  3.0*EXP(T) FOR VO=KO. HERE, T=10*-11/TAU, CS GIVEN IN MICROBARNS.    1/77*
CN   A  ABOLINS 76 IS FNAL 240 GEV/C NEUTRON-BE EXPT. TYPICAL VALUES ABOVE   1/77*
CN   A  ARE FOR M=3.0 GEV. SEE FIG 4 FOR MASS RANGE 2.0-4.0 GEV. OBSERVES    1/77*
CN   A  POSSIBLE K- PI+ ENHANCEMENT AT 2.29+-.03 GEV                         1/77*

CAP    CHARMED HADRON PRODUCTION CROSS SECTION (PBAR NUCLEON)  (CM**2)
CAP  C   0  5. E-29 OR LESS  CL=.95   CARLSSON  75 HBC     PBAR P ANYTHING   2/77*
CAP  C   0  3. E-29 OR LESS  CL=.95   CARLSSON  75 HBC     PBAR P PI+ PI-    2/77*
CAP  E   0  .8 TO 4.4 E-30   OR LESS  CESTER    76 SPEC    12.4 TO 15 GEV/C  2/77*
CAP  C  CARLSSON 75 IS A 9GEV PBAR P CERN EXPT.  LIMITS ARE FOR P PBAR PEAK  2/77*
CAP  C  IN CHANNELS INDICATED. K KBAR CHANNELS CHECKED BUT NO LIMITS GIVEN.  2/77*
CAP  E  CESTER 76 LOOKS AT MASS RANGE 1.8 TO 2.5 GEV. SEE TABLE 1 FOR        2/77*
CAP  E  INDIVIDUAL CHANNELS. VALUES GIVEN ARE CROSS-SEC/NUCLEON ON CARBON.   2/77*

Y      CHARMED HADRON EVIDENCE IN NEUTRINO NUCLEON --> 2 LEPTONS ANYTHING
Y    B  14MU+MU-  OMU-MU-  OMU+MU+     BENVENU1  75 SPEC    PREDOM. NEU BEAM 2/76
Y    B  51MU+MU-  7MU-MU-  3MU+MU+     BENVENU3  75 SPEC    6/7 NEU BEAM     2/76
Y    B   5MU+MU-  OMU-MU-  2MU+MU+     BENVENU5  75 SPEC    9/10ANTINEU BEAM 2/76
Y        4MU+MU-  4 OTHER MU PAIRS     BARISH    76 SPEC    NEU BEAM         7/76*
Y    A   1 EVENT  MU-E+                BARISH    77 DBC     NEU BEAM         3/77*
Y    B  BENVENUTI 75 ARE FNAL NEUTRINO NUCLEON EXPERIMENTS WHICH LOOKED FOR  2/76
Y    B  TWO OR MORE MUONS IN THE FINAL STATE.  NO TRIMUON EVENTS WERE SEEN.  2/76
Y    B  AUTHORS STATE THAT THESE DIMUON EVENTS REQUIRE THE EXISTENCE OF ONE  2/76
Y    B  OR MORE NEW PARTICLES WITH M=2-4GEV AND TAU=10**-10SEC. OR LESS.     2/76
Y    B  BENVENUTI4 75 SHOW THAT THE OBSERVED PROPERTIES OF THESE EVENTS      2/76
Y    B  DO NOT AGREE WITH HYPOTHESES OF HEAVY LEPTON OR INTERMEDIATE VECTOR  2/76
Y    B  BOSON.  THEY SUGGEST A HADRON (Y) WITH A NEW QUANTUM NUMBER.         2/76
Y    A  BARISH 77 EVENT COULD BE NEU P TO MU+ B++. SEE CHARMED BARYON NOTE   3/77*
Y    A  AND LAMBDA/C+ SECTION ABOVE.                                         3/77*

VO     CHARMED HADRON EVIDENCE IN NEUTRINO NUCLEON --> MU- E+ VO ANYTHING
VO      WHERE THE VO IS A KOS OR A LAMBDA
VO   B   1 EVENT                       DEDEN     75 HLBC                     2/76
VO   B   1 EVENT                       BLIETSCHA 76 HLBC                     2/76
VO   V   4 EVENTS                      VONKROGH  76 HLBC                     2/76
VO   E   0 EVENTS                      BERGE     77 HLBC   ANTINEU BEAM      3/77*
VO   B  THE DEDEN 75 AND BLIETSCHAU 76 EVENTS ARE FROM CERN                  2/76
VO   B  GARGAMELLE NEUTRINO EXPOSURES.  THE MASSES OF THE E+ VO SYSTEM FOR   2/76
VO   B  THE TWO EVENTS ARE 1.24, 1.91 GEV FOR LAMBDA OR 0.65, 1.57 FOR KO.   2/76
VO   V  THE VON KROGH 76 EVENTS ARE FROM AN FNAL 15 FT NEON BUBBLE CHAMBER   2/76
VO   V  EXPOSURE.  ALL FOUR E+ EVENTS FOUND HAVE ASSOCIATED KOS.             2/76
VO   E  BERGE 77 USED FNAL 15 FT CHAMBER FILLED WITH H-NEON. SAW TWO         3/77*
VO   E  POSSIBLE BUT UNLIKELY MU E EVENTS, NEITHER WITH ASSOCIATED VO.       3/77*

R1     CHARMED HADRON (Y) BRANCHING RATIO INTO (MU NEU ANYTHING)/HADRONS
R1   B   8    A FEW PERCENT            BENVENU2  75 SPEC    FNAL NEUTRINO NU 2/76
R1   B  BENVENUTI2 75 LOOKS AT ANTINEUTRINO NUCLEON --> MUON HADRONS.  SEES  2/76
R1   B  EXCESS EVENTS ABOVE INCIDENT ENERGY 30 GEV.  COMPARES BENVENUTI1 75  2/76
R1   B  DIMUON EVENTS WITH EXCESS EVENTS TO GET BRANCHING RATIO.             2/76

R2     CHARMED HADRON (ASSOC. VO) BRANCHING RATIO INTO SEMILEPTONICS/ALL
R2   B   2    0.1   OR MORE            BLIETSCHA 76 HLBC    M=2.5-4 GEV      2/76
R2   B  THIS BR.RATIO AND MASS ARE REQD. BY OBSERVED RATE AND CHARM SCHEME.  2/76

CC     CHARMED HADRON EVIDENCE IN COSMIC RAYS
CC   N   1 EVENT                       NIU       71 EMUL                     9/76*
CC   N  NIU 71 DETECTS CHGD PARTICLE DECAYING INTO HADRON+PIO. MASS=1.78GEV  9/76*
CC   N  AND TAU=2.2 E-14 IF SECONDARY IS PION. MASS=2.95 GEV AND TAU=3.6     9/76*
CC   N  E-14 IF IT IS PROTON. POSSIBLE EVIDENCE OF PAIR PRODUCTION.          9/76*
CC   T   8 EVENTS                      TASAKA    73 EMUL                     9/76*
CC   T  SAME TYPE AS NIU EVENT. TAU BETW 1.5 AND 175 E-13.                   9/76*
CC   S   1 EVENT                       SUGIMOTO  75 EMUL                     1/77*
CC   S  SAME TYPE AS NIU EVENT. TWO SUCH PARTICLES PRODUCED TOGETHER.        1/77*
CC   S  TAU1=6.E-13, DECAYS TO CHARGED PRONG + ETA. TAU2=4.E-12, DECAYS TO   1/77*
CC   S  CHARGED PRONG + PIO. MASSES OF BOTH PARTICLES ARE ABOUT 2.0 GEV IF   1/77*
CC   S  DECAY PRONG IS PROTON, 1.7 IF DECAY PRONG IS KAON, AND 1.55 IF       1/77*
CC   S  DECAY PRONG IS PI. COMBINED MASS OT THE TWO NEW PARTICLES = 4.1 GEV  1/77*
CC   S  OR 3.8 GEV ASSUMING THE DECAY PRONGS TO BE KAONS OR PIONS            1/77*
CC   S  RESPECTIVELY. CONSISTENT WITH LAMBDA/C+ LAMBDABAR/C-.SEE GAISSER 76  1/77*

EM     CHARMED HADRON CROSS SEC. IN MISC. EMUL. EXPTS, WHERE LIFETIME SEEN   3/77*
EM   J   1 EVENT                       JAIN      75 EMUL TAU APROX. 10E-13   2/77*
EM   K   2 EVENTS                      KOMAR     75 EMUL    TAU .LT. E-15    4/77*
EM   B   1 EVENT                       BURHOP    76 EMUL    TAU APPROX E-13  3/77*
EM   C   0  1.5E-30 OR LESS  CL=.90   COREMANS  76 EMUL    TAU E-12 TO E-14 3/77*
EM   J  JAIN 75 IS A FNAL 300 GEV PROTON EXPT. EVENT SHOWS DECAY OF NEUTRAL  2/77*
EM   J  INTO HADRON-E-NEU, TAKING PLACE .019 CM FROM THE PROD VERTEX. MAY    2/77*
EM   J  BE LEPTONIC DECAY OF CHARMED PARTICLE.                               2/77*
EM   K  KOMAR 75 IS FNAL 200 GEV/C PROTON EXPT.  SEE 2 EVENTS WITH SINGLE    4/77*
EM   K  ELECTRON EMITTED FROM NEAR INTERACTION.                              4/77*
EM   B  BURHOP 76 EXPT DONE AT FERMILAB HIGH ENERGY NEUTRINO BEAM. USED A    3/77*
EM   B  COMBINATION OF EMULSION AND SPARK CHAMBERS. THEY SEE A PARTICLE      3/77*
EM   B  WITH TAU=ABOUT 6 E-13 SEC DECAYING TO VO + 3 CHGD TRACKS. DECAYING   3/77*
EM   B  PARTICLE NOT CONSISTENT WITH CHARMED D OR LAMBDA/C+.                 3/77*
EM   C  COREMANS 76 USED 300 GEV/C PROTONS, AND LOOKED FOR ABOVE LIFETIMES.  3/77*

****** ********* ********* ********* ********* ********* ********* ********
```


```
                          REFERENCES FOR CHARMED HADRON SEARCHES

NIU       71 PTP 46 1644     +MIKUMO,MAEDA                   (TOKY+YOKOHAMA)
TASAKA    73 PTP 50 1879     +YAMAMOTO                               (KONAN)

AUBERT    75 PRL 35 416      +BECKER,BIGGS,BURGER,CHEN+            (MIT+BNL)
    ALSO  77 PRL 38 172      Z. MING MA, B. Y. OH                      (MSU)
BALTAY    75 PRL 34 1118     +CAUTIS,COHEN,CSORNA,KALELKAR + (COLU+BING)
BENVENU1  75 PRL 34 419      BENVENUTI,CLINE,FORD+ (HARV,PENN,WISC,FNAL)
BENVENU2  75 PRL 34 597      BENVENUTI,CLINE,FORD+ (HARV,PENN,WISC,FNAL)
    ALSO  74 PRL 33 984      AUBERT,BENVENUTI+     (HARV,PENN,WISC,FNAL)
BENVENU3  75 PRL 35 1199     BENVENUTI,CLINE,FORD+ (HARV,PENN,WISC,FNAL)
BENVENU4  75 PRL 35 1203     BENVENUTI,CLINE,FORD+ (HARV,PENN,WISC,FNAL)
BENVENU5  75 PRL 35 1249     BENVENUTI,CLINE,FORD+ (HARV,PENN,WISC,FNAL)
BLESER    75 PRL 35 76       +GOBBI,KENAH,KEREN+   (FNAL+NWES+ROCH+SLAC)
BOYARSKI  75 PRL 35 196      +BREIDENBACH,BULOS,DAKIN,FELDMAN+(SLAC+LBL)
CARLSSON  75 NP B99 451      +EKSPONG,HOLMGREN,NILSSON+       (STOH+LIVP)
DEDEN     75 PL 58B 361            (AACH+BRUX+CERN+EPOL+MILA+ORSA+LOUC)
JAIN      75 PRL 34 1238     P. L. JAIN, B. GIRARD                  (BUFF)
KOMAR     75 JETPL 21 239    +ORLOVA,TRETYAKOVA,CHERNYAYSKII        (LEBD)
PERL      75 PRL 35 1489     +ABRAMS,BOYARSKI,BREIDENBACH +         (SLAC)
SUGIMOTO  75 PTP 53 1540     +SATO,SAITO                      (WASEDA+TOKY)
WARD      75 NP B101 29      +ANSORGE,CARTER,MOUNT,NEALE+           (CAVE)

AAHLIN    76 NP B107 476     +ALPGARD,ANDERSEN,BERGVATN+(OSLO+STOH+HELS)
ABOLINS   76 PRL 37 417      +CARDIMONA,MATTHEWS,SIDWELL+ (MSU+OSU+CARL)
BARISH    76 PRL 36 939      +BARTLETT,BODEK,BROWN,BUCHHOLZ + (CIT+FNAL)
BINKLEY   76 PRL 37 578      +GAINES,PEOPLES,KNAPP+ (FNAL+COLU+HAWA+ILL)
BINTINGE  76 PRL 37 732      BINTINGER,LUNDY,AKERLOF+    (FNAL+MICH+PURD)
BLIETSCH  76 PL 60B 207            (AACH+BRUX+CERN+EPOL+MILA+ORSA+LOUC)
BRAUNSCH  76 PL 63B 471      BRAUNSCHWEIG +    (AACH+DESY+HAMB+MPIM+TOKY)
BUNNELL   76 PRL 37 85       +CHENG,DELPAPA,DORFAN,DOUNGVAN+ (UCSC+SLAC)
BURMESTE  76 PL 64B 369      BURMESTER,CRIEGEE+     (DESY+HAMB+SIEG+WUPG)
BURHOP    76 PL 65B 299       (LOUC+FNAL+BELG+DUUC+CERN+LOIC+ROMA+STRB+)
CESTER    76 PRL 37 1178     +FITCH,KADEL,WEBB,WHITTAKER +      (PRIN+BNL)
COOK      76 PL 64B 221      +CSORNA,HOLMGREN,JONCKHEERE+(WASH+LALO+UCD)
COREMANS  76 PL 65B 480      +SACTON+     (BELG+DUUC+LOUC+ROMA+STRB+WARS)
GHIDINI   76 NP B111 189     +NAVACH,DOWELL,KENYON+         (OMEGA GROUPS)
GOLDHABE  76 PRL 37 255      GOLDHABER,PIERRE,ABRAMS,ALAM+      (LBL+SLAC)
HAGOPIAN  76 PRL 36 296      +WILKINS,WIND,HAGOPIAN,ALBRIGHT+ (FSU+BRAN)
KNAPP     76 PRL 37 882      +LEE,LEUNG,SMITH +       (COLU+HAWA+ILL+FNAL)
PERUZZI   76 PRL 37 569      +PICCOLO,FELDMAN,NGUYEN,WISS +     (SLAC+LBL)
QUINN     76 PR D14 2857     D. J. QUINN, R. H. MILBURN            (TUFTS)
VONKROGH  76 PRL 36 710      +FRY,CAMERINI,CLINE+    (WISC+LBL+CERN+HAWA)

BARISH    77 PR D15 1        +DERRICK,DOMBECK,MUSGRAVE +        (ANL+PURD)
BERGE     77 PRL 38 266      +DIBIANCA,EMANS +        (FNAL+SERP+ITEP+MICH)
BLANAR    77 PRL 38 192      +BOYER,FAISSLER,GARELICK,GETTNER +     (NEAS)
FELDMAN   77 PRL 38 117      +BULOS,LUKE,ABRAMS,ALAM,BOYARSKI+(SLAC+LBL)

                             REVIEWS REFERRED TO IN DATA CARDS

GAISSER   76 PR D14 3153     T.K.GAISSER,F.HALZEN             (BARTOL+WISC)

****** ********* ********* ********* ********* ********* ********* ********
****** ********* ********* ********* ********* ********* ********* ********
```


CHARMONIUM STATES

We group into this section those meson states commonly believed to consist of charmed-quark-charmed-antiquark pairs. Since the discovery of the J/ψ(3100) (AUBERT 74, AUGUSTIN 74[1]) this family has increased to at least 9, of which we tabulate 6 as well-established particles. The current situation is summarized in the accompanying level diagram.

In the 4-4.5 GeV region there is resonance-like structure in at least two places in the ratio R of the total hadronic cross section to the μ-pair production cross section (see accompanying figure). According to FELDMAN 76[1], "[The 4 GeV] region is quite complicated and is not well understood. There are probably several resonances and many thresholds for charmed meson production conspiring to create the complex structure seen in [the figure]. There appears to be an isolated resonance at 4414 MeV/c^2."

Data Card Listings

CHARMONIUM STATES

Excellent reviews on charmonium are given by, for example, FELDMAN 76, WIIK 76, WIIK 77[1], which may be consulted for further details.

The method of extracting narrow resonance widths from e^+e^- colliding beam formation experiments is, by now, well known. For a summary of this method, see p. 140 of our previous edition.[2]

References

1. See reference section of the J/ψ(3100).
2. Particle Data Group, Rev. Mod. Phys. 48, No. 2, Part II (1976).

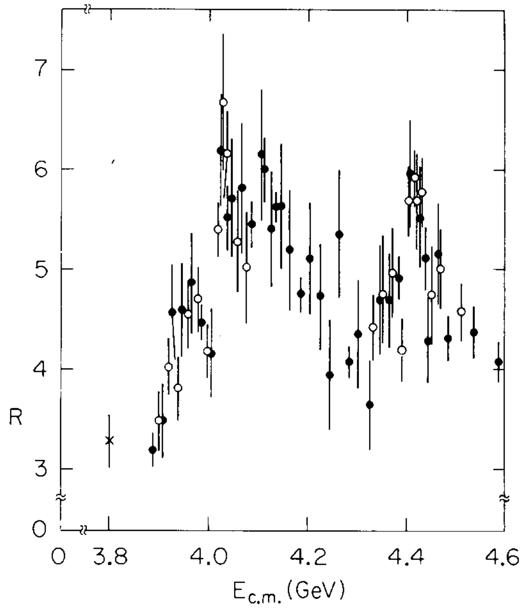

The ratio of cross sections $\frac{\sigma(e^+e^- \to \text{hadrons})}{\sigma(e^+e^- \to \mu^+\mu^-)}$ in the 4-4.5 GeV region, taken from SIEGRIST 76. There is an overall normalization uncertainty of 10%.

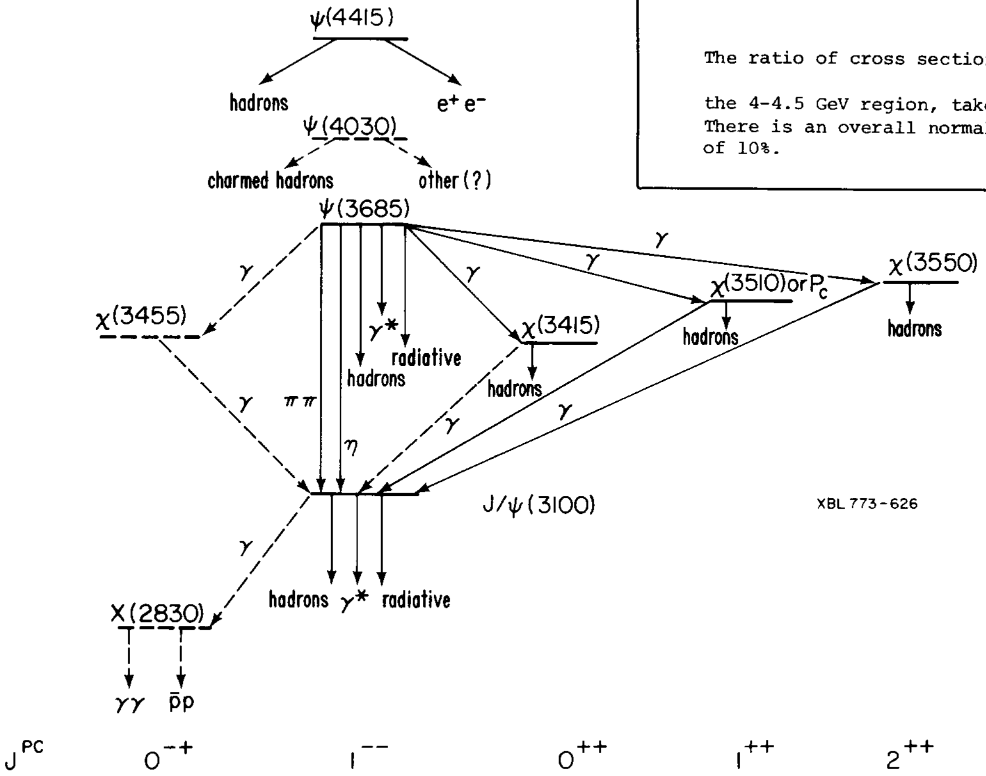

Summary of observed charmonium states and transitions (adapted from FELDMAN 76[1]). Uncertain states and transitions are indicated by dashed lines. J^{PC} quantum number assignments are in some cases tentative, but all are at least consistent with experiment; see individual particle listings for discussion. The notation γ* refers to decay processes involving intermediate virtual photons, including decays to e^+e^- and $\mu^+\mu^-$.

 Data Card Listings

X(2830)

```
               54  X(2830,JPG=    ) I=

                   CPSERVEC IN THE SEQUENTIAL RACIATIVE DECAY OF THE
          J/PSI(3100) INTC X(2830) GAMMA, X(2830) INTC GAMMA GAMMA.
          THIS SUGGESTS QUANTUM NUMBER ASSIGNMENTS C=+, IG=0+ OR 1-.
          NEEDS CONFIRMATION. CMITTED FROM TABLE.

------ --------- --------- --------- --------- --------- --------- --------

               54  X(2830) MASS (MEV)

M    B    8(2700.0)                  BARTEL     76 CNTR    E+E-,3 GAMMA      1/76
M         15(2830.0)    (30.0)       BRAUNSCHW  77 DASP    E+E-,3 GAMMA      1/77*
M    B    SIGNAL IS ONLY 2 STD EFFECT IN BARTEL 76.                          3/77*

------ --------- --------- --------- --------- --------- --------- --------

               54  X(2830) PARTIAL DECAY MODES

                                                          DECAY MASSES
P1      X(2830) INTO GAMMA GAMMA
P2      X(2830) INTO PBAR P

------ --------- --------- --------- --------- --------- --------- --------
               54  X(2830) BRANCHING RATIOS

R       SEE BRANCHING RATIOS R70,R76,R77,R79 OF J/PSI(3100)
R       SEE BRANCHING RATIOS R54 OF PSI(3685)

R1      X(2830) INTO (PBAR P)/TOTAL                        (P2)
R1        2 POSSIBLY SEEN                WIIK      75 CASP        E+E-        1/76

****** ********* ********* ********* ********* ********* ********* ********

                         REFERENCES FOR X(2830)

WIIK       75 STANFORD SYMP.69   B.H.WIIK                           (DFSY)

BARTEL     76 TBILISI CONF.N56   +DUINKER,OLSSON,HEINTZE,+       (DESY+HEID)
FELDMAN    76  SLAC-PUB-1851     G.J.FELDMAN                     (SLAC+LBL)
WIIK       76 TBILISI CONF.N 75  B.H.WIIK RAPPORTEUR                 (DESY)

BRAUNSCH   77  DESY 77/02        BRAUNSCHWEIG,+   (AACH+DESY+HAMB+MPIM+TOKY)
WIIK       77  DESY 77/01        +WOLF                               (DESY)

****** ********* ********* ********* ********* ********* ********* ********
****** ********* ********* ********* ********* ********* ********* ********
```

J/ψ(3100)

```
               70  J/PSI(3100,JPG=1--) I=0
------ --------- --------- --------- --------- --------- --------- --------

               70  J/PSI(3100) MASS (MEV)

M          (3100.)                   AUBERT     74 SPEC    28. PP(E+E-)      2/75
M   L      (3105.)      (3.)         AUGUSTIN   74 SMAG        E+E-          2/75
M   U       3095.        4.          BOYARSKI   75 SMAG        E+E-          3/75
M   S       3089.5      31.          CRIEGEE1   75 PLUT        E+E-          2/75
M           3098.        6.          PREPOST    75 SPEC    13.-21.GAMMA D    1/76
M           3103.        6.          BEMPORAD   75 FRAB        E+E-          1/76
M           3096.0      30.0         SNYDER     76 SPEC    400 P BE,E+E-     1/77*
M
M   L   BOYARSKI 75 IS A REEVALUATION OF AUGUSTIN 74 BASED
M   L   ON A RECALIBRATION OF THE SPEAR BEAM ENERGY.
M
M   O   MASS, WIDTH, PARTIAL WIDTHS, AND BRANCHING RATIOS ALL OBTAINED      3/75
M   O   FROM ONE OVERALL FIT TO DATA OF THIS EXPERIMENT.                    3/75
M
M   S   ERROR OF ABOUT 1 PER CENT FROM THE UNCERTAINTY IN CALIBRATION OF    2/75
M   S   THE BEAM ENERGY.                                                    2/75
M          . . . . . . . . . . .
M    AVG    3097.5      2.9      AVERAGE (ERROR INCLUDES SCALE FACTOR OF 1.0)
M    STUDENT3097.5      3.2      AVERAGE USING STUDENT10(H/1.11) -- SEE 1976 TEXT

------ --------- --------- --------- --------- --------- --------- --------

               70  J/PSI(3100) WIDTH (KEV)

W             69.       15.          BOYARSKI   75 SMAG        E+E-          3/75
W             68.       26.          BALDINI1   75 FRAG        E+E-          1/76
W             60.       25.          ESPOSITO   75 FRAM        E+E-          1/76
W          . . . . . . . . . . .
W    AVG      66.9      11.5     AVERAGE (ERROR INCLUDES SCALE FACTOR OF 1.0)
W    STUDENT  66.9      12.4     AVERAGE USING STUDENT10(H/1.11) -- SEE 1976 TEXT

------ --------- --------- --------- --------- --------- --------- --------

               70  J/PSI(3100) PARTIAL DECAY MODES

                                                          DECAY MASSES
P1      J/PSI(3100) INTO E+ E-                            .5+  .5
P2      J/PSI(3100) INTO MU+ MU-                         105+ 105
P3      J/PSI(3100) INTO HADRONS
P4      J/PSI(3100) INTO VIRTUAL GAMMA INTO HADRONS

P       HADRONIC DECAYS
P       ---------------
P11     J/PSI(3100) INTO PI+ PI-
P12     J/PSI(3100) INTO PI+ PI- PI0
P13     J/PSI(3100) INTO 2(PI+ PI-)
P14     J/PSI(3100) INTC 2(PI+ PI-) PI0
P15     J/PSI(3100) INTO 3(PI+ PI-)
P16     J/PSI(3100) INTO 3(PI+ PI-) PI0
P17     J/PSI(3100) INTC 4(PI+ PI-)
P18     J/PSI(3100) INTC 4(PI+ PI-) PI0
P19     J/PSI(3100) INTO K KBAR
P20     J/PSI(3100) INTO K KBAR PI
P21     J/PSI(3100) INTO PI+ PI- K+ K-
P22     J/PSI(3100) INTO 2(PI+ PI-) K+ K-
P23     J/PSI(3100) INTO PI+ PI- PI0 K+ K-
P24     J/PSI(3100) INTO RHO PI
P25     J/PSI(3100) INTO RHO PI PI PI
P26     J/PSI(3100) INTO OMEGA PI PI
P27     J/PSI(3100) INTO OMEGA 4PI
P28     J/PSI(3100) INTO OMEGA K KBAR
P29     J/PSI(3100) INTO OMEGA F
P30     J/PSI(3100) INTO OMEGA F PRIME
P31     J/PSI(3100) INTO PHI PI PI
P32     J/PSI(3100) INTO PHI 2(PI+ PI-)
P33     J/PSI(3100) INTO PHI K KBAR
P34     J/PSI(3100) INTO PHI ETA
P35     J/PSI(3100) INTO PHI ETA PRIME
P36     J/PSI(3100) INTO PHI F
P37     J/PSI(3100) INTO PHI F PRIME
P38     J/PSI(3100) INTO A2 PI
P39     J/PSI(3100) INTO A2 RHO
P40     J/PSI(3100) INTO K K*(892)
P41     J/PSI(3100) INTO K K*(1420)
P42     J/PSI(3100) INTO K*(892) K*(892)
P43     J/PSI(3100) INTO K*(1420) K*(1420)
P44     J/PSI(3100) INTO K*(892) K*(1420)
P45     J/PSI(3100) INTO P PBAR
P46     J/PSI(3100) INTO P PBAR PI
P47     J/PSI(3100) INTO P NBAR PI
P48     J/PSI(3100) INTO P PBAR PI+ PI-
P49     J/PSI(3100) INTO P PBAR PI+ PI- PI0
P50     J/PSI(3100) INTO P PBAR ETA
P51     J/PSI(3100) INTO P PBAR OMEGA
P52     J/PSI(3100) INTO LAMBDA ANTILAMBDA
P53     J/PSI(3100) INTO LAMBDA ANTISIGMA
P54     J/PSI(3100) INTO XI ANTIXI

P       RADIATIVE DECAYS
P       ----------------
P70     J/PSI(3100) INTO GAMMA GAMMA
P71     J/PSI(3100) INTO 3 GAMMA
P72     J/PSI(3100) INTO PI0 GAMMA
P73     J/PSI(3100) INTO ETA GAMMA
P74     J/PSI(3100) INTO ETA PRIME GAMMA
P75     J/PSI(3100) INTO X(2830) GAMMA

------ --------- --------- --------- --------- --------- --------- --------

               70  J/PSI(3100) PARTIAL WIDTHS (KEV)

W1      J/PSI(3100) INTO E+ E-                      (G1)                     2/75
W1             4.8       0.6         BOYARSKI   75 SMAG        E+E-          3/75
W1  B         (4.6)     (.8)         BALDINI1   75 FRAG        E+E-          1/76
W1             4.6       1.0         ESPOSITO   75 FRAM        E+E-          1/76
W1  B  ASSUMING EQUAL PARTIAL WIDTHS FOR (E+E-) AND (MU+MU-)
W1          . . . . . . . . . . .
W1  AVG        4.75      0.51    AVERAGE (ERROR INCLUDES SCALE FACTOR OF 1.0)
W1  STUDENT    4.75      0.55    AVERAGE USING STUDENT10(H/1.11) -- SEE 1976 TEXT

W2      J/PSI(3100) INTO MU+ MU-                    (G2)                     2/75
W2             4.8       0.6         BOYARSKI   75 SMAG        E+E-          3/75
W2             5.0       1.0         ESPOSITO   75 FRAM        E+E-          1/76
W2          . . . . . . . . . . .
W2  AVG        4.85      0.51    AVERAGE (ERROR INCLUDES SCALE FACTOR OF 1.0)
W2  STUDENT    4.85      0.55    AVERAGE USING STUDENT10(H/1.11) -- SEE 1976 TEXT

W3      J/PSI(3100) INTO HADRONS                    (G3)                     2/75
W3            59.       14.          BOYARSKI   75 SMAG        E+E-          3/75
W3            59.       24.          BALDINI1   75 FRAG        E+E-          1/76
W3            50.       25.          ESPOSITO   75 FRAM        E+E-          1/76
W3          . . . . . . . . . . .
W3  AVG       57.3      10.9     AVERAGE (ERROR INCLUDES SCALE FACTOR OF 1.0)
W3  STUDENT   57.3      11.7     AVERAGE USING STUDENT10(H/1.11) -- SEE 1976 TEXT

W4      J/PSI(3100) INTO GAMMA INTO HADRONS
W4 C          12.        2.          BOYARSKI   75 SMAG        E+E-          1/76
W4 C    INCLUDED IN W3

------ --------- --------- --------- --------- --------- --------- --------

               70  J/PSI(3100) BRANCHING RATIOS

        FOR THE BRANCHING RATIOS R1 - R4, SEE ALSO THE PARTIAL
        WIDTHS ABOVE, AND (PARTIAL WIDTHS)*R1 BELOW.

R1      J/PSI(3100) INTO (E+ E-)/TOTAL              (P1)                     3/75
R1           0.069     0.009         BOYARSKI   75 SMAG        E+E-          3/75

R2      J/PSI(3100) INTO (MU+ MU-)/TOTAL            (P2)                     3/75
R2           0.069     0.009         BOYARSKI   75 SMAG        E+E-          3/75

R3      J/PSI(3100) INTO (HADRONS)/TOTAL            (P3)                     3/75
R3           0.86      0.02          BOYARSKI   75 SMAG        E+E-          3/75

R4      J/PSI(3100) INTO (E+ E-)/(MU+ MU-)          (P1)/(P2)                2/75
R4           1.00      0.05          BOYARSKI   75 SMAG        E+E-          3/75
R4           0.93      0.10          FORD       75 SPEC        E+E-          2/75
R4            .91       .15          ESPOSITO   75 FRAM        E+E-          1/76
R4          . . . . . . . . . . .
R4  AVG      0.980     0.043     AVERAGE (ERROR INCLUDES SCALE FACTOR OF 1.0)
R4  STUDENT  0.980     0.047     AVERAGE USING STUDENT10(H/1.11) -- SEE 1976 TEXT

R5      J/PSI(3100) INTO (GAMMA INTO HADRONS)/TOTAL
R5 C          .17       .02          BOYARSKI   75 SMAG        E+E-          1/76
R5 C    INCLUDED IN R3

R       HADRONIC DECAYS
R       ---------------

R8      J/PSI(3100) INTO (PI+ PI-)/TOTAL         (UNITS 10**-4)
R8        2    1.0       0.7         BRAUNSCHW  76 DASP        E+E-          1/77*
R8        1    1.6       1.6         VANNUCCI   77 SMAG        E+E-          1/77*
R8          . . . . . . . . . . .
R8  AVG        1.10      0.64    AVERAGE (ERROR INCLUDES SCALE FACTOR OF 1.0)
R8  STUDENT    1.10      0.69    AVERAGE USING STUDENT10(H/1.11) -- SEE 1976 TEXT

R9      J/PSI(3100) INTO (2(PI+ PI-))/TOTAL
R9       76     .004      .001          JEAN-MARI 76 SMAG        E+E-          1/76

R10     J/PSI(3100) INTO (2(PI+ PI-) PI0)/TOTAL
R10     675     .04       .01           JEAN-MARI 76 SMAG        E+E-          1/76
R10            (0.044)   (0.005)        BURMESTER 77 PLUT        E+E-          1/77*

R11     J/PSI(3100) INTO (3(PI+ PI-)/TOTAL
R11      32     .004      .002          JEAN-MARI 76 SMAG        E+E-          1/76

R12     J/PSI(3100) INTO (3(PI+ PI-) PI0)/TOTAL
R12     181     .029      .007          JEAN-MARI 76 SMAG        E+E-          1/76
```

Data Card Listings

J/ψ(3100)

```
R13     J/PSI(3100) INTO (4(PI+ PI-) PI0)/TOTAL
R13      13     .009     .003               JEAN-MARI 76 SMAG          E+E-           1/76

R14     J/PSI(3100) INTO (PI+ PI- K+ K-)/TOTAL
R14     205    0.0072   0.0023              VANNUCCI  77 SMAG          E+E-           1/77*

R15     J/PSI(3100) INTO (2(PI+ PI-) K+ K-)/TOTAL
R15      30    0.0031   0.0013              VANNUCCI  77 SMAG          E+E-           1/77*

R16     J/PSI(3100) INTO (RHO PI)/(PI+ PI- PI0)
R16            (.7)  OR MORE  CL=0.90  JEAN-MARI 76 SMAG          E+E-           1/76

R17     J/PSI(3100) INTO (RHO0 PI0)/(RHO+- PI-+)
R17            0.63     0.22                BARTEL 1  76 CNTR          E+E-           1/77*
R17             .59      .17                JEAN-MARI 76 SMAG          E+E-           1/76
R17          . . . . . . . . . .
R17 AVG        0.60     0.13    AVERAGE (ERROR INCLUDES SCALE FACTOR OF 1.0)
R17 STUDENT    0.60     0.14    AVERAGE USING STUDENT10(H/1.11) -- SEE 1976 TEXT

R18     J/PSI(3100) INTO (RHO PI)/TOTAL
R18     543    0.010    0.002               BARTEL 1  76 CNTR          E+E-           1/77*
R18      99    0.012    0.003               BRAUNSCHW 76 DASP          E+E-           1/77*
R18     153     .013     .003               JEAN-MARI 76 SMAG          E+E-           1/76
R18          . . . . . . . . . .
R18 AVG        0.0112   0.0015  AVERAGE (ERROR INCLUDES SCALE FACTOR OF 1.0)
R18 STUDENT    0.0112   0.0016  AVERAGE USING STUDENT10(H/1.11) -- SEE 1976 TEXT

R19     J/PSI(3100) INTO (OMEGA PI PI)/(2(PI+ PI-) PI0)
R19  J         (.2)                         JEAN-MARI 76 SMAG          E+E-           1/76

R20     J/PSI(3100) INTO (RHO PI PI PI)/(2 (PI+ PI-) PI0)
R20  J         (.3)                         JEAN-MARI 76 SMAG          E+E-           1/76
R20  J  FINAL STATE  2(PI+PI-)PI0

R21     J/PSI(3100) INTO (PHI PI+ PI-)/TOTAL
R21      23    0.0014   0.0006              VANNUCCI  77 SMAG          E+E-           1/77*

R22     J/PSI(3100) INTO (K0S K0L)/TOTAL  (UNITS 10**-4)
R22            (0.89) OR LESS  CL=0.90  VANNUCCI  77 SMAG          E+E-           1/77*

R23     J/PSI(3100) INTO (K+ K-)/TOTAL     (UNITS 10**-4)
R23       1    1.4      1.4                 BRAUNSCHW 76 DASP          E+E-           1/77*
R23       2    2.0      1.6                 VANNUCCI  77 SMAG          E+E-           1/77*
R23          . . . . . . . . . .
R23 AVG        1.7      1.1     AVERAGE (ERROR INCLUDES SCALE FACTOR OF 1.0)
R23 STUDENT    1.7      1.1     AVERAGE USING STUDENT10(H/1.11) -- SEE 1976 TEXT

R24     J/PSI(3100) INTO (K0 K*(892)0)/TOTAL
R24      45    0.0027   0.0006              VANNUCCI  77 SMAG          E+E-           1/77*

R25     J/PSI(3100) INTO (K+- K*(892)-+)/TOTAL
R25      39    0.0041   0.0012              BRAUNSCHW 76 DASP          E+E-           1/77*
R25      48    0.0032   0.0006              VANNUCCI  77 SMAG          E+E-           1/77*
R25          . . . . . . . . . .
R25 AVG        0.00338  0.00054 AVERAGE (ERROR INCLUDES SCALE FACTOR OF 1.0)
R25 STUDENT    0.00338  0.00059 AVERAGE USING STUDENT10(H/1.11) -- SEE 1976 TEXT

R26     J/PSI(3100) INTO (K0 K*(1420)0)/TOTAL
R26            (0.002) OR LESS  CL=0.90  VANNUCCI  77 SMAG          E+E-           1/77*

R27     J/PSI(3100) INTO (K+- K*(1420-+)/TOTAL
R27            (0.0033)OR LESS  CL=0.90  BRAUNSCHW 76 DASP          E+E-           1/77*
R27            (0.0015)OR LESS  CL=0.90  VANNUCCI  77 SMAG          E+E-           1/77*

R28     J/PSI(3100) INTO (K*(892)0 K*(892)0)/TOTAL
R28            (0.0005)OR LESS  CL=0.90  VANNUCCI  77 SMAG          E+E-           1/77*

R29     J/PSI(3100) INTO (K*(1420)0 K*(1420)0)/TOTAL
R29            (0.0029)OR LESS  CL=0.90  VANNUCCI  77 SMAG          E+E-           1/77*

R30     J/PSI(3100) INTO (K*(892)0 K*(1420)0)/TOTAL
R30      40    0.0067   0.0026              VANNUCCI  77 SMAG          E+E-           1/77*

R31     J/PSI(3100) INTO (PBAR P)/TOTAL    (UNITS 10**-3)
R31  A  70     2.3      0.3                 BRAUNSCHW 76 DASP          E+E-           1/77*
R31  A 300    (2.0)    (0.15)               GOLDHABER 76 SMAG          E+E-           1/77*
R31  A  ASSUMING ANGULAR DISTRIBUTION (1.+COS(THETA)**2)

R32     J/PSI(3100) INTO (PBAR P)/(MU+ MU-)
R32  A  20    (.051)   (.02)                CRIEGEE2  75 PLUT          E+E-           1/76
R32  A  ASSUMING ANGULAR DISTRIBUTION (1.+COS(THETA)**2)

R33     J/PSI(3100) INTO (LAMBDA ANTILAMBDA)/TOTAL
R33      19     .0016    .0008              ABRAMS    75 SMAG          E+E-           1/76

R34     J/PSI(3100) INTO (P PBAR PI0)/TOTAL
R34            (0.0010) (0.0002)            FELDMAN   76 SMAG          E+E-           1/77*

R35     J/PSI(3100) INTO (P PBAR PI+PI-)/TOTAL
R35            (0.0041) (0.0008)            FELDMAN   76 SMAG          E+E-           1/77*

R36     J/PSI(3100) INTO (P PBAR PI+ PI- PI0)/TOTAL
R36            (0.0011) (0.0004)            FELDMAN   76 SMAG          E+E-           1/77*

R37     J/PSI(3100) INTO (LAMBDA ANTISIGMA)/(LAMBDA ANTILAMBDA)
R37            (.22) OR LESS  CL=0.90  GOLDHABER 75 SMAG          E+E-           2/76

R38     J/PSI(3100) INTO (PI+- A2)/TOTAL
R38            (0.0043)OR LESS  CL=0.90  BRAUNSCHW 76 DASP          E+E-           1/77*

R39     J/PSI(3100) INTO (OMEGA PI PI)/TOTAL
R39            (0.007)  (0.002)             BURMESTER 77 PLUT          E+E-           1/77*
R39     348    0.0068   0.0019              VANNUCCI  77 SMAG          E+E-           1/77*

R40     J/PSI(3100) INTO 2(K+ K-)/TOTAL
R40            0.0007   0.0003              VANNUCCI  77 SMAG          E+E-           1/77*

R41     J/PSI(3100) INTO (OMEGA K+ K-)/TOTAL
R41      22    0.0008   0.0005              VANNUCCI  77 SMAG          E+E-           1/77*

R42     J/PSI(3100) INTO (PHI K+ K-)/TOTAL
R42      14    0.0009   0.0004              VANNUCCI  77 SMAG          E+E-           1/77*

R43     J/PSI(3100) INTO (PHI ETA)/TOTAL
R43       5    0.0010   0.0006              VANNUCCI  77 SMAG          E+E-           1/77*

R44     J/PSI(3100) INTO (PHI ETA PRIME)/TOTAL
R44            (0.0013)OR LESS  CL=0.90  VANNUCCI  77 SMAG          E+E-           1/77*

R45     J/PSI(3100) INTO (PHI F PRIME)/TOTAL
R45       6    0.0008   0.0005              VANNUCCI  77 SMAG          E+E-           1/77*

R46     J/PSI(3100) INTO (P NBAR PI-)/TOTAL
R46            (0.0038) (0.0008)            FELDMAN   76 SMAG          E+E-           1/77*

R47     J/PSI(3100) INTO (P PBAR ETA)/TOTAL
R47            (0.0019) (0.0004)            FELDMAN   76 SMAG          E+E-           1/77*

R48     J/PSI(3100) INTO (P PBAR OMEGA)/TOTAL
R48            (0.0005) (0.0001)            FELDMAN   76 SMAG          E+E-           1/77*

R49     J/PSI(3100) INTO (K0S K+- PI-+)/TOTAL
R49     126    0.0026   0.0007              VANNUCCI  77 SMAG          E+E-           1/77*

R50     J/PSI(3100) INTO (PHI F)/TOTAL     (UNITS 10**-4)
R50            (3.7)  OR LESS  CL=0.90  VANNUCCI  77 SMAG          E+E-           1/77*

R51     J/PSI(3100) INTO (PHI 2(PI+PI-))/TOTAL
R51            (0.0015)OR LESS  CL=0.90  VANNUCCI  77 SMAG          E+E-           1/77*

R52     J/PSI(3100) INTO (OMEGA F)/TOTAL
R52      81    0.0019   0.0008              VANNUCCI  77 SMAG          E+E-           1/77*

R53     J/PSI(3100) INTO (OMEGA F PRIME)/TOTAL  (UNITS 10**-4)
R53            (1.6)  OR LESS  CL=0.90  VANNUCCI  77 SMAG          E+E-           1/77*

R54     J/PSI(3100) INTO (PI+PI-PI0 K+K-)/TOTAL
R54     309    0.012    0.003               VANNUCCI  77 SMAG          E+E-           1/77*

R55     J/PSI(3100) INTO (RHO A2)/TOTAL
R55      36    0.0084   0.0045              VANNUCCI  77 SMAG          E+E-           1/77*

R56     J/PSI(3100) INTO (OMEGA 4PI)/TOTAL
R56     140    0.0085   0.0034              VANNUCCI  77 SMAG          E+E-           1/77*

R57     J/PSI(3100) INTO (XI- ANTIXI-)/TOTAL
R57            (0.0004)                     FELDMAN   76 SMAG          E+E-           1/77*

R58     J/PSI(3100) INTO (RHO+- PI-+)/(K*(892)+- K-+)
R58            (0.26)   (0.09)              PIERRE    76 SMAG          E+E-           4/77*


R       RADIATIVE DECAYS
R       ----------------

R70     J/PSI(3100) INTO (X(2830) GAMMA)/TOTAL  (UNITS 10**-3)
R70 S          (50.)   OR LESS  CL=0.90  BADTKE    76 CNTR          E+E-           1/77*
R70            (39.)   OR LESS  CL=0.90  WHITAKER  76 SMAG          E+E-           4/77*
R70            (17.)   OR LESS  CL=0.90  BIDDICK   77 CNTR          E+E-           3/77*
R70 S   BADTKE 76 IS SUPERCEDED BY BIDDICK 77.                                     3/77*

R71     J/PSI(3100) INTO (2 GAMMA)/TOTAL  (UNITS 10**-3) (P4)
R71            (3.)    OR LESS  CL=0.90  WIIK      75 DASP          E+E-           1/77*
R71            (0.5)   OR LESS  CL=0.90  BARTEL    77 CNTR          E+E-           4/77*

R72     J/PSI(3100) INTO (PI0 GAMMA)/TOTAL (UNITS 10**-3)                          2/75
R72  B         (4.0)   OR LESS  CL=.90   BACCI     75 FRAG          E+E-           1/76
R72  B         (0.5)   OR LESS  CL=0.90  BARTEL    77 CNTR    E+E-,3 GAMMA         1/77*
R72  U   9    (0.075)  (0.048)              BRAUNSCHW 77 DASP    E+E-,3 GAMMA         1/77*
R72  B   RE-STATED BY US USING (HADRONS)/TOTAL=0.86
R72  U   RE-STATED BY US USING TOTAL WIDTH 67 KEV.

R73     J/PSI(3100) INTO (ETA GAMMA)/TOTAL (UNITS 10**-3)
R73            (16.)   OR LESS  CL=.90   BACCI     75 FRAG          E+E-           1/76
R73      21   (1.3)    (0.4)                BARTEL    77 CNTR    E+E-,3 GAMMA         1/77*
R73  U   40   (0.82)   (0.19)               BRAUNSCHW 77 DASP    E+E-,3 GAMMA         1/77*
R73  U   RE-STATED BY US USING TOTAL WIDTH 67 KEV.

R74     J/PSI(3100) INTO (ETA PRIME GAMMA)/TOTAL  (UNITS 10**-3)
R74  B         (15.)   OR LESS  CL=.90   BALDINI2  75 FRAG          E+E-           1/76
R74            (3.3)   OR LESS  CL=.90   BACCI     76 FRAG          E+E-           4/77*
R74      57    2.4      0.7                 BARTEL 1  76 CNTR    E+E-,2 GAMMA RHO     1/77*
R74  U    3   (2.27)   (1.75)               BRAUNSCHW 77 DASP    E+E-,3 GAMMA         1/77*
R74  B   RE-STATED BY US USING (HADRONS)/TOTAL=0.86
R74  U   RE-STATED BY US USING TOTAL WIDTH 67 KEV.

R75     J/PSI(3100) INTO (ETA PRIME GAMMA)/(ETA GAMMA)
R75            (1.8)    (0.8)               BARTEL    77 CNTR    E+E-,3 GAMMA         3/77*

R76     J/PSI(3100) INTO (X(2830) GAMMA)/TOTAL,X TO 2 GAMMA (UNITS 10**-3)
R76  X         (0.14)   (0.08)              BARTEL 2  76 CNTR    E+E-,3 GAMMA         1/77*
R76  U   15   (0.124)  (0.052)              BRAUNSCHW 77 DASP    E+E-,3 GAMMA         1/77*
R76  X  EXISTENCE OF X(2830) IN BARTEL 2 76 DATA IS ONLY 2 STD EFFECT               3/77*
R76  U   RE-STATED BY US USING TOTAL WIDTH 67 KEV.

R77     J/PSI(3100) INTO (X(2830) GAMMA)/TOTAL,X TO P PBAR GAM (UNITS 10**-3
R77            (0.04) OR LESS  CL=0.90  GOLDHABER 76 SMAG          E+E-           1/77*
R77            (0.2)  OR LESS  CL=0.90  WIIK      76 DASP          E+E-           1/77*

R78     J/PSI(3100) INTO (3 GAMMA)/TOTAL  (UNITS 10**-3)
R78  U         (0.08) OR LESS  CL=0.90  BRAUNSCHW 77 DASP    E+E-,3 GAMMA         1/77*
R78  U   RE-STATED BY US USING TOTAL WIDTH 67 KEV.

R79     J/PSI(3100) INTO (X(2830) GAMMA)/TOTAL,X TO RHO GAMMA (UNITS 10**-3)
R79            (0.3)  OR LESS  CL=0.90  BARTEL 2  76 CNTR    E+E-,2 GAMMA RHO     1/77*

R80     J/PSI(3100) INTO (GAMMA + 2 OR MORE NEUTRALS)/TOTAL   (UNITS 10**-3)
R80            7.0      2.0                 BARTEL    77 CNTR          E+E-           1/77*

------ --------- --------- --------- --------- --------- --------- --------

                   70  J/PSI(3100)   G(I)*G(E+E-)/G(TOTAL)  (KEV)


         THIS COMBINATION OF A PARTIAL WIDTH WITH THE PARTIAL WIDTH
         INTO E+E- AND WITH THE TOTAL WIDTH IS OBTAINED FROM THE INTEGRATED
         CROSS-SECTION INTO CHANNEL(I) IN THE E+E- ANNIHILATION.
         WE ONLY LIST DATA NOT HAVING BEEN USED TO DETERMINE THE PARTIAL
         WIDTH G(I) OR THE BRANCHING RATIO G(I)/TOTAL.

G1      G(E+E-)*G(E+E-)/G(TOTAL)
G1  S          (.32)     (.07)              BALDINI1  75 FRAG          E+E-           1/76
G1              .34       .14               BEMPORAD  75 FRAB          E+E-           1/76
G1              .41       .06               DASP1     75 DASP          E+E-           1/76
G1  S          (.34)     (.09)              ESPOSITO  75 FRAM          E+E-           1/76
G1  S          (.36)     (.10)              FORD      75 SPEC          E+E-
G1           . . . . . . . . . .
G1  AVG        0.399     0.055   AVERAGE (ERROR INCLUDES SCALE FACTOR OF 1.0)
G1  STUDENT    0.399     0.060   AVERAGE USING STUDENT10(H/1.11) -- SEE 1976 TEXT
```

J/ψ(3100), χ(3415), χ(3455) — Data Card Listings

```
G2      G(MU+MU-)*G(E+E-)/G(TOTAL)
G2              .31        .09          BEMPORAD  75 FRAB        E+E-           1/76
G2             (.32)      (.08)         CRIEGEE2  75 PLUT        E+E-           1/76
G2              .51        .09          DASP1     75 DASP        E+E-           1/76
G2   S         (.38)      (.05)         ESPOSITO  75 FRAM        E+E-           1/76
G2   S         (.46)      (.10)         LIBERMAN  75 SPEC        E+E-           1/76
G2                 . . . . . . . . . .
G2   AVG       0.41       0.10     AVERAGE (ERROR INCLUDES SCALE FACTOR OF 1.6)
G2   STUDENT   0.410      0.079    AVERAGE USING STUDENT10(H/1.11) -- SEE 1976 TEXT

G3      G(HADRONIC)*G(E+E-)/G(TOTAL)
G3   S         (4.)       (.8)          BALDINI1  75 FRAG        E+E-           1/76
G3   S         (3.9)      (.8)          ESPOSITO  75 FRAM        E+E-           1/76

     S    SEE THE BRANCHING RATIOS AND PARTIAL WIDTHS ABOVE.

****** ********* ********* ********* ********* ********* ********* ********
```

REFERENCES FOR J/PSI(3100)

```
CHRISTEN 70 PRL 25 1523          CHRISTENSEN,HICKS,LEDERMAN+ (COLU+BNL+CERN)

ABRAMS   74 PRL 33 1453          +BRIGGS,AUGUSTIN,BOYARSKI+        (LBL+SLAC)
ASH      74 NCL 11 705           +ZORN,BARTOLI+      (FRAS+UMD+NAPL+PADO+ROMA)
AUBERT   74 PRL 33 1404          +BECKER,BIGGS,BURGER,CHEN,EVERHART(MIT+BNL)
AUGUSTIN 74 PRL 33 1406          +BOYARSKI, ABRAMS.BRIGGS+         (SLAC+LBL)
BACCI    74 PRL 33 1408          +BARTOLI,BARBARINO,BARBIELLINI+  (FRASCATI)
    ALSO 74 PRL 33 1649          FOR ERRATA
BALDINI- 74 NCL 11 711           BALDINI-CELIO,BACCI+         (FRASCATI+ROMA)
BARBIELL 74 NCL 11 718           BARBIELLINI.BEMPORAD+ (FRAS+NAPO+PISA+ROMA)
BRAUNSCH 74 PL 53B 393           BRAUNSCHWEIG+     (AACHEN+HAMB+MUNICH+TOKYO)

ABRAMS   75 STANFORD SYMP.25     G.S.ABRAMS                             (LBL)
ANDREWS  75 PRL 34 231           +HARVEY,LOBKOWICZ,MAY,NORDBERG  (ROCH+CORN)
AUBERT   75 NP B 89 1            +BECKER,RIGGS,BURGER,GLENN,+       (MIT+BNL)
BACCI    75 NCL 12 269           +PENSO,STELLA,BALDINI-CELIO,+   (ROMA+FRAS)
BALDINI1 75 PL 58B 471           BALDINI-CELIO,BOZZO,CAPON,BACCI+(FRAS+ROMA)
BALDINI2 75 PL 58B 475           BALDINI-CELIO,CAPON,DEL FABBRO+ (FRAS+ROMA)
BEMPORAD 75 STANFORD SYMP.113 C.BEMPORAD                    (PISA+FRASCATI)
BLANAR   75 PRL 35 346           +BOYER,FAISSLER,GARELICK,GETTNER,+   (NEAS)
BOYARSKI 75 PRL 34 1357          +BREIDENBACH,BULOS,FELDMAN,+     (SLAC+LBL)JPC
BRAUNSCH 75 PL 53B 491           BRAUNSCHWEIG+     (AACHEN+HAMB+MUNICH+TOKYO)
CAMERINI 75 PRL 35 483           +LEARNED,PREPOST,ASH,ANDERSON,+ (WISC+SLAC)
CRIEGEE1 75 PL 53B 489           +DEHNE,FRANKE,HORLITZ;KRECHLOCK+     (DESY)
CRIEGEE2 75  DESY PREP.75/32     +DEHNE,FOX,FRANKE,HORLITZ,KNIES,+    (DESY)
DAKIN    75 PL 56 B 405          +KREISLER,BOLON,HEILE+       (MASA+MIT+SLAC)
DASP1    75 PL 56B 491           BRAUNSCHWEIG,KONIGS,+ (AACH+DESY+MPIM+TOKY)
DASP2    75 PL 57B 297           BRAUNSCHWEIG,KONIGS,+ (AACH+DESY+MPIM+TOKY)
ESPOSITO 75 NCL 14 73            +BARTOLI,BISELLO,+     (FRAS+NAPO+PADO+ROMA)
FORD     75 PRL 34 604           +BERON,HILGER,HOFSTADTER+       (SLAC+PENN)
GITTELMA 75 PRL 35 1616          GITTELMAN+HANSON+LARSON+LOH+         (CORN)
GOLDHABE 75  LBL-4224            GOLDHABER,JOHNSON,KADYK,+        (LBL+SLAC)
GRECO    75 PL 56B 367           +PANCHERI-SRIVASTAVA,SRIVASTAVA      (FRAS)
HEINTZE  75 STANFORD SYMP.97     J.HEINTZE                      (HEIDELBERG)
JACKSON  75 NIM 128 13           J.D.JACKSON,D.SCHARRE                 (LBL)
KNAPP1   75 PRL 34 1040          +LEE,BRONSTEIN+    (COLU+HAWA+CORN+ILL+FNAL)
KNAPP2   75 PRL 34 1044          +LEE,BRONSTEIN+    (COLU+HAWA+CORN+ILL+FNAL)
LIBERMAN 75 STANFORD SYMP.55     A.D.LIBERMAN                     (STANFORD)
MARTIN   75 PRL 34 288           +BOLON,DAKIN,FELDMAN,HANSON+(MIT+MASA+SLAC)
PREPOST  75 STANFORD SYMP.241 R.PREPOST                          (WISCONSIN)
SIMPSON  75 PRL 35 699           +BERON,FORD,HILGER,HOFSTADTER,+ (STAN+PENN)
WIIK     75 STANFORD SYMP.69     B.H.WIIK                             (DESY)
YENNIE   75 PRL 34 239           D.R.YENNIE                        (CORNELL)

ANTIPOV  76 TBILISI CONF.N 8     +BESSUBOV,BUDANOV,BUSHNIN,DENISOV,+  (IHEP)
BACCI    76 LNF-76/60(P)         +BALDINI-CELIO.CAPON+      (FRAS+ROMA+GENO)
BADTKE   76  PREPRINT            +BARNETT,+   (UMD+PAVI+PRIN+UCSD+SLAC+STAN)
BARTEL 1 76 PL 64 B 483          +DUINKER,OLSSON,STEFFEN,HEINTZE+(DESY+HEID)
BARTEL 2 76 TBILISI CONF.N56     +DUINKER,OLSSON,HEINTZE,+       (DESY+HEID)
BRAUNSCH 76 PL 63 B 487          BRAUNSCHWEIG,+    (AACH+DESY+HAMB+MPIM+TOKY)
FELDMAN  76  SLAC-PUB-1851       G.J.FELDMAN                      (SLAC+LBL)
GOLDHABE 76  LBL-4884            G.GOLDHABER                      (SLAC+LBL)
JEAN-MAR 76 PRL 36 291           +ABRAMS,BOYARSKI,BREIDENBACH,+   (SLAC+LBL)IG
PIERRE   76 SACLAY-DPHPE76-21 F.PIERRE                            (SLAC+LBL)
SNYDER   76 PRL 36 1415          +HOM,LEDERMAN,PAAR,APPEL,+ (COLU+FNAL+STON)
VANNUCCI 76  SLAC-PUB-1724       +ABRAMS,BOYARSKI,BREIDENBACH,+   (SLAC+LBL)
WHITAKER 76 PRL 37 1596          +TANENBAUM,ABRAMS,ALAM,BOYARSKI,+(SLAC+LBL)
WIIK     76 TBILISI CONF.N75     B.H.WIIK RAPPORTEUR                  (DESY)

BARTEL   77  DESY 76/65          +DUINKER,OLSSON,HEINTZE,+       (DESY+HEID)
BIDDICK  77 PRINT-77-0244UCSD +BURNETT+     (UCSD+UMD+PAVI+PRIN+SLAC+STAN)
BRAUNSCH 77  DESY 77/02          BRAUNSCHWEIG,+    (AACH+DESY+HAMB+MPIM+TOKY)
BURMESTE 77  QUOTED BY WIIK76 PLUTO COLLABORATION                     (DESY)
VANNUCCI 77 TO BE PUB PR D       +ABRAMS,ALAM,BOYARSKI,+          (SLAC+LBL)
WIIK     77  DESY 77/01          +WOLF                                (DESY)

****** ********* ********* ********* ********* ********* ********* ********
****** ********* ********* ********* ********* ********* ********* ********
```

χ(3415)

```
56  CHI(3415,JPG=0++) I=0

       OBSERVED IN THE RADIATIVE DECAY OF PSI(3685) INTO
   CHI(3415) GAMMA.THEREFORE C=+. THE OBSERVED DECAY INTO (PI+PI-)
   OR (K+K-) IMPLIES G=+,JP=0+,2+,... . THE ANGULAR DISTRIBUTION
   IS CONSISTENT WITH J=0.

------ --------- --------- --------- --------- --------- --------- --------

                    56  CHI(3415) MASS (MEV)

M    W   2 3412.0      8.0          WIIK      75 DASP   E+E-,J/PSI 2 GAM  1/77*
M        1(3413.0)   (10.0)         FELDMAN   76 SMAG   E+E-,J/PSI 2 GAM  1/77*
M          3415.0     10.0          TRILLING  76 SMAG   E+E-,HADRONS GAM  1/77*
M    Q    (3418.0)    (7.0)         VERNON    76 CNTR   E+E-,MONOCHR.GAM  1/77*
M          3413.0     11.0          WHITAKER  76 SMAG   E+E-,MONOCHR.GAM  1/77*
M          3413.0      9.0          BIDDICK   77 CNTR   E+E-,MONOCHR.GAM  3/77*
M    W  INCREASED 4 MEV BY FELDMAN 76 TO CORRECT FOR ENERGY CALIBRATION.
M    Q  VERNON 76 IS SUPERCEDED BY BIDDICK 77
M             . . . . . . . . .
M    AVG     3413.1      4.7     AVERAGE (ERROR INCLUDES SCALE FACTOR OF 1.0)
M    STUDENT 3413.1      5.0     AVERAGE USING STUDENT10(H/1.11) -- SEE 1976 TEXT

------ --------- --------- --------- --------- --------- --------- --------

                    56  CHI(3415) PARTIAL DECAY MODES

                                                             DECAY MASSES
P1     CHI(3415) INTO PI+ PI-                                139+ 139
P2     CHI(3415) INTO K+ K-                                  493+ 493
P3     CHI(3415) INTO 2(PI+ PI-)                             139+ 139+ 139+ 139
P4     CHI(3415) INTO 3(PI+ PI-)
P5     CHI(3415) INTO PI+ PI- K+ K-                          139+ 139+ 493+ 493
P6     CHI(3415) INTO J/PSI(3100) GAMMA                     3098+   0
P7     CHI(3415) INTO 2 GAMMA
P8     CHI(3415) INTO PI+ PI- P PBAR                         139+ 139+ 938+ 938
P9     CHI(3415) INTO RHO0 PI+ PI-                           773+ 139+ 139
P10    CHI(3415) INTO K*(892)0 K+/- PI-/+                    892+ 493+ 139

------ --------- --------- --------- --------- --------- --------- --------

                    56  CHI(3415) BRANCHING RATIOS

R         SEE ALSO BRANCHING RATIOS R54 OF PSI(3685)

R1        CHI(3415) INTO (2 GAMMA)/TOTAL
R1           (0.0057)OR LESS  CL=0.90  BRAUNSCHW 77 DASP    E+E-,3 GAMMA      1/77*

R2     CHI(3415) INTO 2(PI+ PI-)/TOTAL
R2   T        (.043)    (.017)           TRILLING  76 SMAG PSI(3685)TO GAM CHI  1/77*
R2   T   CALCULATED USING PSI(3685) TO (GAMMA CHI(3415))/TOTAL=.075+/-.026      1/77*

R3     CHI(3415) INTO (PI+ PI- K+ K-)/TOTAL
R3   T        (.036)    (.015)           TRILLING  76 SMAG PSI(3685)TO GAM CHI  1/77*

R4     CHI(3415) INTO 3(PI+ PI-)/TOTAL
R4   T        (.02)     (.01)            TRILLING  76 SMAG PSI(3685)TO GAM CHI  1/77*

R5     CHI(3415) INTO (PI+ PI-)/TOTAL
R5   T        (.01)     (.005)           TRILLING  76 SMAG PSI(3685)TO GAM CHI  1/77*

R6     CHI(3415) INTO (K+ K-)/TOTAL
R6   T        (.01)     (.005)           TRILLING  76 SMAG PSI(3685)TO GAM CHI  1/77*

R7     CHI(3415) INTO (PI+ PI- P PBAR)/TOTAL
R7   T        (.005)    (.002)           TRILLING  76 SMAG PSI(3685)TO GAM CHI  1/77*

R8     CHI(3415) INTO (J/PSI(3100) GAMMA)/TOTAL
R8   T        (.03)     (.03)            TRILLING  76 SMAG PSI(3685)TO GAM CHI  1/77*

R9     CHI(3415) INTO (RHO0 PI+ PI-)/2(PI+ PI-)
R9             .39       .12             TRILLING  76 SMAG PSI(3685)TO GAM CHI  1/77*

R10    CHI(3415) INTO (K*(892)0 K+/- PI-/+)/(PI+ PI- K+ K-)
R10            .41       .10             TRILLING  76 SMAG PSI(3685)TO GAM CHI  1/77*

****** ********* ********* ********* ********* ********* ********* ********
```

REFERENCES FOR CHI(3415)

```
FELDMAN  75 PRL 35 821           +JEAN-MARIE,SADOULET,VANNUCCI,+   (LBL+SLAC)
    ALSO 75 PRL 35 1189  (ERRATA)
TANENBAU 75 PRL 35 1323          TANENBAUM,WHITAKER,ABRAMS,+       (LBL+SLAC)
WIIK     75 STANFORD SYMP.69     B.H.WIIK                             (DESY)

FELDMAN  76  SLAC-PUB-1851       G.J.FELDMAN                      (SLAC+LBL)
PIERRE   76  LBL-5324            F.PIERRE                         (SLAC+LBL)
TRILLING 76 STANFORD SYMP.437 G. H. TRILLING                           (LBL)
VERNON   76 TBILISI CONF.N63     W.VERNON       (UMD+PAVI+PRIN+UCSD+SLAC+STAN)
WHITAKER 76 PRL 37 1596          +TANENBAUM,ABRAMS,ALAM,BOYARSKI,+(SLAC+LBL)
WIIK     76 TBILISI CONF.N75     B.H.WIIK RAPPORTEUR                  (DESY)

BIDDICK  77 PRINT-77-0244UCSD +BURNETT+     (UCSD+UMD+PAVI+PRIN+SLAC+STAN)
BRAUNSCH 77  DESY 77/03          BRAUNSCHWEIG,+    (AACH+DESY+HAMB+MPIM+TOKY)
WIIK     77  DESY 77/01          +WOLF                                (DESY)

****** ********* ********* ********* ********* ********* ********* ********
****** ********* ********* ********* ********* ********* ********* ********
```

χ(3455)

```
              58  CHI(3455,JPG=   ) I=

                 OBSERVED IN THE CASCADE RADIATIVE DECAY OF PSI(3685)
         INTO CHI(3455) GAMMA, CHI(3455) INTO J/PSI(3100) GAMMA
         WHITAKER 76), THEREFORE C=+.  NOT SEEN IN HADRONIC MODES.
         NOT SEEN IN OTHER EXPERIMENTS LOOKING ONLY FOR MONOCHROMATIC
         PHOTONS.  AMBIGUOUS, WITH A (BROADER) STATE AT ABOUT 3340 NOT
         EXCLUDED.  NEEDS CONFIRMATION.  OMITTED FROM TABLE

------ --------- --------- --------- --------- --------- --------- --------

                    58  CHI(3455) MASS (MEV)

M        4 3454.0      10.0           WHITAKER  76 SMAG    E+E-,J/PSI 2 GAM  1/77*

------ --------- --------- --------- --------- --------- --------- --------

                    58  CHI(3455) PARTIAL DECAY MODES

                                                             DECAY MASSES
P1     CHI(3455) INTO J/PSI(3100) GAMMA                     3096+   0

------ --------- --------- --------- --------- --------- --------- --------

                    58  CHI(3455) BRANCHING RATIOS

R        SEE BRANCHING RATIOS R62 OF PSI(3685)

****** ********* ********* ********* ********* ********* ********* ********
```

REFERENCES FOR CHI(3455)

```
FELDMAN  76  SLAC-PUB-1851       G.J.FELDMAN                      (SLAC+LBL)
WHITAKER 76 PRL 37 1596          +TANENBAUM,ABRAMS,ALAM,BOYARSKI,+(SLAC+LBL)
WIIK     76 TBILISI CONF.N75     B.H.WIIK RAPPORTEUR                  (DESY)

WIIK     77  DESY 77/01          +WOLF                                (DESY)

****** ********* ********* ********* ********* ********* ********* ********
****** ********* ********* ********* ********* ********* ********* ********
```

Data Card Listings

P_c or $\chi(3510)$, $\chi(3550)$, $\psi(3685)$

P_c or $\chi(3510)$

```
55   PC OR CHI(3510, JPG=  +) I=0

          OBSERVED IN THE RADIATIVE SEQUENTIAL DECAY OF THE
     PSI(3685) INTO PC GAMMA, PC INTO J/PSI(3100) GAMMA. THEREFORE C=+.
     THE LACK OF DECAYS INTO (PI+PI-) OR (K+K-) IS SUGGESTIVE OF
     JP = ABNORMAL. THE DECAYS INTO 4PI AND 6PI IMPLY C=+, THUS I=0.
     J=0 IS EXCLUDED BY THE ANGULAR DISTRIBUTION IN THE (GAMMA J/PSI)
     DECAY(FELDMAN 76).

------ --------- --------- --------- --------- --------- --------- --------

                    55   PC MASS (MEV)

M    W   40(3500.)     (10.)          TANENBAUM 75 SMAG         HADRONS GAM  1/76
M    W   7 3512.0       7.0           WIIK      75 DASP    E+E-,J/PSI 2 GAM  1/77*
M          3510.0      20.0           BARTEL    76 CNTR    E+E-,J/PSI 2 GAM  1/77*
M       12 3504.0      10.0           WHITAKER  76 SMAG    E+E-,J/PSI 2 GAM  1/77*
M    S    (3512.0)     (7.0)          VERNON    76 CNTR    E+E-,MONOCHR.GAM  1/77*
M          3511.0       7.0           BIDDICK   77 CNTR    E+E-,MONOCHR.GAM  3/77*
M    W   TANENBAUM 75 SUPERCEDED BY WHITAKER 76                              3/77*
M    W   INCREASED 4 MEV BY FELDMAN 76 TO CORRECT FOR ENERGY CALIBRATION.
M    S   VERNON 76 IS SUPERCEDED BY BIDDICK 77                               3/77*
M          . . . . . . . . . .
M    AVG     3510.0      4.3     AVERAGE (ERROR INCLUDES SCALE FACTOR OF 1.0)
M    STUDENT3510.1       4.7     AVERAGE USING STUDENT10(H/1.11) -- SEE 1976 TEXT

------ --------- --------- --------- --------- --------- --------- --------

                    55   PC PARTIAL DECAY MODES

                                                             DECAY MASSES
P1      PC INTO J/PSI(3100) GAMMA                            3098+   0
P2      PC INTO PI+ PI-                                      139+ 139
P3      PC INTO K+ K-                                        493+ 493
P4      PC INTO GAMMA GAMMA
P5      PC INTO 2(PI+ PI-)                                   139+ 139+ 139+ 139
P6      PC INTO 3(PI+ PI-)
P7      PC INTO PI+ PI- K+ K-                                139+ 139+ 493+ 493
P8      PC INTO PI+ PI- P PBAR                               139+ 139+ 938+ 938
P9      PC INTO RHO0 PI+ PI-                                 773+ 139+ 139
P10     PC INTO K*(892)0 K+/- PI-/+                          892+ 493+ 139

------ --------- --------- --------- --------- --------- --------- --------

                    55   PC BRANCHING RATIOS

R       SEE ALSO BRANCHING RATIOS R60 OF PSI(3685)

R1      PC INTO (J/PSI(3100) GAMMA)/TOTAL
R1   D       DOMINANT                 DASP      75 DASP         E+E-         1/76
R1   T       (.26)                    TRILLING  76 SMAG PSI(3685) TO GAM PC  1/77*
R1   D  USING THE UPPER LIMITS OF SIMPSON 75
R1   T  ESTIMATED USING PSI(3685) TO (GAMMA PC)/TOTAL=.09

R2      PC INTO (PI+PI- AND K+K-)/TOTAL
R2          NOT SEEN                  FELDMAN   75 SMAG         E+E-         1/76
R2   T      LESS THAN .002            TRILLING  76 SMAG PSI(3685) TO GAM PC  1/77*

R3      PC INTO (GAMMA GAMMA)/TOTAL
R3          (0.0030)OR LESS  CL=0.90  BRAUNSCHW 77 DASP    E+E-,3 GAMMA      1/77*

R4      PC INTO 2(PI+ PI-)/TOTAL
R4   T       (.012)                   TRILLING  76 SMAG PSI(3685) TO GAM PC  1/77*

R5      PC INTO (PI+ PI- K+ K-)/TOTAL
R5   T       (.007)                   TRILLING  76 SMAG PSI(3685) TO GAM PC  1/77*

R6      PC INTO 3(PI+ PI-)/TOTAL
R6   T       (.019)                   TRILLING  76 SMAG PSI(3685) TO GAM PC  1/77*

R7      PC INTO (PI+ PI- P PBAR)/TOTAL
R7   T       (.001)                   TRILLING  76 SMAG PSI(3685) TO GAM PC  1/77*

R8      PC INTO (RHO0 PI+ PI-)/2(PI+ PI-)
R8            .24       .20           TRILLING  76 SMAG PSI(3685) TO GAM PC  1/77*

R9      PC INTO (K*(892)0 K+/- PI-/+)/(PI+ PI- K+ K-)
R9            .35       .18           TRILLING  76 SMAG PSI(3685) TO GAM PC  1/77*

****** ********* ********* ********* ********* ********* ********* ********
```



```
                             REFERENCES FOR PC

DASP      75 PL 57B 407          BRAUNSCHWEIG,KONIGS,+ (AACH+DESY+MPIM+TOKY)
FELDMAN   75 STANFORD SYMP.39    G.J.FELDMAN                          (SLAC)
HEINTZE   75 STANFORD SYMP.97    J.HEINTZE                      (HEIDELBERG)
SIMPSON   75 PRL 35 699          +BERON,FORD,HILGER,HOFSTADTER,+ (STAN+PENN)
TANENBAU  75 PRL 35 1323         TANENBAUM,WHITAKER,ABRAMS,+      (LBL+SLAC)
WIIK      75 STANFORD SYMP.69    B.H.WIIK                             (DESY)

BARTEL    76 TBILISI CONF.N56    +DUINKER,OLSSON,HEINTZE,+       (DESY+HEID)
FELDMAN   76 SLAC-PUB-1851       G.J.FELDMAN                      (SLAC+LBL)
TRILLING  76 STANFORD SYMP.437   G. H. TRILLING                        (LBL)
VERNON    76 TBILISI CONF.N63    W.VERNON      (UMD+PAVI+PRIN+UCSD+SLAC+STAN)
WHITAKER  76 PRL 37 1596         +TANENBAUM,ABRAMS,ALAM,BOYARSKI,+(SLAC+LBL)
WIIK      76 TBILISI CONF.N75    B.H.WIIK RAPPORTEUR                  (DESY)

BIDDICK   77 PRINT-77-0244UCSD +BURNETT+      (UCSD+UMD+PAVI+PRIN+SLAC+STAN)
BRAUNSCH  77 DESY 77/03          BRAUNSCHWEIG,+   (AACH+DESY+HAMB+MPIM+TOKY)
WIIK      77 DESY 77/01          +WOLF                                (DESY)

****** ********* ********* ********* ********* ********* ********* ********
****** ********* ********* ********* ********* ********* ********* ********
```


$\chi(3550)$

```
57   CHI(3550,JPG=  +) I=0

          OBSERVED IN RADIATIVE DECAY OF PSI(3685) INTO
     CHI(3550) GAMMA. THEREFORE C=+. THE OBSERVED DECAY INTO 4PI
     AND 6PI IMPLY G=+, THUS I=0.
     J=0 IS EXCLUDED BY THE ANGULAR DISTRIBUTION IN THE HADRONIC
     DECAYS (FELDMAN 76)

------ --------- --------- --------- --------- --------- --------- --------

                    57   CHI(3550) MASS (MEV)

M          3550.0      10.0           TRILLING  76 SMAG    E+E-,HADRONS GAM  1/77*
M        4 3543.0      10.0           WHITAKER  76 SMAG    E+E-,J/PSI 2 GAM  1/77*
M    Q    (3561.0)     (7.0)          VERNON    76 CNTR    E+E-,MONOCHR.GAM  1/77*
M          3561.0       7.0           BIDDICK   77 CNTR    E+E-,MONOCHR.GAM  3/77*
M    Q   VERNON 76 IS SUPERCEDED BY BIDDICK 77                               3/77*
M          . . . . . . . . . .
M    AVG     3553.8      5.4     AVERAGE (ERROR INCLUDES SCALE FACTOR OF 1.1)
M    STUDENT3553.8       5.9     AVERAGE USING STUDENT10(H/1.11) -- SEE 1976 TEXT

------ --------- --------- --------- --------- --------- --------- --------

                    57   CHI(3550) PARTIAL DECAY MODES

                                                             DECAY MASSES
P1      CHI(3550) INTO PI+ PI-                               139+ 139
P2      CHI(3550) INTO K+ K-                                 493+ 493
P3      CHI(3550) INTO 2(PI+ PI-)                            139+ 139+ 139+ 139
P4      CHI(3550) INTO 3(PI+ PI-)
P5      CHI(3550) INTO PI+ PI- K+ K-                         139+ 139+ 493+ 493
P6      CHI(3550) INTO J/PSI(3100) GAMMA                     3095+   0
P7      CHI(3550) INTO 2 GAMMA
P8      CHI(3550) INTO PI+ PI- P PBAR                        139+ 139+ 938+ 938
P9      CHI(3550) INTO RHO0 PI+ PI-                          773+ 139+ 139
P10     CHI(3550) INTO K*(892)0 K+/- PI-/+                   892+ 493+ 139

------ --------- --------- --------- --------- --------- --------- --------

                    57   CHI(3550) BRANCHING RATIOS

R       SEE ALSO BRANCHING RATIOS R58 OF PSI(3685)

R1       CHI(3550) INTO (2 GAMMA)/TOTAL
R1          (0.0025)OR LESS  CL=0.90  BRAUNSCHW 77 DASP     E+E-,3 GAMMA     1/77*

R2      CHI(3550) INTO 2(PI+ PI-)/TOTAL
R2   T       (.02)                    TRILLING  76 SMAG PSI(3685)TO GAM CHI  1/77*
R2   T  ESTIMATED USING PSI(3685) TO (GAMMA CHI(3550))/TOTAL=.08             1/77*

R3      CHI(3550) INTO (PI+ PI- K+ K-)/TOTAL
R3   T       (.016)                   TRILLING  76 SMAG PSI(3685)TO GAM CHI  1/77*

R4      CHI(3550) INTO 3(PI+ PI-)/TOTAL
R4   T       (.01)                    TRILLING  76 SMAG PSI(3685)TO GAM CHI  1/77*

R5      CHI(3550) INTO (PI+ PI- AND K+ K-)/TOTAL
R5   T       (.002)                   TRILLING  76 SMAG PSI(3685)TO GAM CHI  1/77*

R6      CHI(3550) INTO (PI+ PI- P PBAR)/TOTAL
R6   T       (.002)                   TRILLING  76 SMAG PSI(3685)TO GAM CHI  1/77*

R7      CHI(3550) INTO (J/PSI(3100) GAMMA)/TOTAL
R7   T       (.12)                    TRILLING  76 SMAG PSI(3685)TO GAM CHI  1/77*

R8      CHI(3550) INTO (RHO0 PI+ PI-)/2(PI+ PI-)
R8            .21       .17           TRILLING  76 SMAG PSI(3685)TO GAM CHI  1/77*

R9      CHI(3550) INTO (K*(892)0 K+/- PI-/+)/(PI+ PI- K+ K-)
R9            .25       .13           TRILLING  76 SMAG PSI(3685)TO GAM CHI  1/77*

****** ********* ********* ********* ********* ********* ********* ********
```



```
                         REFERENCES FOR CHI(3550)

FELDMAN   75 PRL 35 821          +JEAN-MARIE,SADOULET,VANNUCCI,+  (LBL+SLAC)
    ALSO  75 PRL 35 1189  (ERRATA)
TANENBAU  75 PRL 35 1323         TANENBAUM,WHITAKER,ABRAMS,+      (LBL+SLAC)

FELDMAN   76  SLAC-PUB-1851      G.J.FELDMAN                      (SLAC+LBL)
PIERRE    76  LBL-5324           F.PIERRE                         (SLAC+LBL)
TRILLING  76 STANFORD SYMP.437   G. H. TRILLING                        (LBL)
VERNON    76 TBILISI CONF.N63    W.VERNON      (UMD+PAVI+PRIN+UCSD+SLAC+STAN)
WHITAKER  76 PRL 37 1596         +TANENBAUM,ABRAMS,ALAM,BOYARSKI,+(SLAC+LBL)
WIIK      76 TBILISI CONF.N75    B.H.WIIK RAPPORTEUR                  (DESY)

BIDDICK   77 PRINT-77-0244UCSD +BURNETT+      (UCSD+UMD+PAVI+PRIN+SLAC+STAN)
BRAUNSCH  77  DESY 77/03         BRAUNSCHWEIG,+   (AACH+DESY+HAMB+MPIM+TOKY)
WIIK      77  DESY 77/01         +WOLF                                (DESY)

****** ********* ********* ********* ********* ********* ********* ********
****** ********* ********* ********* ********* ********* ********* ********
```


$\psi(3685)$

```
71   PSI(3685,JPG=1--) I=0

------ --------- --------- --------- --------- --------- --------- --------

                    71   PSI(3685) MASS (MEV)

M    L    (3695.)       (4.)          ABRAMS    74 SMAG         E+E-         2/75
M    S     3680.3      37.            CRIEGEE   75 PLUT         E+E-         2/75
M          3684.        5.            LUTH      75 SMAG         E+E-         1/76
M          3684.        9.            PREPOST   75 SPEC    21.  GAMMA C      1/76
M
M    L   LUTH 75 IS A REEVALUATION OF ABRAMS 74.                             2/75
M    S   ERROR OF ABOUT 1 PER CENT FROM THE UNCERTAINTY IN CALIBRATION OF    2/75
M    S   THE BEAM ENERGY.                                                    2/75
M          . . . . . . . . . .
M    AVG     3683.9      4.3     AVERAGE (ERROR INCLUDES SCALE FACTOR OF 1.0)
M    STUDENT3683.9       4.7     AVERAGE USING STUDENT10(H/1.11) -- SEE 1976 TEXT

------ --------- --------- --------- --------- --------- --------- --------

DM               PSI(3685) - J/PSI(3100) MASS DIFFERENCE (MEV)

DM         588.7        .8            LUTH      75 SMAG

------ --------- --------- --------- --------- --------- --------- --------

                    71   PSI(3685) WIDTH (KEV)

W          228.        56.            LUTH      75 SMAG

------ --------- --------- --------- --------- --------- --------- --------

                    71   PSI(3685) PARTIAL DECAY MODES

                                                             DECAY MASSES
P1      PSI(3685) INTO E+ E-                                 .5+  .5
P2      PSI(3685) INTO MU+ MU-                               105+ 105
P3      PSI(3685) INTO HADRONS
P4      PSI(3685) INTO VIRTUAL GAMMA INTO HADRONS
```

ψ(3685)


```
P       DECAYS INTO J/PSI(3100) + ANYTHING
P       ----------------------------------
P11     PSI(3685) INTO J/PSI(3100) + ANYTHING
P12     PSI(3685) INTO J/PSI(3100) + NEUTRALS
P13     PSI(3685) INTO J/PSI(3100) PI+ PI-              3098+ 139+ 139
P14     PSI(3685) INTO J/PSI(3100) PIO PIO              3098+ 134+ 134
P15     PSI(3685) INTO J/PSI(3100) ETA                  3098+ 548
P16     PSI(3685) INTO J/PSI(3100) GAMMA GAMMA

P       HADRONIC DECAYS
P       ---------------
P21     PSI(3685) INTO PI+ PI-
P22     PSI(3685) INTO RHO PI
P23     PSI(3685) INTO K+ K-
P24     PSI(3685) INTO 2(PI+ PI-)
P25     PSI(3685) INTO 2(PI+ PI-) PIO
P26     PSI(3685) INTO PI+ PI- K+ K-
P27     PSI(3685) INTO PBAR P
P28     PSI(3685) INTO LAMBDA ANTILAMBDA
P29     PSI(3685) INTO XI ANTIXI

P       RADIATIVE DECAYS
P       ----------------
P51     PSI(3685) INTO GAMMA GAMMA
P52     PSI(3685) INTO PIO GAMMA
P53     PSI(3685) INTO ETA GAMMA
P54     PSI(3685) INTO ETA PRIME GAMMA
P55     PSI(3685) INTO X(2830) GAMMA                    2830+    0
P56     PSI(3685) INTO CHI(3415) GAMMA                  3413+    0
P57     PSI(3685) INTO CHI(3455) GAMMA                  3454+    0
P58     PSI(3685) INTO PC(3510) GAMMA                   3510+    0
P59     PSI(3685) INTO CHI(3550) GAMMA                  3554+    0
P60     PSI(3685) INTO PC(3510) + ANYTHING
------ --------- --------- --------- --------- --------- --------- --------
```

FITTED PARTIAL DECAY MODE BRANCHING FRACTIONS

The matrix below is derived from the error matrix for the fitted partial decay mode branching fractions, P_i, as follows: The diagonal elements are $P_i \pm \delta P_i$, where $\delta P_i = \sqrt{\langle \delta P_i \delta P_i \rangle}$, while the off-diagonal elements are the normalized correlation coefficients $\langle \delta P_i \delta P_j \rangle / (\delta P_i \cdot \delta P_j)$. For the definitions of the individual P_i, see the listings above; only those P_i appearing in the matrix are assumed in the fit to be nonzero and are thus constrained to add to 1.

	$J/\psi\,\pi^+\pi^-$	$J/\psi\,\pi^0\pi^0$	$J/\psi\,\eta$	J/ψ+OTHER	NON-J/ψ
$J/\psi\,\pi^+\pi^-$	.3289+-.0251				
$J/\psi\,\pi^0\pi^0$	.4767	.1734+-.0178			
$J/\psi\,\eta$	-.0216	-.0102	.0416+-.0071		
J/ψ+OTHER	.2593	-.4156	-.1526	.0334+-.0258	
NON-J/ψ	-.9014	-.4243	-.0537	-.5365	.4227+-.0445

```
------ --------- --------- --------- --------- --------- --------- --------

                       71  PSI(3685) PARTIAL WIDTHS (KEV)

W1      PSI(3685) INTO E+ E-                          (G1)                     2/75
W1           2.1        .3            LUTH       75 SMAG         E+E-          1/76

W3      PSI(3685) INTO HADRONS                        (G3)
W3           224.       56.           LUTH       75 SMAG         E+E-          1/76
------ --------- --------- --------- --------- --------- --------- --------

                       71  PSI(3685) BRANCHING RATIOS

R1      PSI(3685) INTO (E+ E-)/TOTAL
R1 L         .0093      .0016         LUTH       75 SMAG         E+E-          1/76
R1 L    FROM AN OVERALL FIT ASSUMING EQUAL PARTIAL WIDTHS FOR (E+E-)
R1 L    AND (MU+MU-). FOR A MEASUREMENT OF THE RATIO SEE THE ENTRY R4 BELOW

R2      PSI(3685) INTO (MU+ MU-)/TOTAL
R2 H         .0077      .0017         HILGER     75 SPEC         E+E-          1/76
R2 H    RE-STATED BY US USING (J/PSI(3100)+ANYTHING)/TOTAL =0.55

R3      PSI(3685) INTO (HADRONS)/TOTAL
R3   P       .981       .003          LUTH       75 SMAG         E+E-          1/76
R3   P  INCLUDES CASCADE DECAY INTO J/PSI(3100)                                4/77*

R4      PSI(3685) INTO (MU+ MU-)/(E+ E-)
R4          (.89)      (.16)          BOYARSKI   75 SMAG         E+E-          1/76

R5      PSI(3685) INTO (GAMMA INTO HADRONS)/TOTAL
R5 C         .029       .004          LUTH       75 SMAG         E+E-          1/76
R5 C    INCLUDED IN R3


R       DECAYS INTO J/PSI(3100) + ANYTHING
R       ----------------------------------

R10     PSI(3685) INTO (J/PSI(3100) + ANYTHING)/TOTAL
R10          .57        .08           ABRAMS     75 SMAG         E+E-          1/76
R10          . . . . . . . . .
R10 FIT      0.577      0.044   FROM FIT (ERROR INCLUDES SCALE FACTOR OF 1.0)

R11     PSI(3685) INTO (J/PSI(3100) + NEUTRALS)/(J/PSI(3100) + ANYTHING)
R11          .41        .02           TANENBAUM 76 SMAG         E+E-          2/76
R11          . . . . . . . . .
R11 FIT      0.410      0.020   FROM FIT (ERROR INCLUDES SCALE FACTOR OF 1.0)

R12     PSI(3685) INTO (J/PSI(3100) PI+ PI-)/TOTAL
R12          .32        .04           ABRAMS1    75 SMAG         E+E-          1/76
R12          .36        .06           WIIK       75 DASP         E+E-          1/76
R12          . . . . . . . . .
R12 AVG      0.332      0.033   AVERAGE (ERROR INCLUDES SCALE FACTOR OF 1.0)
R12 STUDENT  0.332      0.036   AVERAGE USING STUDENT10(H/1.11) -- SEE 1976 TEXT
R12 FIT      0.329      0.025   FROM FIT (ERROR INCLUDES SCALE FACTOR OF 1.0)

R13     PSI(3685) INTO (J/PSI(3100) PIO PIO)/TOTAL
R13          0.17       0.029         ABRAMS1    75 SMAG         E+E-          1/77*
R13          .18        .06           WIIK       75 DASP         E+E-          1/76
R13          . . . . . . . . .
R13 AVG      0.172      0.026   AVERAGE (ERROR INCLUDES SCALE FACTOR OF 1.0)
R13 STUDENT  0.172      0.028   AVERAGE USING STUDENT10(H/1.11) -- SEE 1976 TEXT
R13 FIT      0.173      0.018   FROM FIT (ERROR INCLUDES SCALE FACTOR OF 1.0)

R14     PSI(3685) INTO (J/PSI(3100) PIO PIO)/(J/PSI(3100) PI+ PI-)
R14 H       (.64)      (.15)          HILGER     75 SPEC         E+E-          1/76
R14          0.53       0.06          TANENBAUM 76 SMAG          E+E-          1/77*
R14 H   IGNORING THE (J/PSI ETA) AND (J/PSI GAMMA GAMMA) DECAYS
R14          . . . . . . . . .
R14 FIT      0.527      0.050   FROM FIT (ERROR INCLUDES SCALE FACTOR OF 1.0)

R15     PSI(3685) INTO (J/PSI(3100) ETA)/TOTAL
R15          .043       .008          TANENBAUM 76 SMAG          E+E-          1/76
R15          .037       .015          WIIK       75 DASP         E+E-          1/76
R15          . . . . . . . . .
R15 AVG      0.0417     0.0071  AVERAGE (ERROR INCLUDES SCALE FACTOR OF 1.0)
R15 STUDENT  0.0417     0.0076  AVERAGE USING STUDENT10(H/1.11) -- SEE 1976 TEXT
R15 FIT      0.0416     0.0071 FROM FIT (ERROR INCLUDES SCALE FACTOR OF 1.0)

R16     PSI(3685) INTO (J/PSI(3100) GAMMA OR J/PSI(3100) PIO)/TOTAL
R16         (.0015)OR LESS CL=.90    TANENBAUM 76 SMAG          E+E-          2/76


R       HADRONIC DECAYS
R       ---------------

R20     PSI(3685) INTO (PI+ PI-)/TOTAL  (UNITS 10**-4)
R20         (3.7)  OR LESS  CL=0.90  BRAUNSCHW 76 DASP          E+E-          1/77*
R20         (0.5)  OR LESS  CL=0.90  FELDMAN   76 SMAG          E+E-          1/77*

R21     PSI(3685) INTO (RHOO PIO)/TOTAL
R21         (.001)OR LESS  CL=.90    ABRAMS    75 SMAG          E+E-          1/76

R22     PSI(3685) INTO (2(PI+ PI-) PIO)/TOTAL
R22          .0035     .0015         ABRAMS    75 SMAG          E+E-          1/76

R23     PSI(3685) INTO (K+ K-)/TOTAL  (UNITS 10**-4)
R23      2  (14.)  OR LESS  CL=0.90  BRAUNSCHW 76 DASP          E+E-          1/77*
R23         (0.5)  OR LESS  CL=0.90  FELDMAN   76 SMAG          E+E-          1/77*

R24     PSI(3685) INTO (PI+ PI- K+ K-)/TOTAL
R24         (0.0014) (0.0004)        PIERRE 1  76 SMAG          E+E-          1/77*

R25     PSI(3685) INTO (PBAR P)/TOTAL  (UNITS 10**-4)
R25         (4.7)  OR LESS  CL=0.90  BRAUNSCHW 76 DASP          E+E-          1/77*
R25         (2.3)      (0.7)         FELDMAN   76 SMAG          E+E-          1/77*

R26     PSI(3685) INTO (RHO PI)/TOTAL
R26         (0.001)OR LESS  CL=0.90  BARTEL 1  76 CNTR          E+E-          1/77*

R27     PSI(3685) INTO 2(PI+PI-)/TOTAL
R27         (0.0008) (0.0002)        PIERRE 1  76 SMAG          E+E-          1/77*

R28     PSI(3685) INTO (LAMBDA ANTILAMBDA)/TOTAL
R28         (0.0004)OR LESS          FELDMAN   76 SMAG          E+E-          1/77*

R29     PSI(3685) INTO (XI- ANTIXI-)/TOTAL
R29         (0.0002)                 FELDMAN   76 SMAG          E+E-          1/77*


R       RADIATIVE DECAYS
R       ----------------

R41     PSI(3685) INTO (GAMMA GAMMA)/TOTAL
R41  U      (.005)OR LESS  CL=.95    HUGHES    75 SPEC          E+E-          1/76
R41         (.008)OR LESS  CL=.90    WIIK      75 DASP          E+E-          1/76

R42     PSI(3685) INTO (PIO GAMMA)/TOTAL
R42  U      (.007)OR LESS  CL=.95    HUGHES    75 SPEC          E+E-          1/76
R42         (.01) OR LESS  CL=.90    WIIK      75 DASP          E+E-          1/76

R43     PSI(3685) INTO (ETA GAMMA)/TOTAL (UNITS 10**-2)
R43  U      (1.8)  OR LESS  CL=.95   HUGHES    75 SPEC          E+E-          1/76
R43  A      (0.04) OR LESS  CL=.95     9 4   86 77 DASP         E+E-
R43  U  RE-STATED BY US USING (MU+MU-)/TOTAL = .0077
R43  A   RESTATED BY US USING TOTAL DECAY WIDTH 228 KEV.

R44     PSI(3685) INTO (ETA PRIME GAMMA)/TOTAL (UNITS 10**-2)
R44         (0.11) OR LESS  CL=0.90  BARTEL 1  76 CNTR          E+E-          1/77*
R44  A      (0.6)  OR LESS  CL=0.90  BRAUNSCHW 77 DASP          E+E-          1/77*
R44  A   RESTATED BY US USING TOTAL DECAY WIDTH 228 KEV.

R53     PSI(3685) INTO (X(2830) GAMMA)/TOTAL (UNITS 10**-2)
R53 S       (5.0)  OR LESS  CL=0.90  BADTKE    76 CNTR          E+E-          1/77*
R53         (1.1)  OR LESS  CL=0.90  WHITAKER  76 SMAG          E+E-          4/77*
R53         (1.0)  OR LESS  CL=0.90  BIDDICK   77 CNTR          E+E-          3/77*
R53 S    BADTKE 76 IS SUPERCEDED BY BIDDICK 77                                3/77*

R54     PSI(3685) INTO (X(2830) GAMMA)/TOTAL (UNITS 10**-2)
R54                    X(2830) INTO CHANNEL SPECIFIED IN COMMENTS
R54         (0.3)  OR LESS  CL=0.95  HUGHES    75 SPEC    X TO (2 GAMMA)      1/76
R54         (0.034)OR LESS  CL=0.90  BRAUNSCHW 77 DASP    X TO (2 GAMMA)      1/77*
R54         (0.042)OR LESS  CL=0.90  BARTEL 2  76 CNTR    X TO (RHO GAMMA)    1/77*

R55     PSI(3685) INTO (CHI(3415) GAMMA)/TOTAL  (UNITS 10**-2)
R55  A       7.5        2.6          WHITAKER  76 SMAG          E+E-          1/77*
R55 QA      (8.)       (3.)          VERNON    76 CNTR    E+E-,MONOCHR.GAM    1/77*
R55  A       7.2        2.3          BIDDICK   77 CNTR    E+E-,MONOCHR.GAM    3/77*
R55  A  ANGULAR DISTRIBUTION (1+COS**2) ASSUMED
R55 Q   VERNON 76 IS SUPERCEDED BY BIDDICK 77                                 3/77*
R55          . . . . . . . . .
R55 AVG      7.3        1.7      AVERAGE (ERROR INCLUDES SCALE FACTOR OF 1.0)
R55 STUDENT  7.3        1.8      AVERAGE USING STUDENT10(H/1.11) -- SEE 1976 TEXT

R56     PSI(3685) INTO (CHI(3415) GAMMA)/TOTAL  (UNITS 10**-2)
R56                   CHI(3415) INTO CHANNEL SPECIFIED IN COMMENTS
R56      1  (0.2)      (0.2)         WHITAKER  76 SMAG CHI TO(J/PSI GAMMA)    1/77*
R56      1  (1.0)                    WIIK      76 DASP CHI TO(J/PSI GAMMA)    4/77*
R56         (3.3)      (1.7)         BIDDICK   77 CNTR CHI TO(J/PSI GAMMA)    3/77*
R56         (0.04) OR LESS  CL=0.90  BRAUNSCHW 77 DASP CHI TO (2 GAMMA)       1/77*
R56         (0.07)     (0.02)        PIERRE 2  76 SMAG CHI TO (K+K-)          1/77*
R56         (0.07)     (0.02)        PIERRE 2  76 SMAG CHI TO (PI+PI-)        1/77*
R56         (0.12)     (0.04)        PIERRE 1  76 SMAG CHI TO (PI+PI-RHOO)    1/77*
R56         (0.17)     (0.08)        PIERRE 1  76 SMAG CHI TO (PI+K-K*0)      1/77*
R56         (0.32)     (0.06)        PIERRE 2  76 SMAG CHI TO 2(PI+PI-)       1/77*
R56          (.04)      (.013)       TRILLING  76 SMAG CHI TO(PI+PI-PBARP)    1/77*
R56         (0.27)     (0.07)        PIERRE 2  76 SMAG CHI TO (K+K-PI+PI-)    1/77*
R56         (0.14)     (0.05)        PIERRE 2  76 SMAG CHI TO 3(PI+PI-)       1/77*

R57     PSI(3685) INTO (CHI(3550) GAMMA)/TOTAL  (UNITS 10**-2)
R57 QB      (8.)       (3.)          VERNON    76 CNTR    E+E-,MONOCHR.GAM    1/77*
R57  B       7.0        2.0          BIDDICK   77 CNTR    E+E-,MONOCHR.GAM    3/77*
R57  B  VALID FOR ISOTROPIC DISTRIBUTION OF THE PHOTON
```

Data Card Listings

$\psi(3685)$, $\psi(4030)$, $\psi(4415)$

```
R58     PSI(3685) INTO (CHI(3550) GAMMA)/TCTAL  (UNITS 10**-2)
R58                   CHI(3550) INTO CHANNEL SPECIFIED IN COMMENTS
R58          (1.0)     (.6)         TRILLING  76 SMAG CHI TO(J/PSI GAMMA)  1/77*
R58          (2.2)     (1.0)        BIDDICK   77 CNTR CHI TO(J/PSI GAMMA)  3/77*
R58           (.02) OR LESS  CL=0.90 BRAUNSCHW 77 DASP CHI TO (2 GAMMA)     1/77*
R58          (0.023)  (0.013)       PIERRE 2  76 SMAG CHI TO (PI+PI-,K+K-  1/77*
R58          (0.050)  (0.030)       PIERRE 1  76 SMAG CHI TO (PI+PI-RHOO   1/77*
R58          (0.053)  (0.030)       PIERRE 1  76 SMAG CHI TO (PI+K-K*0)    1/77*
R58          (0.16)   (0.04)        PIERRE 2  76 SMAG CHI TO 2(PI+PI-)     1/77*
R58           (.002)   (.001)       TRILLING  76 SMAG CHI TO(PI+PI-PBARP)  1/77*
R58          (0.14)   (0.04)        PIERRE 2  76 SMAG CHI TO (PI+PI-K+K-)  1/77*
R58           (.008)   (.005)       TRILLING  76 SMAG CHI TO 3(PI+ PI-)    1/77*

R59     PSI(3685) INTO (PC(3510) GAMMA)/TCTAL  (UNITS 10**-2)
R59 QB       (9.)      (3.)         VERNON    76 CNTR   E+E-,MONOCHR.GAM  1/77*
R59  B        7.1       1.9         BIDDICK   77 CNTR   E+E-,MUNOCHR.GAM  3/77*
R59  B  VALID FOR ISOTROPIC DISTRIBUTION CF THE PHCTON

R60     PSI(3685) INTO (PC(3510) GAMMA)/TOTAL  (UNITS 10**-2)
R60                   PC(3510) INTO CHANNEL SPECIFIED IN COMMENTS
R60          (4.0)     (2.0)        WIIK      75 DASP PC TO (J/PSI GAMMA)  1/77*
R60          (2.4)     (.8)         TRILLING  76 SMAG PC TO (J/PSI GAMMA)  1/77*
R60          (5.0)     (1.5)        BIDDICK   77 CNTR PC TO (J/PSI GAMMA)  3/77*
R60           (.026)OR LESS  CL=0.90 BRAUNSCHW 77 DASP PC TC (2 GAMMA)     1/77*
R60          (0.015)CR LESS  CL=0.90 PIERRE 2  76 SMAG PC TO (PI+PI-,K+K-) 1/77*
R60          (0.026)  (0.022)       PIERRE 1  76 SMAG PC TC (PI+PI-RHOO))  1/77*
R60          (0.032)  (0.019)       PIERRE 1  76 SMAG PC TO (PI+K-K*0)     1/77*
R60          (0.11)   (0.04)        PIERRE 2  76 SMAG PC TO 2(PI+PI-)      1/77*
R60           (.01)    (.008)       TRILLING  76 SMAG PC TC (PI+PI-PBARP)  1/77*
R60          (0.06)   (0.03)        PIERRE 2  76 SMAG PC TO (PI+PI-K+K-)   1/77*
R60           (.17)    (.06)        TRILLING  76 SMAG PC TC 3(PI+ PI-)     1/77*

R61     PSI(3685) INTC (CHI(3455) GAMMA)/TOTAL  (UNITS 10**-2)
R61 SB       (5.)   OR LESS  CL=0.90 BADTKE    76 CNTR          E+E-      1/77*
R61  B       (2.5)  OR LESS  CL=0.90 BIDDICK   77 CNTR          E+E-      3/77*
R61  B  VALID FOR ISOTROPIC DISTRIBUTION OF THE PHOTON
R61 S   BADTKE 76 IS SUPERCEDED BY BIDDICK 77                             3/77*

R62     PSI(3685) INTC (CHI(3455) GAMMA)/TCTAL  (UNITS 10**-2)
R62                   CHI(3455) INTO CHANNEL SPECIFIED IN COMMENTS
R62       4  (0.8)    (0.4)         TRILLING  76 SMAG CHI TO(J/PSI GAMMA)  1/77*
R62          (0.031)OR LESS  CL=0.90 BRAUNSCHW 77 DASP CHI TO (2 GAMMA)     1/77*

------ --------- --------- --------- --------- --------- --------- --------

                    71  PSI(3685)      G(I)*G(E+E-)/G(TOTAL)  (KEV)

        THIS COMBINATION OF A PARTIAL WIDTH WITH THE PARTIAL WIDTH
        INTC E+E- AND WITH THE TCTAL WIDTH IS OBTAINED FROM THE INTEGRATED
        CROSS-SECTION INTO CHANNEL(I) IN THE E+E- ANNIHILATION.
        WE CNLY LIST DATA NOT HAVING BEEN USED TO DETERMINE THE PARTIAL
        WIDTH G(I) CR THE BRANCHING RATIC G(I)/TCTAL.

G3      G(HADRONIC)*G(E+E-)/G(TCTAL)
G3             2.2       .4             ABRAMS    75 SMAG       E+E-        1/76

****** ********* ********* ********* ********* ********* ********* ********
```


```
                         REFERENCES FOR PSI(3685)

ABRAMS    74 PRL 33 1453         +BRIGGS,AUGUSTIN,BOYARSKI+        (LBL+SLAC)

ABRAMS    75 STANFORD SYMP.25   G.S.ABRAMS                             (LBL)
ABRAMS1   75 PRL 34 1181        +BRIGGS,CHINOWSKY,FRIEDBERG,+     (LBL+SLAC)
AUBERT    75 PRL 33 1624        +BECKER,BIGGS,BURGER,GLENN+        (MIT+BNL)
BOYARSKI  75 PALERMO CONF. 54   +BREIDENBACH,BULCS,ABRAMS,BRIGGS+(SLAC+LBL)
CAMERINI  75 PRL 35 483         +LEARNED,PREPOST,ASH,ANDERSON,+ (WISC+SLAC)
CRIEGEE   75 PL 53B 489         +DEHNE,FRANKE,HCRLITZ,KRECHLOCK+      (DESY)
DASP3     75 PL 57B 407         BRAUNSCHWEIG,KCNIGS,+ (AACH+DESY+MPIM+TOKY)
FELDMAN   75 PRL 35 821         +JEAN-MARIE,SADOULET,VANNUCCI,+  (LBL+SLAC)
FELDMAN1  75 STANFORD SYMP.39   G.J.FELDMAN                           (SLAC)
GRECO     75 PL 56B 367         +PANCHERI-SRIVASTAVA,SRIVASTAVA       (FRAS)
HEINTZE   75 STANFORD SYMP.97   J.HEINTZE                       (HEIDELBERG)
JACKSON   75 NIM 128 13         J.D.JACKSON,C.SCHARRE                  (LBL)
HILGER    75 PRL 35 625         +BERON,FORD,HOFSTADTER,HOWELL,+ (STAN+PENN)
HUGHES    75  PREP.HEPL 765     +BERON,CARRINGTON,FORD,HILGER,+ (STAN+PENN)
LUTH      75 PRL 35 1124        +BOYARSKI,LYNCH,BREIDENBACH,+    (SLAC+LBL)JPC
LIBERMAN  75 STANFORD SYMP.55   A.D.LIBERMAN                      (STANFORD)
PREPOST   75 STANFORD SYMP.241  R.PREPOST                        (WISCONSIN)
SIMPSON   75 PRL 35 699         +BERON,FORD,HILGER,HCFSTADTER,+ (STAN+PENN)
TANENBAU  75 PRL 35 1323        TANENBAUM,WHITAKER,ABRAMS,+      (LBL+SLAC)
WIIK      75 STANFORD SYMP.69   B.H.WIIK                              (DESY)

BADTKE    76  PREPRINT          +BARNETT,+   (UMD+PAVI+PRIN+UCSD+SLAC+STAN)
BARTEL 1  76 PL 64 B 483        +DUINKER,OLSSCN,STEFFEN,HEINTZE+(DESY+HEID)
BARTEL 2  76 TBILISI CONF.N56   +DUINKER,OLSSON,HEINTZE,+        (DESY+HEID)
BRAUNSCH  76 PL 63 B 487        BRAUNSCHWEIG,+   (AACH+DESY+HAMB+MPIM+TOKY)
FELDMAN   76  SLAC-PUB-1851     G.J.FELDMAN                       (SLAC+LBL)
PIERRE 1  76  LBL-5324          F.PIERRE                          (SLAC+LBL)
PIERRE 2  76 TBILISI CONF.N46   F.PIERRE                     (SLAC+LBL+SACL)
PIERRE 3  76 SACLAY-DPHPE76-21  F.PIERRE                          (SLAC+LBL)
SNYDER    76 PRL 36 1415        +HOM,LEDERMAN,PAAR,APPEL,+ (COLU+FNAL+STON)
TANENBAU  76 PRL 36 402         TANENBAUM,ABRAMS,BCYARSKI,BULOS,+(SLAC+LBL)IG
TRILLING  76 STANFORD SYMP.437  G. H. TRILLING                         (LBL)
VERNON    76 TBILISI CONF.N63   W.VERNON     (UMD+PAVI+PRIN+UCSD+SLAC+STAN)
WHITAKER  76 PRL 37 1596        +TANENBAUM,ABRAMS,ALAM,BOYARSKI,+(SLAC+LBL)
WIIK      76 TBILISI CONF.N75   B.H.WIIK RAPPORTEUR                   (DESY)

BIDDICK   77 PRINT-77-0244UCSD  +BURNETT+    (UCSD+UMD+PAVI+PRIN+SLAC+STAN)
BRAUNSCH  77  DESY 77/03        BRAUNSCHWEIG,+   (AACH+DESY+HAMB+MPIM+TOKY)
WIIK      77  DESY 77/01        +WCLF                                 (DESY)

****** ********* ********* ********* ********* ********* ********* ********
****** ********* ********* ********* ********* ********* ********* ********
```


$\psi(4030)$

```
                  72  PSI(4030,JPG=1- ) I=

                  SEEN AS A NARROW PEAK IN E+E- INTO HADRONS.  SEE
        CHARMONIUM MINI-REVIEW.  NEEDS CONFIRMATICN.  NO EXPERIMENTAL
        ATTEMPT HAS BEEN MADE TO IDENTIFY SPECIFIC STATES IN THE
        4000-4300 GEV REGION.  THE NUMBER CF D ANC D* MESONS SEEN
        ASSOCIATED WITH THIS REGICN IS LARGER THAN EXPECTED FOR A MERE
        CHARMED PARTICLE PRODUCTION THRESHOLD EFFECT, SUGGESTING
        RESONANCE INTERPRETATICN FOR AT LEAST PART OF THE DATA.  OMITTED
        FROM TABLE.

------ --------- --------- --------- --------- --------- --------- --------

                  72  PSI(4030) MASS (MEV)

M          (4030.)                   PERUZZI   76 SMAG         E+E-        1/77*

------ --------- --------- --------- --------- --------- --------- --------

                  72  PSI(4030) PARTIAL DECAY MODES

                                                             DECAY MASSES
P1      PSI(4030) INTC  D DBAR
P2      PSI(4030) INTO  D* DBAR AND D*BAR D
P3      PSI(4030) INTC  D* D*BAR
P4      PSI(4030) INTO J/PSI(3100) HADRCNS

------ --------- --------- --------- --------- --------- --------- --------

                  72  PSI(4030) BRANCHING RATIOS

R1      PSI(4030) INTO (D D*)/TOTAL                      (P2)
R1          SEEN                     PERUZZI   76 SMAG         E+E-        1/77*

R2      PSI(4030) INTO J/PSI(3100) HADRONS               (P4)
R2          LOOKED FCR               BURMESTER 77 PLUT         E+E-        4/77*

****** ********* ********* ********* ********* ********* ********* ********
```


```
                         REFERENCES FOR PSI(4030)

AUGUSTIN 75 PRL 34 764        +BCYARSKI,ABRAMS,BRIGGS+          (SLAC+LBL)
BACCI    75 PL 58B 481        +BIDOLI,PENSO,STELLA,+           (ROMA+FRAS)
BOYARSKI 75 PRL 34 762        +BREIDENBACH,ABRAMS,BRIGGS,+      (SLAC+LBL)
ESPOSITO 75 PL 58B 478        +FELICETTI,PERUZZI,+  (FRAS+NAPO+PADO+RCMA)
SCHWITTE 75 STANFORD SYMP.5   R.F.SCHWITTERS                        (SLAC)

FELDMAN  76  SLAC-PUB-1851    G.J.FELDMAN                       (SLAC+LBL)
PERUZZI  76 PRL 37 569        +PICCOLO,FELDMAN,NGUYEN,WISS,+    (SLAC+LBL)

BURMESTE 77 DESY 77/19        +CRIEGEE,DEHNE+        (DESY+HAMB+SIEG+WUPP)
WIIK     77  DESY 77/01       +WCLF                                 (DESY)

****** ********* ********* ********* ********* ********* ********* ********
****** ********* ********* ********* ********* ********* ********* ********
```


$\psi(4415)$

```
                  73  PSI(4415,JPG=1- ) I=

                  RESONANCE-SHAPED STRUCTURE IN E+E- INTO HADRONS.
        NUMBER OF STATES IN THIS REGION, ANC SPECIFIC DECAY MODES UNKNOWN.

------ --------- --------- --------- --------- --------- --------- --------

                  73  PSI(4415) MASS (MEV)

M           4414.       7.           SIEGRIST  76 SMAG         E+E-        2/76

------ --------- --------- --------- --------- --------- --------- --------

                  73  PSI(4415) WIDTH (MEV)

W             33.       10.          SIEGRIST  76 SMAG         E+E-        2/76

------ --------- --------- --------- --------- --------- --------- --------

                  73  PSI(4415) PARTIAL DECAY MODES

                                                             DECAY MASSES
P1      PSI(4415) INTO E+ E-                                 .5+  .5

------ --------- --------- --------- --------- --------- --------- --------

                  73  PSI(4415) BRANCHING RATIOS

R1      PSI(4415) INTO (E+ E-)/TOTAL (UNITS 10**-5)
R1            1.3       .3           SIEGRIST  76 SMAG         E+E-        2/76

R2      PSI(4415) INTO HADRONS/TOTAL
R2          DOMINANT                 SIEGRIST  76 SMAG         E+E-        1/77*

****** ********* ********* ********* ********* ********* ********* ********
```


```
                         REFERENCES FOR PSI(4415)

SCHWITTE 75 STANFORD SYMP.5   R.F.SCHWITTERS                        (SLAC)

FELDMAN  76  SLAC-PUB-1851    G.J.FELCMAN                       (SLAC+LBL)
SIEGRIST 76 PRL 36 700        +ABRAMS,BOYARSKI,BREIDENBACH,+    (LBL+SLAC)

WIIK     77  DESY 77/01       +WOLF                                 (DESY)

****** ********* ********* ********* ********* ********* ********* ********
****** ********* ********* ********* ********* ********* ********* ********
```

HEAVY LEPTON SEARCHES AND EVIDENCE

This review is intended to summarize the recent experimental evidence for the existence of heavy leptons produced in e^+e^- collisions and the recent searches in neutrino and proton beams. For a more complete review up to 1974, see Perl and Rapidis.[1] See also the recent review of Llewellyn Smith.[2]

The known leptons are the electron and its neutrino (e^-, ν_e), the muon and its neutrino (μ^-, ν_μ), and their four antiparticles $(e^+, \bar{\nu}_e)$ and $(\mu^+, \bar{\nu}_\mu)$. Some of their properties are summarized in Table I.

TABLE I. Established leptons†

	Charge	Mass (MeV)	Lepton number	Interaction weak	e.m.	strong
e^-	-	0.51100	$n_e = +1$	yes	yes	no
ν_e	0	~0(<0.00006)	$n_e = +1$	yes	no	no
μ^-	-	105.659	$n_\mu = +1$	yes	yes	no
ν_μ	0	~0(<0.65)	$n_\mu = +1$	yes	no	no

†For antileptons, $(e^+, \bar{\nu}_e)$ and $(\mu^+, \bar{\nu}_\mu)$, change sign of charge and lepton number.

All are spin-1/2 fermions. The lepton numbers n_e and n_μ are found experimentally to be separately conserved as is indicated by the absence (at a level $< 2.2 \times 10^{-8}$, ref. 3) of the decay $\mu \to e\gamma$. Experiments are now being carried out to test this at a lower level.

Several types of heavy leptons (that is non-strongly-interacting fermions other than those in Table I) have been proposed. For purposes of discussion we distinguish four types.[1,2] Each has a corresponding antiparticle with opposite charge and lepton number. For convenience we omit writing the antiparticles in the following descriptions. The four types are:

Sequential Leptons (L^-, ν_L). Such a pair is assumed to have its own separately strictly conserved lepton number $n_L = +1$. This means that the radiative decays

$$\left.\begin{array}{l} L^- \to e^- \gamma \\ L^- \to \mu^- \gamma \end{array}\right\} \text{ are forbidden}$$

while the weak decays (assuming m_{L^-} sufficiently massive)

$$\left.\begin{array}{l} L^- \to \nu_L\, e^- \bar{\nu}_e \\ L^- \to \nu_L\, \mu^- \bar{\nu}_\mu \\ L^- \to \nu_L \text{ hadrons} \end{array}\right\} \text{ are allowed .}$$

There could be an increasing mass sequence of such pairs. It is frequently assumed that the neutrinos are massless.

Decay rates are assumed calculable from conventional weak interactions theory. For L^- mass between 1 and 3 GeV, the branching fraction to each of the two leptonic modes should be roughly 10% to 20%. For L^- mass above 1 GeV, the mean life should be $\lesssim 10^{-12}$ sec, too short to be observed in a track chamber.[1]

Paraleptons (E^+, E^0) and (M^+, M^0). These pairs have the same lepton numbers as the opposite-charge ordinary leptons, i.e., e^- and μ^-, respectively. Radiative decays are again forbidden and decays similar to those allowed for L^- are allowed here, e.g.,

$$M^+ \to \nu_\mu\, e^+ \nu_e$$

$$\text{or} \qquad M^+ \to \nu_\mu\, \mu^+ \nu_\mu \quad .$$

However, the lightest member is not stable as is the case for sequential leptons, so that bizarre decay schemes such as (assuming $m_{E^0} < m_{E^+}$)

$$E^+ \to E^0\, \mu^+ \nu_\mu, \qquad E^0 \to e^- e^+ \nu_e$$

are allowed.

Heavy leptons of this type (and/or a neutral intermediate boson Z^0) are desired in unified gauge theories of weak and electromagnetic interactions to cancel unphysical high energy behavior in such processes as $e^+e^- \to W^+W^-$.[4]

Ortholeptons $(F^-$ and $N^-)$. These have the same lepton numbers as e^- and μ^-, respectively. They may or may not have associated neutral leptons.

Data Card Listings

HEAVY LEPTON SEARCHES AND EVIDENCE

Radiative decays are allowed in addition to weak modes similar to those of sequential leptons. The radiative mode can dominate or can be relatively unimportant depending on the model.[5] Decays such as

$$F^- \to e^- + \text{hadrons}$$

are also allowed.

Long-lived Penetrating Particles. Heavy leptons could have long mean lives under certain circumstances. For example, if $m_{\nu_L} > m_{L^-}$, then L^-, the sequential lepton, is completely stable since its lepton number is conserved.

Experimental Results

Recent experimental efforts related to heavy leptons come primarily from e^+e^- experiments, neutrino beam experiments, and proton beam experiments.

e^+e^- colliding beam experiments provide a powerful tool for investigating heavy lepton hypotheses. Charged heavy leptons, regardless of type, are expected to be pair-produced via a massive virtual photon in e^+e^- collisions.

Strong evidence for the existence of a heavy lepton with mass in the range 1.6 - 2.0 GeV has been obtained. PERL 75-76, a SLAC SPEAR magnetic detector experiment, looks for anomalous $e\mu$ events of the form

$$e^+e^- \to e^\pm\mu^\mp + \text{missing momentum} \quad .$$

They find 105 examples after subtracting a 34 event background from hadron misidentification, weak decays of charmless hadrons, $e \to \mu$ misidentification, and other known sources. The missing momentum could include charged tracks or photons outside the acceptance of the detector, neutrons, K^0_L, or neutrinos. Electromagnetic processes (e.g., $e^+e^- \to e^+e^-\mu^+\mu^-$ with two missed charged tracks) can be ruled out by their calculated rates and by the absence of events with $e^+\mu^+$ and $e^-\mu^-$ pairs.

These events have no conventional explanation and signal the existence of an unknown process. Production and weak leptonic decay of a pair of charged heavy leptons (L) or charmed bosons (B) are obvious candidates for the process, e.g.,

$$e^+e^- \to L^+L^- \qquad L^- \to \nu_L\mu^-\bar{\nu}_\mu \,, \qquad L^+ \to \bar{\nu}_L e^+\nu_e$$

or

$$e^+e^- \to B^+B^- \qquad B^- \to \mu^-\bar{\nu}_\mu \,, \qquad B^+ \to e^+\nu_e \quad .$$

The charged-particle momentum spectrum strongly favors three-body decays and limits the mass of the undetected particles to less than 700 MeV (CL = 95%). An analysis of events with an $e^\pm\mu^\mp$ and photons, K^0_S, or additional charged tracks puts an upper limit of 39% (CL = 90%) on the fraction of the anomalous events which could have an undetected γ, π^0, K^0, η, or charged track. Thus if a single hypothesis is to explain all of the data then the heavy lepton hypothesis is strongly favored. However, a conspiracy of charmed particle leptonic and semileptonic decays could conceivably give rise to similar results. PERL 75 estimate the heavy lepton mass to be 1.6 - 2.0 GeV.

Inclusive anomalous (not from well known sources) muon production,

$$e^+e^- \to \mu^\pm \text{ anything} \quad ,$$

has been reported by CAVALLI-SFORZA 76 and FELDMAN 77. CAVALLI-SFORZA 76, another SPEAR experiment, finds ~9 two-prongs and ~0 with three or more prongs. Snow[6] argues that these results are compatible with heavy lepton decay but not with higher multiplicities expected in charmed meson decay. FELDMAN 77, with higher statistics in the same experiment as PERL 75-76, sees both two-prong and three-or-more prong anomalous muon signals with cross sections consistent with CAVALLI-SFORZA 76. A heavy lepton hypothesis can explain the FELDMAN 77 two-prong data for all energies 3.9 GeV < $E_{c.m.}$ < 7.8 GeV, and their lower energy three-and-more-prong data. However, for energies 5.8 - 7.8 GeV, additional sources, e.g., charmed particles, are required to explain the large three-and-more-prong signal.

HEAVY LEPTON SEARCHES AND EVIDENCE

Inclusive anomalous electron production has been studied by BRAUNSCHWEIG 76 (see reference section of Charm Searches and Evidence Data Card Listings), a DORIS DASP experiment at c.m. energy 4.0 - 4.2 GeV. The electron momentum spectrum and the observed multiplicity indicate that these events do not come from sequential lepton production but could come from charmed hadron production. The electron momenta observed here are so low (<800 MeV) that the SLAC experiments would have excluded most of these events from their sample. Based on the FELDMAN 77 anomalous muon cross sections, one expects to see only a few events with electron momentum above 800 MeV, so there is no conflict between these two results.

Assuming that the heavy lepton exists, its type is still undetermined. Neutrino experiments discussed below rule out paramuons M^+ and tend to rule out orthomuons N^-. Ali and Yang[8] suggest that the PERL 75 ee:μe:$\mu\mu$ ratio indicates that the τ (as it is now called by the PERL 75-76, FELDMAN 77 authors) is not a para-electron E^+. This leaves the sequential lepton L^- and the ortho-electron F^- as the most likely candidates.

Neutrino experiments which have a ν_μ beam can produce single heavy leptons which have the same muon number as a μ^-. Signature heavy lepton events are those leading to final-state charged leptons other than the normal charged current μ^-, e.g.,

$$\nu_\mu N \to N^- \text{ hadrons}, \quad N^- \to \nu_\mu e^- \bar{\nu}_e$$

$$\nu_\mu N \to M^+ \text{ hadrons}, \quad M^+ \to \nu_\mu \mu^+ \nu_\mu \text{ or } M^+ \to \nu_\mu e^+ \nu_e$$

$$\nu_\mu N \to M^0 \text{ hadrons}, \quad M^0 \to \mu^- e^+ \nu_e \quad .$$

BARISH 74, a Caltech-Fermilab narrow-band neutrino beam experiment has searched for M^+ via the μ^+ mode. The small μ^+ signal observed is consistent with beam contamination by $\bar{\nu}_\mu$. The expected number of events is calculated as a function of M^+ mass assuming a weak coupling constant equal to the universal Fermi constant and a branching fraction to muons of 30%. Their null signal sets a 90% confidence lower limit of 8.4 GeV < M^+ mass. This poses difficulties for those gauge models using M^+ which require its mass to be less than about 7 GeV in order to be consistent with experimental measurements of the muon magnetic moment.[9]

EICHTEN 73 looks for M^+ via the e^+ decay mode, and, assuming a 15% branching fraction, sets a limit of 2.4 GeV < M^+ mass.

ASRATYAN 74 use the data of EICHTEN 73 on electron and positron production in ν_μ and $\bar{\nu}_\mu$ beams to obtain a lower limit 1.8 GeV < N^- mass at the 90% confidence level. Albright[5] argues that even a 1.8 GeV N^- can probably be ruled out if the y distribution and neutral-to-charged-current ratio are considered.

Proton-nucleon collisions have the advantage of large available c.m. energy for production of heavy particles. They have the disadvantage that the lepton production mechanism is not as well understood as it is for e^+e^- collisions and neutrino collisions. Also, backgrounds from copious strong processes pose problems. Pair production from virtual electromagnetic processes is the expected mode of production.

Several approaches have been used in these searches. One is to assume the existence of long-lived charged heavy leptons and to pass the secondaries through an absorber to filter out strongly interacting particles, and a system of scintillation counters and Čerenkov counters to identify hadrons and muons. The cross-section and differential-cross-section limits given in the Data Card Listings for charged heavy lepton production are done in this manner. Mass limits can also be obtained if a model for the production is assumed. BUSHNIN 73 assumes pair production analogous to $\mu^+\mu^-$ production and scales lower energy μ-pair production to obtain cross-section predictions which rule out stable or long-lived charged leptons in the mass range 0.55 to 4.5 GeV.

Data Card Listings

HEAVY LEPTON SEARCHES AND EVIDENCE

FAISSNER 76 looked for long-lived neutral heavy leptons in

$$pN \to L^{+}\ \text{anything}, \quad L^{+} \to L^{o}\ \text{anything}$$

in a "beam dump" type CERN Gargamelle experiment. The L^+ and L^o here mean any type charged and neutral heavy leptons. The L^o could be detected by its decay or its interaction in the bubble chamber. Protons struck a mercury target in a 22-meter-thick steel muon shield. Most hadrons were absorbed before weak decay, thus suppressing normal neutrino flux. However, prompt decays such as expected of the L^+ would not be suppressed. No signal above background was observed, ruling out L^o with lifetime 1 μsec - 1 msec as proposed by DE RUJULA 75 to explain the KRISHNASWAMI 75 Kolar Gold Mine cosmic ray events.

Another approach to heavy lepton hunting in pN collisions has been to search for high-transverse-momentum direct lepton production, i.e., for high p_T leptons not originating from well known weak decays. Other possible candidates for parents of direct leptons are charmed particles, intermediate bosons, high p_T vector mesons, and massive virtual photons; so we have listed these papers in the Other New Particle Searches section of the Data Card Listings. Recent evidence on absence of muon polarization (LAUTERBACH 76, LEIPUNER 76) and μ-pair origin (KASHA 76, BRANSON 77) favors an electromagnetic origin. However, contradictory evidence indicating non-zero muon polarization and weak decay has also been reported (ANISIMOVA 76).

References

1. M. L. Perl and P. Rapidis, SLAC-Pub-1496 (October 1974).
2. C. H. Llewellyn Smith, Invited paper presented at the Royal Society Meeting on New Particles and New Quantum Numbers, 11 March 1976, Oxford Ref. 33/76.
3. S. Parker, H. L. Anderson, and C. Rey, Phys. Rev. 133B, 768 (1964).
4. J. D. Bjorken and C. H. Llewellyn Smith, Phys. Rev. D7, 887 (1973).
5. F. Wilczek and A. Zee, Nucl. Phys. B106, 461 (1976).
6. G. A. Snow, Phys. Rev. Lett. 36, 766 (1976).
7. C. H. Albright, Phys. Rev. D13, 2508 (1976).
8. A. Ali and T. C. Yang, Phys. Rev. D14, 3052 (1976).
9. J. Primack and H. Quinn, Phys. Rev. D6, 3171 (1972). Additional references in reference 3 of BARISH 74.


```
M        HEAVY LEPTON MASS LIMITS (GEV)
M    B   0    0.6   OR MORE               BACCI      73 ELEC +- ORTHOELECTRON(F)  1/76
M    B   0    2.2   OR MORE               BACCI      73 ELEC +- ORTHOELECTRON(F)  1/76
M    C   0    2.0   OR MORE  CL=.90       BARISH     73 ASPK +  PARAMUON (M)      2/74
M    D   0    1.4   OR MORE  CL=.95       BERNARDIN  73 ASPK +- ANY NON-RAD TYPE  2/74
M    D   0    1.0   OR MORE  CL=.95       BERNARDIN  73 ASPK +- ANY NON-RAD TYPE  2/74
M    N  NONE BETWEEN 0.55 AND 4.5         BUSHNIN    73 CNTR -  LONG-LIVED        2/74
M    E   0    2.4   OR MORE  CL=.90       EICHTEN    73 HLBC +  PARAMUON (M)      3/74
M    A        1.8   OR MORE  CL=.90       ASRATYAN   74 HLBC +- ORTHOMUON (N)    11/75
M    F        8.4   OR MORE  CL=.90       BARISH     74 SPEC +  PARAMUON (M)      7/74
M    O   0    1.15  OR MORE  CL=.95       ORITO      74 ASPK +- ANY NON-RAD TYPE 11/75
M    P  64 BTWN 1.6 AND 2.0               PERL       75 SPEC +- ANY NON-RAD TYPE  1/76
M
M                                 COMMENTS                                        3/77*
M      LIMITS APPLY ONLY TO HEAVY LEPTON TYPE GIVEN IN COMMENT AT RIGHT ON        3/77*
M      DATA CARD.  SEE REVIEW ABOVE FOR DESCRIPTION OF TYPES.                     3/77*
M      IN COMMENTS BELOW; ALL BEAMS ARE MU TYPE NEUTRINO OR ANTINEUTRINO.         3/77*
M      L,E,M,F,N STAND FOR SEQUENTIAL LEPTON,PARA-ELECTRON,PARA-MUON,             3/77*
M      ORTHO-ELECTRON,ORTHO-MUON RESPECTIVLY.                                     3/77*
M
M    B BACCI 73 IS FRASCATI E+E- EXPT. LOOKS FOR F --> E GAMMA.                   1/76
M    B MASS LIMIT DEPENDS ON COUPLING CONSTANT LAMBDA FOR THIS DECAY.             1/76
M    B FIRST VALUE ABOVE IS FOR LAMBDA**2 GT 9*10**-5, 2ND IS FOR                 1/76
M    B LAMBDA**2 GT 10**-3.                                                       1/76
M    C BARISH 73 IS FNAL 50,145 GEV NEU EXPT.  LOOKS FOR (NEU NUCLEON -->         3/77*
M    C M+ ANYTHING). ASSUMES (M+ --> MU+ NEU NEU) WITH BR=.3.                     3/77*
M    D BERNARDINI 73 IS FRASCATI E+E- EXPT. FIRST VALUE ASSUMES UNIVERSAL         2/74
M    D COUPLING TO ORDINARY LEPTONS.  SECOND VALUE ALSO ASSUMES COUPLING          2/74
M    D TO HADRONS.                                                                2/74
M    N BUSHNIN 73 IS SERPUKOV 70 GEV P EXPT. MASSES ASSUME MEAN LIFE ABOVE        2/74
M    N 7E-10 AND 3E-8 RESPECTIVELY. CALCULATED FROM CROSS SEC(DC BELOW)           2/74
M    N AND 30 GEV MUON PAIR PRODUCTION DATA.                                      2/74
M    E EICHTEN 73 IS CERN 1-10GEV NEU EXPT. LOOKS FOR M+ PRODUCED IN              2/76
M    E NEU NUCL --> M+ HADRONS ASSUMING 15 PERCENT DECAY TO E+ NEU NEU.           2/76
M    A ASRATYAN 74 USES EICHTEN 73 DATA ON NEU NUCL --> E- HADRONS AND            2/76
M    A ANTINEU NUCL --> E+ HADRONS TO SET LIMITS ON ORTHOMUON PRODUCTION.         2/76
M    F BARISH 74 IS FNAL 50,135 GEV NEU EXPT.  LOOKS FOR (NEU NUCLEON -->         7/74
M    F M+ ANYTHING).  ASSUMES (M+ -->MU+ NEU NEU) WITH BR=.3.                     7/74
M    O ORITO 74 LOOKED FOR H+H- PAIRS GIVING MU-E PAIRS. MASS LIMIT REFERS        3/74
M    O TO ANY NON-RADIATIVE TYPE HEAVY LEPTON: L, E, M, F, N.                     3/74
M    O COUPLING TO HADRON ASSUMED FROM THEORETICAL MODELS.                        3/74
M    P PERL 75 EVENTS ARE E+ E- TO E+- MU-+ AND TWO OR MORE MISSING               1/76
M    P PARTICLES,DONE AT SLAC (SPEAR). AUTHORS CLAIM NO CONVENTIONAL              1/76
M    P EXPLANATION FOR THESE EVENTS.  TOTAL CM ENERGY 3-7.5 GEV.                  1/76

CE       HEAVY LEPTON PRODUCTION CROSS SECTION (E+ E-) (UNITS 10**-35 CM**2)
CE   P  64   (1.9)    (0.5)             PERL       75 SMAG    ECM=4.8 GEV         2/76
CE   C   9   28.5     15.1     11.3     CAVALLISF  76 SPEC    ECM=4.8 GEV         8/76*
CE   P 105   (1.9)    (0.5)             PERL       76 SMAG    ECM=4.8 GEV         3/77*
CE   F  15   19.4      7.1              FELDMAN    77 SMAG    ECM=3.9-4.3 GEV     2/77*
CE   F  18   25.3      8.6              FELDMAN    77 SMAG    ECM=4.5-4.8 GEV     2/77*
CE   F 105   21.2      4.9              FELDMAN    77 SMAG    ECM=5.8-7.8 GEV     2/77*
CE   P  PERL 75 IS SLAC(SPEAR) EXPT .  EVENTS ARE E+E- TO E+-MU-+ AND 2 OR        2/76
CE   P  MORE MISSING PARTICLES.  CS IS FOR ECM=4.8 GEV AND THETA=50-130DEG.       2/76
CE   P  CROSS SECTION RISES FROM 5X10**-36 AT E=4 TO ABOVE MAX. THEN DROPS        2/76
CE   P  TO 6E-36  AT E=7.5.   AUTHORS SAY THESE EVENTS HAVE NO CONVENTIONAL       2/76
CE   P  EXPLANATION.  SUGGEST HEAVY LEPTON OR CHARMED HADRON, M=1.6-2.0GEV.       2/76
CE   P  PERL 76 INCLUDES PERL 75. NOT CORRECTED FOR DETECTOR ACCEPTANCE.          3/77*
CE   C  CAVALLISF 76 IS SLAC(SPEAR) EXPT AT 4.8 GEV CM. RESULT GIVEN ABOVE        8/76*
CE   C  IS TOTAL MUON INCLUSIVE CS FOR 2 CHARGED PRONGS AND MU MOMENTUM GT        8/76*
CE   C  1.05 GEV/C. ASSUMES ISOTROPY. DIFF CS AT THETA=90 DEG IS 23 PB/SR.        8/76*
CE   C  SNOW 76 SAYS RESULT COMPATIBLE WITH HEAVY LEPTON,NOT CHARMED MESON.       8/76*
CE   F  FELDMAN 77 IS A CONTINUATION OF PERL 75. ABOVE DATA IS FOR TWO-           2/77*
CE   F  PRONG EVENTS. DATA ON 3-PRONG EVENTS IS ALSO GIVEN. FOR THIS DATA,        2/77*
CE   F  SEE MORE ANOMALOUS MUON PROD THAN EXPECTED FROM HEAVY LEPTON DECAYS       2/77*
CE   F  ALONE. COULD BE FROM DECAYS OF CHARMED HADRONS.                           2/77*

DC       HEAVY LEPTON PRODUCTION DIFF. CROSS SEC. (P NUCLEON) (CM**2/SR-GEV)
DC   G   0  1.6E-37 OR LESS  CL=.90    GOLOVKIN   72 CNTR- 70GEV P, SERPUKHOV     1/76
DC B     0  4. E-38 OR LESS  CL=.90    BUSHNIN    73 CNTR- 70GEV P, SERPUKHOV     2/74
DC   G  MASS RANGE 1 TO 4.5 GEV,THETA=0,P=25 GEV/C.                               1/76
DC B    BUSHNIN 73 HEAVY LEPTON PATH TRAVERSES 6800 GM/CM**2 ABSORBER.            2/74
DC B    DIFFERENTIAL CROSS-SECTION MEASURED AT P=30 GEV/C THETA= 2 MRAD.          3/74

IC       INVARIANT HEAVY LEPTON PROD. CROSS SEC. (P NUCLEON) (CM**2/GEV**2)
IC   S   0  5.4E-39 OR LESS  CL=.90    CRONIN     74 SPEC -  M=1-6.8 GEV          1/76
IC   B   0  6.4E-35 OR LESS  CL=.90    BINTINGER  75 SPEC +- M=1-5 GEV            2/76
IC   S  CRONIN 74 IS AN FNAL 300 GEV P CU EXPT.  LOOKED FOR LONG LIVED            2/76
IC   S  PENETRATING PARTICLES.  ABOVE LIMIT ASSUMES STABLE.  MULTIPLY IT BY       2/76
IC   S  EXP(1.22E-8*M/TAU) FOR MASS M(GEV) AND LIFETIME TAU(SEC). LIMIT           2/76
IC   S  OBTAINED AT THETA(LAB) = 77 MRAD, PT = 2.38 GEV/C.                        4/77*
IC   B  BINTINGER 75 IS A 30-300 GEV P C EXPT.  LOOKED FOR LONG LIVED             2/76
IC   B  PENETRATING PARTICLES.  ABOVE LIMIT ASSUMES STABLE.  MULTIPLY IT BY       2/76
IC   B  EXP(3.5E-8*M/TAU/P) FOR MASS M(GEV), LIFETIME TAU(SEC), MOM.P(GEV).       2/76
IC   B  OBTAINED AT THETA(LAB) = 91 MRAD, PT = 1-2.25 GEV/C.                      4/77*

CN       NEUTRAL HEAVY LEPTON PRODUCTION CROSS SECTION  (CM**2)
CN   K    5 (1. E-37 OR MORE)                KRISHNASW  75 CNTR +0-  M=2-5 GEV    2/76
CN   B    0                                  BENVENUTI  75 SPEC  0                2/76
CN   K  KRISHNASWAMY 75 IS KOLAR GOLD MINE COSMIC RAY EXPT.  TYPICAL EVENT        2/76
CN   K  HAS VERTEX IN AIR 70 CM FROM WALL WITH THREE OBSERVED CHARGED             2/76
CN   K  TRACKS.  AUTHORS SUGGEST NEU+ROCK GIVES NEW PARTICLE WITH MEAN LIFE       2/76
CN   K  1OE-9 SEC OR LONGER.  DE RUJULA 75 GIVES ANOTHER INTERPRETATION.          2/76
CN   K  SEE ALSO RAJASEKARAN 75.                                                  8/76*
CN   B  BENVENUTI 75 IS AN FNAL EXPERIMENT WHICH ROUGHLY SIMULATES THE            2/76
CN   B  KRISHNASWAMY 75 EXPT. BUT APPARENTLY CONTRADICTS IT, FINDING NO           2/76
CN   B  EVENTS. SENSITIVE TO DECAYS OF NEUTRAL PENETRATING PARTICLES              3/77*
CN   B  PRODUCED BY THE PRIMARY PROTONS OR BY SECONDARY NEUTRINO                  3/77*
CN      [illegible] THE 1 KM. NEUTRINO BEAM EARTH SHIELD.                         3/77*
```

```
CP      NEUTRAL HEAVY LEPTON PROD. CROSS SEC. (PROTON NUCLEON) (CM**2)
CP   F    0  1. E-29 OR LESS              FAISSNER  76 HLBC 0             1/77*
CP   F  FAISSNER 76 LIMIT ASSUMES STABLE NEUTRAL WEAKLY INTERACTING LEPTON.  1/77*
CP   F  ALSO RULES OUT DE RUJULA 75 INTERP. OF 5 KRISHNASWAMY 75 EVENTS AS   1/77*
CP   F  (P NUCLEON --> L+ X, L+ --> LO X) UNLESS L+ MASS IS ABOVE 3 GEV.     1/77*

RI      HEAVY LEPTON BR INTO (E- OR MU- + 2 NEUTRINOS)/(TOTAL)                3/77*
RI   P 105    0.17       0.06       0.03  PERL       76 SPEC               3/77*
RI   P  ASSUMES EQUAL DECAY RATES TO E- AND MU- MODES, V-A COUPLING, MASS   3/77*
RI   P  OF HEAVY LEPTON=1.8 GEV/C**2, MASS OF ASSOCIATED NEUTRINO=0.        3/77*
RI   P  PERL 76 EXPT IS CONTINUATION OF PERL 75,INCLUDES THE 64 OLD EVENTS.  3/77*

****** ********* ********* ********* ********* ********* ********* ********

                                REFERENCES FOR HEAVY LEPTON SEARCHES

GOLOVKIN 72 PL 42B 136          +GRACHEV,KHODYREV,KUBAROVSKY+          (SERP)

BACCI    73 PL 44B 530          +PARISI,PENSO,SALVINI,STELLA+    (ROMA+FRAS)
BARISH   73 PRL 31 410          +BARTLETT,BUCHHOLZ,HUMPHRIY+      (CIT+FNAL)
BERNARDI 73 NC 17A 383          BERNARDINI,BOLLINI,BRUNINI+(CERN+BGNA+FRAS)
    ALSO 70 LNC 4 1156          ALLES-BORELLI,BERNARDINI,BOLLINI+     (CERN)
BUSHNIN  73 NP B58 476          +DUNAYTZEV,GOLOVKIN,KUBAROVSKY +      (SERP)
    ALSO 72 PL 42B 136          GOLOVKIN,GRACHEV,SHODYREV +           (SERP)
EICHTEN  73 PL 46B 281          +DEDEN+(AACH+BELG+CERN+EPOL+MILA+LALO+LOUC)

ASRATYAN 74 PL 49B 488          +GERSHTEIN,KAFTANOV,KUBANTZEV,LAPIN+ (SERP)
BARISH   74 PRL 32 1387         +BARTLETT,BUCHHOLZ,MERRITT +      (CIT+FNAL)
CRONIN   74 PR D10 3093         +FRISCH,SHOCHET,BOYMOND,MERMOD + (EFI+PRIN)
CRITO    74 PL 48B 165          +VISENTIN,CERADINI,CONVERSI +     (FRAS+ROMA)

BENVENUT 75 PRL 35 1486         BENVENUTI,CLINE,FORO+ (HARV+PENN+WISC+FNAL)
BINTINGE 75 PRL 34 982          BINTINGER,CURRY+        (EFI+HARV+PENN+WISC)
KRISHNAS 75 PL 57B 105          KRISHNASWAMY,MENON+          (BOMBAY+OSAKA)
    ALSO 75 PRL 35 628          DE RUJULA,GEORGI,GLASHOW              (HARV)
    ALSO 75 PRAMANA 5 78        RAJASEKARAN,SARMA                     (TATA)
PERL     75 PRL 35 1489         +ABRAMS,BOYARSKI,BREIDENBACH +    (LBL+SLAC)

CAVALLIS 76 PRL 36 558          CAVALLI-SFORZA,GOGGI +       (PAVI+PRIN+UMD)
    ALSO 76 PRL 36 766          GEORGE SNOW                            (UMD)
FAISSNER 76 PL 60B 401          +HASERT+(AACH+BELG+CERN+EPOL+MILA+OXF+LOUC)
PERL     76 PL 63B 466          +FELDMAN,ABRAMS,ALAM,BOYARSKI +   (SLAC+LBL)

FELDMAN  77 PRL 38 117          +BULOS,LUKE,ABRAMS,ALAM,BOYARSKI+(SLAC+LBL)

                                PAPERS NOT REFERRED TO IN THE DATA CARDS

                                ORTHOLEPTONS WITH LEPTON GAMMA COUPLING
BEHREND  65 PRL 15 900          +BRASSE,ENGLER,GANSSAUGE+        (DESY+KARL)
BETOURNE 65 PL 17 70            +NGUYEN NGOC,PEREZ Y JORBA+           (ORSA)
BUDNITZ  66 PR 141 1313         +DUNNING,GOITEIN,RAMSEY,WALKER,WILSON(HARV)
BOLEY    68 PR 167 1275         +ELIAS,FRIEDMAN,HARTMANN,KENDALL+ (MIT+CEA)
BERNARDI 69 NCL 1 15            BERNARDINI,FELICETTI+       (FRAS+NAPL+ROMA)
LIBERMAN 69 PRL 22 663          +HOFFMAN,ENGELS,IMRIE+(HARV+CASE+MCGI+SLAC)
LICHTENS 70 PR D1 825           LICHTENSTEIN,ASH,BERKELMAN,HARTILL+  (CORN)
HANSON   73 NCL 7 587           +LEONG,NEWMAN,LAW,LITKE+(MIT+HARV+CEA+HAIF)

                                LONGLIVED
COCCONI  60 PRL 5 19            +FAZZINI,FIDECARO,LEGROS,LIPMAN+      (CERN)
COOK     61 PR 123 655          +KEEFE,KERTH,MURPHY,WENZEL,ZIPF        (LRL)
FRANZINI 65 PRL 14 196          +LEONTIC,RAHM,SAMIOS,SCHWARTZ    (BNL+COLU)
BARNA    68 PR 173 1391         +COX,MARTIN,PERL,TAN,TONER,ZIPF+(SLAC+STAN)
ANSORGE  73 PR D7 26            +BAKER,KRZESINSKI,NEALE,RUSHBROOKE+  (CAVE)

                                RAMM TYPE
ROTHE    69 NP B10 241          K.W.ROTHE,A.M.WOLSKY                  (PENN)
RAMM     70 NATURE 227 1323     C.A.RAMM                              (CERN)
RAMM     71 NAT.PH.SC.230 145   C.A.RAMM                              (CERN)
CLARK    72 NATURE 237 388      +ELIOFF,FIELD,FRISCH,JOHNSON,KERTH+    (LBL)

****** ********* ********* ********* ********* ********* ********* ********
****** ********* ********* ********* ********* ********* ********* ********
```

INTERMEDIATE BOSON SEARCHES

```
------ --------- --------- --------- --------- --------- --------- --------

M       W BOSON MASS LIMITS (GEV)
M    B   0      1.7   OR MORE  CL=.99   BERNARDIN 65 HYBR +  NEU N, CERN       2/74
M    B   0      2.0   OR MORE  CL=.90   BURNS     65 OSPK +  NEU N, BNL        2/74
M    C   0      3.8   OR MORE  CL=.90   BARISH    73 ASPK +  W+ TO LEP+NEU=.2  2/74
M    C   0      4.5   OR MORE  CL=.90   BARISH    73 ASPK +  W+ TO LEP+NEU=.5  2/74
M    C   0      4.7   OR MORE  CL=.90   BARISH    73 ASPK +  W+ TO LEP+NEU=.8  2/74
M    E   0      5.0   OR MORE  CL=.95   BERGESON  73 ELEC                      1/76
M    U   0 NONE WITH MASS 10-20 GEV    BUSSER    74 WIRE +-0 P-P,52.7 GEV CM  8/76*
M    B  LOOKED FOR (NEU N) TO (W+ MU- N), W+ TO (MU+ NEU, E+ NEU, OR HDRNS)  2/74
M    C  BARISH 73 LOOKED FOR (NEU N) TO (W+ MU- N), W+ TO (MU+ NEU) AT NAL.  2/74
M    C  RESULT GIVEN FOR THREE ASSUMED BR.FRACS. W+ TO (LEPTON NEU)/ALL.     2/74
M    E  BERGESON 73 LOOKED AT ENERGY DISTR OF NEU-INDUCED MUON FLUX UNDER-   1/76
M    E  GROUND. SCALE INVARIANCE OF THE INELASTIC STRUCT FN ASSUMED.         1/76
M    U  BUSSER 74 IS CERN ISR EXPT. LOOKED FOR ELECTRONS OF LARGE            8/76*
M    U  TRANSVERSE MOMENTUM. RESULT QUOTED ABOVE IS MODEL DEPENDENT.         8/76*

C       W BOSON PRODUCTION CROSS SECTION (10**-36 CM**2)
C    A   0     6.0    OR LESS                ANKENBRAN 71 CNTR +- W TO(MU NEU)=1.0  2/74
C    A  ANKENBRANDT 71 LOOKED FOR (P N)TO(W HADRONS), W TO (MU NEU) AT BNL.  2/74
C    A  THIS ASSUMES BR OF W TO MU NEU IS 1.  IN GENERAL THIS VALUE IS      2/74
C    A  6.0/BR, WHERE BR=(W TO MU NEU)/(W TO ALL).                           2/74

S       SCALAR BOSON MASS LIMITS (GEV)
S    C   0   10.0   OR MORE  CL=.90   CONVERSI  73 ASPK  0 E+E- FRASCATI     3/74
S    C  CONVERSI 73 LOOKED FOR QED VIOLATION IN E+E- SCATTERING AT 2.8 GEV   3/74
S    C  AND ASSUMED W BOSON MASS=10 GEV.  FOR MW=15 GEV, MS LIMIT= 6.5 GEV   3/74

****** ********* ********* ********* ********* ********* ********* ********

                                REFERENCES FOR INTERMEDIATE BOSON SEARCHES

BERNARDI 65 NC 38 608           BERNARDINI,BIENLEIN,BOHM,DARDEL,+     (CERN)
BURNS    65 PRL 15 42           +GOULIANOS,HYMAN,LEDERMAN,LEE +  (COLU+BNL)
ANKENBRA 71 PR D3 2582          ANKENBRANDT,LARSEN,LEIPUNER+     (BNL+YALE)
BARISH   73 PRL 31 180          +BARTLETT,BUCHHOLZ,HUMPHREY+      (CIT+FNAL)
BERGESON 73 PRL 31 66           +CASSIDAY,HENDRICKS                   (UTAH)
CONVERSI 73 PL 46B 269          +D'ANGELO,GATTO,PAOLUZI               (ROMA)
BUSSER   74 PL 48B 371          +CAMILLERI,DI LELLA +       (CERN+COLU+ROCK)

****** ********* ********* ********* ********* ********* ********* ********
****** ********* ********* ********* ********* ********* ********* ********
```

QUARK SEARCHES

We have attempted to make the listings of free quark searches more complete in this edition. To that end, we have relied heavily on the recent review of L. Jones.[1]

There is currently no confirmed evidence for the existence of free quarks. The best searches for quarks in cosmic rays yield upper limits on the flux of quarks of about $10^{-11}cm^{-2}ster^{-1}sec^{-1}$. Cross-section upper limits established from proton accelerator experiments and calculations based on production models[2] imply that free quarks have a mass greater than about 5 GeV. Mass limits from photon and electron beam searches are slightly lower, but more reliable, depending only on the QED calculations for quark pair production. Limits on free quark concentrations in stable matter vary enormously depending on the source of matter and the technique.

We group quark searches by experimental technique — proton accelerators, electron accelerators, cosmic rays, and stable matter. Proton accelerator experiments generally measure quark production cross sections (we quote these in section C) and differential cross sections (section D). Searches with photon or electron beams may measure differential cross sections (section G) and set limits on the quark mass (section M). Cosmic ray experiments measure quark flux (section F), and searches in stable matter measure quark concentration (section RHO). Most of the accelerator and cosmic ray experiments have searched for fractionally charged particles, but some have searched for massive stable particles which would have low velocity. The latter searches are usually sensitive to a range of charges and may appear in the section below on Other New Particle Searches.

References

1. L.W. Jones, Michigan preprint UM-HE-76-42, to be published in Rev. Mod. Phys., Oct. 1977.
2. T.K. Gaisser and F. Halzen, Phys. Rev. D11, 3157 (1975).

Data Card Listings

QUARK SEARCHES

```
        SEARCHES FOR INTEGRALLY CHARGED QUARKS APPEAR ALONG WITH OTHER
        SIMILAR SEARCHES IN 'OTHER NEW PARTICLE SEARCHES' SECTION BELOW.

------ --------- --------- --------- --------- --------- --------- --------

C          QUARK PRODUCTION CROSS SECT. FROM PROTON ACCELERATOR EXPTS. (CM**2)
C          0 2.0E-34 OR LESS  CL=.90   BINGHAM   64  HBC Q= -1/3 M=.5-2.0GEV   3/77*
C          0 1.0E-34 OR LESS  CL=.90   BINGHAM   64 HLBC Q= -2/3 M=.5-2.5GEV   3/77*
C          0 2.0E-35 OR LESS           BLUM      64  HBC Q= -1/3 M=0-2.5GEV    3/77*
C     Z    0 9.5E-36 OR LESS           HAGOPIAN  64  HBC Q= +1/3 M=.5-2.5GEV   3/77*
C          0 1.0E-34 OR LESS           LEIPUNER  64 CNTR Q= -1/3 M=0-2.0GEV    3/77*
C          0 4.0E-34 OR LESS           MORRISON  64  HBC Q= -1/3 M=.5-2.5GEV   3/77*
C          0 1.0E-35 OR LESS           MORRISON  64  HBC Q= -2/3 M=.5-2.5GEV   3/77*
C     W    0 2.0E-35 OR LESS           FRANZINI  65 CNTR Q= -2/3 M=0-2.5GEV    3/77*
C     Y    0 3.2E-39 OR LESS  CL=.90   ALLABY    69 CNTR Q= -1/3 M=2GEV        1/76
C     Y    0 5.5E-38 OR LESS  CL=.90   ALLABY    69 CNTR Q= -2/3 M=2GEV        1/76
C     Y    0 1.8E-35 OR LESS  CL=.90   ALLABY    69 CNTR Q= +1/3 M=2GEV        1/76
C     Y    0 1.0E-35 OR LESS  CL=.90   ALLABY    69 CNTR Q= +2/3 M=2GEV        1/76
C     A    0 4.0E-37 OR LESS  CL=.90   ANTIPOV1  69 CNTR Q= -2/3 M=0-5GEV      2/74
C     A    0 3.0E-39 OR LESS  CL=.90   ANTIPOV2  69 CNTR Q= -1/3 M=4.5-5GEV    1/76
C     A    0 3.0E-37 OR LESS  CL=.90   ANTIPOV2  69 CNTR Q= -2/3 M=2-5GEV      1/76
C     V    0 1.0E-36 OR LESS  CL=.90   ANTIPOV   71 CNTR Q= -4/3 M=4GEV        1/76
C     B    0 3.0E-34 OR LESS           BOTT-BODE 72 CNTR Q=+-1/3 M=0-22GEV     2/74
C     B    0 6.0E-34 OR LESS           BOTT-BODE 72 CNTR Q=+-2/3 M=0-13GEV     2/74
C     P    0 1.0E-32 OR LESS  CL=.90   ALPER     73 SPEC Q=  1/3 M=4-24 GEV    1/76
C     P    0 1.0E-32 OR LESS  CL=.90   ALPER     73 SPEC Q=  4/3 M=4-24 GEV    1/76
C     L    0 1.0E-35 OR LESS           LEIPUNER  73 CNTR Q=  1/3 M=0-12GEV     2/74
C     L    0 1.0E-35 OR LESS           LEIPUNER  73 CNTR Q=  2/3 M=0-12GEV     2/74
C     L    0 5.0E-31 OR LESS           LEIPUNER  73 CNTR Q=  4/3 M=0-12GEV     2/74
C     N    0 5.0E-39 OR LESS  CL=.90   NASH      74 CNTR Q= -1/3 M=4 GEV       2/77*
C     N    0 5.0E-38 OR LESS  CL=.90   NASH      74 CNTR Q= -2/3 M=4 GEV       2/77*
C     F    0 4.0E-35 OR LESS  CL=.90   FABJAN    75 ELEC Q=  1/3 M=0-20 GEV    1/77*
C     F    0 8.0E-35 OR LESS  CL=.90   FABJAN    75 ELEC Q=  2/3 M=0-20 GEV    1/77*
C     Z  HAGOPIAN 64 CROSS SECTION INFERRED FROM FLUX DATA.                    3/77*
C     W  FRANZINI 65 CROSS SECTION INFERRED FROM FLUX DATA.                    3/77*
C     Y  ALLABY 69 IS A CERN 27 GEV P+BE EXPT.  STUDIES MASSES 0-2.7GEV        1/76
C     Y  ASSUMING NN=NNQQ.  CROSS SECTIONS ASSUME ISOTROPIC PROD. IN CM.       1/76
C     Y  CROSS SECTIONS AT 2GEV ARE GIVEN HERE.  SEE FIG.9 FOR MASS DEPEN.     1/76
C     A  ANTIPOV1 69 IS A SERPUKHOV 70 GEV P EXPT.  MASS LIMIT FROM NN=NNQQ.   2/74
C     A  ANTIPOV1 69 AND ANTIPOV2 69 ARE SERPUKHOV 70GEV P EXPTS.  ANTIPOV2    1/76
C     A  GIVES RESULTS FOR M=2-5GEV ASSUMING NN-->NNQQ. HADRONIC OR LEPTONIC   1/76
C     A  QUARKS.  WE QUOTE TYPICAL VALUES.                                     1/76
C     V  ANTIPOV 71 IS A SERPUKHOV 70 GEV P+AL EXPT.  STUDIES DIQUARK MASSES   1/76
C     V  1.9-4.4GEV.  WE SHOW 4GEV VALUE.  SEE THEIR FIG.2 FOR MASS DEPEN.     1/76
C     B  BOTT-BODENHAUSEN 72 IS A CERN ISR 26+26 GEV P+P EXPERIMENT.           2/74
C     P  ALPER 73 IS CERN ISR 26+26 GEV P+P EXPT. ASSUMES ISOTROPIC C.M.       1/76
C     P  PRODUCTION.  SENSITIVE TO ANY Q>2/3.                                  1/76
C     L  LEIPUNER 73 IS AN NAL 300 GEV P EXPERIMENT.                           2/74
C     N  NASH 74 IS FNAL EXPT USING 200 AND 300 GEV PROTONS. SEE FIG 2,PG861   2/77*
C     N  FOR OTHER MASS VALUES AND VARIOUS PRODUCTION MECHANISMS.              2/77*
C     F  FABJAN 75 IS CERN ISR P+P EXPT AT S=2830 GEV**2. INCLUDES RESULTS     1/77*
C     F  OF BOTT-BODE 72 EXPT.                                                 1/77*

D          QUARK PROD. DIFF. CROSS SEC. FROM PROTON ACCL. EXPTS. (CM**2/SR-GEV)
D     D    0 1.5E-36 OR LESS           DORFAN    65 CNTR BE TARG  M=3-7GEV     2/74
D     D    0 3.0E-36 OR LESS           DORFAN    65 CNTR FE TARG  M=3-7GEV     2/74
D     Y    0 7.2E-39 OR LESS  CL=.90   ALLABY    69 CNTR Q=-1/3  THETA= 0 MR   1/76
D     Y    0 5.2E-38 OR LESS  CL=.90   ALLABY    69 CNTR Q=-2/3  THETA=6.5MR   1/76
D     Y    0 2.6E-35 OR LESS  CL=.90   ALLABY    69 CNTR Q=+1/3  THETA=44 MR   1/76
D     Y    0 1.3E-35 OR LESS  CL=.90   ALLABY    69 CNTR Q=+2/3  THETA=44 MR   1/76
D     A    0 7.0E-38 OR LESS  CL=.90   ANTIPOV2  69 CNTR Q=-1/3   M=0-5GEV     1/76
D     A    0 4.0E-38 OR LESS  CL=.90   ANTIPOV2  69 CNTR Q=-2/3   M=0-2.5GEV   1/76
D     V    0 1.6E-36 OR LESS  CL=.90   ANTIPOV   71 CNTR Q=-4/3  THETA=47 MR   1/76
D     V    0 3.8E-36 OR LESS  CL=.90   ANTIPOV   71 CNTR Q=-4/3  THETA=47 MR   1/76
D     N    0 5.6E-36 OR LESS  CL=.90   NASH      74 CNTR Q=-1/3                2/77*
D     N    0 5.0E-35 OR LESS  CL=.90   NASH      74 CNTR Q=-2/3   M GT 1.76    2/77*
D     N    0 8.5E-35 OR LESS  CL=.90   NASH      74 CNTR Q=-2/3   M LT 1.76    2/77*
D     L    0 1.6E-33 OR LESS  CL=.90   ALBROW    75 SPEC Q=+-4/3  M=5-20 GEV   1/77*
D     J    0 5.0E-34 OR LESS  CL=.90   JOVANOVIC 75 CNTR Q=1/3  M=7-15 GEV     2/76
D     J    0 2.0E-34 OR LESS  CL=.90   JOVANOVIC 75 CNTR Q=1/3  M=15-26 GEV   11/75
D     J    0 1.3E-34 OR LESS  CL=.90   JOVANOVIC 75 CNTR Q=2/3  M=10-26 GEV   11/75
D     J    0 8.0E-35 OR LESS  CL=.90   JOVANOVIC 75 CNTR Q=4/3  M=10-26 GEV   11/75
D     B    0 3.9E-36 OR LESS  CL=.90   BALDIN    76 CNTR Q=-2/3  M=1.4-6 GEV   1/77*
D     B    0 2.0E-36 OR LESS  CL=.90   BALDIN    76 CNTR Q=-4/3  M=2.7-12GEV   1/77*
D     D  DORFAN 65 IS A 30 GEV/C P EXPERIMENT AT BNL.   V=.18-.995             2/74
D     Y  SEE FOOTNOTE Y IN SUBSECTION C ABOVE.                                 2/76
D     A  SEE FOOTNOTE A IN SUBSECTION C ABOVE.                                 2/76
D     V  FIRST ANTIPOV 71 VALUE IS FOR M=1.9-2.3,2.7-4.4GEV, SECOND IS FOR     1/76
D     V  M=2.3-2.7GEV.  SEE ALSO NOTE V IN SECTION C ABOVE.                    1/76
D     N  NASH 74 IS FNAL EXPT USING 200 AND 300 GEV PROTONS.  VALUES ARE FOR   2/77*
D     N  A 1MRAD LAB PROD. ANGLE AND OUTGOING MOMENTUM AT MAX OF FOUR BODY     2/77*
D     N  PHASE SPACE FOR QUARK-PAIR PROD.  SEE TABLE I PG. 860 FOR OTHER       2/77*
D     N  LIMITS.                                                               2/77*
D     L  ALBROW 75 IS A CERN ISR EXPT WITH ECM=53 GEV. THETA=40 MR. SEE        1/77*
D     L  FIG. 5 FOR MASS RANGES UP TO 25 GEV.                                  1/77*
D     J  JOVANOVICH 75 FIG.4 COVERS RANGES Q=1/3 TO 2 AND M=3 TO 26 GEV.      11/75
D     J  THIS IS A CERN ISR 26+26, 22+22 GEV P+P EXPERIMENT.                   2/76
D     B  BALDIN 76 IS A 70 GEV SERP EXP.  VALUES ARE PER AL NUCLEUS AT         1/77*
D     B  THETA=0.  ASSUMES STABLE PARTICLE INTERACTING WITH MATTER IN SAME     1/77*
D     B  MANNER AS ANTIPROTON.                                                 1/77*

DG         QUARK PROD. DIFF. CROSS SEC. FROM PHOTOPROD. (CM**2/SR-EQUIV.QUANTA)
DG    G        5.0E-35 OR LESS  CL=.90   GALIK      74 CNTR     THETA=1.2,7 DEG. 11/76*
DG    G  GALIK 74 IS 20 GEV(MAX) GAMMA CU EXPT. USING SLAC 20 GEV SPTRMETER. 11/76*

M          LIMIT ON QUARK MASS FROM ELECTRON ACCELERATORS (GEV/C**2)
M           *LEP QUARK  INDICATES LEPTONIC QUARK
M           *STR QUARK  INDICATES STRONG QUARK
M                  .85   OR MORE  CL=.99   BATHOW    67 CNTR Q=1/3   *LEP QUARK   3/77*
M                  .90   OR MORE  CL=.99   BATHOW    67 CNTR Q=2/3   *LEP QUARK   3/77*
M                  .70   OR MORE  CL=.90   FOSS      67 CNTR Q=1/3   *LEP QUARK   3/77*
M                  .84   OR MORE  CL=.90   FOSS      67 CNTR Q=2/3   *LEP QUARK   3/77*
M                 1.0    OR MORE           BELLAMY   68 CNTR Q=1/3   *LEP QUARK   3/77*
M                 1.5    OR MORE           BELLAMY   68 CNTR Q=2/3   *LEP QUARK   3/77*
M                 0.5    OR MORE           BELLAMY   68 CNTR Q=1/3   *STR QUARK   3/77*
M                  .75   OR MORE           BELLAMY   68 CNTR Q=2/3   *STR QUARK   3/77*
M     G           3.6    OR MORE  CL=.90   GALIK     74 CNTR Q=1/3   *STR QUARK   7/76*
M     G           4.5    OR MORE  CL=.90   GALIK     74 CNTR Q=2/3   *STR QUARK   7/76*
M     G           1.4    OR MORE  CL=.90   GALIK     74 CNTR Q=1/3   *LEP QUARK   7/76*
M     G           1.8    OR MORE  CL=.90   GALIK     74 CNTR Q=2/3   *LEP QUARK   7/76*
M     G  FIRST TWO MASS LIMITS ARE FOR STRONGLY INTERACTING QUARKS,INFERRED    7/76*
M     G  FROM CROSS-SEC LIMITS USING DRELL MODEL. LAST TWO ARE FOR LEPTONIC    7/76*
M     G  QUARKS. EXPT USES PHOTOPRODUCTION ON COPPER.                          7/76*

F          QUARK FLUX FROM COSMIC RAY EXPERIMENTS  (NUMBER/CM**2-SR-SEC)
F           *TD IN THE RIGHT HAND COLUMNS INDICATES A SEARCH FOR MASSIVE
F               QUARKS USING TIME DELAY AFTER AIR SHOWERS. SENSITIVE TO A RANGE
F               OF CHARGES
F           *AS IN THE RIGHT HAND COLUMNS INDICATES A SEARCH IN AIR SHOWERS
F           ALL SEARCHES ARE AT SEA LEVEL UNLESS OTHERWISE INDICATED
F          0 1.6E-8    OR LESS  CL=.90   BOWEN     64 CNTR Q=-1/3  ALT=2750M      3/77*
F          0 2.0E-7    OR LESS  CL=.90   SUNYAR    64 CNTR Q=1/3                  3/77*
F          0 8.7E-9    OR LESS  CL=.90   DELISE    65 CNTR Q=1/3   ALT=2750M      3/77*
F          0 1.8E-8    OR LESS  CL=.90   DELISE    65 CNTR Q=2/3   ALT=2750M      3/77*
F          0 5.0E-8    OR LESS  CL=.90   MASSAM    65 CNTR Q=2/3                  3/77*
F     V    0 1.4E-10   OR LESS           BARTON    66 CNTR Q=2/3                  3/77*
F          0 1.5E-9    OR LESS  CL=.90   BUHLER-BR 66 CNTR Q=1/3   ALT= 450M      3/77*
F          0 1.4E-9    OR LESS  CL=.90   BUHLER-BR 66 CNTR Q=2/3   ALT= 450M      3/77*
F          0 2.6E-9    OR LESS           KASHA     66 CNTR Q=1/3                  3/77*
F          0 2.1E-9    OR LESS           KASHA     66 CNTR Q=2/3                  3/77*
F          0 4.5E-10   OR LESS  CL=.90   LAMB      66 CNTR Q=1/3                  3/77*
F          0 1.6E-9    OR LESS  CL=.90   LAMB      66 CNTR Q=2/3                  3/77*
F     W    0 1.4E-10   OR LESS           BARTON    67 CNTR Q=2/3                  3/77*
F     Q    0 1.6E-7    OR LESS           BUHLER-1  67 CNTR Q=4/3   ALT= 450M      3/77*
F     Q    0 4.5E-10   OR LESS  CL=.90   BUHLER-2  67 CNTR Q=1/3   ALT= 450M      3/77*
F     Q    0 1.7E-10   OR LESS           BUHLER-2  67 CNTR Q=2/3   ALT= 450M      3/77*
F          0 1.7E-10   OR LESS  CL=.90   GOMEZ     67 CNTR Q=1/3                  3/77*
F          0 3.4E-10   OR LESS  CL=.90   GOMEZ     67 CNTR Q=2/3                  3/77*
F          0 2.0E-9    OR LESS  CL=.90   KASHA     67 CNTR Q=2/3                  3/77*
F     C    0 3.0E-10   OR LESS           BJORNBOE  68 CNTR M=5GEV OR MORE *TD     2/74
F     R    0 1.8E-10   OR LESS  CL=.90   BRIATORE  68 CNTR Q=1/3                  5/76*
F     R    0 1.8E-10   OR LESS  CL=.90   BRIATORE  68 CNTR Q=2/3                  5/76*
F     R    0 3.7E-8    OR LESS  CL=.90   BRIATORE  68 CNTR Q=4/3                  5/76*
F     Y    0 2.2E-8    OR LESS           FRANZINI  68 CNTR V=.5-.9C  M=2GEV UP    2/74
F          0 6.6E-11   OR LESS  CL=.95   GARMIRE   68 CNTR Q=1/3                  3/77*
F          0 8.8E-11   OR LESS  CL=.95   GARMIRE   68 CNTR Q=2/3                  3/77*
F          0 3.1E-10   OR LESS  CL=.90   HANAYAMA  68 CNTR Q=1/3                  3/77*
F          0 2.4E-8    OR LESS  CL=.95   KASHA1    68 OSPK V=.5-.75C M=5-15GEV    2/74
F          0 1.2E-10   OR LESS  CL=.90   KASHA2    68 CNTR Q=2/3                  3/77*
F          0 1.3E-10   OR LESS  CL=.90   KASHA3    68 CNTR Q=4/3                  3/77*
F     Z    0 5.0E-11   OR LESS           CAIRNS    69 CC   Q=2/3                  3/77*
F     F    0 5.0E-11   OR LESS  CL=.90   FUKUSHIMA 69 CNTR Q=1/3                  2/74
F     F    0 7.5E-10   OR LESS  CL=.90   FUKUSHIMA 69 CNTR Q=2/3                  2/74
F     M    1  EVENT CLAIMED              MCCUSKER  69 CC   Q=2/3          *AS     2/74
F     U    1  EVENT CLAIMED              CHU       70 HLBC                *AS     5/76*
F          0 1.9E-9    OR LESS  CL=.90   FAISSNER  70 CNTR Q=1/3                  3/77*
F          0 9.8E-11   OR LESS  CL=.90   KRIDER    70 CNTR Q=1/3   ALT=750M       3/77*
F          0 1.6E-10   OR LESS  CL=.90   KRIDER    70 CNTR Q=2/3   ALT=750M       3/77*
F          0 1.3E-10   OR LESS  CL=.90   CHIN      71 CNTR Q=1/3                  3/77*
F          0 5.7E-11   OR LESS  CL=.90   CHIN      71 CNTR Q=1/3   ALT=2770M      3/77*
F          0 3.0E-10   OR LESS  CL=.90   CLARK     71 CC   Q=1/3          *AS     3/77*
F          0 3.0E-11   OR LESS  CL=.90   CLARK     71 CC   Q=2/3          *AS     3/77*
F          0 1.0E-10   OR LESS  CL=.90   HAZEN     71 CC   Q=1/3,2/3      *AS     2/77*
F          0 4.1E-10   OR LESS           BEAUCHAMP 72 CNTR Q=4/3   ALT=2750M      3/77*
F          0 1.0E-10   OR LESS  CL=.90   BOHM      72 CNTR Q=1/3          *AS     2/74
F          0 1.0E-10   OR LESS  CL=.90   BOHM      72 CNTR Q=2/3          *AS     2/74
F          0 8.3E-11   OR LESS  CL=.90   COX       72 ELEC Q=1/3   ALT=2750M      3/77*
F          0 9.6E-11   OR LESS  CL=.90   COX       72 ELEC Q=2/3   ALT=2750M      3/77*
F          0 2.2E-10   OR LESS  CL=.90   CROUCH    72 CNTR Q=2/3                  3/77*
F     X    0 3.0E-8    OR LESS           DARDO     72                     *TD     3/77*
F          0 4.0E-9    OR LESS  CL=.95   EVANS     72 CC   Q=1/3          *AS     1/77*
F          0 1.5E-9    OR LESS           TONWAR    72 CNTR M.GT.10GEV     *TD     3/77*
F          0 8.0E-11   OR LESS           ASHTON    73 CNTR Q=1/3          *AS     3/77*
F     H    0 1.7E-8    OR LESS  CL=.90   HICKS     73 CNTR Q=1/3                  1/76
F     H    0 1.7E-8    OR LESS  CL=.90   HICKS     73 CNTR Q=2/3                  1/76
F          0 1.0E-7    OR LESS  CL=.90   CLARK     74 CC   Q=1/6          *AS     1/77*
F          0 7.0E-10   OR LESS  CL=.90   CLARK     74 CC   Q=1/4          *AS     1/77*
F          0 8.0E-11   OR LESS  CL=.90   CLARK     74 CC   Q=1/3          *AS     1/77*
F          0 1.0E-6    OR LESS  CL=.90   CLARK     74 CC   Q=4/9          *AS     3/77*
F          0 2.0E-11   OR LESS  CL=.90   CLARK     74 CC   Q=2/3          *AS     1/77*
F     K    0 3.0E-10   OR LESS  CL=.95   KIFUNE    74 CNTR Q=1/3                  7/76*
           0 1.2E-11   OR LESS  CL=.90   HAZEN     75 CC   Q=1/3          *AS     7/76*
           0 7.0E-11   OR LESS  CL=.90   KRISOR    75 CNTR Q=1/3                  3/77*
S          0 5.0E-11   OR LESS  CL=.90   KRISOR    75 CNTR Q=2/3  GAMMA = 10      3/77*
S          0 1.5E-10   OR LESS  CL=.90   KRISOR    75 CNTR Q=2/3  GAMMA GT1000    3/77*
F          0 1.0E-9    OR LESS           BRIATORE  76 ELEC                *TD     1/77*
F     V  BARTON 66 HAD 220000 G/CM**2 EXTRA SHIELDING                             3/77*
F     W  BARTON 67 HAD 6000 G/CM**2 EXTRA SHIELDING                               3/77*
F     Q  BUHLER-1 67 AND BUHLER-2 67 HAD 760 G/CM**2 EXTRA SHIELDING              3/77*
F     C  BJORNBOE 68 -TWO EXPERIMENTS HAVING 1650 AND 3600 G/CM**2 SHIELDING      3/77*
F     R  BRIATORE 68 SEARCHES FOR LEPTONIC QUARKS WITH 6300 G/CM2 SHIELDING       3/77*
F     R  BRIATORE 68 GIVES (1.1+-1.8)E-10 FOR Q=4/3  . WE CONV. TO CL=.90         3/77*
F     Z  CAIRNS 69 OBSERVED 4 POSSIBLE QUARK CANDIDATES                           3/77*
F     Y  FRANZINI 68 MEASURES VELOCITY DIRECTLY BY TOF                            3/77*
F     F  FUKUSHIMA 69 DOES NOT RULE OUT QUARKS HEAVIER THAN 10 GEV.               7/76*
F     M  MC CUSKER 69 CLAIMS 1 CANDIDATE.   LATER SIMILAR EXPTS. SEE NONE.        2/74
F     U  Q=2/3 IF MASS LT 6.5 GEV, Q=1/3 IF MASS = 8 GEV.                         5/76*
F     U  COULD BE AN EARLY-TIME NORMALLY CHARGED COSMIC RAY. SEE ALLISON 70.      2/77*
F     X  DARDO 72 HAD 7000 G/CM**2 EXTRA SHIELDING                                3/77*
F     H  HICKS 73 LOOKED AT LARGE ZENITH ANGLES, THUS USING THE ATMOSPHERE        1/76
F     H  AS AN EXTENDED FILTER FOR HADRONIC QUARKS. THEIR SEARCH PUTS AN          1/76
F     H  UPPER LIMIT ON LEPTONIC QUARK FLUX IN COSMIC RAYS.                       1/76
F     K  KIFUNE 74 LOOKED AT LARGE ZENITH ANGLES. FROM THEIR FLUX LIMIT,THEY      7/76*
F     K  GET A LOWER LIMIT ON QUARK MASS OF 20 GEV.                               7/76*

RHO        QUARK CONCENTRATION IN MATTER (QUARKS PER NUCLEON)
RHO   S    0 1.0E-22   OR LESS           HILLAS     59                            3/77*
RHO   R    0 1.0E-10   OR LESS           BENNETT    66 SOLAR SPECTRUM             3/77*
RHO        0 1.0E-17   OR LESS           CHUPKA     66 METORITES                  3/77*
RHO        0 1.0E-16   OR LESS           GALLINARO  66   GRAPHITE LEVITOMETER   . 3/77*
RHO        0 4.0E-19   OR LESS           STOVER     67 IRON LEVITOMETER           2/74
RHO        0 1.0E-17   OR LESS           BRAGINSKI  68 GRAPHITE LEVITOMETER       3/77*
RHO        0 1.0E-20   OR LESS           RANK       68 OIL DROPS                  3/77*
RHO   T    0 1.0E-18   OR LESS           RANK       68 SEA WATER                  3/77*
RHO   T    0 1.0E-17   OR LESS           RANK       68 SEA SALT, ETC.             3/77*
RHO   T    0 1.0E-18   OR LESS           RANK       68 LAKE WATER                 3/77*
RHO   V    0 1.0E-24   OR LESS           COOK       69  SEAWATER                  2/74
RHO   V    0 1.0E-23   OR LESS           COOK       69  ROCK SAMPLES              2/74
RHO   V    0 1.0E-23   OR LESS           COOK       69 LAVA                       3/77*
RHO   V    0 5.0E-23   OR LESS           COOK       69 LIMESTONE                  3/77*
RHO        0 1.0E-15   OR LESS           ELBERT     70 ION SPECTROMETER           3/77*
RHO        0 5.0E-19   OR LESS           MORPURGO   70 GRAPHITE LEVITOMETER       3/77*
RHO   Z    0 1.0E-21   OR LESS           STEVENS    76 DEEP OCEAN SEDIMENT        3/77*
RHO   Z    0 1.0E-22   OR LESS           STEVENS    76 LUNAR SOIL                 3/77*
RHO   S  HILLAS 59 WAS INSENSITIVE TO QUARKS ACCORDING TO SUNYAR 64.              3/77*
RHO   R  BENNETT 66 LIMIT INFERRED BY JONES 76.                                   3/77*
RHO   T  RANK 68 USES U.V. SPECTROSCOPY.                                          3/77*
RHO   V  COOK 69 USES MOLECULAR BEAMS.                                            3/77*
RHO   Z  STEVENS 76 USES AN ION SPECTROMETER.                                     3/77*

****** ********* ********* ********* ********* ********* ********* ********
```

QUARK SEARCHES, MAGNETIC MONOPOLE SEARCHES

Data Card Listings

```
                              REFERENCES FOR QUARK SEARCHES

HILLAS    59 NATURE 184 892    HILLAS,CRANSHAW                          (AERE)

BINGHAM   64 PL 9 201          +DICKINSON,DIEBOLD,KOCH,LEITH+   (CERN+EPOL)
BLUM      64 PRL 13 353A       +BRANDT,COCCONI,CZYZEWSKI,DANYSZ+      (CERN)
BOWEN     64 PRL 13 728        BOWEN,DELISE,KALBACH,MORTARA           (ARIZ)
HAGOPIAN  64 PRL 13 280        +SELOVE,EHRLICH,LEBOY,LANZA,RAHM+(PENN+BNL)
LEIPUNER  64 PRL 12 423        LEIPUNER,CHU,LARSEN,ADAIR          (BNL+YALE)
MORRISON  64 PL 9 199          MORRISON                               (CERN)
SUNYAR    64 PR 136B 1157      SUNYAR,SCHWARZSCHILD,CONNORS            (BNL)

DELISE    65 PR 140B 458       DELISE,BOWEN                           (ARIZ)
DORFAN    65 PRL 14 999        +EADES,LEDERMAN,LEE,TING               (COLU)
FRANZINI  65 PRL 14 196        +LEONTIC,RAHM,SAMIOS,SCHWARTZ      (BNL+COLU)
MASSAM    65 NC 40A 589        MASSAM,MULLER,ZICHICHI                 (CERN)

BARTON    66 PL 21 360         BARTON,STOCKEL                         (NCPL)
BUHLER-B  66 NC 45A 520        BUHLER-BROGLIN,FORTUNATO,MASSAM+       (CERN)
CHUPKA    66 PRL 17 60         CHUPKA,SCHIFFER,STEVENS                 (ANL)
GALLINAR  66 PL 23 609         GALLINARO,MORPURGO                     (GENO)
KASHA     66 PR 150 1140       KASHA,LEIPUNER,ADAIR               (BNL+YALE)
LAMB      66 PRL 17 1068       LAMB,LUNDY,NOVEY,YOVANOVITCH            (ANL)

BARTON    67 PRSL 90 87        BARTON                                 (NOPL)
BATHOW    67 PL 25B 163        BATHOW,FREYTAG,SCHULZ,TESCH            (DESY)
BUHLER-1  67 NC 49A 209        BUHLER-BROGLIN,FORTUNATO,MASSAM+       (CERN)
BUHLER-2  67 NC 51A 837        BUHLER-BROGLIN,DALPIAZ,MASSAM,ZICHICH(CERN)
FOSS      67 PL 25B 166        +GARELICK,HOMMA,LOBAR,OSBORNE,UGLUM     (MIT)
GOMEZ     67 PRL 18 1022       +KOBRAK,MOLINE,MULLINS,ORTH,VANPUTTEN+(CIT)
KASHA     67 PR 154 1263       +LEIPUNER,WANGLER,ALSPECTOR,ADAIR(BNL+YALE)
STOVER    67 PR 164 1599       +MORAN,TRISCHKA                        (SYRA)

BELLAMY   68 PR 166 1391       +HOFSTADTER,LAKIN,PERL,TONER      (STAN+SLAC)
BJORNBOE  68 NC B53 241        +DAMGARD,HANSEN,CHATTERJEE+       (BOHR+BERN)
BRAGINSK  68 JETP 27 51        BRAGINSKII,ZELDOVICH,MARTYNOV          (MOSU)
BRIATORE  68 NC 57A 850        +CASTAGNOLI,BOLLINI,MASSAM+       (TORI+CERN)
FRANZINI  68 PRL 21 1013       FRANZINI,SHULMAN                       (COLU)
GARMIRE   68 PR 166 1280       GARMIRE,LEONG,SREEKANTAN                (MIT)
HANAYAMA  68 CJP 46 S734       +HARA,HIGASHI,KITAMURA,MIONO+          (OSAK)
KASHA1    68 PR 172 1297       +STEFANSKI                         (BNL+YALE)
KASHA2    68 PRL 20 217        KASHA,LARSEN,LEIPUNER,ADAIR        (BNL+YALE)
KASHA3    68 CJP 46 S730       KASHA,LARSEN,LEIPUNER,ADAIR        (BNL+YALE)
RANK      68 PR 176 1635       D.M.RANK                               (MICH)

ALLABY    69 NC 64A 75         +BIANCHINI,DIDDENS,DOBINSON,HARTUNG+ (CERN)
ANTIPOV1  69 PL 29B 245        +KARPOV,KHROMOV,LANDSBERG,LAPSHIN+     (SERP)
ANTIPOV2  69 PL 30B 576        +BOLOTOV,DEVISHEV,DEVISHEVA,ISAKOV+    (SERP)
CAIRNS    69 PR 186 1394       +MCCUSKER,PEAK,WOOLCOTT              (SYDNEY)
COOK      69 PR 188 2092       +DEPASQUALI,FRAUENFELDER,PEACOCK +      (ILL)
FUKUSHIM  69 PR 178 2058       FUKUSHIMA,KIFUNE,KONDO,KOSHIBA+        (TOKY)
MCCUSKER  69 PRL 23 658        MCCUSKER,CAIRNS                      (SYDNEY)

CHU       70 PRL 24 917        CHU,KIM,BEAM,KWAK            (OSU+ROSE+KANS)
   ALSO   70 PRL 25 550        ALLISON,DERRICK,HUNT,SIMPSON,VOYVODIC (ANL)
ELBERT    70 NP B20 217        +ERWIN,HERB,NIELSEN,PETRILAK,WEINBERG(WISC)
FAISSNER  70 PRL 24 1357       +HOLDER,KRISOR,MASON,SAWAF,UMBACH      (AACH)
KRIDER    70 PR D1 835         KRIDER,BOWEN,KALBACH                   (ARIZ)
MORPURGO  70 NIM 79 95         MORPURGO,GALLINARO,PALMIERI            (GENO)

ANTIPOV   71 NP B27 374        +KACHANOV,KUTJIN,LANDSBERG,LEBEDEV + (SERP)
CHIN      71 NC 2A 419         CHIN,HANAYAMA,HARA,HIGASHI,TSUJI       (OSAK)
CLARK     71 PRL 27 51         +ERNST,FINN,GRIFFIN,HANSEN,SMITH+ (LLL+LBL)
HAZEN     71 PRL 26 582        W.E.HAZEN                              (MICH)

BEUCHAMP  72 PR D6 1211        BEUCHAMP,BOWEN,COX,KALBACH             (ARIZ)
BOHM      72 PRL 28 326        +DIEMONT,FAISSNER,FASOLO,KRISOR+       (AACH)
BOTT-BOD  72 PL 40B 693        BOTT-BODENHAUSEN,CALDWELL+        (CERN+MPIM)
COX       72 PR D6 1203        COX,BEUCHAMP,BOWEN,KALBACH             (ARIZ)
CROUCH    72 PR D5 2667        CROUCH,MORI,SMITH                      (CASE)
DARDO     72 NC 9A 319         DARDO,NAVARRA,PENENGO,SITTE            (TORI)
EVANS     72 PRSE A70 143      +FANCEY,MUIR,WATSON               (EDIN+LEED)
TONWAR    72 JPA 5 569         TONWAR,NARANAN,SREEKANTAN              (TATA)

ALPER     73 PL 46B 265          (CERN+LIVP+LUND+BOHR+RHEL+STOH+BERG+LOUC)
ASHTON    73 JPA 6 577         ASHTON,COOPER,PARVARESH,SALEH          (DURH)
HICKS     73 NC 14A 65         +FLINT,STANDIL                         (MANI)
LEIPUNER  73 PRL 31 1226       +LARSEN,SESSOMS,SMITH,WILLIAMS+    (BNL+YALE)

CLARK     74 PR D10 2721       +FINN,HANSEN,SMITH                      (LLL)
GALIK     74 PR D9 1856        +JORDAN,RICHTER,SEPPI,SIEMANN +   (SLAC+NAL)
KIFUNE    74 JPSJ 36 629       +HIEDA,KUROKAWA,TSUNEMOTO,KIMURA+(TOKY+KEK)
NASH      74 PRL 32 858        +YAMANOUCHI,NEASE,SCULLI     (FNAL+CORN+NYU)

ALBROW    75 NP B97 189        +BARBER,BENZ+ (CERN+DARE+FOM+LANC+MCHS+UTR)
FABJAN    75 NP B101 349       +GRUHN,PEAK,SAULI,CALDWELL+       (CERN+MPIM)
HAZEN     75 NP B95 189        +HODSON,WINTERSTEIN,GREEN,KASS+(MICH+LEEDS)
JOVANOVI  75 PL 56B 105        JOVANOVICH+ (MANI+AACH+CERN+GENO+HARV+TORI)
KRISOR    75 NC 27A 132        KRISOR                                 (AACH)

BALDIN    76 SJNP 22 264       +VERTOGRADOV,VISHNEVSKII,GRISHKEVICH+(JINR)
BRIATORE  76 NC 31A 553        +DARDO,PIAZZOLI,MANNOCCHI+   (LCG+FRAS+FREI)
STEVENS   76 PR D14 716        +SCHIFFER, CHUPKA                       (ANL)

                                 REVIEW ARTICLES

ZAITSEV   72 SJNP 15 656       +LANDSBERG                             (SERP)
JONES     76 MICH-HE-76-42     JONES (TO BE PUB. IN REV.MOD.PHYS.)    (MICH)

****** ********* ********* ********* ********* ********* ********* ********
****** ********* ********* ********* ********* ********* ********* ********
```

MAGNETIC MONOPOLE SEARCHES

There is little new to report in this section. However, we include the listings for completeness. One interesting development is the proposed reinterpretation of the PRICE 75 event by HAGSTROM 77 as a heavy antinucleus.

```
C        MONOPOLE PROD. CROSS SECTION - ACCELERATOR EXP.      (CM**2)/NUCLEON
C    A    0    1 E-40 OR LESS  CL=.95   AMALDI    63 EMUL   M=0 TO 3 GEV        12/75
C    A    0    5 E-41 OR LESS  CL=.95   AMALDI    63 EMUL   M=0 TO 3.4 GEV      12/75
C    P    0    2 E-40 OR LESS           PURCELL   63 CNTR   M=0 TO 3 GEV        12/75
C    G    0    4 E-43 OR LESS  CL=.95   GUREVICH  72 EMUL   M=0-5 GEV            3/74
C    C    0    6 E-42 OR LESS  CL=.95   CARRIGAN  73 CNTR Q=1/6-24 DIRAC CHAR    3/74
C    M    0    5 E-42 OR LESS  CL=.95   CARRIGAN  74 CNTR   Q=1/30 TO 24        12/75
C    N    0    1 E-39 OR LESS  CL=.95   CARRIGAN  75 HLBC   NEU ENERGY=1.0       1/76
C    N    0    4 E-38 OR LESS  CL=.95   CARRIGAN  75 HLBC   NEU ENERGY=5.0       1/76
C    N    0    1 E-37 OR LESS  CL=.95   CARRIGAN  75 HLBC   NEU ENERGY=8.0       1/76
C    E    0    5 E-44 OR LESS  CL=.95   EBERHARD  75 CNTR   M=0 TO 12 GEV       11/75
C    I    0    2 E-36 OR LESS  CL=.95   GIACOMELL 75 PLAS   M=0 TO 20 GEV        2/76
C    A  AMALDI 63 USES 28 GEV PROT BEAM AT CERN PS. FIRST RESULT IS FOR        12/75
C    A  PROTON TARGET, SECOND IS FOR NUCLEON TARGET INSIDE NUCLEUS.            12/75
C    P  PURCELL 63 LOOKS FOR MONOPOLES PRODUCED BY 30 GEV PROT AT THE AGS.     12/75
C    G  GUREVICH 72 IS A SERPUKHOV 70 GEV/C P EXP. MASS LIMIT FROM PP=PPMM      3/74
C    C  CARRIGAN 73 IS NAL 300 GEV P EXP. MASS LIMIT 0-12 GEV FROM PP=PPMM      3/74
C    M  CARRIGAN 74 IS NAL 400 GEV EXP.  MASS LIMIT 0-13.7 GEV/MONOPOLE.       12/75
C    N  CARRIGAN 75 REEXAMINES OLD CERN NEUTRINO EXPTS IN HLBC. NEU ENERGY      1/76
C    N  GIVEN AT RIGHT REPRESENTS NEUTRINO THRESHOLD ENERGY.                    1/76
C    N  THESE VALUES ARE IN UNITS CM**2/NUCLEUS.                                1/76
C    E  EBERHARD 75 USED NAL TARGETS - 300 GEV AND 400 GEV P ON ALUMINUM.       2/76
C    E  Q=1-7 DIRAC CHGS.  USED SAME TYPE OF DETECTOR AS ROSS 73.               2/76
C    I  GIACOMELLI 75 IS CERN ISR EXP., M=0-30 GEV, Q=0.4-2.5 DIRAC CHGS.       2/76

CS       MONOPOLE PROD. CROSS SECTION - SEARCH IN MATTER     (CM**2)/NUCLEON
CS   G    0    5 E-38 OR LESS           GOTO      63 EMUL   M=1 GEV             12/75
CS   G    0    5 E-36 OR LESS           GOTO      63 EMUL   M=10 GEV            12/75
CS   G    0    5 E-33 OR LESS           GOTO      63 EMUL   M=100 GEV           12/75
CS        0    3 E-40 OR LESS  CL=.95   PETUKHOV  63 CNTR   METEORITE           12/75
CS   C    0    1 E-38 OR LESS  CL=.90   CARITHERS 66 ELEC   M=2 GEV             12/75
CS   C    0    7 E-37 OR LESS  CL=.90   CARITHERS 66 ELEC   M=10 GEV            12/75
CS   C    0    1 E-35 OR LESS  CL=.90   CARITHERS 66 ELEC   M=25 GEV            12/75
CS   F    0    5 E-43 OR LESS  CL=.90   FLEISCH1  69 CNTR   M=1 GEV              2/76
CS   F    0    2 E-40 OR LESS  CL=.90   FLEISCH1  69 CNTR   M=10 GEV             2/76
CS   F    0    3 E-37 OR LESS  CL=.90   FLEISCH1  69 CNTR   M=100 GEV            2/76
CS   F    0    5 E-34 OR LESS  CL=.90   FLEISCH1  69 CNTR   M=1000 GEV           2/76
CS   F    0    1 E-29 OR LESS  CL=.90   FLEISCH1  69 CNTR   M=10000 GEV          2/76
CS   K    0    1 E-42 OR LESS  CL=.95   KOLM      71 CNTR   M=1.5 GEV            3/74
CS   K    0    1 E-42 OR LESS  CL=.95   KOLM      71 CNTR   M=10 GEV             3/74
CS   K    0    1 E-37 OR LESS  CL=.95   KOLM      71 CNTR   M=100 GEV            3/74
CS   K    0    1 E-34 OR LESS  CL=.95   KOLM      71 CNTR   M=1000 GEV           3/74
CS   K    0    1 E-31 OR LESS  CL=.95   KOLM      71 CNTR   M=1500 GEV           3/74
CS   R    0    1 E-43 OR LESS  CL=.95   ROSS      73 ELEC   M=2 GEV              3/74
CS   R    0    5 E-41 OR LESS  CL=.95   ROSS      73 ELEC   M=10 GEV             3/74
CS   R    0    5 E-38 OR LESS  CL=.95   ROSS      73 ELEC   M=100 GEV            3/74
CS   G  GOTO 63 EXAMINES MAGNETITE ROCK IN THE ADIRONDACK MOUNTAINS.           12/75
CS   C  CARITHERS 66 LIMITS ABOVE ARE FOR NUCLEON-NUCLEON INTERACTIONS.        12/75
CS   C  LIMITS FOR PHOTONUCLEON PRODUCTION ARE 10**3 TIMES LARGER.             12/75
CS   F  FLEISCHER 69 LOOKED FOR MONOPOLES IN SEDIMENTS AT BOTTOM OF OCEAN       3/74
CS   F  DEPOSITED DURING THE LAST 16 MILLION YEARS. Q=60 DIRAC CHAR.OR LESS     3/74
CS   K  KOLM 71 TRIED TO DETECT MONOP. IN DEEP SEAWATER Q=.2-27 DIRAC CHAR.     2/76
CS   R  ROSS 73 TRIED TO DETECT MONOP. IN LUNAR DUST    Q=.4-36 DIRAC CHAR      2/76
CS   R  OR LARGER CHARGES EXCEPT FOR G= N*36*G0, WITH N INTEGER.  THEY ALSO     3/74
CS   R  REPORT LIMIT OF DENSITY IN LUNAR MATERIAL AS 1.7*10**-4 MONOP./GM.      2/76

F        MONOPOLE FLUX IN COSMIC RAYS (NUMBER/CM**2-SEC-SR)
F         0    1 E-13 OR LESS           GOTO      63 EMUL   KE TO 10**4 GEV     12/75
F         0    5 E-15 OR LESS  CL=.90   CARITHERS 66 ELEC                       12/75
F    F    0    3 E-19 OR LESS  CL=.90   FLEISCH2  69 SCAN   KE TO 10**10 GEV    12/75
F         0    2 E-18 OR LESS           KOLM      71 CNTR   KE TO 10**5 GEV     12/75
F    R    0    5 E-19 OR LESS  CL=.95   ROSS      73 ELEC   KE TO 10**4 GEV     12/75
F   P     1    1 E-13                   PRICE     75 EMUL   M GT 200 GEV        12/75
F    F  FLEISCHER 2 69 LOOKED FOR MONOPOLE TRACKS LEFT IN OBSIDIAN AND MICA    12/75
F    F  OVER GEOLOGICAL TIMES.                                                 12/75
F    R  ROSS 73 INCLUDES DATA OF EBERHARD 71 PAPER.                            12/75
F    P  THE PRICE 75 EVENT COULD BE EXPLAINED AS DUE TO A FRAGMENTING HEAVY   11/76*
F    P  NUCLEUS.  SEE ALVAREZ 75, FLEISCHER 75, FRIEDLANDER 75,AND ROSS 76.   11/76*
F    P  SEE EBERHARD 75 FOR DISCUSSION OF CONFLICT WITH OTHER EXPERIMENTS.     12/75
F    P  NOT CONSIDERED CONVINCING EVIDENCE FOR THE EXISTENCE OF MONOPOLES.     12/75
F    P  HAGSTROM 77 GIVES A REINTERPRETATION AS A HEAVY ANTINUCLEUS.            3/77*

D        MONOPOLE DENSITY IN MATTER      (NUMBER/LITER)
D    S    0  1.6E-4  OR LESS            SCHATTEN  70 ELEC  MOON                 4/77*
D    C    0  4.4E-5  OR LESS  CL=.95    CARRIGAN  76 CNTR    AIR                1/77*
D    C    0  1.8E-3  OR LESS  CL=.95    CARRIGAN  76 CNTR    SEA WATER          1/77*
D    S  SCHATTEN 70 EXAMINED SATELITE DATA FOR PERTURBATIONS IN THE LUNAR       4/77*
D    S  MAGNETIC WAKE. LIMIT IS FOR THE DIFFERENCE IN NUMBERS OF NORTH AND      4/77*
D    S  SOUTH MONOPOLES.                                                        4/77*
D    C  CARRIGAN 76 IS SENSITIVE TO MONOPOLES WITH DIRAC CHARGE Q=1/6 TO 24     1/77*
D    C  AND MASS AS LARGE AS (7500 GEV)*Q.                                      1/77*

****** ********* ********* ********* ********* ********* ********* ********

                      REFERENCES FOR MAGNETIC MONOPOLE SEARCHES

AMALDI    63 NC 28 773         +BARONI,MANFREDINI,BRADNER+(ROMA+UCSD+CERN)
GOTO      63 PR 132 387        +KOLM,FORD                    (TOKY+MIT+BRAN)
PETUKHOV  63 NP 49 87          +YAKIMENKO                             (LEBD)
PURCELL   63 PR 129 2326       +COLLINS,FUJII,HORNBOSTEL,TURKOT (HARV+BNL)
CARITHER  66 PR 149 1070       CARITHERS,STEFANSKI,ADAIR              (YALE)
FLEISCH1  69 PR 184 1393       FLEISCHER,HART,JACOBS+       (GESC+UNCS+GSCO)
    ALSO  70 JAP 41 958        FLEISCHER,HART,JACOBS,PRICE,SCHWARTZ+(GESC)
FLEISCH2  69 PR 184 1398       FLEISCHER,PRICE,WOODS                  (GESC)
    ALSO  70 JAP 41 958        FLEISCHER,HART,JACOBS,PRICE,SCHWARTZ+(GESC)

SCHATTEN  70 PR D1 2245        SCHATTEN                               (NASA)
KOLM      71 PR D4 1285        +VILLA,ODIAN                       (MIT+SLAC)
GUREVICH  72 PL 38B 549        +KHAKIMOV,MARTEMIANOV+       (KIAE+NOVO+SERP)
    ALSO  70 PL 31B 394        GUREVICH,KHAKIMOV +          (KIAE+NOVO+SERP)
    ALSO  72 JETP 34 917       BARKOV, GUREVICH,            (KIAE+NOVO+SERP)
CARRIGAN  73 PR D8 3717        +NEZRICK,STRAUSS                       (FNAL)
ROSS      73 PR D8 698         +EBERHARD,ALVAREZ,WATT             (LBL+SLAC)
    ALSO  71 PR D4 3260        EBERHARD,ROSS,ALVAREZ,WATT         (LBL+SLAC)
CARRIGAN  74 PR D10 3867       +NEZRICK,STRAUSS                       (FNAL)

CARRIGAN  75 NP B91 279        +NEZRICK                               (FNAL)
    ALSO  71 PR D3 56          CARRIGAN,NEZRICK                       (FNAL)
EBERHARD  75 PR D11 3099       +ROSS,TAYLOR,ALVAREZ,OBERLACK      (LBL+MPIM)
GIACOMEL  75 NC 26A 21         GIACOMELLI,ROSSI+       (BGNA+CERN+SACL+ROMA)
PRICE     75 PRL 35 487        +SHIRK,OSBORNE,PINSKY           (UCB+HOUSTON)
    ALSO  75 LBL-4260          LUIS ALVAREZ                            (LBL)
    ALSO  75 LBL-4289          PHILIPPE EBERHARD                       (LBL)
    ALSO  75 PRL 35 1412       R.L. FLEISCHER,R.M.WALKER         (GESC+WUSL)
    ALSO  75 PRL 35 1167       M.W. FRIEDLANDER                       (WUSL)
    ALSO  76 LBL-4665          RONALD ROSS                             (LBL)
    ALSO  77 PRL 38 729        RAY HAGSTROM                            (LBL)

CARRIGAN  76 PR D13 1823       +NEZRICK,STRAUSS                       (FNAL)

****** ********* ********* ********* ********* ********* ********* ********
****** ********* ********* ********* ********* ********* ********* ********
```

Data Card Listings

OTHER NEW PARTICLE SEARCHES

OTHER NEW PARTICLE SEARCHES

We collect here those searches which do not fit neatly into one of the above search categories.

```
LEP      DIRECT LEPTON PRODUCTION IN PROTON NUCLEON INTERACTIONS
LEP      THESE LEPTONS DO NOT RESULT FROM PIO, ETA OR KNOWN WEAK DECAYS.
LEP      CANDIDATES FOR PARENTS OF DIRECT LEPTONS INCLUDE VIRTUAL MASSIVE
LEP      PHOTONS, HIGH PT VECTOR MESONS, INTERMEDIATE BOSONS, CHARMED
LEP      PARTICLES AND HEAVY LEPTONS.
LEP  A                                 APPEL2    74 SPEC FNAL 300GEV P+BE    3/77*
LEP  A   APPEL2 74 OBSERVE DIRECT ELECTRON AND MUON SIGNALS 10**-4 TIMES THE  3/77*
LEP  A   PION YIELD FOR PPERP RANGE 1.-4 GEV.  ELECTRON SOURCE LIFETIME LESS  3/77*
LEP  A   THAN (10**-11 SEC)*(PARENT MASS/GEV).  SUGGESTS LIGHT VEC.MES.(PHI). 3/77*
LEP  B                                 BOYMOND   74 SPEC FNAL 300GEV P+CU,W  3/77*
LEP  B   BOYMOND 74 SEE DIRECT MUON SIGNAL 0.8E-4 TIMES THE PION YIELD FOR   3/77*
LEP  B   PT RANGE 1.5-4.4GEV.  SUGGEST STRONGLY INTERACTING, SHORT LIFETIME  3/77*
LEP  B   SOURCE.  RHO AND PHI ARE POSSIBLE SOURCES.                          3/77*
LEP  U                                 BUSSER    74 SPEC CERNISR 26+26GEV PP 3/77*
LEP  U   BUSSER 74 SEE DIRECT ELECTRON SIGNAL 10**-4 TIMES PION YIELD FOR    3/77*
LEP  U   PT RANGE 1.6-4.7GEV.  CANT BE PHI ALONE SINCE PHI TO K+K- NOT SEEN. 3/77*
LEP  L                                 LEDERMAN  75 RVUE                     3/77*
LEP  L   LEDERMAN 75 DISCUSSES ABOVE EXPTS AND RECENT UNPUBLISHED RESULTS.  3/77*
LEP  L   SUGGESTS NEW LIGHT(1-5 PION MASSES) VECTOR MESON, WEAKLY DECAYING.  3/77*
LEP  -                                 ABRAMOV   76 CNTR 35-70 GEV P+BE,CU   3/77*
LEP  -   ABRAMOV 76 SEE DIRECT MUON SIGNAL 2.5E-5 TIMES PION YIELD FOR       3/77*
LEP  -   PT RANGE 1.9-3.1 GEV. RATIO MU+/MU- = 1.2. RATIO MU+/PI+ INCREASES  3/77*
LEP  -   WITH INCREASING PROTON ENERGY, INDICATING DECAY OF HEAVY PARTICLE   3/77*
LEP  -   WITH TAU LT 10**-11 SEC.                                            3/77*
LEP  N                                 ANISIMOVA 76 ELEC 70 GEV PROT ON CU   3/77*
LEP  N   ANISIMOVA 76 MEASURES LONG. POLARIZ. OF DIRECT MUONS WITH PT=2 -2.8 3/77*
LEP  N   GEV/C. FIND POL.=-0.85+-0.36. THIS WOULD INDICATE THAT MUONS COME   3/77*
LEP  N   FROM PARTICLE DECAYING VIA WK INTERACTIONS. OPPOSITE RESULT IS      3/77*
LEP  N   SEEN BY LAUTERBACH 76 AND LEIPUNER 76.                              3/77*
LEP  K                                 KASHA     76 CNTR FNAL 400GEV P+NUCL  3/77*
LEP  K   KASHA 76 FIND THAT MUON PAIR PRODUCTION CAN ACCOUNT FOR MOST OF THE 3/77*
LEP  K   DIRECT MUONS INDICATING ELECTROMAGNETIC PRODUCTION MECHANISM.       3/77*
LEP  T                                 LAUTERBAC 76 CNTR FNAL 400GEV P+CU    3/77*
LEP  T   LAUTERBACH 76 MEASURES LONG. POLARIZ. OF HIGH PT DIRECT MUONS TO BE 3/77*
LEP  T   P=-0.135+-0.20 AS EXPECTED FOR ELECTROMAGNETIC PROCESS, NOT WK.DEC. 3/77*
LEP  F                                 LEIPUNER  76                          3/77*
LEP  F   LEIPUNER 76 MEASURES LONG. POLARIZ. OF FORWARD DIRECT MUONS TO BE   3/77*
LEP  F   P=-0.00+-0.10 AS EXPECTED FOR ELECTROMAGNETIC PROCESS, NOT WK. DEC. 3/77*
LEP  S                                 BRANSON   77 SPEC 200 GEV/C PROT + FE 3/77*
LEP  S   BRANSON 77 FINDS MU/PI RATIO= 2.E-5 FOR PT LESS THAN 1 GEV/C.       3/77*
LEP  S   ALSO FINDS THAT 0.7+-0.2 OF ALL PROMPT MUS ARE PRODUCED IN PAIRS.   3/77*

ICL      CHARMONIUM-LIKE STATES - INTEG. CROSS SECTION * B.P. (CM**2-MEV)
ICL  H    0  1.5E-30 OR LESS  CL=.90   BOYARSKI  75 SMAG                     4/77*
ICL  A    0  9.0E-31 OR LESS           BARBIELLI 76 CNTR M=2.5-3 GEV         4/77*
ICL  C    0  5.5E-31 OR LESS  CL=.90   BACCI     76 CNTR M=2.5-3 GEV         4/77*
ICL  E    0  9.0E-31 OR LESS           ESPOSITO  76 CNTR M=2.5-3 GEV         4/77*
ICL  H   BOYARSKI 75 IS A SPEAR EXPT. LIMIT IS FOR ECM=3.2-5.9 GEV,          4/77*
ICL  H   EXCLUSIVE OF THE PSI(3700). LIMIT RANGES FROM 1.1 TO 1.7 E-30.      4/77*
ICL  H   FOR A WIDTH OF 10 MEV, FROM  E+E- HADRONS.                          4/77*
ICL  A   BARBIELLINI 76 IS AN ADONE E+ E- EXPT. CROSS SECT. CONVERTED FROM   4/77*
ICL  A   RATIO TO E+E- --> J/PSI CROSS SECT.                                 4/77*
ICL  C   BACCI 76 IS AN ADONE E+ E- EXPT.                                    4/77*
ICL  E   ESPOSITO 76 IS AN ADONE E+ E- EXPT. CROSS SECT. CONVERTED FROM      4/77*
ICL  E   RATIO TO E+E- --> J/PSI CROSS SECT.                                 4/77*

CL       CHARMONIUM-LIKE STATES   CROSS-SECTION * B.P. (CM**2)
CL   A    0  1.0E-34   OR LESS         APEL      75 CNTR  M=2-5 GEV          4/77*
CL   E                                 EARTLY    76 CNTR  SHOULDER AT 6 GEV  4/77*
CL   H   12  5.2E-36      2.0E-36      HOM1      76 CNTR    PEAK AT 6 GEV    4/77*
CL   H    0  2.0E-36   OR LESS         HOM2      76 CNTR                     4/77*
CL   T    0  2.0E-33   OR LESS         THEODOSIC 76 CNTR    M=1.2-3.5 GEV    4/77*
CL   A   APEL 75 IS A 40 GEV PI- P EXP. SENSITIVE TO MULTI-GAMMAS. DOES NOT  4/77*
CL   A   SEE J/PSI OR PSI(3700).                                             4/77*
CL   E   EARTLY 76 IS A 300 GEV  P NUCLEUS EXPT.  STRUCTURE AT 6 GEV IS      4/77*
CL   E   ABOUT 5 PER CENT THE J/PSI CROSS SECT. DOES NOT SEE THE PSI(3700).  4/77*
CL   H   HOM1 76 AND HOM2 76 ARE FROM A 400 GEV P NUCLEUS EXPT. CROSS SECTS. 4/77*
CL   H   ARE FOR THE 6 GEV MASS REGION, WHERE AN ENHANCEMENT IS REPORTED IN  4/77*
CL   H   E+E-(HOM1 76) BUT NOT IN MU+MU-(HOM2 76). E+E- BUMP MAY BE A        4/77*
CL   H   STATISTICAL FLUCTUATION.                                            4/77*
CL   T   THEODOSIOU 76 IS A CORNELL GAMMA BE EXPT., WITH MAX. ENERGY OF      4/77*
CL   T   11 GEV, LOOKING FOR ELECTRONS AND/OR GAMMAS. CROSS SECTION IS       4/77*
CL   T   CONVERTED FROM DIFF. C.S. GIVEN AS 130EXP(3T) NB/GEV2 EXPECTED FOR  4/77*
CL   T   THE 0- CHARM-ANTICHARM STATE                                        4/77*

CH       HEAVY PARTICLE PRODUCTION CROSS SECTION (CM**2)
CH   L    0  1. E-31 OR LESS           LEIPUNER  73 CNTR +- M=3-11 GEV       5/76*
CH   L   LEIPUNER 73 IS AN NAL 300 GEV P EXPT. WOULD HAVE DETECTED PARTICLES 4/76*
CH   L   WITH LIFETIME GREATER THAN 200 NSEC.                                4/76*

CS       HEAVY PARTICLE PRODUCTION CROSS-SECTION (CM**2/NUCLEON)
CS   G    0  2.5E-35 OR LESS           GUSTAFSON 76 CNTR 0  TAU GT 10**-7    1/77*
CS   G   GUSTAFSON 76 IS A 300 GEV FNAL EXPT LOOKING FOR HEAVY (M GT 2 GEV)  1/77*
CS   G   LONGLIVED NEUTRAL HADRONS IN THE M4 NEUTRAL BEAM. THE ABOVE TYPICAL 1/77*
CS   G   VALUE IS FOR M=3 GEV AND ASSUMES AN INTERACTION CROSS SECTION OF    1/77*
CS   G   1 MB.  VALUES AS A FUNCTION OF MASS AND INTERACTION CROSS SECTION   1/77*
CS   G   ARE GIVEN IN FIG. 2.                                                1/77*

D        HEAVY PARTICLE PRODUCTION DIFFERENTIAL CROSS SECTION (CM**2/SR-GEV)
D         0  1.5E-36 OR LESS           DORFAN    65 CNTR BE TARGET  M=3-7GEV 5/76*
D    C    0  3.0E-36 OR LESS           DORFAN    65 CNTR FE TARGET  M=3-7GEV 5/76*
D         0  2.4E-35 OR LESS  CL=.90   BINON     69 CNTR Q=- M=1-1.8 GEV     3/77*
D    S    0  2.4E-35 OR LESS  CL=.90   ANTIPOV1  71 CNTR Q=- M=1.2-1.7,2.1-4 3/77*
D    T    0  1.2E-35 OR LESS  CL=.90   ANTIPOV2  71 CNTR Q=- M=2.2-2.8       3/77*
D    L    0  5.8E-34 OR LESS  CL=.90   ALPER     73 SPEC +- M=1.5-24 GEV     5/76*
D    A    0  1. E-31 OR LESS  CL=.90   APPEL1    74 CNTR +- M=3.2-7.2 GEV    2/76
D    L    0  2.2E-33 OR LESS  CL=.90   ALBROW    75 SPEC Q=+-1 M=4-15 GEV    1/77*
D    L    0  1.1E-33 OR LESS  CL=.90   ALBROW    75 SPEC Q=+-2 M=6-27 GEV    1/77*
D    J    0  8. E-35 OR LESS  CL=.90   JOVANOVIC 75 CNTR +- M=15-26 GEV      2/76
D    J    0  1.5E-34 OR LESS  CL=.90   JOVANOVIC 75 CNTR Q=+-2, M=3-10 GEV   2/76
D    J    0  6. E-35 OR LESS  CL=.90   JOVANOVIC 75 CNTR Q=+-2, M=10-26 GEV  2/76
D    B    0  2.6E-36 OR LESS  CL=.90   BALDIN    76 CNTR Q=-1, M=2.1-9.4 GEV 1/77*
D        ... (TO 2.4 GEV/C) EXPT AT FNL. UNITS ARE PER GEV MOMENTUM         5/76*
D    C   PER NUCLEUS.                                                        5/76*
D    S   ANTIPOV1 71 LIMIT INFERRED FROM FLUX RATIO. 70 GEV P EXPERIMENT.    3/77*
D    T   ANTIPOV2 71 IS FROM SAME 70 GEV P EXP. AS ANTIPOV1 71 AND BINON 69. 3/77*
D    L   ALPER 73 IS CERN ISR 26+26 GEV P+P EXPT.  P>.9 GEV, .2< BETA <.65.  5/76*
D    A   APPEL1 74 IS NAL 300 GEV P+W EXPERIMENT. STUDIES FORWARD PRODUCTION 2/76
D    A   OF HEAVY (UP TO 24 GEV) CHARGED PARTICLES WITH MOMENTA 24-200GEV(-) 2/76
D    A   AND 40-150GEV (+CHG).  ABOVE TYPICAL VALUE IS FOR 75 GEV AND IS     5/76*
D    A   PER GEV MOMENTUM PER NUCLEON.                                       5/76*
D    L   ALBROW 75 IS A CERN ISR EXPT WITH ECM=53 GEV. THETA=40 MR. SEE      1/77*
D    L   FIG. 5 FOR MASS RANGES UP TO 35 GEV.                                1/77*
D    J   JOVANOVICH 75 IS A CERN ISR 26+26 AND 15+15 GEV P+P EXPERIMENT.     2/76
D    J   FIG.4 COVERS RANGES Q=1/3 TO 2 AND M=3 TO 26 GEV.                   2/76
D    J   VALUE IS PER GEV MOMENTUM.                                          5/76*
D    B   BALDIN 76 IS A 70 GEV SERP EXP.  VALUE IS PER AL NUCLEUS AT         1/77*
D    B   THETA=0.  FOR OTHER CHARGES IN RANGE -0.5 TO -3.0, CL=.90 LIMIT IS  1/77*
D    B   (2.6E-36)/ABS(CHARGE) FOR MASS RANGE (2.1 TO 9.4GEV)*ABS(CHARGE).   1/77*
D    B   ASSUMES STABLE PARTICLE INTERACTING WITH MATTER AS DO ANTIPROTONS.  1/77*

CA       CROSS-SEC FOR PROD AND CAPT OF LONG-LIVED MASSIVE PARTICLES (CM**2)
CA   F    0   .1-9E-36 OR LESS         FRANKEL   74 CNTR TAU=1 TO 1000 HRS   7/76*
CA   R    0  1.4-9E-36 OR LESS         FRANKEL   75 CNTR TAU=50 MS TO 10 HRS 2/77*
CA   A    0   2-20E-34 OR LESS         ALEKSEE1  76 ELEC TAU*100 MS TO 1 DAY 4/77*
CA   A    0   .2-8E-34 OR LESS         ALEKSEE2  76 ELEC TAU=5 MS TO 1 DAY   3/77*
CA   F   FRANKEL 74 LOOKS FOR PARTICLES PRODUCED IN THICK AL TARGETS BY      7/76*
CA   F   300-400 GEV/C PROTONS.                                              7/76*
CA   R   FRANKEL 75 IS EXTENSION OF FRANKEL 74.                              2/77*
CA   A   ALEKSEEV(1,2) 76 ARE 61-70 GEV P SERP EXPT. CS IS PER PB NUCLEUS.   3/77*

F        HEAVY PARTICLE FLUX IN COSMIC RAYS (NUMBER/CM**2-SEC-SR)
F         0  3.0E-10 OR LESS           BJORNBOE  68 CNTR     M ABOVE 5 GEV   4/77*
F         0  5.0E-11 OR LESS  CL=.90   JONES     67 ELEC     M=5 TO 15 GEV   3/77*
F         0  3.0E-8  OR LESS           DARDO     72 CNTR                     4/77*
F         0  1.5E-9  OR LESS           TONWAR    72 CNTR     M GT 10 GEV     4/77*
F    Y    5  6. E-9  OR MORE           YOCK      74 CNTR     M GT 6 GEV      1/76
F         0  7. E-10 OR LESS  CL=.90   YOCK      75 ELEC +- Q GT 7 OR LT -7E 9/76*
F         0  1.0E-9  OR LESS           BHIATORE  76 ELEC                     4/77*
F    Y   YOCK 74 EVENTS COULD BE TRITONS.                                    1/76

C        LIGHT (BETWEEN MU AND E MASSES) PARTICLE MASS(UNITS-ELECTRON MASSES)
C         0    NONE BETWEEN 6 AND 25     BELOUSOV  60 CNTR   SPINOR,TAU>1 E-8   5/76*
C         0    NONE BETWEEN 2 AND 25     GORBUNOV  60 CC     SPINOR,TAU>1 E-9   5/76*
C         0    NONE BETWEEN 5 AND 175    COWARD    63 CNTR   SPINOR,TAU>22 E-10 5/76*
C         0    NONE BETWEEN 5 AND 175    COWARD    63 CNTR   SCALAR,TAU>68 E-10 5/76*
C    D    0    NONE BETWEEN 2 AND 13     BLAGOV    75 CNTR  SPINOR,TAU>2E-10SEC 2/76
C    D    0    NONE BETWEEN 2 AND 10.6   BLAGOV    75 CNTR  SCALAR,TAU>2E-10SEC 2/76
C    D   BLAGOV 75 BOUNDS ON LIFETIME DEPEND ON MASS AND IMPROVE AS MASS        4/77*
C    D   DECREASES.  AT 2 GEV THE EXPERIMENT IS SENSITIVE TO TAU>3E-11 SEC      4/77*
C    D   FOR SPINOR, TAU>5E-11 SEC FOR SCALAR.                                  4/77*
```

****** ********* ********* ********* ********* ********* ********* ********

REFERENCES FOR OTHER NEW PARTICLE SEARCHES


```
BELOUSOV 60 JETP 11 1143      +RUSAKOV,TAMM,CERENKOV                  (LEBD)
GORBUNOV 60 JETP 11 51        +SPIRIDONOV,CERENKOV                    (LEBD)
COWARD   63 PR 131 1782       +GITTELMAN,LYNCH,RITSON                 (STAN)
DORFAN   65 PRL 14 999        +EADES,LEDERMAN,LEE,TING                (COLU)
JONES    67 PR 164 1584        (MICH+WISC+LBL+UCLA+MINN+COSU+COLO+MURA)
BJORNBOE 68 NC B53 241        +DAMGARD,HANSEN,CHATTERGEE+    (BOHR+BERN)
BINON    69 PL 30B 510        DUTEIL,KACHANOV,KHROMOV,KUTYIN+         (SERP)

ANTIPOV1 71 PL 34B 164        +DENISOV,DONSKOV,GORIN,KACHANOV+        (SERP)
ANTIPOV2 71 NP B31 235        +DENISOV,DONSKOV,GORIN,KACHANOV+        (SERP)
DARDO    72 NC 9A 319         DARDO,NAVARRA,PENENGO,SITTE             (TORI)
TONWAR   72 JPA 5 569         TONWAR,NARANAN,SREEKANTAN               (TATA)
ALPER    73 PL 46B 265         (CERN+LIVP+LUND+BOHR+RHEL+STOH+BERG+LOUC)
LEIPUNER 73 PRL 31 1226       +LARSEN,SESSOMS,SMITH,WILLIAMS+   (BNL+YALE)

APPEL1   74 PRL 32 428        +BOURQUIN,GAINES,LEDERMAN,PAAR+ (COLU+FNAL)
APPEL2   74 PRL 33 722        +BOURQUIN,GAINES,HOM,LEDERMAN+  (COLU+FNAL)
BOYMOND  74 PRL 33 112        +MERMOD,PIROUE,SUMNER,CRONIN+    (PRIN+EFI)
BUSSER   74 PL 53B 212        +CAMILLERI,DILELLA+     (CERN+COLU+ROCK+SACL)
FRANKEL  74 PR D9 1932        +FRATI,RESVANIS,YANG,NEZRICK     (PENN+NAL)
YOCK     74 NP B76 175        P.C.M.YOCK                (UNIV OF AUCKLAND)

ALBROW   75 NP B97 189        +BARBER,BENZ+ (CERN+DARE+FOM+LANC+MCHS+UTR)
APEL     75 PL 56B 190        +AUGENSTEIN,BERTOLUCCI,DONSKOV,+(SERP+CERN)
BLAGOV   75 YAD.FIZ. 21,300   +KOMAR,MURASHOVA,SYREISHCHIKOVA+        (LEBD)
FRANKEL  75 PR D12 2561       +FRATI,RESVANIS,YANG,NEZRICK    (PENN+FNAL)
JOVANOVI 75 PL 56B 105        JOVANOVICH+ (MANI+AACH+CERN+GENO+HARV+TORI)
LEDERMAN 75 PRL 35 1543       +WHITE                                  (COLU)
YOCK     75 NP B86 216        P.C.M. YOCK          (UNIV OF AUCKLAND+SLAC)

ABRAMOV  76 PL 64B 365        +SULYAEV,BONDARENKO,DOBRETSOV + (SERP+MEPI)
ALESKEE1 76 SJNP 22 531       ALESKEEV,ZAITSEV,KALININA,KRUGLOV+    (JINR)
ALEKSEE2 76 SJNP 23 633       ALEKSEEV,ZAITSEV,KALININA,KRUGLOV+    (JINR)
ANISIMOV 76 PL 65B 85         ANISIMOVA,BONDARENKO,GOVOROV +   (SERP+MEPI)
BACCI    76 PL 58B 190        +BIDOLI,PENSO,STELLA,+           (ROMA+FRAS)
BALDIN   76 SJNP 22 264       +VERTOGRADOV,VISHNEVSKII,GRISHKEVICH+(JINR)
BARBIELL 76 PL 64B 359        BARBIELLINI,NICOLETTI+(FRAS+NAPL+PISA+ROMA)
BRIATORE 76 NC 31A 553        +DARDO,PIAZZOLI,MANNOCCHI+ (LCG+FRAS+FREI)
EARTLY   76 PRL 36 1355       +GIACOMELLI,PRETZL           (FNAL+BGNA+MUNI)
ESPOSITO 76 PL 64B 362        +FELICETTI,MARINI,+  (FRAS+ROMA+PADO+NAPL)
GUSTAFSO 76 PRL 37 474        GUSTAFSON,AYRE,JONES,LONGO,MURTHY     (MICH)
HOM1     76 PRL 36 1236       +LEDERMAN,PARR,SNYDER+      (COLU+FNAL+STON)
HOM2     76 PRL 37 1374       +LEDERMAN,PAAR,SNYDER,+     (COLU+FNAL+STON)
KASHA    76 PRL 36 1007       +KELLOGG,LAUTERBACH,ADAIR+  (YALE+BNL+FNAL)
LAUTERBA 76 PRL 37 1436       LAUTERBACH,ADAIR,CARTER,GRANNAN+ (YALE+BNL)
LEIPUNER 76 PRL 36 1011       +LARSEN,ADAIR,CARTER+         (BNL+YALE+FNAL)
THEODOSI 76 PRL 37 126        THEODOSIOU,GITTELMAN,HANSON,LARSON+  (CORN)

BRANSON  77 PRL 38 457        +SANDERS,SMITH,THALER,ANDERSON+ (PRIN+EFIN)
```


****** ********* ********* ********* ********* ********* ********* ********
****** ********* ********* ********* ********* ********* ********* ********

CROSS SECTION PLOTS

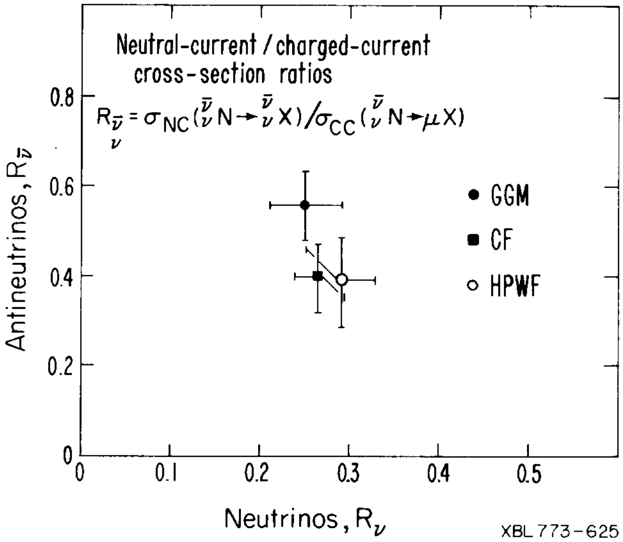

Neutral-current-to-charged-current cross-section ratios, neutrinos vs. antineutrinos. Determination by three separate experiments: Gargamelle collaboration [J.Blietschau et al., Nucl. Phys. B118, 218 (1977)]; Caltech-Fermilab [F.S.Merritt, Ph.D. Thesis, California Institute of Technology (1977); point has been corrected for experimental cuts assuming a scaling model for charged currents and an antiquark fraction in the nucleon of 17%]; and Harvard-Penn-Wisconsin-Fermilab [A.Benvenuti et al., Phys. Rev. Lett. 37, 1039 (1977)]. Because of the different energy regions and experimental cuts involved, some care should be exercised in making direct comparisons.

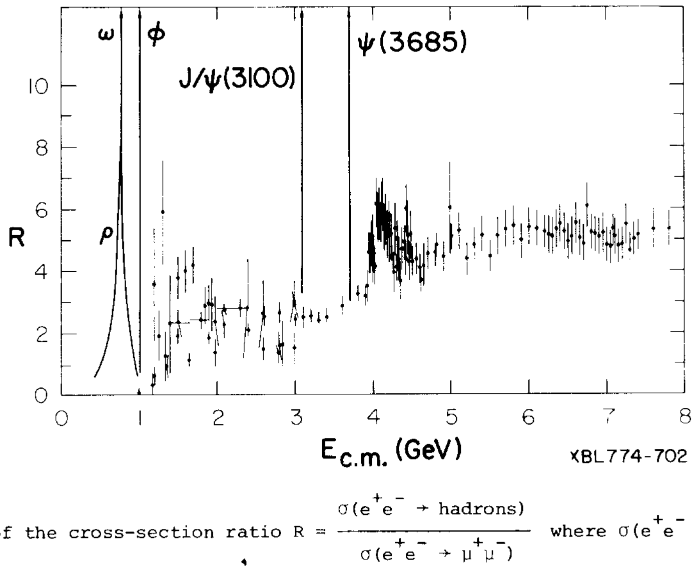

A summary of the cross-section ratio $R = \dfrac{\sigma(e^+e^- \to \text{hadrons})}{\sigma(e^+e^- \to \mu^+\mu^-)}$ where $\sigma(e^+e^- \to \mu^+\mu^-)$ is taken from QED as $86.8/E^2_{c.m.}$ nb-GeV^2, and $\sigma(e^+e^- \to \text{hadrons})$ is generally taken as the cross section of 3-or-more-prongs plus non-coplanar 2-prongs, as compiled by Schwitters and Straunch [Ann. Rev. Nucl. Sci. 26, 89 (1976)]. Between 3 and 8 GeV there is an overall normalization uncertainty of the order of 10%, and a further slowly varying uncertainty of as much as 15%. Below 3 GeV, the normalization uncertainty is of the order of 50%.

ERRATA

The following corrections should be made in the 1976 edition of "Review of Particle Properties", Particle Data Group [Rev. Mod. Phys. 48, No. 2, Part II (1976)]. A second page number given in parentheses following the first number refers to the corresponding page in the 1976 Particle Properties Data Booklet; where the second number is absent, the correction was already made in the Data Booklet before it was issued.

Page S21: The mass squared of the π^0 should read 0.0182 instead of 0.182.

Page S24 (8): The magnetic moment of the μ should read 1.001 165 897 $\frac{e\hbar}{2m_\mu c}$ instead of 1.001 166 897 $\frac{e\hbar}{2m_\mu c}$.

Page S26: The width of the π^0 should read 7.95±0.55 eV instead of 7.8±0.9 eV; the width of the η should read 0.85±0.12 keV instead of 2.63±0.58 keV; and the percentage decay of the η into neutral and charged modes should read 71.0 and 29.0, respectively, instead of 71.1 and 28.9. These values (or their equivalents) are all given correctly in the Stable Particle Table.

Page S32: The J^P of the $\Lambda(1860)$ should read $3/2^+$ instead of $1/2^+$.

Page S33: The mass of the $\Sigma(1765)$ should read 1773 instead of 1723.

Page S35 (39): On the line giving the value of what is called "μ_p", the notation should be changed to "μ_N"; this is the nuclear magneton, not the proton magnetic moment. The next line, giving μ_p/μ_{Bohr}, should be completely replaced by

$$\mu_p/\mu_{Bohr} = 0.001521032210(18) \qquad 0.012 \; ;$$

the μ_p appearing here is the proton magnetic moment. Additionally, the third expression for R_∞ should read $m_e c\alpha^2/2h$ instead of $m_e c\alpha^2/2\hbar$; the numerical value is correct as it stands. Also, the gravitational constant should read $6.6720(41)\times10^{-8}\,\mathrm{cm}^3\,\mathrm{g}^{-1}\,\mathrm{sec}^{-2}$ instead of $6.6732(31)\times10^{-8}\,\mathrm{cm}^{-3}\,\mathrm{g}^{-1}\,\mathrm{sec}^{-2}$. And finally, on the line giving the pressure of 1 atmosphere, the word "dynes" should be replaced by "g(force)"; also note that 1 bar = 10^6 dynes/cm^2.

Pages S40-S41 (52-53): Equation II-19 should be deleted; also, both parts of Eq. II-20 and the first part of Eq. II-23 (defining u) should be marked to indicate that they apply in the (ab) c.m. system only.

Page S45 (72): In Section C.3, on multiple Coulomb scattering, the expression given for $\theta^{1/e}_{proj}$ should have referred to θ^{rms}_{proj} [see V. L. Highland, Nucl. Instr. and Meth. 129, 497 (1975); also private communication]; the proper equation, for θ^{rms}_{proj}, is given below. The correct description of multiple scattering is as follows. The probability of scattering through a space angle θ into an element of solid angle $d\Omega = \sin\theta d\theta d\phi$ in terms of a parameter θ_0 is given to a good approximation by

$$f(\theta)d\Omega = Ke^{-\theta^2/\theta_0^2}\,d\Omega \; ,$$

with $K \cong 1/(\pi\theta_0^2)$. For this distribution, $\theta^{1/e}$, the angle such that $f(\theta^{1/e})/f(0) = 1/e$, is equal to $\theta^{rms} = \sqrt{\langle\theta^2\rangle} = \theta_0$. This distribution may be expressed in terms of the two projected angles θ_x and θ_y, with $d\Omega = d\theta_x d\theta_y$, and the probability of one of the projected angles, say θ_x, derived as

$$g(\theta_x)d\theta_x = \frac{1}{\sqrt{2\pi}\,\theta_x^{rms}}\, e^{\left\{-\frac{\theta_x^2}{2(\theta_x^{rms})^2}\right\}}\, d\theta_x$$

with $2(\theta_x^{rms})^2 = \theta_0^2$. For this distribution, $\theta_x^{rms} = \theta_x^{1/e}/\sqrt{2}$ is given by the expression

$$\theta^{rms}_{proj} = z\,\frac{14\mathrm{MeV}/c}{p\beta}\sqrt{\frac{L}{L_R}}\left[1+\frac{1}{9}\log_{10}\left(\frac{L}{L_R}\right)\right]\left[1+\frac{M^2}{Em_s}\right]$$

for the scattering of a particle of mass M, charge $z|e|$, velocity β, and energy E in a thickness L of a medium of radiation length L_R and atomic mass m_s. The distribution for $g(\theta_x)$ is accurate experimentally at the 5-10% level except in the tails, which are broader than the Gaussian form. For this reason, the notation "rms", which has come into general use in this problem, is somewhat of a misnomer. It should be understood that this refers to the $1/\sqrt{e}$ point of the distribution, i.e., $g(\theta^{rms}_{proj})/g(0) = e^{-1/2} = 0.606$, and not to the true rms projected scattering angle (which is larger than θ^{rms}_{proj} due to the large tails). Note that for incident electrons, positrons, or heavy nuclei, this formula is inaccurate.

ACKNOWLEDGMENTS

We would like to thank V. E. Barnes and D. Carmony for their very useful suggestions for new items to be included in the Review of Particle Properties. Some of these suggestions have been incorporated into this edition and others will be added to the next full edition in April 1978. We would also like to thank C. Ballagh, W. Chinowsky, G. Feldman, G. Goldhaber, R. Hagstrom, B. Knapp, R. Madaras, M. Perl, R. Schwitters, and J. Wiss for their useful comments and suggestions for this edition.

A SPECIAL REQUEST

The Particle Data Group is currently compiling a database of experimental high energy physics reports and proposals. We publish an account of active high energy physics experiments (LBL-91) and will publish an index of high energy physics reports (LBL-90). Our database will eventually become directly accessible to users at any institution. An important feature of our system will be a link between each report and the experimental proposal that generated the data in that report. In order to help make this link, we request that publications include the accelerator and proposal number in a footnote.

MASS DEPENDENCE OF STATISTICAL FISSION PARAMETERS*

M. BECKERMAN and M. BLANN
Department of Chemistry,
and Nuclear Structure Research Laboratory[1], *University of Rochester, Rochester, N.Y. 14627, USA*

Received 4 February 1977

Statistical fission parameters B_f and a_f/a_ν are extracted from analyses of recently measured heavy-ion induced fission and evaporation residue excitation functions for medium mass systems using a formalism with spin dependent level densities and multiple particle/fission competition. Results are compared with those of the less rigorous s-wave approximation as treated in the code ALICE.

One property of nuclei at high angular momenta is an increase in fissionability, such as that described by the rotating liquid drop model (RLD) of Cohen et al. [1]. The parameters which govern the (statistical) fission of these nuclei are therefore of interest since they are related to the property of deformation versus angular momentum. Most analyses have been performed using formulations which either did not use appropriate spin dependent level densities, or which ignored consequences of multiple particle emission, or both. Thus, it is not clear whether the parameters extracted represent the approximations in formulations used or the characteristics of the nuclei involved.

An additional problem of heavy ion fission data analyses has been the data themselves. These have often been only fission excitation functions, necessitating arbitrary assumptions concerning the compound nucleus formation cross sections and, therefore, the limiting angular momenta (l_{crit}) for compound nucleus formation.

Recently, a large body of data [2, 3] has become available for which both fission and evaporation residue excitation functions have been measured, spanning a fairly broad compound nucleus mass range (A = 97–176). In this letter, we report analyses of these data using a code [4] which treats multiple particle emission with spin dependent nuclear level densities. We seek a description of the fission excitation functions in terms of a parameter which scales the fission barrier of the RLD model of [1], B_f, and a parameter which represents the ratio of single particle level densities at the saddle point to those at equilibrium deformation, a_f/a_ν. A recent application [5] of this code to the system $^{40}Ar + ^{109}Ag$ required a surprising liquid drop barrier reduction of 40%. In this paper we investigate the compound nucleus mass dependence of these fission parameters. Since many analyses are now being performed with the simpler statistical code "ALICE" [6], we also compare results of the new code with those of ALICE; the degree of agreement is found to be mass dependent.

The fission and particle (n, p, α) emission widths are given by

$$\Gamma_f \propto (2I+1) \int_0^{E-E_{sp}(I)} \rho_f(E - E_{sp}(I) - k)\, dk, \qquad (1)$$

and

$$\Gamma_\nu \propto (2S_\nu + 1) \sum_{l=0}^{\infty} \sum_{J=|I-l|}^{I+l} (2J+1) \int_0^{E-E_{min}(J)-B_\nu}$$

$$\times\, \rho_\nu(E - E_{min}(J) - B_\nu - \epsilon) T_\nu^l(\epsilon)\, d\epsilon,$$

where I and J represent emitting and residual nucleus angular momentum, respectively, and S_ν the intrinsic spin of particle ν; ϵ its channel energy, and B_ν its binding energy. The transmission coefficients $T_\nu^l(\epsilon)$ at orbital angular momentum l are computed using the nuclear optical model with parameters given by global sets [7]. Level densities given by $\rho_K(U) = U^{-2} \times \exp[2(a_K U)^{1/2}]$ are used; following Lang [8], the

* Work supported in part by the U.S. Energy Research and Development Administration.
1 Supported by a grant from the National Science Foundation.

excitation energies are decremented by the appropriate rotational energies. A value of $a_\nu = A/10$ is used. The maximum compound nucleus angular momenta used are determined from experimental fusion cross sections using the sharp cutoff model.

The rotational energy of each nucleus in its equilibrium deformed state, $E_{\mathrm{min}}(I)$, and at the saddle point, $E_{\mathrm{sp}}(I)$ are initially calculated using the RLD model. The saddle point energies are then adjusted in the calculations by scaling the fission barrier $B(I)$ by the constant, B_f:

$$E_{\mathrm{sp}}(I) = E_{\mathrm{min}}(I) + B(I)\cdot B_\mathrm{f} \qquad (2)$$

where $B(I)$ is the difference in RLD energies between the saddle point and equilibrium deformed nucleus.

The code evaluates decay widths for the energy (E) and angular momentum (J) cross section population elements of each nuclide, with a mesh size of 1 MeV by $1\hbar$, using a logic previously described [9] to follow the entire decay chain.

This code was used to analyze both the fission and evaporation residue excitation functions for the system ^{40}Ar + ^{109}Ag at bombarding energies between 169 and 340 MeV (Lab). While different parameter sets could reproduce narrow ranges of these excitation functions, it was found [5] that the entire range could be reproduced only by $a_\mathrm{f}/a_\nu = 1.03 \pm 0.03$, and $B_\mathrm{f} = 0.60 \pm 0.05$.

Beginning with this parameter set, we search for best sets for the fission excitation functions for ^{35}Cl + ^{62}Ni, ^{120}Sn, and ^{141}Pr at lab energies from 155 to 170 MeV, and for the system ^{20}Ne + ^{107}Ag at lab energies of 110–170 MeV. As before, analyses are restricted to l_{crit} values given by the sharp cutoff approximation to the experimental fusion cross sections. The binary division yields from the system ^{35}Cl + ^{62}Ni show some signs of mass asymmetry [2]. The compound nucleus may be below the point at which fission is stable against asymmetry [10]. The yields therefore may not be due to equilibrium fission and, if they are, the statistical fission [11] approach may not be applicable. The analyses are presented with these reservations in mind; only a lower limit to B_f is deduced for the ^{62}Ni system for these reasons.

The results of table 1 clearly show that the fission barriers must be reduced by factors of 30–50% from results given by the RLD model; a value of a_f/a_ν of 1.03 ± 0.03 seems adequate for the entire mass range which we have investigated. The B_f factors of table 1 indicate a minimum near $A = 127$. However, there are uncertainties in the experimental data analyzed and in the sharp cutoff approximation. The Cl-induced reaction data span a dynamic excitation range of less than 15 MeV, which makes unambiguous extraction of parameters difficult. In view of these difficulties in the data and analyses, a constant barrier reduction factor cannot be ruled out.

Some indication of the sensitivity of calculated results to parameter choices is indicated in the set of results of fig. 1 obtained using $B_\mathrm{f} = 1.0$, $a_\mathrm{f}/a_\nu = 1.25$. It may be seen that the sensitivity to parameter change over a given excitation energy range decreases with increasing mass. To further emphasize the desirability of data over a broad range of excitation energies we note the following example: At 200 MeV ^{35}Cl (lab) + ^{141}Pr, the calculated evaporation residue cross section is $\approx$200 mb for $B_\mathrm{f} = 0.65$, $a_\mathrm{f}/a_\nu = 1.03$, and only $\lesssim$50 mb for $B_\mathrm{f} = 1.00$, $a_\mathrm{f}/a_\nu = 1.25$. A more detailed illustration of this sensitivity may be found in [5].

We can only speculate at this point as to the rea-

Table 1
Statistical fission parameters deduced in this work

Target and projectile	A_{CN}	E_{lab} (MeV)	E^* (MeV)	J_{crit} ($\hbar$)	B_f	a_f/a_ν
^{62}Ni + ^{35}Cl [2]	97	155–170	86–95	58–66	$\gtrsim$0.54	1.04
^{107}Ag + ^{20}Ne [3]	127	118–166	75–122	37–60	0.51 ± 0.06	1.04 ± 0.03
^{109}Ag + ^{40}Ar [15]	149	169–337	71–194	49–108	0.60 ± 0.05 [a]	1.03 ± 0.03 [a]
^{116}Sn + ^{35}Cl [2]	151	155–170	63–74	43–60	0.57	1.02
^{141}Pr + ^{35}Cl [2]	176	155–170	49–61	24–49	$0.65^{+0.10}_{-0.05}$	$1.03^{+0.07}_{-0.03}$

[a] Result from [5].

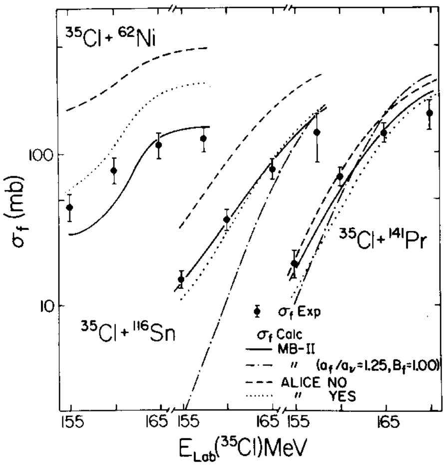

Fig. 1. Experimental and calculated fission excitation functions. Filled circles denote the experimental fission cross sections from [2]. Solid curves represent the present (MB-II) calculations using the parameters given in table 1: dashed and dotted curves denote s-wave (ALICE) calculations for NO and YES options, respectively. Dash-dot curves also shown for ^{35}Cl + ^{116}Sn and ^{35}Cl + ^{141}Pr denote (MB-II) calculations with a_f/a_ν = 1.25 and B_f = 1.00.

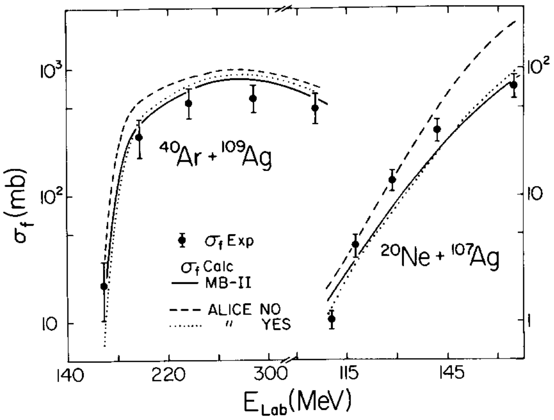

Fig. 2. Experimental and calculated fission excitation functions. Filled circles denote the experimental fission cross sections for ^{40}Ar + ^{109}Ag [15] and ^{20}Ne + ^{107}Ag [3]. Solid, dashed and dotted curves represent the same quantities as in fig. 1.

sons for what may seem to be large discrepancies between the barriers deduced from these analyses and the RLD model results. First, barrier calculations which include an estimate of the finite range of nuclear forces [12] give 10–30% decreases in $l = 0$ barrier heights in the mass range considered in this letter. Second, for the partial waves relevant to these analyses, the barriers are differences between two energies, and the percent error in the saddle point energies themselves are on the order of only 10%. Finally, it must be kept in mind that the compound nucleus model may itself be failing in the excitation ranges under consideration since the lifetime is no longer far in excess of the recurrence time [13]. Furthermore, inverse reaction cross sections may not be represented well by ground state capture cross sections [14]. These questions must be investigated more thoroughly before the significance of the results of this work are fully understood.

Statistical fission parameters often are deduced from analyses using a code due to Blann and Plasil [6] which makes use of the s-wave approximation; in order to understand how parameters deduced by means of the s-wave approximation may differ from those deduced using the more rigorous angular momentum coupling formalism of this work, s-wave calculations are also shown in figs. 1 and 2.

In the formalism of [6], there are two options available for fixing the angular momenta for which E_{sp} and E_{min} are evaluated. For one option (denoted by NO), the angular momenta are taken as the entrance channel orbital angular momenta; for the other (denoted by YES), they are taken as the orbital angular momenta decremented by a fixed amount following particle emission ($2\hbar$ for neutrons, $3\hbar$ for protons and $10\hbar$ for alpha particles). Results of calculations performed for each option are shown in figs. 1 and 2; the YES option provides results in better agreement with those of this work. The differences between each of the calculations increase as the mass number decreases, indicating an expected greater dependence upon the angular momentum treatment for lighter systems. The comparisons shown in fig. 1 apply to the parameters of table 1. Further investigations reveal that such differences are sensitive to a_f/a_ν and B_f (they depend upon the relative importance of multiple-chance fission contributions and upon the steepness, with angular momenta, of the fission branching ratios). However, for a fixed parameter set the mass dependence should follow a similar trend to that of figs. 1 and 2.

To summarize, for all systems investigated we find that the RLD fission barriers must be reduced by from 30 to 50% (B_f = 0.7 to 0.5) and $a_f/a_\nu \approx 1.03$.

There is some indication that B_f reaches a minimum near $A = 127$; in order to firmly establish parameters for $^{35}Cl + ^{141}Pr$ and for heavy mass systems high energy evaporation residue measurements are required with a simultaneous fitting criterion applied. In general, the YES option of [6] gives results similar to those of the present work except for the lightest mass system, although this last conclusion is not parameter independent.

References

[1] S. Cohen, F. Plasil and W.J. Swiatecki, Ann. of Phys. (NY) 82 (1974) 557.
[2] J. Bisplinghoff et al., Bull. Am. Phys. Soc. 21 (1976) 656.
[3] F. Plasil, R.L. Ferguson, F. Pleasonton and R.L. Hahn, preliminary results, cited by F. Plasil, in: Proc. of the Int. Conf. on Reactions between complex nuclei, eds. R.L. Robinson, F.K. McGowan, J.B. Ball and J.H. Hamilton, Nashville, 1974, p. 107.
[4] M. Beckerman and M. Blann, University of Rochester Nuclear Structure Research Laboratory Rpt. UR-NSRL-135, "MB-II description".
[5] M. Beckerman and M. Blann, Phys. Rev. Lett. 38 (1977) 272; Bull. Am. Phys. Soc. 21 (1976) 974.
[6] M. Blann and F. Plasil, Phys. Rev. Lett. 29 (1972) 303; F. Plasil and M. Blann, Phys. Rev. C11 (1975) 508; M. Blann, Reports COO-3494-29, COO-3494-32, "Overlaid Alice, description, revisions".
[7] D. Wilmore and P.E. Hodgson, Nucl. Phys. 55 (1964) 673; F.G. Perey and B. Buck, Nucl. Phys. 32 (1962) 353; F.G. Perey, Phys. Rev. 131 (1963) 745; G.R. Satchler, Nucl. Phys. 70 (1965) 177.
[8] D.W. Lang, Nucl. Phys. 77 (1966) 545.
[9] M. Blann, Phys. Rev. 157 (1967) 860.
[10] U.L. Businaro and S. Gallone, Nuovo Cim. 5 (1957) 315.
[11] N. Bohr and J.A. Wheeler, Phys. Rev. 56 (1939) 426.
[12] H.J. Krappe and J.R. Nix, in: Proc. of the Third Int. Atomic Energy Symposium on Physics and chemistry of fission, vol. I (International Atomic Energy Agency, Vienna, 1974) p. 159.
[13] M. Blann, in: Proc. Int. Symp. on Highly excited states, Jülich, 1975, eds. A. Faessler, C. Mayer-Böricke and P. Turek, p. 120.
[14] M. Beckerman and M. Blann, Progress Report COO-3494-31, Rochester (1976, unpublished) p. 75; O. Sauer, H. Chandra and U. Mosel, Nucl. Phys. A264 (1976) 221.
[15] H.C. Britt et al., Phys. Rev. C13 (1976) 1483.

ON THE FOCUSSING EFFECT AND THE LARGE ENERGY LOSS IN THE QUASI-FISSION REACTION

A. IWAMOTO and K. HARADA
Japan Atomic Energy Research Institute, Tokai-mura, Naka-gun, Ibaraki-ken, Japan

Received 14 July 1976
Revised version received 4 February 1977

A classical dynamical model is applied to the deep inelastic reactions between heavy ions. Assuming that the range of the nuclear interaction depends on the intrinsic excitation energies, the sharp angular distribution and the large energy loss in the quasi-fission reaction are explained systematically.

In the heavy ion collision with energy above the Coulomb barrier, it was found that the most of the total reaction cross section σ_R is distributed among the deep inelastic process σ_{DI} and the fusion process σ_{FUS}, and the ratio σ_{DI}/σ_{FUS} changes considerably depending on the masses of the entrance channel. For the reactions induced by Ar or even lighter ions on heavy targets [1], a large part of the reaction cross section goes to the fusion channel and the critical angular momentum l_{cr} for this process increases with the incident energy. However, for the reactions induced by Kr or even heavier ions on heavy targets [2–7] the fusion cross section is only a fraction of the total reaction cross section and the most part of it goes to the deep inelastic process. Of particular interest is that the mass of the outgoing particle is very near to the projectile's, whereas the total kinetic energy is grossly equal to what would be expected for the fission of the compound nucleus (quasi-fission). In addition, the angular distribution is peaked very sharply near the grazing angle, irrespective of the incident energy.

Gross et al. [8], Bondorf et al. [9] and Tsang [10] proposed a classical model with a phenomenological friction force for these reactions. It was found that the general trend of the critical angular momentum for the fusion reaction could be reproduced with this model when the incident ion is Ar or even lighter ones [8, 9, 11, 12], however for the reaction induced by the heavier projectile it was hard to fit the angular distribution and energy loss of the quasi-fission reaction and fusion cross section simultaneously. In fact Gross et al. [11] calculated the Kr + Bi reaction at laboratory energies 525 MeV and 600 MeV, and succeeded in obtaining the sharp angular distribution of 600 MeV data. However, they could not reproduce the angular distribution of the 525 MeV data well. For the 525 MeV data, Deubler and Dietrich [13] showed that the angular distribution could be understandable as a consequence of the "double rainbow" type deflection function. However, these treatments [11, 13] could not reproduce the energy loss well and moreover the comparison with experiments was limited to one or two cases. These circumstances lead us to examine if the characteristic features for very heavy ion reactions could be reproduced systematically with a simple model.

We start with the same equations of motion for the classical system as used by Bondorf et al. [9]. In this model, the Lagrangian of the system is written as

$$\mathcal{L} = \tfrac{1}{2}(\mu\dot{r}^2 + \mu r^2\dot{\theta}_0^2 + I_1\dot{\theta}_1^2 + I_2\dot{\theta}_2^2) - V_N(r) - V_C(r) \quad (1)$$

where r is the distance between mass centers, θ_0 the rotational angle of the molecular axis, θ_i the rotational angle of the nucleus i, μ the reduced mass of the relative motion and I_i the moment of inertia of the nucleus i. After a suitable transformation of the variables, we introduce three types of phenomenological frictional forces which are assumed to be diagonal and proportional to the velocities with respect to new variables. They are called as radial, tangential and rolling frictions, respectively. To reduce the number of parameters, we have set the coefficient of the rolling friction to be zero. This will be admissible from the analogy of classical mechanics where the rolling friction is much weaker than the tangential one. We have also assumed that two nuclei have initially zero spins and the moment of inertia I_i is given by that of the rigid body since the typical intrinsic excitation energy is more than several tens of MeV. After some calculations, we obtain the following equations of motion

$$\mu\ddot{r} - l^2/\mu r^3 + \frac{\partial}{\partial r}(V_N + V_C) = -C_r f(r)\dot{r} \,.$$

$$\mu\dot{l} = C_t g(r)\,[5\,l_0/2 - \{5/2 + (R_1 + R_2)^2/r^2\}\,l] \,. \tag{2}$$

Here, C_r and C_t are the strength of the radial and tangential frictions, $f(r)$ and $g(r)$ the form factors of the radial and tangential frictions, l the relative orbital angular momentum given by $l = \mu r^2 \dot{\theta}_0$ and l_0 the initial value of the orbital angular momentum.

For the nuclear potential $V_N(r)$, we adopt the "Orsey potential" parametrized by Ngô et al. [14]. It consists of the attractive Gaussian potential and the repulsive one with quadratic form. It was found that the potential reproduces the interaction barrier [15] and the critical angular momentum for fusion [12] fairly well. For simplicity we use the same value for the radius parameters r_0 as those given in table 2 of ref. [14] to calculate the matter and charge radii $R_i = r_0 A_i^{1/3}$. The Coulomb potential is assumed as

$$\begin{aligned} V_C &= Z_1 Z_2\, e^2/r \quad \text{for} \quad r \geqslant R_1 + R_2 \,, \\ V_C &= V_0 - kr^n \quad \text{for} \quad r \leqslant R_1 + R_2 \,. \end{aligned} \tag{3}$$

where the value V_0 is given by

$$V_0 = 3Z_1 Z_2 e^2 (5/R_2 - R_1^2/R_2^3)/10 \quad \text{for} \quad R_1 \leqslant R_2 \,. \tag{4}$$

The form of V_C, and the value of k and n are taken from ref. [9], but the value of V_0 is determined by using the sudden approximation under which the charge density distribution at $r = 0$ is expressed as a completely overlapped liquid drops. The form factors $f(r)$ and $g(r)$ of radial and tangential frictions are assumed to be equal and to have the same forms as those given in ref. [9] inside the touching radius $r = R_1 + R_2$. For the outer region, we assume that they have the same forms as that of the nuclear potential $V_N(r)$, although the strengths are normalized so that they are joined smoothly with each other at the touching radius. This assumption was made in order to reduce the number of the fitting parameters. The coefficients C_r and C_t are given in units of MeV/c fm^4 = $10^{-23}/3$ MeV sec/fm^5 throughout this article.

Next, we introduce a new assumption about the nuclear potential and friction form factors. It is motivated by the fact that most of the classical dynamical models give the smaller energy loss of the quasi-fission reaction than the experimental data. This difference amounts more than 30 MeV. In this respect, Bondorf et al. [16] has pointed out that the potentials in the incident and exit channels may differ very much. Deubler and Dietrich [13] have performed the calculation taking into account the deformability of the nucleus and showed that this effect causes the increase of the energy loss. Instead of introducing other collective coordinates, we have taken into account the asymmetry of the incident and exit channels by requiring that the range of the nuclear potential increases with the intrinsic excitation energy. We have assumed in this paper that the width parameter a in the Gaussian tail of the nuclear potential be expressed as

$$a = a_0(l + C_e\sqrt{\Delta E}) \,, \tag{5}$$

where a_0 is the original width parameter and has the value ($\sqrt{1/0.27} = 1.92$) fm [14], ΔE is the energy loss and C_e the parameter with the dimension (MeV)$^{-1/2}$. The quantities ΔE and a are functions of time and are calculated at every instant in the reaction process. This assumption is phenomenological and in particular, the functional form in eq. (5) is adopted tentatively as a first choice. The underlying physical consideration is the following.

In the Thomas–Fermi model of the nucleus, the local matter density $\rho(r)$ is expressed as a function of the single-particle potential $u(r)$ and the temperature θ. If the function $u(r)$ is approximated by the linear function of r near and slightly beyond the surface region, then the density $\rho(r)$ behaves as an exponential decaying function of r in that region, the width of which is proportional to the temperature θ. The Fermi-gas model gives the relation $\theta \propto \sqrt{\Delta E}$, and so the density $\rho(r)$ stretches proportional to $\sqrt{\Delta E}$. We assume that the stretch of the density $\rho(r)$ causes the stretch of the ion-ion interaction $V_N(r)$, which is proportional to the former. This is approximately satisfied if we construct the potential by folding the elementary interaction with the density $\rho(r)$.

If we use eq. (5), the attractive part of the ion–ion potential becomes too large for high energy reactions where the energy loss is very large. So we postulate a kind of normalization that the potential depth at the

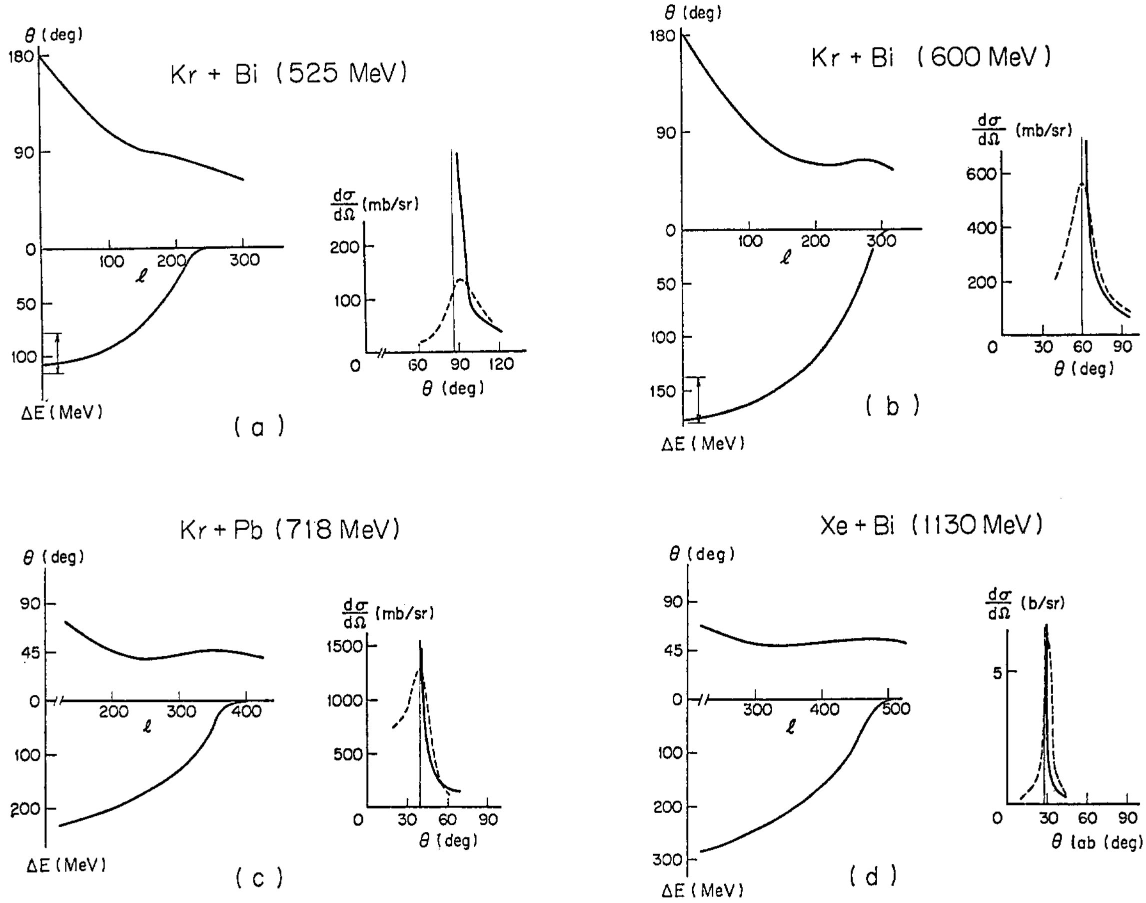

Fig. 1. Scattering angles θ and energy losses ΔE as functions of the initial orbital angular momenta l, and the angular distributions for several reactions. Values of the friction coefficients (C_r, C_t) are set to be (500, 300) for all reactions and the parameter C_e is set to be 0.07, 0.07, 0.05, 0.06 respectively for (a)–(d). Scattering angle θ is defined in the center-of-mass frame except for that used in the angular distribution of (d) where the scattering angle in the laboratory frame is adopted. The arrows in the energy loss curves represent the experimental data. In the angular distribution curves, the solid lines are the calculated results and the dashed lines are experimental data. Data are taken from (a) ref. [2]; (b) ref. [3]; (c) ref. [5]; (d) ref. [6].

touching radius decreases as ΔE increases under the condition that the potential depth at the half-depth point of the original potential is kept fixed. Since the friction form factors are assumed to be the same as those of the nuclear potential, eq. (5) is also applied to them except for the normalization.

In fig. 1, we show the results of our calculation for typical very heavy ion reactions. Shown are the scattering angles and energy losses as functions of the incident angular momenta, and the angular distributions together with the experimental data. The coefficients of frictional forces are fixed to $(C_r, C_t) = (500, 300)$ for all reactions. As is seen in this figure, our model is able to reproduce the focussing effect and the large energy loss systematically. The deflection functions tell us that the focussing effect in fig. 1(a) occurs owing to the "shoulder" region located at $l = 140, 160$, on the other hand, the focussing in the higher energy reactions (fig. 1(b)–1(d)) is due to the "double rainbow" scattering as discussed in ref. [13]. In accordance

Table 1
Comparison of the calculated results with the experimental data. Listed are: E_{lab}, incident laboratory energy; C_e, the parameter defined in eq. (5); l_{cr}, the critical angular momentum for fusion (l_{cr} = 0 means no fusion cross section); ΔE, the energy loss in the focussing region; Δl, the angular momentum loss at the focussing angle. The value of the friction coefficients (C_r, C_t) are set to be (500, 300) for all systems.

System	E (lab) (MeV)	C_e (MeV)$^{-1/2}$	l_{cr}(th) ($\hbar$)	l_{cr}(exp) ($\hbar$)	ΔE (th) (MeV)	ΔE (exp) (MeV)	Δl (th) ($\hbar$)	θ (th) (deg)	θ (exp) (deg)	Ref.
Kr + Bi	525	0.07	0	~0	107–48	100	31	86,5	90	[2]
	600	0.07	0	~0	175–108	140	35	59.7	58	[3]
Kr + Pb	494	0.07	0	~0	81–34	–	26	99.0	90	[5]
	510	0.07	0	~0	97–42	–	29	90.6	80	[5]
	718	0.05	0	small	253–165	–	43	39.0	42	[5]
Xe + Bi	1130	0.06	0	–	324–210	300–0	56	27.3 [a]	30 [a]	[6]
Ar + Sb	199	0.01	74	84 ± 6	15 [b]	–	13	0.0	–	[17]
	300	0.01	97	107 ± 10	77 [b]	–	18	0.0	–	[17]

[a] Focussing angle in the laboratory frame. [b] Maximum energy loss.

with ref. [13], the rainbow angle located at lower l corresponds to the quasi-fission peak where the energy loss is very large. Our calculation always yields either "shoulder" or "double rainbow" type deflection function for the reactions induced by Kr or Xe.

In table 1, we show our results of calculations together with some experimental results. Here, the focussing of the angular distributions for 525 MeV Kr + Bi and 494 and 510 MeV Kr + Pb are "shoulder" types, and for the remaining 600 MeV Kr + Bi, 718 MeV Kr + Pb and 1130 MeV Xe + Bi are "double rainbow" types. As seen in this table, no fusion cross section is obtained for the reaction induced by Kr and Xe. This is consistent with the experiments [2–7] where the fusion cross section is a very little fraction of the total reaction cross section. This is a natural consequence of using the "Orsay potential", because its nuclear plus Coulomb potential for l = 0 wave has a potential pocket with almost zero depth for Kr + Bi and Kr + Pb systems, and has no pocket for Xe + Bi system. This is in contrast with the system Ar + Sb where the total potential for l = 0 wave has a pocket with a depth of about 15 MeV, which yields a large fusion cross section as shown in table 1. In this respect, the "Orsey potential" may be better than the folding potential because the latter yields a moderately large fusion cross section even for Kr induced reactions [11].

As seen in fig. 1 and table 1, the energy losses in the quasi-fission reactions are nicely reproduced with our model. This is entirely due to the assumption (5), that is, the ranges of the nuclear and frictional forces stretch as the nuclei are excited intrinsically. Comparing with the entrance channel, the barrier of the exit channel potential moves to the larger center separation while reducing its height. As a result, the kinetic energy of the outgoing particle could be lower than the barrier height of the incident channel, yielding a large energy loss as obtained in the experiments. The most interesting result in our calculation is that the assumption (5) causes the focussing effect as well as the increase of energy loss. This was checked by setting the coefficient C_e being zero. In this case, the 600 MeV Kr + Bi reaction still exhibits the double rainbow structure but the second rainbow angle is about 10 degrees lower than the experimental quasi-fission peak. Moreover, 525 MeV Kr + Bi reaction does not exibit a focussing effect at all.

Though the parameter C_e is treated as a free parameter in our model, it will be considered to represent the "softness" of the nucleus. The word "softness" is used here to express how large the nuclear potential stretches for a given intrinsic excitation energy. This characteristic of the coefficient C_e is seen from the comparison in table 1 between the Kr and Ar induced reactions. In the latter case, we must use the value C_e ~0.01 to reproduce the experimental data of the critical angular momentum, and the value C_e ~0.07 in the former. Since the heavy nucleus is softer than the light nucleus for the collective vibration, it may be reasonable that the heavier system has a larger value of C_e. However, in table 1, we can see two exceptional cases of 718 MeV Kr + Pb and 1130 MeV Xe + Bi reactions where the values of C_e are 0.05 and 0.06 respectively. On the other hand, a pure statistical consideration based on the Thomas–Fermi model, which was used to derive the functional form in eq. (5), gives a contrary result. There, the larger mass system has larger heat capacity and so results in a smaller increment of the force range for a given ΔE. Therefore we can say, comparing eq. (5) with table 1, that neither a pure statistical consideration nor a pure collective consideration cannot explain the whole data. So at this stage, we regard eq. (5) as a phenomenological assumption. Since we have got a fairly good result with this assumption, we can say at least that the range stretches according to the excitation energy and the ratio C_e becomes larger the larger the mass of the system as a whole. In this respect, we do not want to attach a definit physical meaning to the functional form $\sqrt{\Delta E}$.

We have also examined the dependence of our whole results on the value of parameters C_r and C_t. As a typical example, 600 MeV Kr + Bi reaction was chosen. When the parameter set (C_r, C_t) is varied from (400, 200) to (600, 400), the second rainbow angle changes ±2 degrees. The energy loss corresponding to this angle changes ±10 MeV from the value obtained with the set (500, 300) used in the present analysis. Thus we could say that our results are not very sensitive to the value of (C_r, C_t). We think that this insensitivity in our model is welcome when we think of the crudity of the classical model.

In conclusion, our model could reproduce the angular distribution and the energy loss of the quasi-fission reaction systematically. The introduction of the "softness parameter" is very useful in the phenomenological analysis of the heavy ion reaction.

We are indebted to Dr. S. Igarasi for helpfull discussions.

References

[1] M. Lefort, Y. Le Beyec and J. Peter, in: Proc. Int. Conf. on Reactions between complex nuclei, Nashville, Tenn., 1974, vol. 1 (North-Holland, Amsterdam, 1974) p. 81.
[2] F. Hanappe et al., Phys. Rev. Lett. 32 (1974) 738.
[3] K.L. Wolf et al., Phys. Rev. Lett. 33 (1974) 1105.
[4] J.V. Kratz, A.E. Norris and G.T. Seaborg, Phys. Rev. Lett. 33 (1974) 502.
[5] R. Vandenbosch, M.P. Webb and T.D. Thomas, Phys. Rev. Lett. 36 (1976) 459.
[6] W.U. Schroder et al., Phys. Rev. Lett. 36 (1976) 514.
[7] R.J. Otto, M.M. Fowler, D. Lee and G.T. Seaborg, Phys. Rev. Lett. 36 (1976) 135.
[8] D.H.E. Gross and H. Kalinowski, Phys. Lett. 48B (1974) 302.
[9] J.P. Bondorf, M.I. Sobel and D. Sperber, Phys. Rep. 15 (1974) 83.
[10] C.F. Tsang, Physica Scripta 10A (1974) 90.
[11] D.H.E. Gross, H. Kalinowski and J.N. De, in: Proc. Symp. on Classical and quantum mechanical aspects of heavy ion collisions, Heidelberg, 1974 (Springer-Verlag, Berlin, 1975) p. 194.
[12] E. Seglie, D. Sperber and A. Sherman, Phys. Rev. C11 (1975) 1227.
[13] H.H. Deubler and K. Dietrich, Phys. Lett. 56b (1975) 241.
[14] C. Ngo, B. Tamain et al., Nucl. Phys. A252 (1975) 237.
[15] C. Ngo et al., Nucl. Phys. A240 (1975) 353.
[16] J.P. Bondorf, J.R. Huizenga, M.I. Sobel and D. Sperber, Phys. Rev. C11 (1975) 1265.
[17] B. Tamain, C. Ngô and J. Péter, Nucl. Phys. A252 (1975) 187.

THE EFFECT OF p–h CORRECTIONS ON THE PROTON PAIRING VIBRATIONS AT $Z = 50$ ★

E.R. FLYNN and P.D. KUNZ
Nuclear Physics Laboratory, Department of Physics and Astrophysics, University of Colorado, Boulder, Colorado 80309, USA

Received 30 November 1976
Revised version received 28 February 1977

Recent experimental results from Cd(^{3}He, n)Sn reactions on a variety of Cd targets indicate that the proton pairing vibration lies at an excitation energy nearly 2 MeV below the value suggested by binding energy systematics. It is shown here that this large discrepancy, which is in contrast to the case of neutron pairing vibrations, may be explained by the effects of particle–hole (p–h) interactions which are large because of the Coulomb contribution. The p–h matrix elements are obtained empirically from observed p–h separations and also calculated theoretically for both Coulomb and nuclear contributions. These average empirical matrix elements from the Cd experiments give excellent agreement to the 2p–1h states in the ^{115}In(^{3}He, n) experiment populated via $L = 0$ transfers. The agreement in the latter case indicates a simple scaling of the interaction with the number of particles and holes.

The study of pairing vibrations in nuclei has proven to be a significant facet in the field of elementary excitations [1]. The preponderance of existing data on pairing vibrations for medium to heavy nuclei is in the two-neutron transfer reactions rather than the two-proton reactions because of experimental difficulties. These two-neutron transfer reactions show remarkably small deviations in energy of the pairing vibration state when compared to a simple harmonic description of noninteracting phonons [2]. Such deviations vary from less than 5% (100 keV) of the phonon energy in the lead nuclei to 10% in those cases where only the neutron shell is closed. In contrast to this, recent two-proton stripping reactions to the closed $Z = 50$ shell [3] have shown over 40% reduction in the centroid energy of the excited 0^+ state strength as compared to the harmonic model prediction. It is the purpose of the present paper to show that this discrepancy is due to the large Coulomb particle–hole (p–h) interaction and that when this correction is taken into account, the proton pairing vibration has similar features to the neutron pairing vibration.

Results published on proton pairing vibration studies previously have been confined to the f–p and s–d shells where protons and neutrons are in similar orbits and an isospin representation of the data is required [4]. The results of Fielding et al. [3] represent the first data in the heavier nuclei where the isospin T is sufficiently high that almost all of the transfer strength appears in the lower T state. The actual $L = 0$ strength is fragmented among several levels, presumably states of the same T, and it is assumed that these are two quasiparticle neutron states which are mixing with the two-particle-two-hole proton pairing vibration. In the present discussion we are only concerned with the parentage of the $L = 0$ proton excited strength and thus the total observed strength and energy weighted centroid. These latter values are shown in table 1 as columns 3 and 2 respectively for each final nucleus (column 1) observed in the work of ref. [3]. The strength is given in terms of the enhancement factor, ϵ, where $d\sigma/d\Omega = N\epsilon(d\sigma/d\Omega_{DWBA})$ so that ϵ represents a relative cross section strength corrected for Q-value and mass effects. The protons were assumed to strip into the $2d_{5/2}$ orbit. At the bottom of each column is the average value for all nuclei considered. The errors on these numbers are probably on the order of ±20–25% if both absolute cross section errors of ±15% quoted by Fielding et al. [3] and possible missing strength are considered. A definite trend with neutron number is difficult to establish.

Columns 4 and 5 of table 1 contain the harmonic estimates of the pairing vibration energy and strength

★ Work supported in part by the U.S. Energy Research and Development Administration.

Table 1

A compilation of the (^{3}He, n) L = 0 energy centroids and total strengths leading to residual tin nuclei (column 1) is given in columns 2 and 3, respectively. Columns 4 and 5 give the harmonic model predictions and expected total strength based on the Te ground state intensities. Empirical p–h corrections are in column 6 with their predicted effect on the P.V. energy in column 7. Theoretical Coulomb and nuclear matrix elements for the ^{114}Sn case are given in columns 8 and 9, respectively, with the predicted P.V. energy from this method in column 10.

Final nucleus	Experimental results		Harmonic predictions		Empirical p–h corrections		Theoretical values		
	$\bar{E}_x$ (P.V.) (MeV)	$\Sigma\epsilon$	E_x (P.V.) (MeV)	$\Sigma\epsilon$	E (p–h) (MeV)	$\bar{E}_x$ (P.V.) (MeV)	Coulomb E (p–h) (MeV)	Nuclear E (p–h) (MeV)	E (P.V.) (MeV)
^{108}Sn	3.49	1.99	–	–	–	–			
^{112}Sn	3.59	1.40	(4.77) a)	1.93	–	–			
^{114}Sn	2.89	1.60	5.14	–	−0.46	3.30	−0.267 b)	−0.078 b)	3.76
^{116}Sn	3.02	2.12	5.54	1.52	−0.60	3.14	−0.274 c)	−0.053 c)	3.83
^{118}Sn	2.57	1.30	5.19	1.10	−0.55	2.99			
^{120}Sn	–		5.26	1.53	−0.54	3.10			
Average	3.11	1.68	5.28	1.52	−0.54	3.13			

a) Mass uncertain. b) Based on $g_{9/2}^{-1} d_{5/2}$. c) Based on $g_{9/2}^{-1} g_{7/2}$.

respectively. The energy is found from the usual procedure (see, e.g. ref. [1]).

$$\bar{E}_x(\mathrm{P.V.}) = B_{2p}(^A\mathrm{Sn}) - B_{2p}(^{A+2}\mathrm{Te}) ,$$

where $B_{2p}(^AZ)$ is the two-proton binding energy of the elements Z with the atomic number A. The harmonic strength expected, as given in column 5, is the ground state $^A\mathrm{Sn} \rightarrow {}^{A+2}\mathrm{Te}$ enhancement factor which is assumed to be the addition phonon which yields the strength seen in the (two-phonon) pairing vibrations of the tin nuclei. Excited 0^+ states in the Te nuclei have been ignored. A comparison of columns 3 and 5 indicate a reasonable consistency of total pairing vibration strength to harmonic strength supporting the concept of parentage in this one-phonon state and that no major unexplained mixing is occurring. The average values at the bottom of the table more clearly show this. The deviation between harmonic energies and observed energy centroids is in excess of 2 MeV, however, far larger than the values observed in neutron cases [2].

In order to understand the existence of a weakly excited 0^+ state in the ^{210}Pb(p, t)^{208}Pb reaction [5] at ~5.2 MeV in excitation, Blomqvist [6] suggested the possibility of a proton pairing vibration which was weakly mixed with the neutron pairing vibration and brought down from an unperturbed energy of 6.60 MeV to 5.30 MeV by p–h interaction. The exact nature of this state in ^{208}Pb is still unknown and this interpretation remains unconfirmed. However, the same concept may be applied to the new Cd(^{3}He,n)Sn data. Column 6 of table 1 contains an empirical estimate of the proton p–h matrix element using single-proton transfer data. These results are from the (^{3}He,d) reaction on targets of ^{112}Cd [7], ^{114}Cd [8] and ^{116}Cd [9] and the ^{121}Sb(d,^{3}He) reaction [10]. The relations used to obtain the p–h energies were (following the usual procedure, see e.g. ref. [11])

$$(^3\mathrm{He,d}),\quad 2E(\mathrm{p{-}h}) = B_p(^{A+2}\mathrm{Sb}) + \bar{E}_x(\mathrm{p}) - B_p(^A\mathrm{In}) ,$$

$$(\mathrm{d},^3\mathrm{He}),\quad E(\mathrm{p{-}h}) = B_p(^{A+1}\mathrm{Sb}) + \bar{E}_x(\mathrm{h}) - B_p(^A\mathrm{Sn}) ,$$

where $B_p(^AZ)$ refers to the binding energy of a proton and $\bar{E}_x(\mathrm{p})$ and $\bar{E}_x(\mathrm{h})$ are the energy centroids of the $d_{5/2}$ and $g_{7/2}$ particle and $g_{9/2}$ hole orbitals respectively. This calculation gives a difference between the unperturbed particle and hole states given by the B(p) values and the perturbed particle–hole state given by the observed excitation energy. The $2J + 1$ weighted averages for the values of E(p–h) for the $(g_{9/2}^{-1} d_{5/2})_J$ and $(g_{9/2}^{-1} g_{7/2})_J$ configurations are quite close together and the results tabulated in column 6 of the table represent an average of the two values for each nucleus. This procedure should be considered as somewhat of an upper estimate of the p–h energy for these p–h configurations as missing strength may occur at higher energies which effectively reduces E(p–h). Column 6 of the table indicates a remarkable uniformity among the values obtained for the different reactions with an average value of E(p–h) = –0.54 MeV obtained. An empirically corrected pairing vibration energy is then given by

$$E(\mathrm{P.V.}) = E(\mathrm{HAR}) + 4 \times E(\mathrm{p{-}h})\,,$$

which yields the values given in column 7 of the table. The average expected excitation energy of the pairing vibration centroid is thus at 3.13 MeV which agrees with the observed energy average of 3.11 MeV. Indeed, the close agreement must be considered fortuitous because of the intrinsic errors associated with the energy centroids of the particle and hole states in the reactions cited. The factor of 4 above assumes a simple scaling of the p–h interaction.

The values of E(p–h) may be used to predict the centroid of the $L = 0$ transitions to the 2p–1h proton states seen in the ^{115}In(^{3}He,n)^{117}Sb [12] reaction. The centroid position is given by

$$\bar{E}_{\mathrm{x}}(\mathrm{2p{-}1h}) = B_{\mathrm{2p}}(^{116}\mathrm{Sn}) - B_{\mathrm{2p}}(^{118}\mathrm{Te}) - 2E(\mathrm{p{-}h})$$

which results in values of 1.83 MeV and 1.71 MeV using the single-particle transfer value of E(p–h) = –0.54 MeV and the (^{3}He,n) value E(p–h) = –0.59 MeV respectively. The experimental energy of the centroid is 1.83 MeV. This close agreement shows that the effects of the particle hole interaction can be approximately scaled with the numbers of particles and holes.

It is also possible to estimate the E(p–h) term from shell model considerations. The Coulomb term may be calculated for various orbitals separately from the nuclear term using Woods–Saxon wave functions for the orbitals. Columns 8 and 9 of the table give the theoretical estimates of the Coulomb and nuclear contributions for the ^{114}Sn case. Both $(\pi g_{9/2}^{-1}\pi d_{5/2})$ and $(\pi g_{9/2}^{-1}\pi g_{7/2})$ are shown and it is seen that they yield similar results. The nuclear contribution was obtained using matrix elements supplied by Vary [13]. The matrix elements will have a slow A dependence over the Sn isotopes and will not modify the conclusions presented. The dominant term, as expected, is seen to be the Coulomb term which explains the large discrepancy between neutron and proton pairing vibration agreements with harmonic model predictions. The nuclear and Coulomb terms do add constructively to give a value of ~–0.34 MeV. This number still lies about 0.2 MeV below the empirical E(p–h) resulting in an 0.7–0.8 MeV discrepancy with the experimental E(P.V.) centroid. It is not clear whether the error between the empirical and the theoretical E(p.h.) lies in the value of $\bar{E}$(p) used in the first case or the nuclear matrix elements from the latter. The major effect in the energy shift is certainly explained by the theoretical estimate.

We have explained here the large energy shift from the expected value which was noted in proton pairing vibration strength in the Cd(^{3}He,n) reaction studies by Fielding et al. [3]. These effects can be expected for all medium to heavy nuclei and substantiate the suggestion by Blomqvist that the proton pairing vibration state in ^{208}Pb will also be lower than originally anticipated.

We are grateful to the authors of ref. [3] and [12] for providing us with their data on the (^{3}He,n) reaction prior to publication, as well as to S. Harar for data on the (^{3}He, d) reaction. We would also like to thank J.P. Vary for the nuclear matrix elements.

References

[1] A. Bohr and B. Mottelson, Nuclear structure, vol. II (W.A. Benjamin, Inc., Reading, Mass., 1975) p. 646.
[2] See e.g. E.R. Flynn, Problems of vibrational nuclei (North-Holland, Amsterdam, 1975) p. 423.
[3] H.W. Fielding, R.E. Anderson, C.D. Zafiratos, D.A. Lind, F.E. Cecil, H.H. Wieman and W.P. Alford, Nucl. Phys., to be published.
[4] B.F. Bayman, D.R. Bes and R.A. Broglia, Phys. Rev. Lett. 23 (1969) 1299.
[5] G. Igo, P.D. Barnes and E.R. Flynn, Ann. Phys. 66 (1971) 60.
[6] J. Blomqvist, Phys. Lett. 33B (1970) 541.
[7] R.G. Markham and H.W. Fulbright, Phys. Rev. C 9 (1974) 1633.
[8] E. Thuriere, Thesis, University of Paris (1970).
[9] S. Harar and R.N. Horoshko, Nucl. Phys. A183 (1972) 161.
[10] R.F. Leonard, cited by D.C. Kocher, in: Nucl. Data Sheets 17 (1976) 49.
[11] E.A. McClatchie, C. Galshausser and D.L. Hendrie, Phys. Rev. C1 (1970) 1828.
[12] R.E. Anderson, H.W. Fielding, C.D. Zafiratos, D.A. Lind, F.E. Cecil and H.H. Wieman, private communication.
[13] J.P. Vary, private communication.

FOUR-BODY CALCULATIONS OF ^{3}He(p, pp)d AND ^{3}He(p, pd)p BREAK-UP REACTIONS

Mikolaj SAWICKI[1]
Inst. für Theoret. Kernphysik der Universität Bonn, D-5300 Bonn, Germany

Received 20 December 1976

We calculate the differential cross sections at various angles for reactions ^{3}He(p, pp)d and ^{3}He(p, pd)p at 35 MeV and 45 MeV incident proton laboratory energy, solving the integral equations of four-body theory with separable, S-wave, spin-dependent two body forces.

We have applied the four-body theory of Grassberger-Sandhas [1] to calculation of differential cross sections in ^{3}He(p, pp)d and ^{3}He(p, pd)p reactions at 35 MeV and 45 MeV incident proton laboratory energy. Our calculations are performed with model separable, S-wave, spin-dependent nucleon-nucleon interaction with Yamaguchi form-factors.

Even with such an extremely simple two-body interaction and after partial wave decomposition we have to deal with a system of integral equations in two variables, which at present seem to be numerically untractable.

Approximating by separable expressions the T-operators for scattering in all possible subsystems entering the kernel of equations, one obtains a system of multichannel integral equations in single variable. However, the complicated structure of singular kernel causes, that the contour deformation technique, so helpful for finding an exact solution of genuine three-body problem [2], is here impracticable, since in fact we do not know a full analytic structure of kernel, but only its numerical behaviour. Therefore, we have to look for another technique, keeping in mind, that any approximation to be used should preserve the unitarity of solutions, if we want to avoid the drastic deviations from the exact solution.

The most powerful method for appropriate handling with unitarity constraints is the K-matrix method, where we explicitly include the cut structure of integral kernel. The applicability of this method as well as a failure of standard non-unitary Born-type approximations has been numerically demonstrated in three-body calculations of n–d elastic scattering [3], in calculations of three-body break-up process n + d → n + n + p [4], and in our previous work [5] in four-body calculations of n + ^{3}He → n + ^{3}He and d + d → n + ^{3}He reactions. In this paper we consequently apply K-matrix method for calculations of four-body break-up collision p + ^{3}He → d + p + p.

In Grassberger-Sandhas theory the desintegration occurs via the production, free propagation and subsequent decay of clusters in all possible two-fragment channels. The general expression for break-up amplitude describing the transition from r-state in initial two-fragment channel ρ (in our case r represents helium or triton, since we do not include Coulomb forces) to nucleon pair β in deuteron state and two free nucleons is

$$X^{\beta d}_{0,\rho r} = -\sum_{\lambda}\sum_{p}\sum_{\gamma\subset\lambda}\sum_{n=d,\phi}\sum_{\alpha\subset\rho}\sum_{m=d,\phi} T^{\beta d,\gamma n}_{\lambda p}\, \tau^{\gamma n}\, U^{\gamma n,\alpha m}_{\lambda\rho}\, |\phi^{\alpha m}_{\rho r}\rangle. \tag{1}$$

The summation over index λ extends over all these among two-fragments channels in which interacting pair β can be found, i.e.

(i) over two among four channels if (ijk) (l) type with three simultaneously interacting nucleons i, j, k and

(ii) over one among three channels of (ij) (kl) type with two independent pairs of interacting nucleons. The internal summation over γ and α involves all pairs of interacting nucleons to be found in channels λ or ρ, respectively. We have assumed that any pair of interacting nucleons can be only in deuteron state d or in virtual singlet state ϕ.

[1] On leave of absence from Institute of Theoretical Physics, Warsaw University, Warsaw, Poland.

The operator $T_{\lambda p}^{\beta m,\gamma n}$ is the transition operator for elastic or rearrangement scattering inside cluster λ and index p denotes the set of quantum numbers of cluster. For example, if $\lambda = (123)(4)$ and $p = \{S_\lambda, I_\lambda\} = \{\frac{1}{2}, \frac{1}{2}\}$ then $T_{\lambda p}^{(12)\phi,(23)d}$ describe the rearrangement process in three nucleon system with triton quantum numbers, transforming the initial configuration with free nucleon 1 and nucleons 2 and 3 in deuteron state into final configuration with nucleons 1 and 2 in virtual singlet state ϕ and free nucleon 3. This is exactly three-body amplitude $X^{\beta m,\gamma n}$ of Lovelace [6], immersed in the four-body Hilbert space with fourth nucleons as a spectator.

When λ represents one of 3 channels (ij) (kl), i.e. $\lambda = (12)(34)$, then $T_{\lambda p}^{(34)\phi,(34)d}$ transforms the initial configuration with nucleons 3 and 4 in deuteron state and free nucleons 1 and 2 into final configuration with nucleons 3 and 4 in virtual singlet state ϕ and free nucleons 1 and 2. Since the relative motion of groups (12) and (34) is here unaffected, operator $T_{\lambda p}^{(34)\phi,(34)d}$ represents in fact the scattering of nucleon 1 from nucleon 2, whereas the spectator pair (34) changes its quantum numbers, but the sum of internal energies of both pair is fixed, as well as the sum p of their quantum numbers.

The ket $|\phi_{\rho \mathrm{r}}^{\alpha m}\rangle$ is the component of initial state wave function describing the relative position of pair α with quantum numbers m inside the state r of cluster ρ, and operators $U_{\lambda\rho}^{\gamma n,\alpha m}$ are the basic transition operators of four-body theory [1]. Finally, the propagator $\tau^{\gamma n}$ is the energy-dependent part of two-nucleon separable T-operator t_γ,

$$t_\gamma = -\sum_{k=d,\phi} |\gamma k\rangle\, \tau^{\gamma k} \langle \gamma k|, \tag{2}$$

where $|\gamma k\rangle$ are the Yamaguchi formfactors with parameters fixed by low-energy two-nucleon data.

When all cluster-operators T_λ in (1) are approximated by the separable expression

$$T_{\lambda p}^{\beta n,\gamma m} = -\sum_{\nu\nu'} \left|\begin{matrix}\beta n\\ \lambda p\nu\end{matrix}\right\rangle \tilde{\tau}_{\lambda p,\nu\nu'}^{n,m} \left\langle\begin{matrix}\gamma m\\ \lambda p\nu'\end{matrix}\right|, \tag{3}$$

we obtain

$$X_{0,\rho\mathrm{r}}^{\beta d} = -\sum_{\lambda}\sum_{p}\sum_{\gamma\subset\lambda}\sum_{\nu\nu'}\sum_{n=d,\phi}\sum_{\alpha\subset\rho}\sum_{m=d,\phi} \left|\begin{matrix}\beta d\\ \lambda p\nu\end{matrix}\right\rangle \tilde{\tau}_{\lambda p,\nu\nu'}^{d,n}\, X_{\lambda p\nu',\rho\mathrm{r}}^{\gamma n,\alpha m}, \tag{4}$$

where $X_{0,\rho\mathrm{r}}^{\gamma n,\alpha m}$ are matrix elements for rearrangement transitions between two-fragment channels. We have used the Bateman method for generating the separable form (3) and indices ν, ν' denote Bateman formfactors. We have included only $l = 0$ partial wave and all possible combinations of quantum numbers p of intermediate clusters λ. Details of these procedure are given elsewhere [7], here we point out that resulting propagators $\tilde{\tau}_{\lambda p,\nu\nu'}$ for λ of type (i) have the pole on real energy axis when p is a state with triton quantum numbers. The two-deuteron pole, which appears in propagators of type (ii) do not contribute to actual process due to isospin conservation. Finally, the form factor of physical state r appears to be (on-energy shell) a linear combination of Bateman formfactors.

The rearrangement amplitudes $X_{\lambda p,\rho\mathrm{r}}$ satisfy after partial wave decomposition the system of integral equations (hereafter we omit for simplicity all subindices)

$$X_{\sigma s,\rho\mathrm{r}}(q'_\sigma, q_\rho; E) = Z_{\sigma s,\rho\mathrm{r}}(q'_\sigma, q_\rho; E) - \sum_{\lambda p} \int \mathrm{d}q''_\lambda q''^2_\lambda Z_{\sigma s,\lambda p}(q'_\sigma, q''_\lambda; E)\tilde{\tau}_{\lambda p}(E - q''^2_\lambda/2\mu_\lambda) X_{\lambda p,\rho\mathrm{r}}(q''_\lambda, q_\rho; E) \tag{5}$$

where potentials $Z_{\sigma s,\rho\mathrm{r}}$ are constructed from form-factors entering eq. (3) and propagators $\tau^{\gamma k}$ given by eq. (2). The details of equations, as well as the discussion of consequences of identity of nucleons and spin-isospin analysis are given in separate paper [8].

We split the integration over triton pole in $\tilde{\tau}_{\lambda p}$ in principal value integral and delta-part integration

$$\frac{1}{q'' - (q_0 + \mathrm{i}\epsilon)} = \mathcal{P}\frac{1}{q'' - q_0} + \mathrm{i}\pi\delta(q'' - q). \tag{6}$$

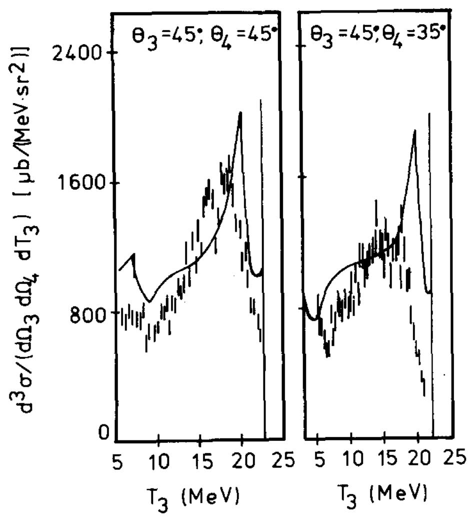

Fig. 1. ^{3}He(p, pd)p cross sections at 35 MeV in first-order K-matrix Born approximation. Coplanar angles $\theta_3 = \theta_4 = 45°$ and $\theta_3 = 45°, \theta_4 = 35°$. Data from ref. [9].

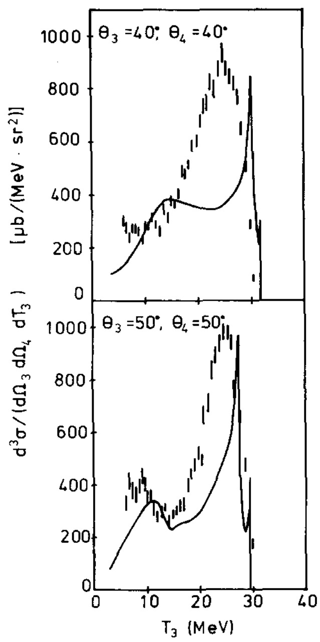

Fig. 2. ^{3}He(p, pd)p cross sections at 45 MeV in first-order K-matrix Born approximation. Symmetric coplanar angles $\theta_3 = \theta_4 = 40°$ and $\theta_3 = \theta_4 = 50°$. Data from ref. [10].

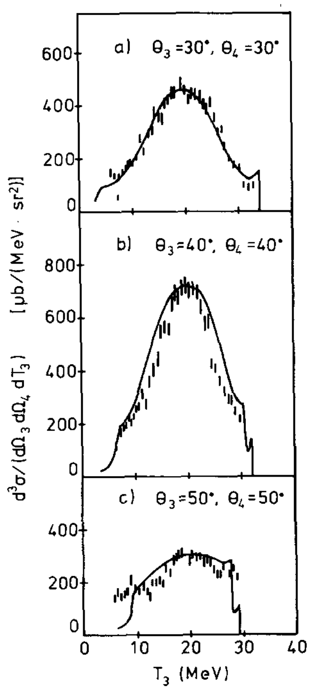

Fig. 3. ^{3}He(p, pp)d cross sections at 45 MeV in first-order K-matrix Born approximation. Symmetric coplanar angles: (a) $\theta_3 = \theta_4 = 30°$; (b) $\theta_3 = \theta_4 = 40°$; (c) $\theta_3 = \theta_4 = 50°$. Data from ref. [10]. Theoretical curves normalized to pp QFS peak i.e. divided by 5.0, 1.57 and 1.35 at (a), (b) and (c) respectively.

Then the half-on-energy-shell amplitudes $X_{\sigma s, \rho r}$ are given by set of algebraic equations

$$X_{\sigma p,\rho r}(q_0, q'_\rho; E) = K_{\sigma p,\rho r}(q_0, q'_\rho; E) - i\pi \sum_\lambda K_{\sigma p,\lambda p}(q_0, q_0; E) R_{\lambda p} X_{\lambda p,\rho r}(q_0, q'_\rho; E), \tag{7}$$

where quantities $R_{\lambda p}$ are the residua of propagators $\widetilde{\tau}_{\lambda p}$ at triton pole. The amplitudes $K_{\sigma p,\rho r}$ are the solutions of eq. (5) with integral replaced by principal-value integration and can be found in iterative way. However, the calculation of higher orders in perturbative expansions is extremely time-consuming, due to considerable number of amplitudes, and on the other side the higher orders give only small corrections, since they involve the principal-value integration of monotonic functions over a simple pole. Therefore, we restricted ourselves to first-order Born-approximation to K-matrix

$$K_{\sigma p,\rho r}(q'_\sigma, q_\rho; E) = Z_{\sigma p,\rho r}(q'_\sigma, q_\rho; E) \tag{8}$$

and put this expression into eq. (7).

In figs. 1–3 we present the resulting cross sections. In general, despite the very simple model interaction used in calculations, the agreement with experiment is not bad, especially for ^{3}He(p, pd)p spectra. Further we point out, that the observed shift in position of p–d QFS peak away from theoretically predicted position [12] in ^{3}He(p, pd)p data, previously fitted by addition of the neutron pick-up amplitude to the QFS amplitude [9], is not reproduced by our four-body theory. Since the contribution of neutron pick-up mechanism is here provided by inclusion of channels (ii) in intermediate propagation in eq. (1), and on the other hand the off-shell effects in analogy to the three-body case [11] are expected to be of minor importance in region of QFS peak, our results seem to suggest that the inclusion of Coulomb forces is necessary for explanation of this phenomenon as well as for obtaining the quantitative agreement in the ^{3}He(p, pp)d spectra, where our theory gives too big values for p–p QFS peak (fig. 3). The calculation with Coulomb forces are actually in progress.

The author would like to thank Professor Konrad Bleuler for his kind hospitality extended to him at the Institut für Theoretische Kernphysik der Universität Bonn where this work was done and Professor W.T.H. van Oers for providing his with details of experimental data [10].

References

[1] P. Grassberger and W. Sandhas, Nucl. Phys. B2 (1967) 181.
[2] R. Aaron and R.D. Amado, Phys. Rev. 150 (1966) 857;
R.T. Cahill and I.H. Sloan, Nucl. Phys. A165 (1971) 161;
W. Ebenhöh, Nucl. Phys. A191 (1972) 97.
[3] I.H. Sloan, Phys. Rev. 185 (1969) 1361.
[4] W. Böttger, Bonn University preprint IR-76-11 (1976).
[5] M. Sawicki and J.M. Namyslowski, Phys. Lett. B60 (1976) 331.
[6] C. Lovelace, Phys. Rev. 135 (1964) B 1225.
[7] M. Sawicki and J.M. Namyslowski, in: Proc. of the VIIth Intern. Conf. on Few body problems in nuclear and particle physics, Delhi, 1975, in print.
[8] M. Sawicki, to be published.
[9] M.B. Epstain et al., Phys. Lett. 36B (1971) 305.
[10] S.N. Bunker et al., Phys. Rev. C12 (1975) 1396.
[11] M.I. Haftel et al., Nucl. Phys. A269 (1976) 359.
[12] I. Slaus et al., Phys. Rev. Lett. 27 (1971) 751.

AVERAGE EFFECTIVE-INTERACTION CALCULATIONS IN A SIMULATED HARTREE-FOCK BASIS

P. GOODE[1]
Department of Physics, Rutgers University, New Brunswick, New Jersey 08903, USA

and

B.R. BARRETT[2]
Department of Physics, University of Arizona, Tucson, Arizona 85721, USA

The averaged effective interaction for mass-18 nuclei is computed through fourth-order perturbation theory in both a pure harmonic-oscillator basis and a simulated Hartree-Fock basis. Going to a Hartree-Fock basis does not eliminate the large fourth-order averages found earlier by Goode and Koltun using an harmonic-oscillator basis.

A major problem in nuclear effective-interaction ($\mathcal{V}_{\text{eff}}$) calculations is whether or not meaningful results can be obtained for $\mathcal{V}_{\text{eff}}$ using low-order perturbation theory. The work of Schucan and Weidenmüller [1] demonstrated that the perturbation expansion for $\mathcal{V}_{\text{eff}}$, using the Bloch-Horowitz-Brandow linked-cluster theory [2], will diverge in most cases of physical interest, due to the presence of so-called "intruder states" in the same energy regime as the model-space states. In such cases the perturbation expansion for $\mathcal{V}_{\text{eff}}$ can, at best, be asymptotically convergent. The unsolved problem is then to determine at what order of the perturbation expansion the results for $\mathcal{V}_{\text{eff}}$ has converged to its asymptotic value. Much formal work is being carried out on this problem at the present time, but no conclusive results have been obtained [3].

Another related problem is the very large results obtained for the average value of $\mathcal{V}_{\text{eff}}$ in fourth-order perturbation theory by Goode and Koltun [4]. They calculated the average value of $\mathcal{V}_{\text{eff}}$ from first through fourth order for mass-6 and mass-18 nuclei and found in all cases that the fourth-order average values were as large or larger than either the second- or the third-order average values. They pointed out in this work that the large fourth-order values were due to the structure of the number conserving sets (ncs) [5, 6] in this order (and also higher orders). The most disturbing result of their investigation was that these large fourth-order values for the ncs appear to be in *no way* connected with the intruder state problem, discussed by Schucan and Weidenmüller. Thus, even if one had some criteria for predicting the particular order at which the expansion should be asymptotically converged due to the effects of intruder states, fourth- and higher-order results would still be large due to the ncs.

Since most perturbation-theory calculations of $\mathcal{V}_{\text{eff}}$ have been performed in an harmonic-oscillator (HO) single-particle (s.p.) basis, it has been suggested [7] as a possible solution to the above problem that performing the same calculations in a Hartree-Fock (HF) s.p. basis would cause the fourth- and higher-order ncs to be significantly smaller and would also improve the relative convergence of the perturbation expansion in the lower orders. The purpose of this letter is to redo the average calculations of Goode and Koltun for mass-18 in a simulated HF basis and to compare the results with those obtained using an HO basis.

In order to carry out our simulated HF calculations we use the technique of Goodin, Ellis, and Goede (GEG) [7]. For the 0s and 0p orbitals, which make up the ^{16}O core, they employed HO wavefunctions with a fixed oscillator parameter of $b_0 = 1.7$ fm. For the (1s 0d) and (1p 0f) shells they also used HO wavefunc-

[1] Work supported in part by the NSF (Grant No. MPS75-06858).
[2] Work supported in part by the NSF (Grant No. MPS75-07320).

Table 1
Average effective interaction $\mathcal{V}_{ab}^{(n)}$ [a]

Pure Harmonic Oscillator basis ($b_0 = b_u = 1.7$ fm)

Order in PT [b]	Configuration (a, b) [c]					
	(4, 4)	(4, 5)	(4, 6)	(5, 5)	(5, 6)	(6, 6)
First	−1.034	−0.534	−1.060	−3.863	−0.534	−1.019
Second	−0.008	0.240	0.099	−0.200	0.240	−0.069
Third	−0.079	0.138	−0.115	0.153	0.138	−0.051
Fourth	−0.461	−0.022	−0.551	−0.755	−0.022	−0.558

Simulated Hartree Fock basis ($b_0 = 1.7$ fm, $b_u = 2.0$ fm)

Order in PT	Configuration (a, b)					
	(4, 4)	(4, 5)	(4, 6)	(5, 5)	(5, 6)	(6, 6)
First	−0.761	−0.510	−0.771	−1.847	−0.510	−0.756
Second	−0.057	0.040	−0.010	−0.191	0.040	−0.084
Third	−0.042	0.040	−0.054	−0.068	0.040	−0.034
Fourth	−0.148	−0.019	−0.166	−0.311	−0.019	−0.199

[a] See eq. (1).
[b] PT ≡ Perturbation theory.
[c] a and b denote the s.p. orbitals, i.e. $4 \equiv 0d_{5/2}$, $5 \equiv 1s_{1/2}$, $6 \equiv 0d_{3/2}$.

tions but allowed the oscillator parameter b_u to vary. In order to make the wavefunctions orthogonal when $b_0 \neq b_u$, they performed a Schmidt orthogonalization, in which a small 0s component was admixed into the 1s wavefunction, with a similar treatment for the p orbitals. Since HO wavefunctions with $b_u = 2.0$ fm have been found to overlap quite well with their HF counterparts, GEG took $b_u = 2.0$ fm to simulate an HF basis. We make the same choice for our calculations.

Using the two-body central interaction employed by GEG for both $b_0 = b_u = 1.7$ fm and $b_0 = 1.7$ fm and $b_u = 2.0$ fm, we calculated the Goode-Koltun average-values of $\mathcal{V}_{\text{eff}}$ from first through fourth order in G for mass-18 nuclei, which we defined by

$$\mathcal{V}_{ab}^{(n)} = \frac{\Sigma_{J,T}\hat{J}\hat{T}\langle abJT|\mathcal{V}_{\text{eff}}^{(n)}|abJT\rangle}{\Sigma_{J,T}\hat{J}\hat{T}}, \tag{1}$$

where the superscript n denotes the nth order term in perturbation theory, a and b denote s.p. states and $\hat{J} \equiv 2J+1$, etc. These results are given in table 1. Table 2 lists the simple average of the *absolute value* of the averages in table 1. We call this "the average of the averages" and define it by

$$\langle\mathcal{V}^{(n)}\rangle = \frac{1}{6}\sum_{a\leqslant b}|\langle\mathcal{V}_{ab}^{(n)}\rangle|, \tag{2}$$

where $\mathcal{V}_{ab}^{(n)}$ is given by eq. (1). We take only a simple average, so as not to give too much emphasis to states of high J (which are related to large values of j_a and j_b), since these have already been weighted in eq. (1).

Table 2
Average of the absolute values of the averages $\langle\mathcal{V}^{(n)}\rangle$ [a].

Order in PT [b]	HO [c]	SHF [d]	Reduction factor [e]
First	1.341	0.859	0.64
Second	0.143	0.070	$(0.70)^2$
Third	0.112	0.046	$(0.74)^3$
Fourth	0.395	0.144	$(0.78)^4$

[a] See eq. (2).
[b] PT ≡ Perturbation theory.
[c] Pure harmonic oscillator basis ($b_0 = b_u = 1.7$ fm).
[d] Simulated Hartree Fock basis ($b_0 = 1.7$ fm, $b_u = 2.0$ fm).
[e] See the text and ref. [7].

Column four in table 2 also indicates the factor by which the pure HO results must be multiplied in order to obtain the simulated HF results.

The numbers in table 1 clearly show that the simulated HF results are generally reduced relative to the pure HO results but that the fourth-order averages are still larger than either the second- or third-order averages.

Column four of table 2 shows that each order in $\langle \mathcal{V}^{(n)} \rangle$ is reduced by a different amount, defined by X^n for $n = 1$ to 4, respectively, in going to the simulated HF basis and that the factor X steadily increases as the order n increases. Hence, the fourth-order results are reduced proportionally less than the lower orders, and the fourth-order averages are still significantly larger than either the second- or third-order averages, even in the simulated HF basis.

In general, most fourth-order terms are small and fall off fast or faster than the $(0.78)^4$ listed in table 2. This overall larger factor comes from the fourth-order ncs, which can contain a hole-hole interaction. This argument is similar to but more complicated than the one given by Goode and Koltun for why the ncs can be large in fourth order, as can be seen from the following examples.

Let us first consider the fourth-order ncs generated by fig. 1(a). Fig. 1(b) shows one *particular* averaged diagram which can be obtained from fig. 1(a). The solid arrows denote valence particles. The ncs denoted by fig. 1(a) is similar in structure to the second ncs in third order [6]. Because of the presence of a hole-hole interaction in this ncs, each term in this ncs falls off more slowly than other fourth-order terms, namely as $(0.77)^4$. This result is simple to understand, since the hole-hole interaction is totally within the ^{16}O core (i.e. b_0 is fixed at 1.7 fm), and, consequently, does not change in going to the simulated HF basis. It is worth noting that the factor would be $(1.0)^4$ if *all* interactions in the diagram were hole-hole interactions.

Now let us consider the fourth-order ncs coming from fig. 2(a), of which fig. 2(b) is one *particular* averaged diagram in this ncs. The ncs denoted by fig. 2(a) is similar in structure to the first ncs in third order [6]. It contains no hole-hole interaction, but instead a particle-particle or particle-valence interaction. As a result, the terms in this ncs fall off more rapidly than the terms in the ncs illustrated in fig. 1(a).

We would also like to point out that the degree of cancellation among the terms in the ncs depicted in fig. 1(a) is *not* increased by going to a simulated HF basis. This can be understood in the following manner. From fig. 1(a) we can generate two terms, one in which the bare valence line interacts with a particle in the "dressed valence" line and the other in which the bare valence line interacts with a hole in the "dressed valence" line. This produces a valence-valence interaction in the former case (see fig. 1(b)) and a valence-hole interaction in the latter case. As one goes to the simulated HF basis the overlap between valence and hole wavefunctions is reduced, while the valence-valence interaction is also weakened. Consequently, the degree of internal cancellation among terms in the ncs also remains the same.

(a) (b)

Fig. 1(a). A fourth-order number conserving set (ncs) similar to the second ncs in third order (ref [6]). (b) One particular averaged term in this ncs.

Thus, the ncs tell the story in fourth order. They can contain hole-hole interactions and hence fall off at a slower rate than other fourth-order terms and all lower-order terms.

In conclusion, the most important result of our calculations is that going to an HF s.p. basis does *not* eliminate the large fourth-order averages found by Goode and Koltun using a pure HO s.p. basis. Consequently, further investigations must still be carried out to understand the real significance of these large fourth-order results and how to incorporate them correctly into future perturbation theory calculations of $\mathcal{V}_{\mathrm{eff}}$.

(a) (b)

Fig. 2(a) A fourth-order ncs similar to the first ncs in third order (ref. [6]). (b) One particular averaged term in this ncs.

We would like to thank Paul Ellis and Frank Goodin for their two-body matrix elements. We also thank the late, great Sigma-5 computer at Rutgers for the numbers and the research group at the Rutgers Nuclear Physics Laboratory, whose support and cooperation made this calculation possible. One of us (BRB) would like to thank Prof. H.A. Weidenmüller for the hospitality of the Max-Planck-Institute for Nuclear Physics in Heidelberg, where part of this work was carried out, and the Alexander-von-Humboldt Stiftung for partial support during this period.

References

[1] T.H. Schucan and H.A. Weidenmüller, Ann. Phys. (N.Y.) 73 (1972) 108; 76 (1973) 483.
[2] C. Bloch and J. Horowitz, Nucl. Phys. 8 (1958) 91; B.H. Brandow, Rev. Mod. Phys. 39 (1967) 771.
[3] C.M. Vincent and S. Pittel, Phys. Lett. 47B (1973) 327; S. Pittel, C.M. Vincent and J.D. Vergados, Phys. Rev. C13 (1976) 412; C.M. Vincent, Phys. Rev. C14 (1976) 660.
[4] P. Goode and D.S. Koltun, Nucl. Phys. A243 (1975) 44.
[5] B.H. Brandow, in: Lectures in theoretical physics, Vol. XIB, ed. K.T. Mahanthappa and W.E. Brittin (Gordon and Breach, New York, 1969) p. 55.
[6] B.R. Barrett and M.W. Kirson, Phys. Lett. 30B (1969) 8; Nucl. Phys. A148 (1970) 145.
[7] F.L. Goodin, P.J. Ellis and P. Goode, to be published.

GAMMA-RAYS FROM AN INCOMPLETE FUSION REACTION INDUCED BY 95 MeV ^{14}N

T. INAMURA, M. ISHIHARA, T. FUKUDA[1] and T. SHIMODA[2]
Cyclotron Laboratory, The Institute of Physical and Chemical Research, Wako-shi, Saitama 351, Japan

and

H. HIRUTA
Department of Physics, Tokyo Gakugei University, Koganei-shi, Tokyo 184, Japan

Received 18 March 1976

Gamma-rays from the $^{159}Tb(^{14}N, \alpha xn)^{169-x}Yb$ reaction, in which non-evaporation α-particles are emitted, have been identified. Yields of E2 cascade transitions suggest that the angular momentum distribution of the entrance channel leading to this reaction is localized just above the critical angular momentum for complete fusion.

It was first pointed out by Quinton et al. [1] that in the bombardment of Ni, Au and Bi with ^{12}C, ^{14}N and ^{16}O, high-energy α-particles were emitted predominantly in the forward direction. Recently, Galin et al. [2] have reported a similar phenomenon for the $^{103}Rh + {}^{14}N$ reaction. Their results indicate that the process, in which high-energy α-particles are emitted in the forward direction only, exists generally in ^{12}C, ^{14}N and ^{16}O-induced reactions, and competes with the evaporation following compound-nucleus formation. Observation of γ-rays, following such forward-peaked high-energy α-particle emission, would be interesting because the starting population for γ-emission might be different from that in the compound nucleus.

Here, following Britt and Quinton [1], we shall refer to the forward-peaked high-energy α-particles as "direct" α-particles.

^{159}Tb was bombarded with 95 MeV ^{14}N beams from the IPCR cyclotron, this combination being chosen because the likely reaction products are well-known rotational nuclei. The ^{159}Tb target was a self-supporting metallic foil 2.1 mg/cm^2 thick. The "direct" α-particles were detected with a Si surface-barrier annular detector at 0° to the beam, the solid angle subtended being 0.73 sr ($\theta = 16.7° - 32.6°$). In order to make the contribution from the evaporation process negligible, α-particles with energies below 33 MeV were cut off by placing a 400 μm thick annular aluminum foil in front of the Si detector. Gamma-rays were observed in coincidence with the α-particles thus detected, the γ-detector being a 60 cm^3 Ge(Li) counter placed at 90° to the beam and at a distance of 4 cm from the target.

Protons and α-particles were separated by operating the Si detector with a depletion depth which was thin to protons. The yields of d, t and ^3He were shown to be negligible by using a $\Delta E - E$ counter telescope. The energy spectrum of α-particles, observed at 25° to the beam, was found to peak at about 25 MeV, the highest energy being at about 60 MeV.

For comparison, we also observed γ-rays in coincidence with "compound" α-particles emitted in the backward direction. The same annular detector was placed at 180° to the beam, the detection angle being 147.4°–163.3°, but the 400 μm foil was replaced by one of 100 μm.

Fig. 1 shows γ-ray spectra observed in coincidence with (a) "direct" α-particles and (b) "compound" α-particles, together with a singles spectrum (c) for comparison. Accidental coincidences have been subtracted. Energies of the γ-rays identified agree with those reported already [3–5] within 0.5 keV.

As is seen in fig. 1a, the strongest γ-rays coincident with "direct" α-particles are from the $^{159}Tb(^{14}N, \alpha 3n)^{166}Yb$ reaction. This suggests that the "direct" α-particle is emitted first and in most cases

[1] Present address: Department of Physics, Osaka University, Osaka, Japan.
[2] On leave from Department of Physics, Kyoto University, Kyoto, Japan.

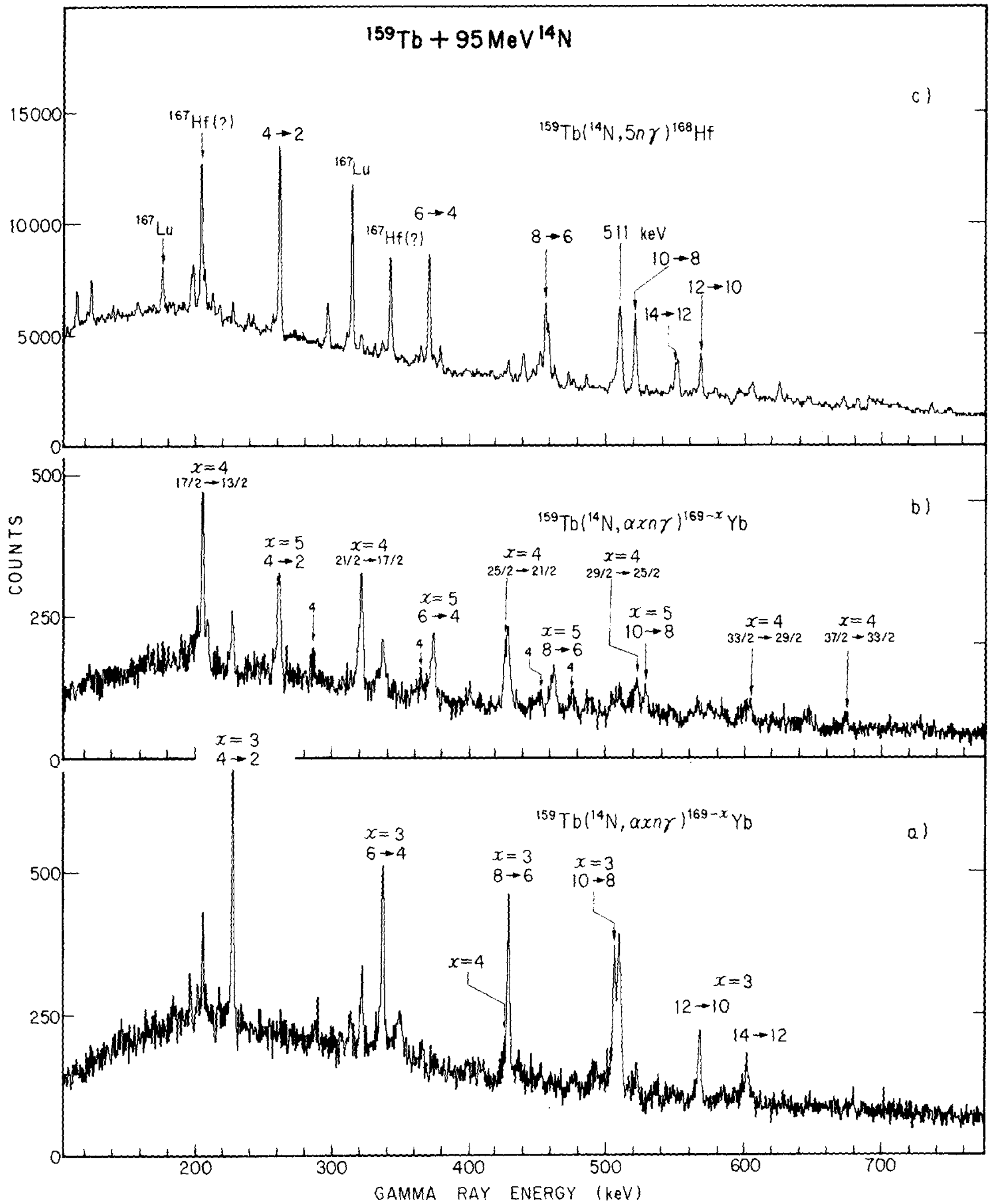

Fig. 1. Gamma-ray spectra observed in coincidence with (a) "direct" α-particles emitted in the forward direction ($E_\alpha \gtrsim 33$ MeV) and (b) "compound" α-particles emitted in the backward direction ($E_\alpha \gtrsim 15$ MeV) in the bombardment of ^{159}Tb with 95 MeV ^{14}N. A singles spectrum (c) is also shown for comparison. The indication $x = 4$ relates to γ-rays from the other bands of ^{165}Yb.

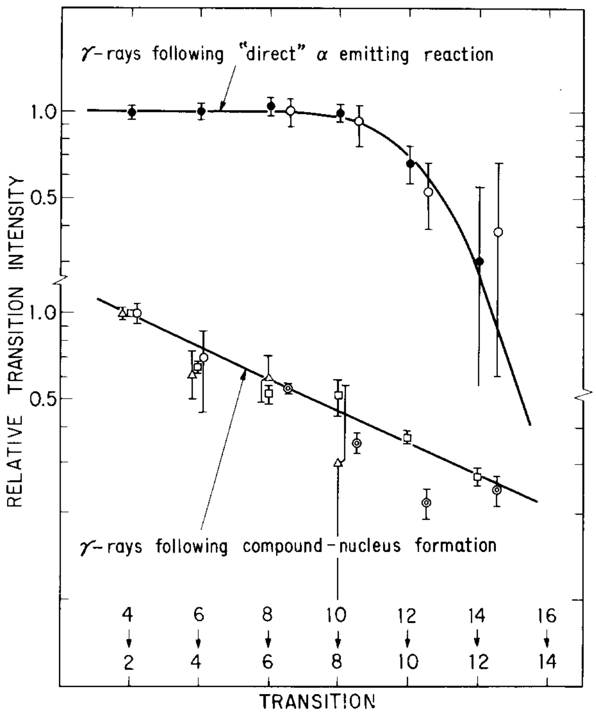

Fig. 2. Gamma-transition intensities relative to the $4^+ \to 2^+$ ($17/2^+ \to 13/2^+$ for ^{165}Yb) transition in de-excitation of the ^{159}Tb + 95 MeV ^{14}N reaction products. The upper drawing shows the data obtained in coincidence with "direct" α-particles: • for ^{166}Yb and ○ for ^{165}Yb; the solid line was obtained for ^{166}Yb (see text). The lower drawing shows the data on the residues of compound-nucleus formation: □ for ^{168}Hf, ○ for ^{166}Yb, ◎ for ^{165}Yb, and △ for ^{164}Yb; for ^{165}Yb the normalization was made at 0.54 on account of the spin concerned, and a line is drawn just to guide the eye.

is followed by three neutrons. This reaction can be regarded as incomplete fusion. It is interesting to note that γ-rays from the ^{159}Tb(^{14}N, α5n)^{164}Yb reaction are hardly seen in fig. 1a.

Fig. 2 shows intensities of E2 cascade transitions relative to the $4^+ \to 2^+$ transition of the residual nuclei, ^{164}Yb, ^{166}Yb and ^{168}Hf; for ^{165}Yb, the intensities are given relative to the $17/2^+ \to 13/2^+$ transition which is associated with the $i_{13/2}$ decoupled band [4]. For ^{166}Yb produced by the incomplete fusion reaction (fig. 1a), intensities of the cascade transitions have been found equal up to the $10^+ \to 8^+$ member, and then the yield decreases considerably. This indicates that the starting population for γ-emission was localized somewhat larger than $J = 10$ and only the ground-state band members were fed. This tendency also seems to hold for ^{165}Yb. For the residual nuclei associated with compound-nucleus formation (fig. 1b, c), however, the yields of successively higher cascades showed a near exponential fall, conforming to the general trend reported so far on γ-deexcitation of compound-nuclear reaction products in this mass region.

It seems possible to reproduce the γ-transition yields recorded in coincidence with the "direct" α-particles by assuming a Gaussian shape for the spin distribution of the starting population for γ-emission. The upper solid line in fig. 2 shows a fit to the data on ^{166}Yb corresponding to Gaussian distribution with a half-width of $2\hbar$ and a mean of $13\hbar$. Here, we have tentatively assumed four statistical dipole transitions prior the entry point into the ground state band.

The change in angular momenta during the particle emission can be approximately estimated as follows: the angular momentum removed by the "direct" α-particle emission is on average $21\hbar$, this being a semiclassical value determined from the average kinetic energy (40 MeV in lab) of the recorded α-particles; and according to the prescription given by Alexander and Simonoff [6], three neutron evaporation will remove $6\hbar$. Thus we have a mean value $\langle l \rangle = 40\hbar$ for the angular momentum distribution of the entrance channel of this reaction. This seems quite a reasonable result because the ^{14}N projectile probably just grazes the ^{159}Tb nucleus in order to transfer as many as ten nucleons and the impact parameter should be rather close to the value corresponding to the critical angular momentum l_{cr} for compound-nucleus formation, which is estimated to be $37\hbar$ on the basis of cross-section measurements [7].

In conclusion, we have indicated that for the ^{159}Tb + 95 MeV ^{14}N reaction, unlike compound-nucleus formation, the "direct" α-particle emitting reaction involves incoming partial waves with angular momenta restricted to values just above l_{cr}. Because of this, high-spin states in the residual nuclei can be populated selectively. This is probably true for other heavy ions, such as ^{12}C, ^{16}O and ^{20}Ne. Therefore, measurements of γ-rays coincident with "direct" α-particles appear to be a promising technique to study properties of the yrast region, for example band intersection in deformed nuclei. A detailed study of the angular momentum distribution of "direct" α-particles would provide important additional information.

We would like to thank Prof. H. Kamitsubo and Dr. T. Nomura for valuable discussion in connection with this study. Comments on the presentation of the manuscript by Dr. J.C. Lisle are gratefully acknowledged.

References

[1] W.J. Kox, A.R. Quinton and C.E. Anderson, Phys. Rev. 120 (1960) 2120;
H.C. Britt and A.R. Quinton, Phys. Rev. 124 (1961) 877.
[2] J. Galin et al., Phys. Rev. C9 (1974) 1126.
[3] O. Saethre et al., Nucl. Phys. A207 (1971) 486.
[4] L.L. Riedinger et al., Phys. Rev. Lett. 33 (1974) 1346.
[5] Nucl. Data Sheets 17, no. 1 (1976).
[6] J.M. Alexander and G.N. Simonoff, Phys. Rev. 133 (1964) 93.
[7] T. Fukuda et al., Contributions INS International Symposium on Collectivity of medium and heavy nuclei, and the Colloque Franco-Japonais, Tokyo (1976) p. 31.

THE OCTUPOLE GIANT RESONANCE STRENGTH IN ^{16}O

G. PERRIN, D. LEBRUN, J. CHAUVIN, P. MARTIN, P. De SANTIGNON
Institut des Sciences Nucléaires, F-38 Grenoble, France

D. EPPEL, H.V. GERAMB
I. Institut für theor. Physik, Universität Hamburg, West Germany

and

H.L. YADAV and V.A. MADSEN
Institut für Kernphysik, Kernforschungsanlage Jülich, D-5170 Jülich, West Germany

Received 15 March 1977

Angular distributions for polarized proton inelastic scattering cross sections along with the analysing power for the reaction $^{16}O(\vec{p}, p')\,^{16}O^*(2^-, 8.88$ MeV) at $E_p = 42.5, 44.0$ and 49.3 MeV have been measured. A semidirect reaction analysis augments the evidence for octupole giant resonance strength in the 30 to 50 MeV energy region.

The identification of hadronic inelastic excitation of giant-multipole resonances [1] (GR) other than E1 and E2 modes is still in a rudimentary stage. The lack of information about higher modes is partly due to their appearance at high energies, where smooth, featureless spectra loaded with pile-up background make identification difficult. In this unyielding situation the semidirect approach involving analysis of inelastic scattering mediated by virtual excitation of giant resonances has been useful.

Recently reported measurements [2] along with the theoretical analysis of polarized proton inelastic scattering to the 8.88 MeV 2^- state in ^{16}O gave evidence for excitation of the octupole GR. The extracted strength distributions permitted the conjecture of the existence of a sizeable fraction of the E3 mode localized above 40 MeV. To check this possibility earlier measurements have been extended to higher energies, $E_p = 42.5, 44.0$, and 49.3 MeV using an improved polarized ion source but with otherwise the same experimental procedure as described in ref. [2].

The distorted wave theory [3], used in the evaluation of the theoretical transition amplitude, distinguishes a direct and semirdirect process in the form

$$T_{\beta\alpha} = T_{\beta\alpha}(\mathcal{H}_{pp}) + \langle\Psi^{(-)}(\beta)|\mathcal{H}_{PR}\, G^{(+)}\, \mathcal{H}_{RP}|\Psi^{(+)}(\alpha)\rangle. \tag{1}$$

In the evaluation of the semidirect amplitude (the second term in eq. (1)) excitation of E1 through E4 modes are allowed. The strength of each is determined by the coupling constant

$$y_\lambda(\bar{Q}) = -\sum\!\!\!\!\!\!\int \langle 0|\alpha^+_{\lambda\mu}|\phi_\lambda\rangle \times \frac{1}{(\bar{Q} - E_\lambda + (i/2)\Gamma^\uparrow)} \langle\tilde{\phi}_\lambda|\alpha_{\lambda\mu}|0\rangle \, dE_\lambda \tag{2}$$

in which $|\phi_\lambda\rangle$ denotes the intermediate states with excitation energy E_λ; $\alpha_{\lambda\mu}$ are the collective transition operators, $\Gamma^\uparrow$ signifies the escape width, and $\bar{Q}$ is related to the projectile energy E_p and the binding energy of the spectator ϵ_j with $\bar{Q} = E_p + \epsilon_j (\epsilon_j = 0.6$ MeV). The coupling constant is obtained from the experimental angular distributions by a χ^2 fitting procedure.

The final results of this calculation along with the data are shown in figs. 1a and 1b. The analysis [2] yielded the coupling constants $y_\lambda(\bar{Q})$ for each multipolarity and energy $\bar{Q}$ as shown in fig. 2 for the E3 mode supplemented by the results of ref. [2].

As expected, we observe $\lambda = 3$ excitation to prevail in the 40 to 50 MeV region with diminishing strength towards higher energy. The contribution

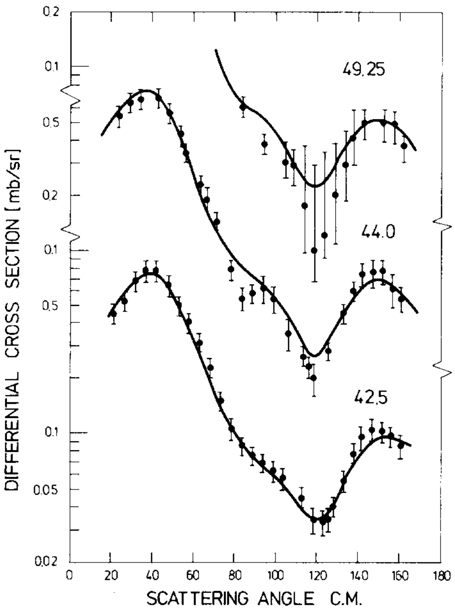

(a)

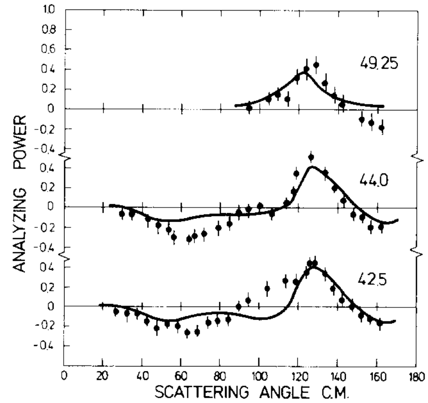

(b)

Fig. 1. (a) The differential cross section for the transition to the 2^- level in ^{16}O with the best fit curves obtained in the present analysis. (b) The analysing power analysis of the data in (a).

from other excitation modes was found to be small and smooth. The contributions from E1 and E2 modes have a slight influence on the quality of the fit but no concentration of strength was seen.

In order to have a closer comparison with the RPA calculations and the information available from the experiment we feel here the need of a detailed discussion concerning the strength distribution, in particular for the octupole GR, which is related with the coupling constant $y_3(\bar{Q})$. This will yield an estimate of the linear energy-weighted sum rule [5] (EWSR) depletion and other relevant information expected to be useful in the understanding of the higher modes. Towards this end, first we consider eq. (2) which on evaluation of the two matrix elements contained in it, can be written as

$$y_\lambda(\bar{Q}) = -\frac{\beta_\lambda^2}{(2\lambda+1)}$$

$$\times \sum\!\!\!\!\!\!\int \frac{1}{(\bar{Q} - E_\lambda + (1/2)\mathrm{i}\Gamma^\uparrow)} |a(E_\lambda)|^2 \, \mathrm{d}E_\lambda . \qquad (3)$$

Here β_λ is identified with the usual collective model deformation parameter which measures the total transition strength whereas $|a(E_\lambda)|^2$ is the normalized strength distribution. The integrated value of the imaginary part of the coupling constant can be expressed as

$$\mathrm{Im} \int y_\lambda(\bar{Q})\, \mathrm{d}\bar{Q}$$

$$= \frac{\beta_\lambda^2}{2\lambda+1} \sum\!\!\!\!\!\!\int \int \frac{\frac{1}{2}\Gamma^\uparrow}{(\bar{Q}-E_\lambda)^2 + \{(\Gamma^\uparrow)^2/4\}} \, \mathrm{d}\bar{Q} \, |a(E_\lambda)|^2 \, \mathrm{d}E_\lambda$$

$$\leqslant \frac{\beta_\lambda^2}{2\lambda+1} \sum\!\!\!\!\!\!\int \int_{-\infty}^{\infty} \frac{\frac{1}{2}\Gamma^\uparrow}{(\bar{Q}-E_\lambda)^2 + \{(\Gamma^\uparrow)^2/4\}} \mathrm{d}\bar{Q} \, |a(E_\lambda)|^2 \, \mathrm{d}E_\lambda$$

$$= \frac{\pi\beta_\lambda^2}{2\lambda+1}, \qquad (4)$$

where the integral on $\bar{Q}$ written without explicit limits means the integral over the region of experimental ex-

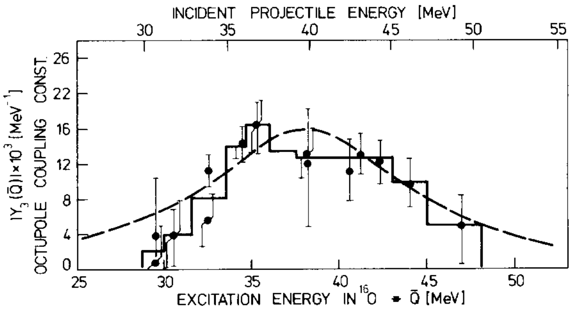

Fig. 2. Strength distribution $|y_3(\bar{Q})|$ for the excitations in the octupole giant resonance region of ^{16}O. The dashed curve is a Breit-Wigner distribution, which was not used in the fitting procedure and has been drawn only to guide the eye.

citation energies. The integral on the left hand side of eq. (4) is a lower limit to the total λ-pole strength. Because $\mathrm{Im}\, y(\bar{Q})$ falls off fairly rapidly away from a resonance, the left hand side is also a fair approximation (errors of ≈ 10% might be expected) to the total strength within the experimental region of $\bar{Q}$. Unfortunately, the phases of $y(\bar{Q})$ are not well determined by the current analysis, so the value of eq. (4) is diminished, and we use it here only for a consistency check.

We have therefore gone to an alternative procedure for the determination of the fraction of the octupole strength in the experimental region. We simply try to reproduce $|y_3(\bar{Q})|$ obtained from the analysis using several discrete resonances, each with its own strength and width,

$$y_3(\bar{Q}) = -\frac{\beta_3^2}{7} \sum_n \frac{|a_n|^2}{\bar{Q} - E_n + \frac{1}{2}\Gamma_n \mathrm{i}}. \qquad (5)$$

Although the parameters and number of pole terms are not unique, the value of $(\Sigma_n |a_n|^2)\beta_3^2$ summed in the region $\bar{Q}$ = 30–50 MeV is stable within extremes of about 16%. The effect of putting in known low-lying octupole states and an assumed isovector resonance of 15 MeV width at 60 MeV was tested and, as expected, their inclusion does not alter the result by more than 10%.

Estimates of β_3^2 obtained from the fit are 0.28 ± 0.02, while the estimate from eq. (4) obtained by roughly integrating the experimental data and using the phase from the fitted curve also gives β_3^2 = 0.28. Integration of the fitted curve directly in eq. (4) gives β_3^2 = 0.26.

Estimates of the quantity $\Sigma\, \beta_3^2 |a_n|^2 E_n$ are in the range 11.2 ± 0.8 considering the error bars and the non-uniqueness of the parameters of eq. (5) determined from the data. The percent depletion of the EWSR is obtained from the formulas given by Satchler [5], with the density parameter k = 1 as required for consistency with the collective inelastic form factor. The result is

$$0.0653 \times \sum E_n |a_n|^2 \beta_3^2 A \frac{R_{\mathrm{rms}}^4 R^2}{\langle r^4 \rangle} [\%] \qquad (6)$$

where R is the half-maximum density radius.

For a light nucleus like ^{16}O the expectation value $\langle r^4 \rangle$ depends very sensitively on the details of the mass distribution. From electron scattering reliable information is available about the RMS radius (2.71 fm) and skin thickness (2.0 ± 0.2 fm) of ^{16}O. Using these values and a Saxon-Woods mass density gives parameters R = 1.085 $A^{1/3}$ fm, a = 0.455 fm. The EWSR depletion evaluated taking into account the uncertainties in the determination of β_3 and in the skin thickness amounts to (70 ± 10)%. It is only a coincidence that this number agrees with the sum rule fraction of ref. [2]. That value was calculated with a Breit-Wigner fit to the data between 30 and 40 MeV and the uniform model for calculating moments of the mass density, both of which lead to an overestimate of the EWSR fraction. By comparison, theoretical calculations of Krewald et al. [6] give a depletion of 130% of isoscalar EWSR, but there both isoscalar and isovector excitations appear in the 30 to 50 MeV region. Similar results are given by Liu and Brown [7] as well as by Shlomo and Bertsch [8]. In the lower energy regions up to 20 MeV sum rule depletions of 20% have been attributed to the 6.13, 15.41 and 19.0 MeV states by Harakeh et al. [9].

Adding these values to the 30 to 50 MeV region gives the result that (90 ± 10)% of the octupole isoscalar sum rule value is exhausted by the observed E3 strength.

References

[1] F.E. Bertrand, Ann. Rev. Nucl. Sci. 26 (1976) 457.
[2] D. Lebrun et al. Nucl. Phys. A265 (1976) 291.
[3] H.V. Geramb et al., Phys. Rev. C12 (1975) 1697.
[4] S.M. Austin et al., Phys. Rev. C3 (1971) 1514.
[5] G.R. Satchler, Nucl. Phys. A195 (1972) 1.
[6] S. Krewald et al., Nucl. Phys., to be published.
[7] K.F. Liu and G.E. Brown, Nucl. Phys. A265 (1976) 335.
[8] S. Shlomo and G. Bertsch, Nucl. Phys. A243 (1975) 507.
[9] M.N. Harakeh et al., Nucl. Phys. A265 (1976) 189.

THE EFFECT OF PION RESCATTERING THROUGH THE $\Delta(1236)$ ON THE $\gamma D \to pp\pi^-$ REACTION FOR HIGH NUCLEON MOMENTUM

J.M. LAGET

Département de Physique Nucléaire, CEN Saclay, BP 2, 91190 Gif-sur-Yvette, France

Received 20 December 1976

The high momentum tail of the momentum distribution of the nucleons, emitted in the $\gamma D \to pp\pi^-$ reaction, is explained in terms of single pion nucleon rescattering.

The usefulness of the $\gamma D \to pp\pi^-$ reaction, for measuring the $\gamma n \to p\pi^-$ reaction cross-section, has been recognized a long time ago. Several bubble chamber experiments were performed [1, 2]. They were analysed in the frame work of the spectator nucleon model, where the cross section is related to the elementary process cross section $d\sigma(Q, \omega)/d\Omega_\pi$ and to the momentum distribution $\rho(p_s)$, of the spectator nucleon, by

$$\frac{d\sigma}{d\boldsymbol{p}_s \, d\Omega_\pi} = (1 + \beta_s \cos\theta_s)\rho(p_s)\frac{d\sigma}{d\Omega_\pi}(Q, \omega) . \tag{1}$$

The total energy in the πN center of mass is Q, and the angle between the incoming photon and the outgoing pion is ω. The momentum, the angle and the velocity of the recoiling nucleon are respectively p_s, θ_s and β_s. The flux factor $(1 + \beta_s \cos\theta_s)$ appears because the incoming photon sees a moving neutron target. This model has been proven to be successful for low momentum values of the spectator nucleon [1, 2]. However, strong discrepancies appear when this momentum becomes high. In fig. 1 we have plotted the experimental momentum distribution

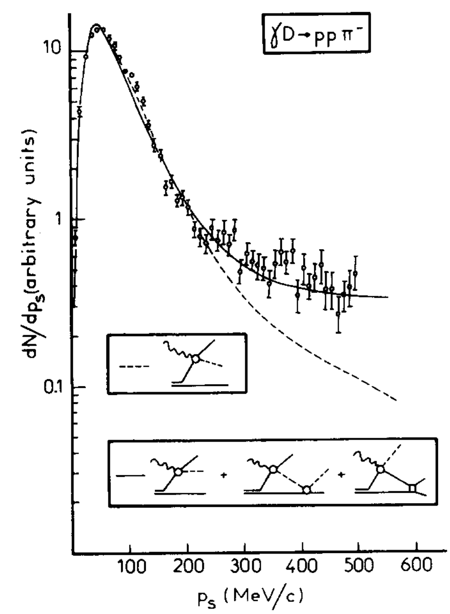

Fig. 1. The momentum distribution of the slowest emitted nucleon: $dN/dp_S \propto p_S^2 \rho(p_S)$. Dashed line curve: spectator nucleon model. Full line curve: rescattering effects included. Experimental points from ref. [1].

obtained in [1]: in the framework of spectator nucleon model it is nothing but the wavefunction of the deuteron in the momentum space (dashed line curve). As said above the agreement is good for low values of p_s, but the theoretical momentum distribution falls too quickly above 200 MeV/c, and one has to explain a factor of about four between the theory and the experiment when $p_s \sim 500$ MeV/c.

In this note we are interested in that region where the spectator nucleon model fails: we do not consider the deuteron as a neutron target but we use the $\gamma D \to pp\pi^-$ reaction as a way to manufacture the $\Delta(1236)$ resonance and we consider the deuteron as a laboratory to study the Δ–N interaction.

We showed in [3] that it is possible to reproduce the pion photoproduction reactions on free nucleon by considering the few number of diagrams labelled I in fig. 2. The creation of $\Delta(1236)$ in the s-channel (diagram Ie) plays a capital role, but the Born terms (diagram Ia, b, c, d) are also important and are computed with pseudo-vector coupling for the πNN vertex. We were able to reproduce the experimental multipoles [4] with a great degree of accuracy; the details are given in [3]. If the target nucleon is bound in deuterium and if the emitted π-N pair is not disturbed by the other nucleon, we are left with the spectator nucleon model (diagrams II in fig. 2) where the elementary process occurs on a quasi-free nucleon. Of course final state interactions exist and they are depicted by diagrams III (pion single rescattering) and IV (proton-proton rescattering) in fig. 2.

Considering this set of diagrams we have been able to reproduce the high momentum part of the recoiling nucleon distribution (full line curve in fig. 1). Before detailing our method we would like to put the emphasis on the two following points, which qualitatively explain this flattening of the momentum distribution. Firstly, when the recoiling nucleon momentum increases, the contribution due to the graph II decreases as the momentum distribution of the nucleon inside deuterium. But this momentum is shared between the two nucleons when rescattering occurs (III and IV) and we are mainly sensitive to the low momentum part of the wavefunction, even if the recoiling momentum is high. The second important point is that the pion nucleon scattering (or proton-proton scattering) can occur on shell. Two consequences immediately follow: (i) the singularity of the matrix element lies very close to the physical region and it is therefore strongly enhanced; (ii) there are no (or little) ambiguities in the choice of the elementary operators and we can use their on shell parametrization [3], which provides also a good way to extrapolate near the mass shell.

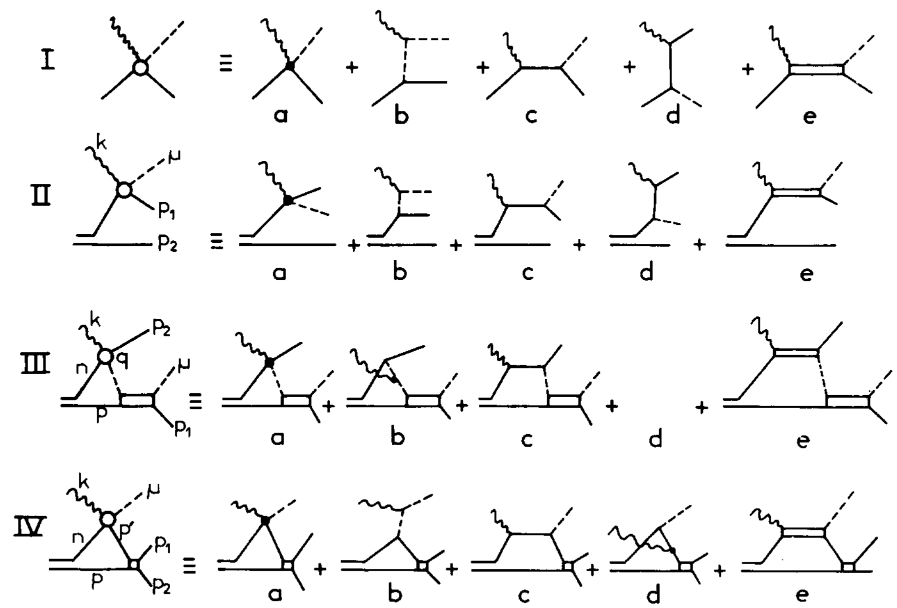

Fig. 2. The relevant diagrams. I: reaction $\gamma N \to N\pi$; II: Spectator nucleon model; III: pion nucleon single rescattering (note that the diagram IIId is forbidden by isospin conservation); IV: proton-proton rescattering.

Let

$$(k^0 = |\boldsymbol{k}|, \boldsymbol{k}), (\mu^0, \boldsymbol{\mu}), (p_1^0, \boldsymbol{p}_1), (p_2^0, \boldsymbol{p}_2)$$

and $(E_\Delta = p_1^0 + \mu^0,\ p_\Delta = \boldsymbol{p}_1 + \boldsymbol{\mu})$ the quadrimomenta of the incoming photon, the outgoing pion, the two outgoing nucleons and the outgoing $\Delta(1236)$. The cross-section is related to the matrix element via:

$$\frac{\mathrm{d}\sigma}{\mathrm{d}\boldsymbol{p}_2\,\mathrm{d}\Omega_\pi} = A \sum_{\substack{\boldsymbol{\epsilon}, M\\ m_1, m_2}} |M(\boldsymbol{p}_1, m_1, \boldsymbol{p}_2, m_2, \boldsymbol{\epsilon}, M) - M(\boldsymbol{p}_2, m_2, \boldsymbol{p}_1, m_1, \boldsymbol{\epsilon}, M)|^2, \tag{2}$$

where A is a kinematical factor including phase space and normalization factors and where the indiscernability of the two outgoing nucleons has been taken into account. The sum runs over the magnetic quantum numbers of the deuteron M, of the two nucleons m_1 and m_2 and the photon polarization vector $\boldsymbol{\epsilon}$. According to fig. 2 the matrix element is split into three parts

$$M = M_{\mathrm{II}} + M_{\mathrm{III}} + M_{\mathrm{IV}}\,. \tag{3}$$

Describing the nucleons in a non relativistic way, the photon and the pion in a relativistic way, the matrix element for the quasi free process II is (see [3]):

$$M_{\mathrm{II}} = \mathrm{i} \sum_{l,s} \sum_{m_l, m_s, m_n} T_{\gamma\mathrm{n}}(\boldsymbol{n}, m_{\mathrm{n}}, \boldsymbol{p}_1, m_1)\, \langle l m_l s m_s | 1\, M\rangle \langle \tfrac{1}{2} m_{\mathrm{n}} \tfrac{1}{2} m_2 | s m_s\rangle \mu_1(p_2)\, Y_l^{m_l}(\hat{\boldsymbol{p}}_2), \tag{4}$$

where the elementary process matrix element $T_{\gamma\mathrm{n}}$ was obtained in [3] by computing the non relativistic limit, up to the order p^2/m^2, of the relativistic matrix element associated to the diagrams I. The wavefunction in the momentum space $u_0(p)$ and $u_2(p)$ are chosen of the form:

$$u_0(p) = 4\pi N \sum_{i=1}^{5} \frac{c_i}{p^2 + \alpha_i^2}, \qquad u_2(p) = 4\pi N\rho \sum_{i=1}^{6} \frac{d_i}{p^2 + \beta_i^2} \frac{p^2}{\alpha_i^2}, \tag{5}$$

where the constants $N, \rho, c_i, \alpha_i, d_i$, and β_i are given in [5]. This is a good parametrization of the standard deuteron wavefunctions.

The matrix element for the single pion scattering diagram III is:

$$M_{\mathrm{III}} = -\mathrm{i} \frac{1}{(2\pi)^3\sqrt{4\pi}} \sum_{m_{\mathrm{n}} m_{\mathrm{p}}} \langle \tfrac{1}{2} m_{\mathrm{n}} \tfrac{1}{2} m_{\mathrm{p}} | 1\, M\rangle \{T(\gamma\mathrm{n} \to \mathrm{p}\pi^-)T(\pi^-\mathrm{p} \to \pi^-\mathrm{p}) - T(\gamma\mathrm{p} \to \mathrm{p}\pi^0)T(\pi^0\mathrm{n} \to \mathrm{p}\pi^-)\}$$
$$\times \int \frac{\mathrm{d}\boldsymbol{p}\, u_0(p)}{q^2 - m_\pi^2}\,. \tag{6}$$

The energy integration, in the loop, has been replaced by the residue associated with the nucleon pole: the nucleon which does not absorb the photon is put on his energy shell. We have done further assumptions to obtain this simple formula: each of them has been checked numerically. The influence of the D-state in the deuteron wavefunction is negligible, and we restrict ourselves to the dominant S-state part. The most important contribution to the integral comes from the low momentum part of the wavefunction and it is legitimate to single out the elementary matrix elements $T_{\gamma\mathrm{N}}$ and $T_{\pi\mathrm{N}}$: the corrections coming from the Fermi motion do not affect qualitatively the results reported here. Therefore we have kept in the integral the two quantities which are quickly varying in the integration domain: the wavefunction and the pion propagator. It is essential to keep this propagator inside the integral, because its denominator vanishes for some values of the integration variable $\boldsymbol{p}$. The pion can be on its mass shell and we have to deal with on shell pion nucleon rescattering. The form [5] of the wavefunction allows to compute analytically this integral and to split it into its singular (on shell) and its principal (off shell) parts:

$$\int \frac{\mathrm{d}p\, u_0(p)}{q^2 - m^2} = \frac{4\pi^3 \mathcal{N}}{p_\Delta} \sum_{i=1}^{5} c_i \left\{ -\frac{\mathrm{i}}{2} \log \frac{p_+^2 + \alpha_i^2}{p_-^2 + \alpha_i^2} - \operatorname{arctg} \frac{p_+}{\alpha_i} - \operatorname{arctg} \frac{p_-}{\alpha_i} \right\}, \tag{7}$$

where $p_\pm = (p_\Delta/Q)E_\mathrm{p}' \pm (p_\Delta^0/Q)p'$, the energy and the momentum of the nucleon, in the center of mass of the interacting πN pair in the final state, being respectively E_p' and p'. The momenta $|p_-|$ and p_+ are nothing but the limits of the physical region for an on mass shell pion-nucleon scattering. It should be noted that the most important contribution coming from this integral is its singular (on shell) part, which is a strongly varying function of the external kinematics. By varying the experimental kinematical conditions it is possible to maximize the singularity of the rescattering diagram and to obtain strong variations in the cross-section.

The elementary pion photoproduction amplitudes $T(\gamma \mathrm{n} \to \mathrm{p}\pi^-)$ and $T(\gamma \mathrm{p} \to \mathrm{p}\pi^0)$ are those of ref. [3], whereas the pion-nucleon matrix element $T_{\pi\mathrm{N}}$ is described by the s-channel $\Delta(1236)$ formation diagram:

$$T_{\pi\mathrm{N}} = 2MC_\pi G_3^2 \left(\chi_{m_1} \left| \frac{s \cdot \boldsymbol{\mu} s^+ \cdot \boldsymbol{q}}{Q^2 - M^2 + \mathrm{i}M\Gamma} \right| \chi_{m_\mathrm{p}} \right), \tag{8}$$

with the following parameters:

$$M = 1231\ \mathrm{MeV}, \quad \Gamma = 109 \left[\frac{|\boldsymbol{q}|}{|\boldsymbol{q}_\Delta|} \right]^3 \frac{M}{Q} \frac{1 + (R|\boldsymbol{q}_\Delta|)^2}{1 + (R|\boldsymbol{q}|)^2}, \quad G_3 = \frac{g_3}{m_\mathrm{n}} \sqrt{\frac{1 + (R|\boldsymbol{q}_\Delta|)^2}{1 + (R|\boldsymbol{q}|)^2}}, \quad R = 0.00552\ \mathrm{MeV}^{-1},$$
$$g_3 = 2.13 \text{ or } g_3^2/4\pi = 0.37\,. \tag{9}$$

The isospin coefficient C_π depends on the charge of the exchanged pion ($C_\pi = 1/3$ for π^- exchange and $C_\pi = \sqrt{2/3}$ for π^0 exchange). This amplitude is a good parametrization of the dominant $J = T = 3/2$ channel, the other channels being much more smaller.

The proton-proton rescattering amplitude has been computed in the same way and we have parametrized the nucleon-nucleon elementary amplitude by its partial wave expansion [6] up to and including $L = 2$.

With these formulae we have computed the momentum distribution of the spectator nucleon in the following way. Firstly we define the spectator nucleon as the nucleon with the lowest momentum. We then compute the cross section (2) and extract, with the aid of (1), what we call the momentum distribution $\rho(p_\mathrm{s})$ and we compute a mean value of $\rho(p_\mathrm{s})$ by a Monte Carlo procedure, varying the remaining independent variables θ_r, Q, ω and ϕ_π (the pion azimuthal angle) in the whole available phase space. This is a way to simulate the experiment [1].

The results are depicted in fig. 1, and have already been discussed in the beginning of this note. However, it should be pointed out that the contribution coming from the proton-proton rescattering diagram is very small (a few percent for $p_\mathrm{s} \sim 500$ MeV/c) and the effect is entirely due to the single pion-nucleon rescattering process. The assumptions that we have done in evaluating the matrix element (6) lead to variations of the results of the order of magnitude of the experimental error bars; our model is precise enough to reproduced the factor four needed to fill the gap between the experimental data and the spectator model prediction. The exchange current diagrams IIIa and IIIb lead to contribution as important as the contribution due to the $\Delta(1236)$ formation diagram IIIe.

We have also computed the matrix element corresponding to double rescattering of the pion and we have found that its contribution do not change significantly the results. An important conclusion for the Δ–N system immediately follows: the diagram in which a single pion is exchanged, without iteration (diagram IIIe in fig. 2) would be responsible for the main part of the Δ–N interaction. This is not surprising since the exchanged pion can be real, and therefore the singularity of this diagram is strong.

Of course more detailed experimental studies are needed to check this idea. We have compared our model to an integrated quantity, mainly sensitive to the main features of the Δ–N interaction. A detailed (exclusive) experiment, with high statistics and in which all the kinematical quantities would be measured, would be of great help. Such an experiment is being performed in Saclay [7] and we are carefully comparing our model to it. The results of this comparison, together with the details of the calculation reported here, will be published elsewhere.

References

[1] P. Benz et al., Nucl. Phys. B65 (1973) 158.
[2] M. Beneventano et al, Nuovo Cim. 19A (1974) 529.
[3] I. Blomquist and J.M. Laget, Internal report DPh-N/HE 76-2; Nucl. Phys. A, in press.
[4] F.A. Berends and A. Donnachie, Nucl. Phys. B84 (1975) 342;
W. Pfeil and D. Schwela, Nucl. Phys. B45 (1972) 379.
[5] I. McGuee, Phys. Rev. 151 (1966) 772.
[6] M.H. McGregor et al., Phys. Rev. 169 (1969) 1128.
[7] P.E. Argan et al., in: Intern. Symp. on Interaction studies in nuclei, Mainz, 1975, eds. H. Jochim and B. Ziegler;
G. Tamas, Topical meeting on Intermediate energy physics, Zuoz, 1976.

HIDDEN SYMMETRY AND THE POSSIBILITY OF SPIN-ZERO LEPTONS*

Ernest MA[1]
Department of Physics and Astronomy, University of Hawaii at Manoa, Honolulu, Hawaii 96822, USA

Received 8 March 1977

Hidden in a class of gauge theories is a global symmetry which is only apparent after spontaneous breakdown of the local gauge symmetry. A particularly interesting outcome of this hidden symmetry is the possibility of spin-zero leptons, which could be responsible for the anomalous $e\mu$ events seen in e^+e^- annihilation, as recently proposed by Ma, Pakvassa and Tuan.

In a spontaneously broken gauge theory, the original symmetry of the Lagrangian is represented in the unitarity gauge (U-gauge) by a certain set of relationships among the coupling constants. The simplest example is that of a vector gauge boson A_μ interacting with a complex scalar field ϕ. This Lagrangian is given by

$$\mathcal{L} = -\tfrac{1}{4}(\partial_\mu A_\nu - \partial_\nu A_\mu)^2 + (\partial_\mu + ieA_\mu)\phi^*(\partial^\mu - ieA^\mu)\phi - \mu^2(\phi^*\phi) - \tfrac{1}{2}\lambda(\phi^*\phi)^2. \tag{1}$$

For $\mu^2 < 0$, spontaneous symmetry breakdown occurs and the resulting Lagrangian in the U-gauge takes the form

$$\mathcal{L} = -\tfrac{1}{4}(\partial_\mu A_\nu - \partial_\nu A_\mu)^2 + \tfrac{1}{2}(e^2v^2)A_\mu^2 + \tfrac{1}{2}(\partial_\mu H)^2 - \tfrac{1}{2}(\lambda v^2)H^2 - \tfrac{1}{2}\lambda v H^3 - \tfrac{1}{8}\lambda H^4$$
$$+ e^2 v A_\mu^2 H + \tfrac{1}{2}e^2 A_\mu^2 H^2, \tag{2}$$

where $v = (-\mu^2/\lambda)^{1/2}$ and $H = \sqrt{2}\,\mathrm{Re}\,\phi - v$. It is clear that the right-hand side of eq. (2) has more terms than there are independent parameters; but it is not obvious at all how one could use this information to deduce eq. (1). The original symmetry of the theory is therefore no longer apparent.

Remarkably, the reverse of this situation can also happen. In the following, it will be shown that there exists a class of gauge theories, in which a particular (global) symmetry is only apparent *after* spontaneous breakdown of the local gauge symmetry. This *hidden* symmetry will be represented in the original Lagrangian as a relationship among coupling constants, in analogy to the situation described above. In particular, if two Higgs doublets are introduced into the standard SU(2) × U(1) gauge model of the weak and electromagnetic interactions, it is possible to have a pair of spin-zero particles which behave exactly like leptons with their own conserved lepton number, such as to explain [1] the e^+e^- anomalous $e\mu$ events [2].

Consider a local gauge theory based on the group SU(N). Let the symmetry be broken with m scalar multiplets $\phi^{(a)}$, ($a = 1, ..., m$), each belonging to the fundamental representation. Let the Langrangian be invariant under the discrete reflections $\phi^{(a)} \to -\phi^{(a)}$, as well as the interchange of any two scalar multiplets $\phi^{(a)}$ and $\phi^{(b)}$. Then the most general gauge-invariant Higgs potential (i.e., the interaction Lagrangian of the scalar multiplets) is given by [3]

$$-\mathcal{L}_{\rm int} = \tfrac{1}{2}\lambda \sum_{a=1}^{m} [\phi^{(a)i}\phi^{(a)}{}_i]^2 + \tfrac{1}{2}\eta \sum_{a\neq b} [\phi^{(a)i}\phi^{(a)}{}_i]\,[\phi^{(b)j}\phi^{(b)}{}_j] + \tfrac{1}{2}\rho \sum_{a\neq b} [\phi^{(a)i}\phi^{(b)}{}_i]\,[\phi^{(b)j}\phi^{(a)}{}_j]$$
$$+ \tfrac{1}{4}\sigma \sum_{a\neq b} \{[\phi^{(a)i}\phi^{(b)}{}_i]^2 + [\phi^{(b)i}\phi^{(a)}{}_i]^2\}, \tag{3}$$

* Work supported in part by the U.S. Energy Research and Development Administration under Contract E(04-3)-511.
[1] On leave of absence from Institute of Theoretical Science, University of Oregon, Eugene, Oregon 97403.

where the sums over i and j from 1 to N are understood. The four coupling constants $(\lambda, \eta, \rho, \sigma)$ are in general unrelated; but if the condition

$$\lambda - \eta - \rho + \sigma = 0 \tag{4}$$

is imposed, then there will always be a global symmetry left over in the physical Lagrangian after spontaneous breakdown of the local symmetry. The former symmetry is therefore *hidden* in eq. (3), and is only represented by eq. (4). An example of this has been given [4] in the case of two triplets in SU(3), where a global SU(2) symmetry is recovered by using eq. (4).

To show that eq. (4) is a consistent assumption even after renormalization of the field theory, one can either demonstrate explicitly that a global symmetry results for the spontaneously broken theory in the U-gauge, or calculate the effect of renormalization on the quantity $\lambda - \eta - \rho + \sigma$. Both of these were done [4] for the specific SU(3) example cited above. However, for the general case under discussion here, it is best to use the latter method. The renormalization-group equations for the quartic scalar couplings in eq. (3) are given in Appendix B of ref. [3]. They are

$$8\pi^2 \frac{\mathrm{d}\lambda}{\mathrm{d}t} = (N+4)\lambda^2 + (m-1)(N\eta^2 + \rho^2 + \sigma^2) + 2(m-1)\eta\rho - \frac{3(N^2-1)}{N}\lambda g^2 + \frac{3(N-1)(N^2+2N-2)}{4N^2} g^4, \tag{5}$$

$$8\pi^2 \frac{\mathrm{d}\eta}{\mathrm{d}t} = [(m-2)N+2]\eta^2 + \rho^2 + \sigma^2 + 2(N+1)\lambda\eta + 2\lambda\rho + 2(m-2)\eta\rho - \frac{3(N^2-1)}{N}\eta g^2 + \frac{3(N^2+2)}{4N^2} g^4, \tag{6}$$

$$8\pi^2 \frac{\mathrm{d}\rho}{\mathrm{d}t} = (N+m-2)\rho^2 + (N+2)\sigma^2 + 2\lambda\rho + 4\eta\rho - \frac{3(N^2-1)}{N}\rho g^2 + \frac{3(N^2-4)}{4N} g^4, \tag{7}$$

and

$$8\pi^2 \frac{\mathrm{d}\sigma}{\mathrm{d}t} = \sigma\left[2\lambda + 4\eta + 2(N+1)\rho - (m-2)\sigma - \frac{3(N^2-1)}{N} g^2\right], \tag{8}$$

where, as usual, the parameter t is minus the logarithm of the scale by which the renormalization point is changed, and g is the gauge coupling. Combining these four equations, one easily finds

$$8\pi^2 \frac{\mathrm{d}}{\mathrm{d}t}(\lambda - \eta - \rho + \sigma) = (\lambda - \eta - \rho + \sigma)\left[(N+4)\lambda - (N-2)\eta + N\rho - (N+2)\sigma - \frac{3(N^2-1)}{N} g^2\right], \tag{9}$$

which shows clearly that if eq. (4) is satisfied by the bare couplings, it will also be satisfied by the renormalized couplings. (Notice that $\lambda - \eta = 0$, for example, is *not* a consistent assumption.)

Consider now the case of spontaneous symmetry breakdown of SU(2) × U(1) via two scalar doublets $\phi^{(1)}$ and $\phi^{(2)}$. Of the initial eight degrees of freedom contained in them, three are absorbed to form the massive intermediate vector bosons $W^{\pm}$ and Z, but the other five will remain physical and they can be arranged to define the U-gauge as follows:

$$\phi^{(1)} = \begin{bmatrix} \frac{1}{\sqrt{2}}\psi^+ \\ \frac{1}{2}(H + \xi + \mathrm{i}\chi) \end{bmatrix}, \qquad \phi^{(2)} = \begin{bmatrix} -\frac{1}{\sqrt{2}}\psi^+ \\ \frac{1}{2}(H - \xi - \mathrm{i}\chi) \end{bmatrix}. \tag{10}$$

Eq. (3) then becomes

$$\begin{aligned} -\mathcal{L}_{\mathrm{int}} = {} & \tfrac{1}{4}(\lambda + \eta + \rho + \sigma)[\psi^+\psi^- + \tfrac{1}{2}(\xi^2 + \chi^2)]^2 + \tfrac{1}{4}(\lambda + \eta - \rho - \sigma)H^2[\psi^+\psi^- + \tfrac{1}{2}(\xi^2 + \chi^2)] \\ & + \tfrac{1}{16}(\lambda + \eta + \rho + \sigma)H^4 + \tfrac{1}{4}(\lambda - \eta)H^2\xi^2 + \tfrac{1}{4}(\rho - \sigma)H^2\chi^2 + \mu^2[\psi^+\psi^- + \tfrac{1}{2}(H^2 + \xi^2 + \chi^2)], \end{aligned} \tag{11}$$

where the last term has been added to provide the spontaneous symmetry breaking, so that $\langle H \rangle = v\sqrt{2}$ and $\mu^2 = -\frac{1}{2}v^2(\lambda + \eta + \rho + \sigma)$. It is clear from eq. (11) that if $\lambda - \eta - \rho + \sigma = 0$, then $\xi^2 + \chi^2$ is an invariant and a global U(1) symmetry exists. The respective masses of the physical scalar particles are now

$$m(H) = v(2\eta + 2\rho)^{1/2}, \qquad m(\psi^\pm) = v(\lambda - \eta - 2\rho)^{1/2}, \tag{12}$$

and

$$m(\xi \pm \mathrm{i}\chi) = v(2\lambda - 2\eta - 2\rho)^{1/2}.$$

Let $\xi + \mathrm{i}\chi$ be denoted by ψ^0, then it can easily be shown that the doublet (ψ^+, ψ^0) interacts with the vector gauge bosons $W^\pm$, Z, and A in exactly the same way as a lepton doublet with its own conserved lepton number. This conservation comes about because the discrete symmetry of the Lagrangian under the interchange of $\phi^{(1)}$ and $\phi^{(2)}$ holds even after spontaneous breakdown of the local gauge symmetry, so that the states $\psi^+ = (\phi^{(1)+} - \phi^{(2)+})/\sqrt{2}$ and $\psi^0 = (\phi^{(1)0} - \phi^{(2)0})/\sqrt{2}$ which are odd under this transformation must only appear in pairs. This means that there can be no three-point coupling between ψ^+ or ψ^0 with a pair of fermions, even if $\phi^{(1)}$ and $\phi^{(2)}$ are coupled to them to begin with. (The other Higgs boson H behaves as usual and is coupled to fermions in the normal manner.)

Once ψ^+ is produced, it will either be stable or decay via a W^+ into ψ^0 plus a pair of leptons or quarks (which recombine to form one or more hadrons). This is then a possible explanation [1] of the anomalous $e\mu$ events seen in e^+e^- annihilation [2]. Notice that ψ^+ and ψ^0 must have different masses, because according to eq. (12), if their masses were equal, then $\lambda - \eta = 0$ which is an untenable situation as indicated earlier. Finally, it should be pointed out that from eq. (8), σ can be set equal to zero, so that $\lambda - \eta - \rho = 0$ and by eq. (12), $m(\psi^0)$ becomes zero as well. Therefore, not only can there be a pair of spin-zero leptons (ψ^+, ψ^0) with their own conserved lepton number, but it is also possible to make ψ^0 a spin-zero counterpart of a massless neutrino. The analogy is therefore complete.

I thank Professor S. Pakvasa for useful discussions.

References

[1] E. Ma, S. Pakvassa and S.F. Tuan, University of Hawaii preprint UH-511-231-77.
[2] M.L. Perl et al., Phys. Rev. Lett. 35 (1975) 1489; Phys. Lett. 63B (1976) 466; G.J. Feldman et al., Phys. Rev. Lett. 38 (1977) 117.
[3] T.P. Cheng, E. Eichten and L.-F. Li, Phys. Rev. D9 (1974) 2259.
[4] E. Ma, Nucl. Phys. B116 (1976) 195; Phys. Lett. 62B (1976) 347.

PHOTOPRODUCTION OF CHARMONIUM★

Benedikt HUMPERT
Stanford Linear Accelerator Center, Stanford University, Stanford, California 94305, USA
and Department of Theoretical Physics, University of Geneva, Geneva, Switzerland

Received 2 November 1976
Revised manuscript received 2 March 1977

Photoproduction of ortho and para charm-anticharm bound states is considered in the framework of the Cheng-Wu picture. Non-Abelian gauge gluons mediate the interaction between the $c\bar{c}$-pair and the nucleon. The angular distributions of ψ_c and η_c are determined. The influence of multigluon exchanges and quark mass variation is studied.

Photoproduction of particles which are bound states of heavy quarks [1] permits the study of several theoretical assumptions in strong interaction dynamics and gives the possibility of investigating the dynamical implications of the large charmed quark mass [2]. The binding of the quarks into physical particles is supposed to be due to a linearly growing confinement potential [3]; this assumption was extensively used in charmonium calculations [4] and there have been many attempts to explore its deeper foundation in field theory [3]. The interaction between the quarks is commonly thought to be due to the exchange of colored gauge gluons whose interaction strength decreases with increasing gluon mass [5]; the attractive features of a gauge theory as a basic concept [6], as well as its successful application in phenomenology [7], give strong arguments in favour of such a point of view. The large charmed quark mass has dynamical implications which have been pursued in deep inelastic processes [8] but are little understood in photoproduction reactions [9]. On the phenomenological side one wonders why ψ-photoproduction is suppressed in comparison to photoproduction of the lighter vector mesons and why its angular distribution turns out to be less peaked in the forward direction [1].

In this note we assume that strong interaction dynamics is correctly described by field theories of the non-Abelian type with colored gauge gluons mediating between the quarks. We therefore study the interaction of a bound constituent pair with a nucleon by gluon exchange. Within the framework of quantum electrodynamics such a problem has been studied previously by Cheng and Wu [10] and a number of other authors [11].

In the following we present the results of a simple model, which, we believe, already shows many of the characteristics resulting from our stated framework. We consider the scattering process of a pair of charmed quarks in a scalar $1/r$ (long range) potential. The influence of the bound state nature of the quark-pair is indicated in the formal presentation of the model; however, it is dropped in its numerical evaluation since we are mostly concerned here with the consequences of gluon exchange. We first present the form of the scattering amplitude as given by Cheng and Wu [12]. Subsequently, we give the angular distribution of the ortho and para $c\bar{c}$-states; and, thirdly, we numerically determine the dependence of the scattering amplitude on the quark mass and study the influence and behaviour of the multigluon exchange contributions.

In the present approach the scattering process shown in fig. 1 occurs in three steps: first, the incoming physical photon fluctuates into a system of freely moving constituents (c-quarks), the partons in the DLY approach [13]. Second, each individual constituent undergoes instantaneous, elastic multiscattering processes in the gluon potential of the nucleon. There is no interaction between the quarks during this process. However, they finally interact to form the observed bound state. Within the gluon exchange framework, this three-step picture is expected to be valid at

★ Work supported in part by the Energy Research and Development Administration.

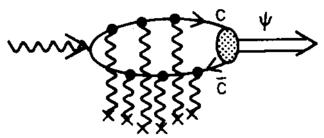

Fig. 1. Three step picture of $\psi(c\bar{c})$ photoproduction in the gluon potential of the nucleon.

high energies where the fluctuation life time is much larger than the time needed for the interaction with the external gluon potential.

This picture has been elegantly formulated by Bjorken et al. [14], using the infinite momentum frame calculus [15]. The incoming photon state is expanded in terms of the bare photon and the parton states $|\bar{1}\rangle$ as:

$$|\gamma\rangle = \sqrt{z_\gamma}\left[|\bar{\gamma}\rangle + \int d\Gamma_{12}\cdot M_{12}^{\gamma}|\bar{1}\rangle|\bar{2}\rangle + ...\right], \tag{1}$$

where $d\Gamma$ represents the phase space factor for the parton states and M^γ is the matrix element describing the fluctuation of the photon into these states; both quantities are determined in the infinite momentum frame.

The "fluctuation wave function" M^γ is determined in the infinite momentum frame [14] and depends in a simple way on a longitudinal momentum η and a transverse momentum $\boldsymbol{p}$ formed by the photon and the two constituents' momenta.

The same reasoning can be applied on the final state $|\psi\rangle$ (where we however exclude the existence of a bare state $|\psi\rangle$) leading to the bound state fluctuation wave function $M^\psi(\boldsymbol{p}', \beta')$. It is related to the ordinary Schroedinger wave function $\phi_B(\boldsymbol{p})$ (which describes the bound $c\bar{c}$-pair), via the arguments of Cheng and Wu [12]:

$$M^\psi(\boldsymbol{p}', \beta') = \sqrt{2M_B}\,\phi_B(\boldsymbol{p}', \beta' M_B)C(\tfrac{1}{2}, \lambda_1, \tfrac{1}{2}, \lambda_2|s, \lambda). \tag{2}$$

$\boldsymbol{p}'$ and β' are transverse and longitudinal momenta of the $c\bar{c}$-bound state system and M_B is its mass. The Clebsch-Gordan coefficient $C(...)$ describes the spin coupling of two fermions with helicities λ_i into the ortho and para charmonium state of spin s and helicity λ. This spin-coupling approximation is legitimate since the constituents' internal motion is small in the infinite momentum frame. The overall amplitude is constructed by sandwiching the scattering operator $R \equiv S - 1$ between the above initial and final states $|\psi\rangle$ and $|\gamma\rangle$ leading to the amplitude

$$T_{\lambda'\lambda} = \int \frac{d\boldsymbol{q}}{(2\pi)^2}[F_-(\boldsymbol{u}+\boldsymbol{q})F_+(\boldsymbol{u}-\boldsymbol{q}) - (2\pi)^4\delta^2(\boldsymbol{u}+\boldsymbol{q})\delta^2(\boldsymbol{u}-\boldsymbol{q})]\,J_{\lambda'\lambda}(\boldsymbol{u},\boldsymbol{q}), \tag{3}$$

where $\boldsymbol{\Delta} \equiv (\boldsymbol{p}_i - \boldsymbol{p}_f) \equiv 2\boldsymbol{u}$ and $\boldsymbol{p}_i(\boldsymbol{p}_f)$ represents the transverse momentum of the initial γ-state (final ψ-state). The "impact factor" $J_{\lambda'\lambda}$ contains all information on the creation process and final state binding of the constituent system through the fluctuation wave functions introduced above:

$$J_{\lambda'\lambda}(\boldsymbol{u},\boldsymbol{q}) = \int_{-1/2}^{+1/2} d\beta \int_{-\infty}^{+\infty} \frac{d\boldsymbol{l}}{(2\pi)^2} \sum M_{\lambda'}^{\psi*}(\boldsymbol{l}+\boldsymbol{m},\beta)M_{\lambda}^{\gamma}(\boldsymbol{l}-\boldsymbol{m},\beta), \tag{4}$$

where $\boldsymbol{m} = \frac{1}{2}\boldsymbol{q} - \beta\boldsymbol{u}$ and the sum extends over the fermion helicities which we have omitted. The differential cross section is

$$\frac{d\sigma}{d\Delta^2} = \frac{1}{(4\pi)^3}\overline{\sum}|T_{\lambda'\lambda}|^2. \tag{5}$$

The S-matrix amplitude describing the interaction of each constituent with the gluon potential is parametrized by the eikonal form

$$F_\pm(\boldsymbol{q}) = \int_{-\infty}^{+\infty} d\boldsymbol{b}\, e^{-i\boldsymbol{q}\boldsymbol{b}} e^{\pm i\chi(\boldsymbol{b})}, \tag{6}$$

such that each constituent acquires an eikonal phase shift whereas their longitudinal momenta and helicities remain unchanged. Assuming a Coulomb-like gluon potential one finds

$$F_\pm(\boldsymbol{q}) = \pm i\,\frac{4\pi\alpha_s}{(\boldsymbol{q}^2)^{2(1\mp i\alpha_s)}}\,e^{\mp i\Phi(\alpha_s,\mu)} \tag{7}$$

with the phase factor $\Phi_s(\alpha_s\mu)$ depending logarithmically on the small photon mass μ which was introduced in order to prevent infrared divergence. $\alpha_s \equiv e_s^2/4\pi$ stands for the strong coupling constant with the strong interaction "charge" e_s.

We now have assembled the necessary ingredients of the T-matrix for the description of photoproduction of a bound quark-pair. In the following we ignore

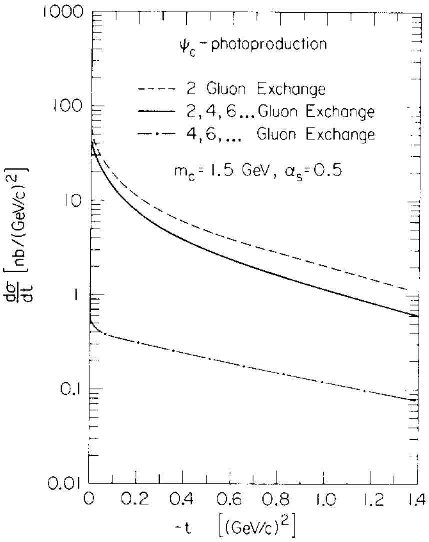

Fig. 2(a) Photoproduction of ortho-charmonium (ψ_c). The solid line represents 2, 4, 6, ... gluon exchange, the dashed line indicates the importance of 2-gluon exchange alone, whereas the dash-dotted line shows the cross section size of 4, 6, ... gluon exchange. The parameters are: m_c = 1.5 GeV and α_s = 0.5.

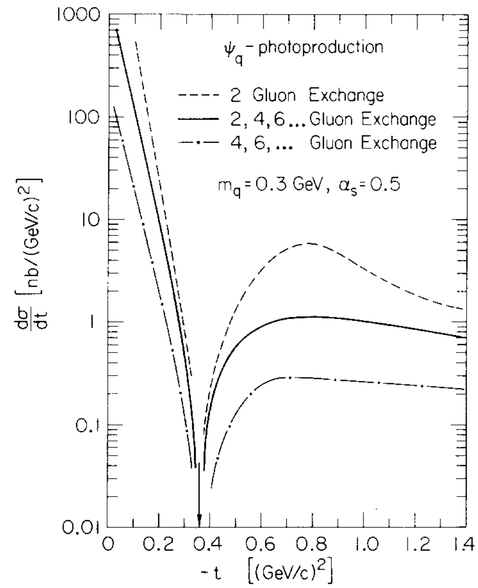

Fig. 2(b) Photoproduction of an ortho $q\bar{q}$-state (ψ_q). The solid line, dashed line and dash-dotted line represent 2, 4, 6, ... gluon exchange. The parameters are: m_q = 0.3 GeV and α_s = 0.5.

the influence of the bound state and replace the bound state wave function by a δ-function. Defining the amplitudes for ortho and para charmonium production as

$$T^1 \equiv T_{\pm 1,\pm 1} = \sqrt{2}\, r R^1, \qquad T^0_\pm \equiv T_{0,\pm 1} = r R^0_\pm, \quad (8, 9)$$

we have

$$R^0_\pm = \sigma_\pm [L_1(\sigma) + L_3(\sigma) + ...] = \sigma_\pm L_1(\sigma) \frac{V(\epsilon)}{V(1)}, \quad (10)$$

$$R^1 = [L_2(\sigma) + L_4(\sigma) + ...] = L_2(\sigma) \frac{W(\epsilon)}{V(1)} \frac{\epsilon^{3/2}}{\ln(1-\epsilon)}, \quad (11)$$

where the variables

$$\sigma = \frac{|\boldsymbol{u}|}{m_c}, \quad \epsilon = \left(\frac{1-\sigma^2}{1+\sigma^2}\right)^2, \quad \sigma_\pm = \frac{u_\pm}{m_c}, \quad u_\pm = u_x \pm i u_y, \quad (12)$$

have been introduced. The two functions

$$V(\epsilon) \equiv {}_2F_1(-i\alpha_s, +i\alpha_s, 1; \epsilon) \quad (13)$$

$$W(\epsilon) \equiv {}_2F_1(1 - i\alpha_s, 1 + i\alpha_s, 2; \epsilon), \quad (14)$$

describe the modification of the "Born amplitude" due to multigluon exchanges. The normalization factor is given by

$$r = -8\pi^2 e \psi_B(0) \alpha_s^2 m_c^{-7/2} \quad (15)$$

with $\psi_B(0)$ the bound state wave function at the origin in configuration space. The functions $L_i(\sigma)$ correspond to 1, 3, 5, ... (2, 4, 6, ...) gluon exchange in para (ortho) charmonium [19] and are determined by use of Mellin transformation techniques [12, 16] for small Δ^2 with the result:

$$L_1(\sigma) = \frac{i}{2\alpha_s} \frac{1}{\sigma^2(1+\sigma^2)} \quad (16)$$

$$L_3(\sigma) = 2i\alpha_s[2\,\mathrm{Re}\,\psi(1 + i\alpha_s) - 2\psi(1) - 1 + \ln 4],$$

$$L_2(\sigma) = \left(\frac{1}{1-\sigma^2}\right)^2 \ln\left(\frac{2\sigma}{1+\sigma^2}\right)^2. \quad (17)$$

These results reveal the following properties:

(1) Keeping only L_1 in R^0, we find the Born amplitude of single gluon exchange (forbidden by color conservation!) which reveals an angular distribution with a sharp spike near the forward direction and which then falls to zero.

(2) The amplitude R^1 reveals a zero at $|\Delta| = 2m_c$ due to the ln-term in $L_2(\sigma)$; in $L_2(\sigma)$ there appears

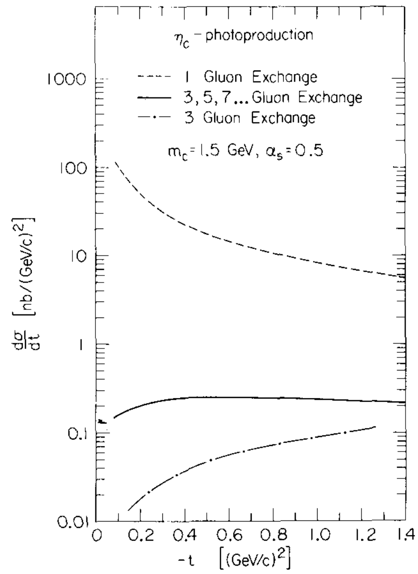

Fig. 3(a) Photoproduction of para-charmonium (η_c). The solid line represents 3, 5, 7 ... gluon exchange, the dashed line indicates single gluon exchange (which is forbidden by color conservation!) and the dotted line indicates the size of the 3-gluon exchange near the forward direction. The parameters are: m_c = 1.5 GeV and α_s = 0.5.

also a pole at $\sigma = 1$ which is cancelled by the $\epsilon^{3/2}$-term in R^1.

(3). Both amplitudes depend on the variable $\sigma = |\boldsymbol{\Delta}|/2m_c$ and therefore scale in the c-quark mass (apart from the normalization).

(4) As we go to larger m_c-values, the amplitudes decrease like $\sim m_c^{-7/2}$ and the shape of the angular distribution is shifted towards the origin.

(5) Since we are working in the infinite momentum frame, the dependence on the initial energy E_{CM} has completely dropped out; our formalism is therefore only valid in the asymptotic region where diffraction dominates.

(6) The above results show no dependence on the target (nucleon) size since we have used an infinitely extended $1/r$-potential.

(7) Our formulas are easily extended to photoproduction of electromagnetic bound-state systems as for instance "heavy leptonium" [17] ; the bound-state wave function at the origin reads:

$$\psi_B(0) = \frac{1}{\sqrt{\pi R_0^3}}, \qquad R_0 = \frac{2}{m_c\alpha}, \qquad \alpha = \frac{e^2}{4\pi} \tag{18}$$

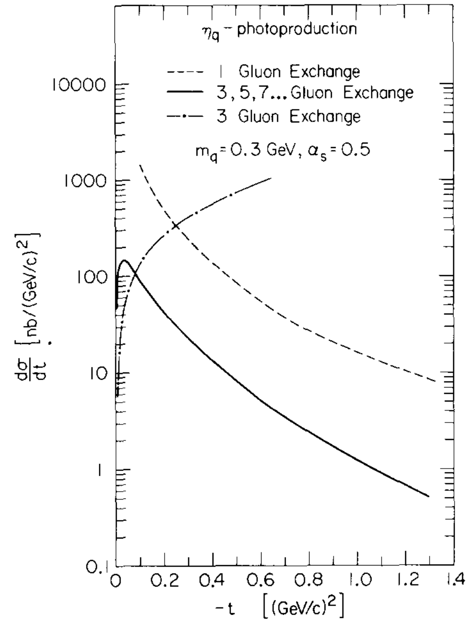

Fig. 3(b) Photoproduction of a para $q\bar{q}$-state (η_q). The solid line, dashed line and dotted line represent 3, 5, 7, ... gluon exchange, single-gluon exchange and 3-gluon exchange. The parameters are: m_q = 0.3 GeV and α_s = 0.5.

and the replacement $\alpha_s \to (Z\alpha)$ is used. $Z(\sim 100)$ stands for the electromagnetic charge of the target atom.

We have numerically evaluated the shape of the differential cross section for ψ_c-photoproduction adjusting $\psi_B(0)$ in eq. (15) such that its size agrees with the data at $E_{CM} \sim 120$ GeV. In fig. 2a (and fig. 2b) we show its shape for m_c = 1.5 GeV (and m_q = 0.3 GeV) and α_s = 0.5. The dashed lines (2-gluon exchange represent the lowest order contribution. The solid lines (2, 4, 6 ... gluon exchanges) take multigluon corrections into account and the dashed-dotted lines (4, 6, ... gluon exchanges) have the 2-gluon exchange subtracted. One notices that the 2-gluon exchange approximation is damped down by the higher order multigluon exchanges which however interfer such that their contribution is about one order of magnitude smaller. An exponential fit in the region $0.1 \leqslant -t \leqslant 0.6$ (GeV/c)^2 gives a slope parameter $b \sim 2-4$ GeV^{-2}; it is less for 4, 6, ... gluon exchange. Mass extrapolation to m_q = 0.3 GeV (fig. 2b) brings the zero-point in the amplitude R^1 (see eq. (11)) to $-t$ = 0.36 (GeV/c)^2. This diffraction minimum is not observed in ρ-photoproduction [18] and it might well disappear in our model if the relativistic bound state nature of the ρ-meson is taken into account‡.

In figs. 3a and 3b we show the analogous curves for photoproduction of the para states η_c and η_q. For illustrative purposes we have drawn the Born-approximation (which however is forbidden by color conservation); it is strongly peaked for small $|t|$-values. 3, 5, ... gluon exchange is flat over a long t-range and bends off towards zero in the extreme forward direction. The same calculation with $m_c = 0.3$ GeV shows a rising curve towards smaller $|t|$-values with $b \sim 5$ GeV^{-2} and a falloff to zero in the extreme forward direction.

Increasing α_s leads to a stronger influence of the higher order gluon terms besides rapidly increasing the amplitudes. The global features as presented in figs. 2 and 3 are however not substantially changed.

In this note an attempt at the descriptions of ψ-photoproduction in the gauge theory framework is sketched by assuming that gluons are responsible for the interaction between the quarks. This picture leads to characteristic consequences in the shape and size of the angular distributions of ψ_c and η_c. In particular, the differential cross section for η_c-production is 1–2 orders of magnitude smaller in comparison to ψ_c-photoproduction and remains constant at large energies. The above presented results are distinct from other approaches and permit experimental tests.

I would like to thank Hannu Miettinen and Fred Gilman for their reading of the manuscript and clearing discussions and I have enjoyed the warm hospitality of Prof. S.D. Drell and SLAC. A fellowship from the Swiss National Science Foundation is gratefully acknowledged.

‡ Note that three ... (four ...) gluon exchanges could also contribute to ortho (para) charmonium production by taking tree-like gluon exchanges into account which have been ignored here. A simple estimate shows that their contribution is small and that no substantial changes may be expected. In addition, we have neglected higher symmetry factors due to color.

References

[1] See e.g., G.S. Abrams, in: Proc. of the Int. Symp. on Lepton and photon interactions at high energies, Stanford University, ed. W.T. Kirk (Stanford Linear Accelerator Center, Stanford University, Stanford, California 1975) p. 25;
R. Prepost, in: Proc. of the Int. Symp. on Lepton and photon interactions at high energies, Stanford University, ed. W.T. Kirk (Stanford Linear Accelerator Center, Stanford University, Stanford, California 1975) p. 241;
For a review see: B. Humpert, Dynamical concepts on scaling violation and the new resonances in e^+e^- annihilation, Lecture notes in physics 45 (Springer Verlag, Heidelberg, 1976).

[2] M.K. Gaillard, B.W. Lee and J.L. Rosner, Rev. Mod. Phys. 47 (1975) 277.

[3] S.D. Drell, Stanford Linear Accelerator Center preprint SLAC-PUB-1683 (November 1975);
H. Joos, DESY preprint 76/36 (July 1976);
S. Yankielowicz, Stanford Linear Accelerator Center preprint SLAC-PUB-1800 (August 1976).

[4] A. DeRujula, Newly discovered resonances, Harvard University (1976).

[5] H.D. Politzer, Phys. Report 14C (1974) 130.

[6] B.W. Lee, in: Proc. of the Int. Symp. on Lepton and photon interactions at high energies, Stanford University, ed. W.T. Kirk (Stanford Linear Accelerator Center, Stanford University, Stanford, California 1975) p. 635.

[7] F.E. Low, Phys. Rev. D12 (1975) 163;
S. Nussinov, Phys. Rev. Lett. 34 (1975) 1286; Phys. Rev. D14 (1976) 246;
T. Appelquist and H.D. Politzer, Phys. Rev. Lett. 34 (1975) 43.

[8] M. Barnett, Phys. Rev. D14 (1976) 70.

[9] B. Humpert and A.C.D. Wright, Stanford Linear Accelerator Center preprint SLAC-PUB-1814 (1976); SLAC-PUB-1853 (1976).

[10] H. Cheng and T.T. Wu, in: Int. Symp. on Electron and photon interactions at high energies, Cornell University, Ithaca, New York, (1971), p. 147; and ref. [12].

[11] S.J. Chang, Diagrammatic approach to geometrical models, preprint ILL-(Th-)76-13 (June 1976).

[12] H. Cheng and T.T. Wu, Phys. Rev. 182 (1969) 1873; Phys. Rev. D5 (1972) 3077; Phys. Rev. D6 (1972)2637.

[13] S.D. Drell, D.J. Levy and T.M. Yan, Phys. Rev. D1 (1972) 1617.

[14] J.D. Bjorken, J.B. Kogut and D.E. Soper, Phys. Rev. D3 (1971) 1382.

[15] S. Brodsky, R. Roskies and R. Suaya, Phys. Rev. D8 (1973) 4576.

[16] R.J. Eden, P.V. Landshoff, D.I. Olive and J.C. Polkinghorne, The analytic S-matrix (Cambridge University Press, 1969).

[17] J.W. Moffat, Phys. Rev. Lett. 35 (1975) 1605.

[18] W. Lee, in: Proc. of the Int. Symp. on Lepton and photon interactions at high energies, Stanford University, ed. W.T. Kirk (Stanford Linear Accelerator Center, Stanford University, Stanford, California 1975) p. 213.

RIGHT-HANDED NEUTRAL HEAVY LEPTONS IN e^+e^- ANNIHILATION? ★

Benedikt HUMPERT and P.N. SCHARBACH
Stanford Linear Accelerator Center, Stanford University, Stanford, California 94305, USA

Received 28 February 1977

The experimental implications of neutral heavy leptons N in e^+e^- annihilation are examined. We calculate the production rate of both right-handed and left-handed N's at SPEAR and PEP/PETRA energies and show that observation of the process $e^+e^- \to \bar{\nu}N$, $N \to e$ (or μ)π allows the determination of both the mass and handedness of N.

Considerable interest has recently been shown [1–6] in the possible enlargement of the leptonic world to encompass right-handed neutral heavy leptons. In such schemes, neutral leptons E and M, forming right-handed doublets

$$\begin{pmatrix} E \\ e \end{pmatrix}_R \qquad \begin{pmatrix} M \\ \mu \end{pmatrix}_R \tag{1}$$

are added to the original Weinberg-Salam (W-S) model [7]. Here

$$\begin{aligned} E &= \cos\phi\, N_e + \sin\phi\, N_\mu \\ M &= -\sin\phi\, N_e + \cos\phi\, N_\mu , \end{aligned} \tag{2}$$

N_e and N_μ are mass eigenstates, and ϕ is an undetermined mixing angle. The neutrino neutral current is as in the W-S model; however, it follows immediately from the assignment (1) that the electronic and muonic neutral currents are purely vector. Consequently, parity-violating effects in atoms are suppressed, a desirable feature if the measurements of the optical rotation in bismuth by the Oxford and Washington groups [8] remain at their present value. Further, the mixing scheme (2) implies the existence of lepton number nonconserving processes such as $\mu \to e + \gamma$ for which the current limit [9] on the branching ratio is 2.2×10^{-8}. This may be just an order of magnitude above the value predicted by the model (1) ‡1. The N's are expected to decay into a pair of conventional leptons (plus a neutrino), a lepton and hadrons such as π, ρ, A_1, and, if sufficiently massive, into a conventional lepton plus a heavy charged lepton. They may be produced in deep inelastic μp and ep experiments and would be expected to appear in the decay products of charmed mesons D, D^*, F, F^*.

In this letter we examine the experimental implications of such leptons in e^+e^- annihilation. We address ourselves to the question how and where they can be found and what theoretical information can be extracted from the data.

We begin our discussion with N production and distinguish between the reactions $e^+e^- \to \bar{\nu}N_e$ ($\nu\bar{N}_e$) and $e^+e^- \to N_e\bar{N}_e$. The former occurs through W-exchange whereas the latter receives contributions from W- and Z-exchange diagrams.

The distributions in the center-of-mass scattering angle θ_N for single and pair production of N_e-leptons are

★ Work supported in part by the Energy Research and Development Administration.
‡1 For example with the choice $\phi = \pi/4$, $m_{N_e} = 1$ GeV, $m_{N_\mu} = 2.4$ GeV, $\Gamma_{\mu e\gamma}/\Gamma \sim 10^{-9}$.

$$\frac{d\sigma}{d\cos\theta_N}(e^+e^- \to \bar{\nu}N_e) = \frac{G_F^2 s \cos^2\phi (1 - m_N^2/s)^2}{32\pi(1 - t/M_W^2)^2}\{2(1+\lambda)(1 - m_N^2/s) + (3+\lambda)(1 + m_N^2/s)$$

$$+ 2(1-\lambda)\cos\theta_N + (1-\lambda)(1 - m_N^2/s)\cos^2\theta_N\} \equiv \cos^2\phi \frac{d\hat{\sigma}}{d\cos\theta_N} \quad (3a)$$

$$\frac{d\sigma}{d\cos\theta_N}(e^+e^- \to N_e\bar{N}_e) = \frac{G_F^2 \delta s}{16\pi}\left\{\cos^4\phi \frac{(1+\delta\cos\theta_N)^2}{(1 - t/M_W^2)^2} + \frac{\cos^2 2\theta_W(1 + \delta^2\cos^2\theta_N)}{2[(1 - s/M_Z^2)^2 + \Gamma_Z^2/M_Z^2]}\right.$$

$$\left. + \frac{\cos 2\theta_W \cos^2\phi\,(1+\delta\cos\theta_N)^2(1 - s/M_Z^2)}{(1 - t/M_W^2)[(1 - s/M_Z^2)^2 + \Gamma_Z^2/M_Z^2]}\right\} \equiv \cos^4\phi \frac{d\hat{\sigma}_W}{d\cos\theta_N} + \frac{d\hat{\sigma}_Z}{d\cos\theta_N} + \cos^2\phi \frac{d\hat{\sigma}_{int}}{d\cos\theta_N}\,. \quad (3b)$$

s is the center-of-mass energy squared, t is the momentum transfer squared, Γ_Z is the width of the neutral intermediate vector boson, and $\delta \equiv (1 - 4m_N^2/s)^{1/2}$. The phenomenological possibility of a left-handed N has been allowed for by the introduction of the parameter $\lambda = \pm 1$ for V ± A e–N_e coupling. In the case of N_μ-production, $\cos\phi$ is replaced by $\sin\phi$.

For right-handed coupling, the distribution (3a) is isotropic as expected from angular momentum considerations[‡2]. The V − A case shows a characteristic $(1 + \cos\theta_N)^2$ behaviour in the region $s \gg m_N^2$: a left-handed heavy lepton is produced preferentially in the forward direction.

Eqs. (3a) and (3b), integrated over θ, are plotted in fig. 1 as functions of s[‡3]. Single N-production outweighs N-pair production by one order of magnitude outside the Z-resonance region; N-pair production obviously dominates around the Z. Changing V + A to V − A does not affect $\sigma(N_e, \bar{N}_e)$, whereas the single-N channel is reduced

[‡2] There is some suppression in the backward direction due to the effect of the intermediate vector boson propagator.
[‡3] Here we have assumed for definiteness a mixing angle $\phi = \pi/4$ and take the Weinberg angle to be $\sin^2\theta_W = 0.35$.

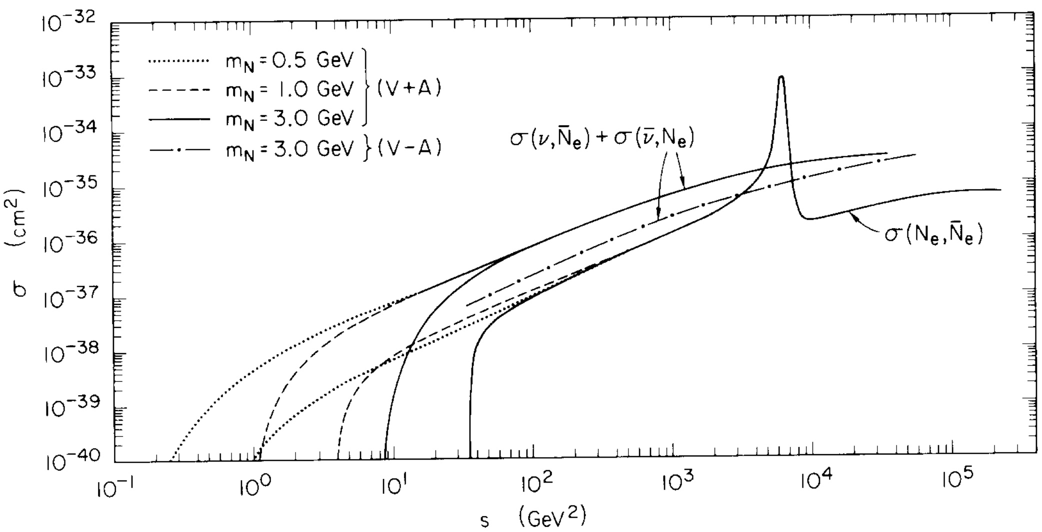

Fig. 1. The total cross section for the processes $e^+e^- \to \bar{\nu}N_e$ and $e^+e^- \to N_e\bar{N}_e$, computed from eqs. (3a) and (3b), with $\phi = \pi/4$ and $\sin^2\theta_W = 0.35$.

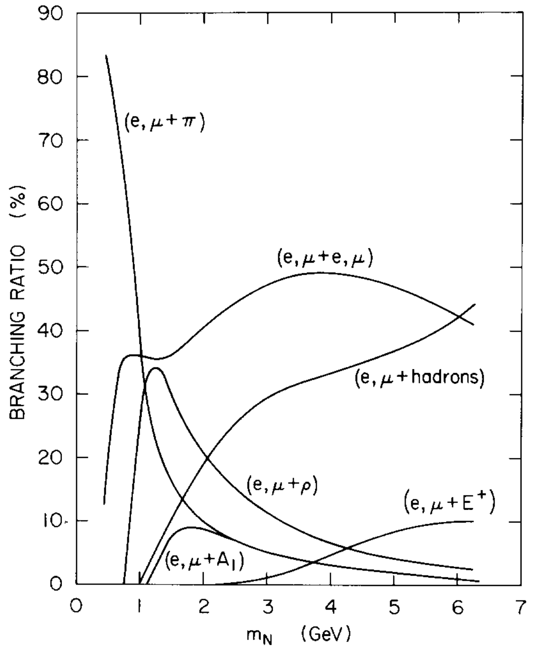

Fig. 2. Branching ratios for the decays $N \to e^-$ (or μ) + ... as a function of m_N.

Table 1
Production rate of neutral heavy leptons at representative SPEAR and PEP/PETRA energies.

	Coupling	Events/day	Percentage pair-produced
$\frac{\sqrt{s}}{2} = 4$ GeV (SPEAR)	V + A	0.9	12%
	V − A	0.4	41%
$\frac{\sqrt{s}}{2} = 16$ GeV (PEP/PETRA)	V + A	128	20%
	V − A	50	48%

by a factor 2–3. When $(m^2_{N_\mu} - m^2_{N_e}) \ll s$, the total heavy lepton production cross section becomes independent of the mixing angle and is

$$\sigma_{tot} = \sum_{i=e,\mu} \sigma(e^+e^- \to \bar{\nu}N_i) + \sigma(e^+e^- \to \nu\bar{N}_i) + \sum_{i,j} \sigma(e^+e^- \to N_i\bar{N}_j) = 2(\hat{\sigma} + \hat{\sigma}_Z) + \hat{\sigma}_W + \hat{\sigma}_{int} \tag{4}$$

From eqs. (3a), (3b), and (4) we find that, for a PEP/PETRA energy of $\sqrt{s}/2 = 16$ and a projected luminosity of 10^{32} cm^{-2} sec^{-1}, the production rate of right-handed N's is 128/day, of which 20% are pair-produced. The corresponding results for the V − A case and the rate at maximum SPEAR energy $\sqrt{s}/2 = 4$ and luminosity 10^{31} cm^{-2} sec^{-1} are shown in table 1.

A particularly clean reaction for the detection and the study of N-leptons and their dynamical behaviour is the chain

$$e^+e^- \to \bar{\nu}N, \quad N \to e(\text{or } \mu) + \pi, \tag{5}$$

as has been emphasized by Bjorken [10]. The N-momentum can be reconstructed from events with only a charged pion and lepton in the final state, allowing determination of the heavy lepton mass. Furthermore, the differential distributions of the final state products depend sensitively on the handedness of the N-e (μ) coupling. The N's are produced polarized, leading to a characteristic decay angular distribution in the N-rest frame.

The counting rates for this reaction depend on the branching ratios for N decay; these have been calculated following refs. [11] and [12]. For $m_\mu/m_N \ll 1$, they are independent of the mixing angle ϕ. Our results are shown in fig. 2[‡4]. The e (μ) π mode is dominant for $m_N \lesssim 1$ GeV, dropping rapidly to 5% at $m_N = 3$ GeV. As an example, let us assume right-handed N_e and N_μ of masses 1.0 and 2.4 GeV. Then the cross section for reaction (5) is 2.0

[‡4] We have assumed the existence of a charged sequential heavy lepton of mass 1.9 GeV [13].

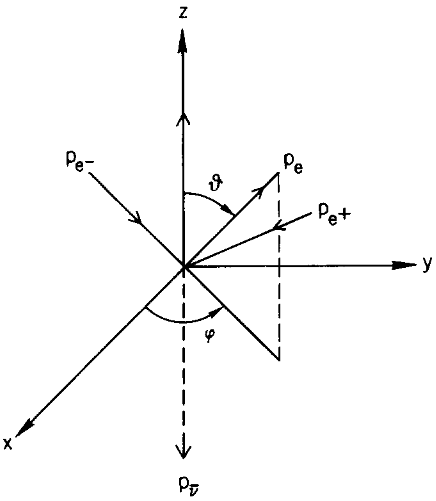

Fig. 3. The decay $N \to e\,(\mu)\pi$ in the heavy lepton rest frame. The initial e^- and e^+ define the z-y plane and the positive z-axis is opposite the direction of the produced antineutrino.

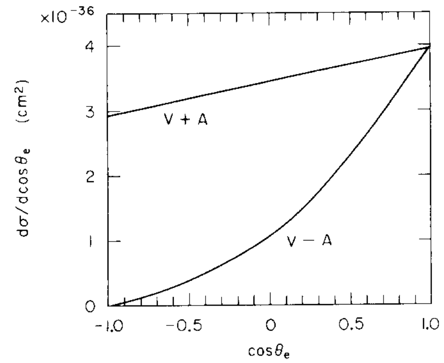

Fig. 4. Distribution of the decay electron of reaction (5) in the center-of-mass frame for (V ± A) coupling with m_N = 1 GeV and $\sqrt{s}$ = 30 GeV.

2.0×10^{-37} cm^2 and 2.7×10^{-36} cm^2 at $\sqrt{s}/2$ = 4 and 16 GeV respectively. This means 0.2 and 23 events per day; in the V − A case the corresponding numbers are reduced by a factor 4. The rate may be an order of magnitude smaller if N_e is as heavy as 5 GeV.

The electron decay angular distribution in the N-rest frame (see fig. 3) is

$$\frac{d\sigma}{d\Omega}(e^+e^- \to \bar{\nu}N_e \underset{\hookrightarrow e\pi}{}) = \frac{G_F^4 f_\pi^2 m_N^3 \cos^4\phi}{2^{11}\Gamma_N \pi^3}(1 - m_\pi^2/m_N^2)^2 (1 - m_N^2/s)^2 \int_{-1}^{1} \frac{d\cos\theta_N}{(1 - t/M_W^2)^2}$$

$$\times \{4s(1+\lambda)(1+\lambda\cos\vartheta) + (1-\lambda)(1+\cos\theta_N)[s + m_N^2 + (s - m_N^2)\cos\theta_N$$

$$-\lambda\cos\vartheta(s - m_N^2 + (s + m_N^2)\cos\theta_N)] + 2m_N\sqrt{s}(1-\lambda)\sin\theta_N(1+\cos\theta_N)\sin\vartheta\sin\varphi\} \tag{6}$$

where f_π is the pion decay constant. The dependence on the azimuthal angle disappears for V + A coupling and in any case is suppressed at high s. In the high energy regime, the N is preferentially polarized along its flight direction if its coupling to the familiar leptons is right-handed or opposite if the coupling is left-handed. In both cases the decay electron prefers to emerge in a direction close to that of its parent.

The characteristics of the center-of-mass distributions of the final state electron are:

(i) $d\sigma/dE_e$ grows linearly within the kinematical limits

$$E_e^{min} = \frac{m_N^2 - m_\pi^2}{2\sqrt{s}}, \qquad E_e^{max} = \frac{m_N^2 - m_\pi^2}{2m_N^2}\sqrt{s}.$$

(ii) The slope of the curve for (V + A) e-N coupling is substantially bigger than for V − A coupling.

(iii) The average electron energy $\langle E_e \rangle \simeq 2.5$ (10.0) GeV for $\sqrt{s}$ = 7.0 (30.0) GeV grows linearly with $\sqrt{s}$.

(iv) $d\sigma/d\cos\theta_e$ is represented in fig. 4. One notices a near isotropic angular distribution for (V + A) coupling whereas a (V − A) coupling leads to an angular distribution which is strongly suppressed in the backward hemisphere These characteristics reflect the behaviour of $d\sigma/d\cos\theta_N$ as given in eq. (3a).

Our investigation shows that neutral right-handed heavy leptons, if they exist, should be detectable at PEP/ PETRA energies and their dynamical characteristics can be determined in several ways by the experiment.

The authors thank Fred Gilman for invaluable discussions. One of us (B.H.) appreciates the financial support of the Swiss National Science Foundation, and the other (P.S.) wishes to thank the Lindemann Trust for a Fellowship. We are grateful for the warm hospitality of Professor S.D. Drell and SLAC.

References

[1] T.P. Cheng and L.F. Li, Invited talk at Orbis Scientiae, Coral Gables, Florida, 17-21 Jan 1977 (Preprint); Missouri-Carnegie preprint (1977).
[2] J.E. Kim, Brown preprint HET-346 (1976).
[3] S.M. Bilensky, S.T. Petcov and B. Pontecorvo, Dubna preprint E2-10374 (1977).
[4] V. Barger and D.V. Nanopoulos, Wisconsin preprint COO-583 (1977).
[5] A. Pais, Rockefeller preprint COO-2232-118 (1977).
[6] A closely related model is that of A. De Rújula, H. Georgi and S.L. Glashow, Harvard preprint HUTP-771A002, based on the gauge group $SU(2)_L \times SU(2)_R \times U(1)$.
[7] S. Weinberg, Phys. Rev. Lett. 19 (1967) 1264;
A. Salam, in: Proc. 8th Nobel Symposium, Stockholm, 1968.
[8] P.E.G. Baird et al., Nature 264 (1976) 528.
[9] S. Parker, H.L. Anderson,and C. Rey, Phys. Rev. 133B (1964) 768.
[10] J. Bjorken, SLAC seminar, January 1977.
[11] Y.S. Tsai, Phys. Rev. D4 (1971) 2821.
[12] J.D. Bjorken and C.H. Llewellyn Smith, Phys. Rev. D7 (1973) 887.
[13] G.J. Feldman et al., Phys. Rev. Lett. 38 (1977) 117.

CHARM CONTRIBUTION TO THE MUON INDUCED DIMUONS

D.P. ROY
Tata Institute of Fundamental Research, Bombay 5, India

Received 8 February 1977

Using a Schwarz inequality, derived recently from unitarity and Zweig suppression, we estimate a lower bound on the muoproduction of charm, in terms of forward ψ-electro(muo)production, which in turn is extrapolated from ψ-photoproduction. The resulting bound on the $\sigma(\mu N \to \mu\mu X)/\sigma(\mu N \to \mu X)$ ratio ($\gtrsim \frac{1}{500}$) is already comparable to the experimental rate, which strongly suggests charm as the dominant mechanism for muon induced dimuons.

Muon induced dimuon events (fig. 1) have been reported by the Michigan State-Fermi Lab Group [1] recently, with a 150 GeV muon beam. Their estimated rate is

$$\frac{\sigma(\mu N \to \mu\mu X)}{\sigma(\mu N \to \mu X)} \sim \frac{1}{1000}\,. \tag{1}$$

This rate is of course, based on an extrapolation because of the experimental cut in the slow muon energy $E_{\mu_2} > 11$ GeV. And since the statistics is rather low (~25 events), the extrapolation is strongly model dependent. In fact an extrapolation from the same data by Barger and Phillips [2], using a detailed model for charm excitation and decay, gives a rate

$$\frac{\sigma(\mu N \to \mu\mu X)}{\sigma(\mu N \to \mu X)} \sim \frac{1}{200}\,. \tag{2}$$

Their detailed model may or may not be valid, but it illustrates, the range of uncertainty involved.

On the theoretical side, the charmed particle excitation is the leading candidate for these dimuons as in the neutrino induced case ($\nu N \to \mu^- \mu^+ X$). From the standard frame work of the Quark Parton Model and the GIM prescription, however, one cannot estimate the rate of muon induced dimuons unlike the neutrino induced case. For, we have here a diagonal excitation of charm which can come only from the $c\bar{c}$ component in the sea. One has no estimate of this component, but it is usually assumed to be much smaller than the other three (n, p and λ) in view of the large SU(4) breaking. There is also a kinematic suppression here, since the diagonal excitation can only produce charmed particles in pairs. Thus one expects the rate of muon induced dimuons to be significantly smaller than the neutrino induced case, but one has no estimate of this rate.

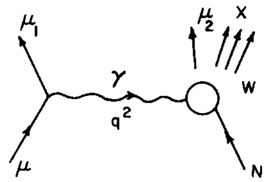

Fig. 1. The muon induced dimuons $\mu N \to \mu\mu X$. The γ 4-momentum square is q^2 and the energy of the γN system is W.

We have tried to estimate the charm contribution to these muon induced dimuons without invoking the Quark Parton Model or even the GIM prescription for charm. Our result would be valid for generic charm. What we are able to obtain in fact, is only a lower bound on the charm contribution. None the less it is a phenomenologically significant estimate, since the bound is already comparable to the observed rate.

The starting point is the usual assumptions of unitarity, Hermitian analyticity and crossing, which give the well-known Schwarz inequality

$$|\mathrm{Im}\, A_{if}(\theta=0)| = |\sum_M A_{iM} A^\dagger_{Mf}| \leqslant \left(\sum_M |A_{iM}|^2\right)^{1/2} \left(\sum_M |A_{fM}|^2\right)^{1/2}, \tag{3}$$

i.e. for a dominantly imaginary amplitude

$$\frac{d\sigma_{if}(\theta=0)}{dt} \leqslant \frac{1}{16\pi}\left(\frac{k^f}{k^i}\right) \sigma_i^T \sigma_f^T\,. \tag{4}$$

This relation has often been used before to obtain a bound on diffractive excitation in terms of the total cross-sections of the initial and final state particles [3].

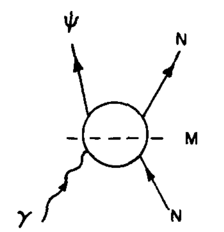

Fig. 2. The diffractive amplitude $\gamma N \to \psi N$. The intermediate states are indicated by M.

Recently Sivers et al. [4] have noted a very interesting consequence of this relation, for the diffractive process $\gamma N \to \psi N$ (fig. 2). It involves splitting the intermediate state M in (3) into C, containing charmed particle pairs and NC containing non-charmed particles, and applying Schwarz inequality to each part. We get

$$\frac{\mathrm{d}\sigma_{\gamma N\to\psi N}(\theta=0)}{\mathrm{d}t} \leqslant \frac{1}{16\pi}\left(\frac{k^{\psi N}}{k^{\gamma N}}\right)(\sigma^{C\frac{1}{2}}_{\gamma N}\sigma^{C\frac{1}{2}}_{\psi N} + \sigma^{NC\frac{1}{2}}_{\gamma N}\sigma^{NC\frac{1}{2}}_{\psi N})^2 . \tag{5}$$

where the first part includes contributions from the bound $c\bar{c}$ states like ψ and ψ', which are however, quite small phenomenologically. Now in the limit of exact Zweig rule $\sigma^{NC}_{\psi N} \to 0$, giving rise to a stronger relation

$$\frac{\mathrm{d}\sigma_{\gamma N\to\psi N}(\theta=0)}{\mathrm{d}t} \leqslant \frac{1}{16\pi}\left(\frac{k^{\psi N}}{k^{\gamma N}}\right)\sigma^{C}_{\gamma N}\sigma^{C}_{\psi N} . \tag{6}$$

Although Zweig rule is not exact (exact Zweig rule would, in fact conflict with unitarity) any phenomenological estimate of the Zweig suppression factor Z_ψ would suggest the $\sigma^{NC}_{\psi N}$ term in (5) to be negligible compared to the left hand side. To see this we can compare (5) with the analogous relation for ρ, which is known to be an approximate equality

$$\frac{\mathrm{d}\sigma_{\gamma N\to\rho N}(\theta=0)}{\mathrm{d}t} \approx \frac{1}{16\pi}\left(\frac{k^{\rho N}}{k^{\gamma N}}\right)(\sigma^{NC}_{\gamma N}\sigma^{NC}_{\rho N}) . \tag{5'}$$

The left hand side is suppressed by a factor $\sim 10^{-3}$. However the $\sigma^{NC}_{\psi N}$ is suppressed relative to $\sigma^{NC}_{\rho N}$ by the Zweig factor Z_ψ, which is $\lesssim 10^{-5}$. This is most easily seen by recalling that the analogous factor for $\varphi \sim 10^{-2}$ and the ratio $\Gamma(\psi \to \rho\pi)/\Gamma(\varphi \to \rho\pi) \sim 10^{-3}$, despite a bigger phase space for $\psi \to \rho\pi$. Thus we expect (6) to be a good approximation to the Schwarz inequality i.e.[‡1]

$$\sigma^{C}_{\gamma N} \gtrsim 16\pi\left(\frac{k^{\gamma N}}{k^{\psi N}}\right)\frac{\mathrm{d}\sigma_{\gamma N\to\psi N}(\theta=0)}{\mathrm{d}t} \Big/ \sigma^{T}_{\psi N} . \tag{7}$$

This relation is expected to hold not only for on-shell photon, but for any general value of q^2.

Thus we have a lower bound on the electro(muo)-production of charmed particles in terms of the ψ-electroproduction. Unfortunately we have only data on ψ-photoproduction, but not so far on electroproduction of ψ. Therefore, we have to do an extrapolation from $q^2 = 0$. The standard VMD extrapolation

$$\left[\frac{\mathrm{d}\sigma(q^2)}{\mathrm{d}t}\right]_{\theta=0} = \left[\frac{\mathrm{d}\sigma(0)}{\mathrm{d}t}\right]_{\theta=0}\left(1-\frac{q^2}{m_V^2}\right)^{-2} \times \left(\frac{k(0)}{k(q^2)}\right)\exp\{B\,(t_{\min}(q^2) - t_{\min}(0))\} \tag{8}$$

is known to work reasonably well for the electroproduction of ρ and ω, where B denotes the slope and m_V the vector meson mass [5]. For ψ, however, VMD seems to be inadequate over the time like region $0 < q^2 < m_\psi^2$. An adequate representation over this region is obtained, both for ψ and the ρ, ω, φ mesons, by incorporating a form factor of the type [6]

$$F(q^2) = (1 - q^2/(m_V + 1)^2)^{-2} . \tag{9}$$

Therefore we incorporate this form factor in the extrapolation formula (8) to estimate $\gamma(q^2)N \to \psi N$ forward cross-section[‡2] from the photoproduction data [7]. The form factor is, of course, a fairly mild one over the space like region of interest. Its effect on the integrated cross-section (10) below is only 30%.

Putting the above $\gamma(q^2)N \to \psi N$ forward cross-section and the experimental value [7] $\sigma^{T}_{\psi N} \simeq 2.75$ mb in the inequality (7), we get a lower bound on $\sigma^{C}_{\gamma N}(q^2, W)$. Using the standard relation between this virtual photon cross-section and the electro(muo)production cross-section [8] $\mathrm{d}\sigma/\mathrm{d}q^2\,\mathrm{d}W$, and integrating over q^2 and W we get a lower bound on charm contribution

$$\sigma^{C} \geqslant 0.35 \text{ nb} . \tag{10}$$

The integration incorporates the experimental cuts

‡1 We replace $\sigma^{C}_{\psi N}$ by $\sigma^{T}_{\psi N}$ since we are only interested in an inequality and besides the total ψN cross-section is expected to be saturated by the charm contribution, any way.

‡2 This ignores the longitudinal photon contribution. However, we are only interested in a lower bound, and besides, the longitudinal contribution is pressumably small as in the ρ, ω case.

[1] on the fast muon energy $E_{\mu_1} > 17$ GeV and angle $\theta_{\mu_1} > 13$ mrad.; and uses a charm threshold of $W = 5$ GeV as suggested by ψ-photoproduction [7,9]. The corresponding quantity from ordinary (noncharmed) final states is obtained by integrating the SLAC electroproduction cross-section with the same cuts. Using the parametrisation of ref. [8] for the SLAC structure functions we get

$$\sigma = 60 \text{ nb} . \tag{11}$$

The alternative parametrisation of ref. [10] gives practically the same value.

The resulting lower bound on charm contribution to the dimuon rate is

$$\frac{\sigma(\mu\text{N} \to \mu\mu\text{X})}{\sigma(\mu\text{N} \to \mu\text{X})} = 2B_\mu \frac{\sigma^C}{\sigma} \gtrsim \frac{1}{500} , \tag{12}$$

where the muonic branching ratio of the charmed particles is taken as $B_\mu \simeq 0.2$. A value of 0.2–0.25 is suggested both by the latest dimuon rate from narrow band neutrino beam [11] and the DESY rate [12] on $e^+e^- \to e^\pm K^0$ + Hadrons. It is also consistent with the relative rate of trimuons to dimuons in the above muon beam experiment [1].

The above inequality becomes an equality in specific models like the VMD. However, the VMD is known to breakdown for the electroproduction cross-section in the deep inelastic region, and specific modifications like the generalised VMD [10] have been suggested. Without invoking any such specific model, we can only obtain a lower bound on the charm contribution, It is significant, however, that this lower bound is already in the range of the experimental estimate $(\frac{1}{1000} - \frac{1}{200})$. It is strongly suggestive of charm excitation as the dominant mechanism for muon induced dimuons.

We believe the uncertainty in the estimated bound is around 50%, arising largely from the off shell extrapolation. Of course, the uncertainty in the present experimental estimates, including the E_{μ_2} extrapolation, is much bigger. This situation should improve soon, as the Michigan State-Fermi Lab. group are planning to increase their dimuon sample [1] by a factor of fifty. The lower bound estimate can be made more precise if we have data on electro(muo)production of ψ. More importantly this will enable us to estimate the bound as a function of q^2, to see for instance the charm contribution to the 15% scaling violation observed in the large negative q^2 region [1]. It seems to us possible to measure ψ electroproduction and muoproduction at SLAC and Fermi Lab.

I gratefully acknowledge discussions with my colleagues here and correspondences with Roger Phillips and Vernon Barger, I am also grateful to S.M. Roy for a careful reading of the manuscript.

References

[1] K.W. Chen, in: Proc. of the Int. Conf. on New particles with new quantum numbers, Madison, Wisconsin, 1976.
[2] V. Barger and R.J.N. Phillips, Phys. Lett. 65B (1976) 167.
[3] See e.g. D.P. Roy and R.G. Roberts, Nucl. Phys. 77B (1974) 240.
[4] D. Sivers, J. Townsend and G. West, Phys. Rev. 13D (1976) 1234.
[5] G. Wolf, in: Proc. of the Int. Conf. on Lepton and photon interaction, Stanford, 1975.
[6] D.P. Roy, Phys. Lett. 63B (1976) 324.
[7] R.L. Anderson, in: Proc. of the Int. Conf. on New particles with new quantum numbers, Madison, Wisconsin, 1976.
[8] G. Miller et al., Phys. Rev. 5D (1972) 528.
[9] V. Barger and R.J.N. Phillips, Phys. Lett. 58B (1975) 433.
[10] J.J. Sakurai and D. Schildknecht, Phys. Lett. 40B (1972) 121.
[11] B.C. Barish et al., Phys. Rev. Lett. 36 (1976) 939, and presentation at the APS meeting "Particles and fields" at BNL, 1976.
[12] Braunschweig et al., Phys. Lett. 63B (1976) 471.

CONFORMAL ANOMALIES IN A GENERAL BACKGROUND METRIC

HUNG-SHENG TSAO[1]
The Rockefeller University, New York, N.Y. 10021, USA

Received 12 February 1977

By using the dimensional regularization procedure, we explicitly calculate the coefficients of conformal anomalies in a general background metric due to scalar, spin 1/2 fermion, gauge and gravitation fields.

Recently there has been renewed interest and progress in understanding the problem of regularization of the energy momentum tensor of a matter field in a general background metric [1–10]. The connection between the conformal anomalies and the Hawking effect [5] adds a special physical significance to the former. In the dimensional regularization procedure the existence of the conformal anomalies was noted some time ago by Capper and Duff [3], a general formal discussion has been presented by Deser, Duff and Isham [4] and the form of anomalies has been clarified by Duncan [7]. In brief, the anomalies arise because of the need to regularize the theory by adding a counter term to the original Lagrangian; i.e.,

$$L = L_o + (1/\epsilon)L_c, \tag{1}$$

where ϵ vanishes at the physical space-time dimension. The trace of the energy momentum tensor is defined[‡] to be

$$T^\mu{}_\mu = \frac{-2}{(-g)^{1/2}} g^{\mu\nu} \frac{\delta L}{\delta g^{\mu\nu}}, \tag{2}$$

$$= T_o{}^\mu{}_\mu + (1/\epsilon)\, T_c{}^\mu{}_\mu .$$

For a conformal invariant theory, one has

$$(-g)^{1/2}\, T_o{}^\mu{}_\mu = \epsilon L_o$$

$$(-g)^{1/2}\, T_c{}^\mu{}_\mu = \epsilon L_c$$

so

$$(-g)^{1/2}\, T^\mu{}_{\mu|\epsilon=0} = L_{c|\epsilon=0}. \tag{3}$$

This is the conformal anomaly. In general we have

$$T^\mu{}_\mu(n=2) = \frac{1}{4\pi}(K_0 R)$$
$$T^\mu{}_\mu(n=4) = \frac{1}{16\pi^2}(K_1 H + K_2 G) \tag{4}$$

with

$$H = R_{\mu\nu}R^{\mu\nu} - \tfrac{1}{3}R^2$$
$$G = R_{\mu\nu\lambda\delta}R^{\mu\nu\lambda\delta} - 4R_{\mu\nu}R^{\mu\nu} + R^2 \tag{5}$$

and possible matter contributions. The numerical values of K_0, K_1 and K_2 in some special cases have been calculated [6–10].

The purpose of this note is to point out that these coefficients can all be calculated by an algorithm, which is a generalization of that of 't Hooft and Veltman [12]. We state the *algorithm*: given a Lagrangian function of ϕ_i in a general background metric $g_{\mu\nu}$ and external fields $N_\mu{}^i{}_j, X_{ij}$ in n space-time dimensions

$$L = (-g)^{1/2}\,[\varphi^* g^{\mu\nu}(D_\mu + N_\mu)(D_\nu + N_\nu)\varphi + \varphi^* X \varphi]^{\ddagger 1},$$

the one loop counter terms are of the form

$$L_c\,(n\to 2) = \frac{1}{2\pi}(-g)^{1/2}\,[\tfrac{1}{6}R + X] \tag{8}$$

$$L_c\,(n\to 4) = \frac{1}{8\pi^2}(-g)^{1/2}\,[\tfrac{1}{2}(\tfrac{1}{6}R + X)^2 + \tfrac{1}{12}Y_{\mu\nu}Y^{\mu\nu} + \tfrac{1}{60}H + \tfrac{1}{180}G] \tag{9}$$

[1] Work supported in part by the U.S. Energy Research and Development Administration under Contract Grant No. EY-76-C-02-2232B*.000.

[‡] We use the convention of Misner et al. [11], and natural units.

[‡1] [ ] means trace over the internal index of ϕ_i, D_μ is the covariant derivative of the metric $g_{\mu\nu}$.

with

$$Y_{\mu\nu} = D_\mu N_\nu - D_\nu N_\mu + N_\mu N_\nu - N_\nu N_\mu .$$

This algorithm can be derived by using the n-dimensional generalized [8, 9, 14] proper time method of Schwinger and DeWitt [2]. All the key elements are contained in the thesis of Christensen [15]. Note that in eq. (8) and eq. (9), we do *not* make use of the topological identities:

$$\int R(-g)^{1/2}\, d^2x = \text{constant},$$
$$\int G(-g)^{1/2}\, d^4x = \text{constant}. \qquad (10)$$

As emphasized by Duncan [7], *in the spirit of dimensional regularization, one can only use these identities that have meaning for all n.*

By using the algorithm, it is straightforward to calculate the L_c and hence $T^\mu{}_\mu$, for a matter field in a general background metric, we only list the results:

(i) conformal scalar, $K_0 = \frac{1}{6}, K_1 = \frac{1}{60}, K_2 = \frac{1}{180}$,

(ii) real spin 1/2 fermion, $K_0 = \frac{1}{12}, K_1 = \frac{1}{20}, K_2 = \frac{7}{720}$,

(iii) gauge field [13], $K_1 = r/5, K_2 = -\frac{13}{180}r$ and in addition one has $T^\mu{}_\mu$ $(n = 4)$ matter $= (1/16\pi^2)e^2 \times \frac{11}{12}C(F^a_{\mu\nu})^2$, with r = rank of the gauge group, $C = f_{abc}f_{abc}$, e = gauge coupling.

(iv) gravitational field [12, 15], $K_0 = \frac{-38}{12}, K_2 = \frac{53}{45}$, and if we do not use the equation $R_{\mu\nu} - \frac{1}{2}g_{\mu\nu}R = 0$ we have additional contribution

$$T^\mu{}_\mu\ (n = 4) = \frac{1}{16\pi^2}\left(\tfrac{7}{10}\, R_{\mu\nu}R^{\mu\nu} + \tfrac{1}{60}R^2\right)$$

Our results in the scalar and fermion case agree with other calculation [8, 10]. For a U(1) gauge field, our result agrees with Brown and Cassidy [9] but not with Buch and Davis [10], they get $K_2 = \frac{1}{90}$. In the gravitational case, because $K_0 < 0$, it seems to indicate that in $2 + \epsilon$ space time dimension‡ the Einstein theory is asymptotically "safe" in the sense of Weinberg [16]. Finally, we would like to point out that one can use our algorithm to calculate the full one loop counter terms of quantum gravity interacting with a matter field [12, 13]. Only the "G" term need be added to previous calculations.

‡ Detail will be published elsewhere.

In summary, we have presented a general algorithm for calculating the counter terms at two and four space time dimensions and we have calculated the conformal anomalies of scalar, spin 1/2 fermion, gauge and gravitation fields.

The author would like to thank S.L. Adler, L.S. Brown, A. Duncan and L. Ford for helpful discussions and J. Bernstein and W. Marciano for critical reading of the manuscript.

References

[1] L. Parker, Quantized fields and particle creation in curved spacetime, lectures presented at the second Latin American Symposium on Relativity and gravitation, Caracas, Venezuela, December (1975).

[2] B.S. DeWitt, Phys. Reports C19 (1975) 295.

[3] D.M. Capper and M.J. Duff, Nuovo Cim. 23A (1974) 173.

[4] S. Deser, M.J. Duff and C.J. Isham, Nucl. Phys. B 111 (1976) 45.

[5] S.M. Christensen and S.A. Fulling, Trace anomalies and the Hawking effects, Phys. Rev. D, in press.

[6] S.L. Adler, J. Lieberman and Y.J. Ng, Regularization of stress-energy tensor for vector and scalar particles propagating in a general background metric, Ann. Phys., in press.

[7] A. Duncan, Phys. Lett. 66B (1977) 167.

[8] L.S. Brown, Stress tensor trace anomaly in a gravitational metric: scalar fields, Univ. of Washington preprint (1976), unpublished.

[9] L.S. Brown and J.P. Cassidy, Stress tensor trace anomaly in a gravitational metric general theory, Maxwell field, Univ. of Washington preprint (1976), unpublished.

[10] S.S. Bunch and P.C.W. Davies, Stress tensor and conformal anomalies for massless fields in a Robertson-Walker Universe, King's College preprint (1976), unpublished.

[11] C.W. Misner, K.S. Thorne and J.A. Wheeler, Gravitation (W.H. Freeman).

[12] G. 't Hooft, Nucl. Phys. B62 (1972) 444;
G. 't Hooft and M. Veltman, Ann. Inst. Henri Poincaré XX, No. 1 (1964) 69.

[13] S. Deser and P. van Nieuwenhuizen, Phys. Rev. D10 (1974) 401, 411;
S. Deser, H.-S. Tsao and P. van Nieuwenhuizen, Phys. Rev. D10 (1974) 3337.

[14] H.-S. Tsao, Institute for Advanced Study note (1976), unpublished.

[15] S.M. Christensen, Covariant coordinate space methods for calculation in the quantum theory of gravity, thesis, The Univ. of Texas at Austin (1975).

[16] S. Weinberg, Critical phenomena for field theories, Lectures presented at Erice, Italy July (1976).

EQUIVALENCE BETWEEN THE UNIFIED DUAL MODEL AND POMERON–REGGEON AMPLITUDES

A. D'ADDA, R. D'AURIA, E. NAPOLITANO
Istituto di Fisica dell'Università di Torino, and
Istituto Nazionale di Fisica Nucleare, Sezione di Torino, Italy

and

P. DI VECCHIA [1], F. GLIOZZI and S. SCIUTO [2]
CERN, Geneva, Switzerland

Received 1 April 1974

We show that a recently proposed unified dual model for interacting open and closed strings actually describes Pomeron–Reggeon amplitudes of the conventional Veneziano model. We prove, in particular, that the Pomeron amplitudes are given by the Shapiro–Virasoro model.

It is not clear whether the existing dual models [1] could be modified to describe the real world of hadrons, or whether they will ultimately be supplanted by completely different models. However, it is a matter of fact that the internal consistency of these models is so accurate that it may compete with field theory. A beautiful example of this consistency is the way in which the second order perturbative unitarity is restored at the critical value of the space-time dimension. Indeed it is well known that at non-critical value of the dimension the simple non-planar orientable loop shows, besides the unitarity cuts, new unitarity violating singularities [2] in the channel with vacuum quantum numbers. At the critical value of the space-time dimension these singularities become a series of poles [3, 4] located on a linear Regge trajectory with twice the intercept and half the slope of the input trajectory; they have been identified with the Pomeron poles.

Since these poles are factorizable [5, 6], they represent a new set of resonances which are required by unitarity. Then one is urged to answer the following questions:

(i) what is the spectrum of the Pomeron resonances?
(ii) what are their scattering amplitudes?
(iii) what are their couplings with the ordinary resonances?

The first question has been recently answered by Olive and Scherk [7], who showed that the Pomeron sector of the conventional Veneziano model coincides at the critical dimension with the spectrum of the Shapiro–Virasoro (SV) model [8].

In this paper we answer the latter two questions by showing that:

(a) the scattering amplitude of on-shell Pomeron states coincides with the corresponding SV amplitude, in agreement with a previous conjecture [9];

(b) the mixed amplitudes among Pomeron states and ordinary resonances coincide with the ones we have constructed in the framework of a unified version (ref. [10] hereafter quoted as I) of the conventional and SV model.

Our starting point is the string picture [11] of dual models or, more precisely, the formulation of the interacting dual string given in ref. [12]. In this work it has been shown that the interaction among strings can be represented by switching on a suitable external field acting on a free string. Indeed this procedure allows to reproduce quite naturally the dual amplitudes in their most manageable form [13], that is, schematically

[1] Address after May 15, 1974: NORDITA, Copenhagen.
[2] Permanent address: Istituto di Fisica dell'Universita di Torino.

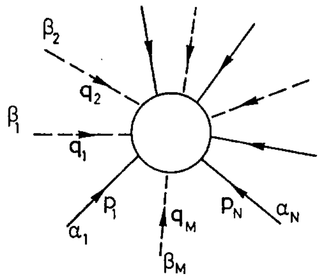

Fig. 1.

$$A(1,2,\ldots N) = \int \mathrm{d}V \langle 1 | \mathcal{V}_2 \mathcal{V}_3 \ldots \mathcal{V}_{N-1} | N \rangle \,, \tag{1}$$

where the vertex $\mathcal{V}$ is the interacting part of the Lagrangian of the string and the physical states $|N\rangle$ and $\langle 1|$ are respectively the initial and the final state of the string.

Such a string picture gives a simple and intuitive description of both the conventional model (open string) and the SV model (closed string) and suggests, as noted in ref. [12], a way to construct a unified model of interacting closed and open strings which include as special cases the conventional model and the SV model.

The detailed features of this model are discussed in I. In order to prove the equivalence between this unified model and the Pomeron–Reggeon amplitudes, we quote here the main result, that is the amplitude $A(N\mathbf{R}, M\mathbf{P})$ for the interaction among N open strings and M closed strings (see fig. 1, where continuous (dotted) lines represent open (closed) string states) that can be written for instance in the form:

$$A(N\mathbf{R}, M\mathbf{P}) = \int_0^1 \prod_{i=2}^{N-2} \frac{\mathrm{d}x_i}{x_i} \,\vartheta(x_{i+1} - x_i) \int \prod_{j=1}^{M} \frac{\mathrm{d}^2 z_j}{|z_j|^2}$$

$$\times \langle \alpha_1, -p_1 | T[\mathcal{V}_{\alpha_2}(x_2; p_2) \ldots \mathcal{W}_{\beta_1}(z_1, \bar{z}_1; q_1)\, \mathcal{W}_{\beta_2}(z_2, \bar{z}_2; q_2) \ldots \mathcal{W}_{\beta_M}(z_M, \bar{z}_M; q_M)] | \alpha_N, p_N \rangle \,. \tag{2}$$

In eq. (2) $\mathcal{V}_\alpha(x,p)$ is the usual vertex [13] of the conventional model associated with a physical state $|\alpha, p\rangle$ of momentum p and labelled by the set of indices α; $\mathcal{W}_\beta(z,\bar{z};q)$ is the vertex associated with the closed string and is related to $\mathcal{V}$ by [‡1]

$$\mathcal{W}_\beta(z, \bar{z}; q) = \mathcal{V}_\alpha(z; q/2)\, \mathcal{V}_{\bar{\alpha}}(\bar{z}; q/2) \tag{3}$$

where α and $\bar{\alpha}$ are the two sets of indices of open string which characterize the closed string [‡2] labelled by the indices β.

The open string variables x are integrated over the real axis ($x_{N-1} = 1$) while the closed string variables z are integrated over the upper half part of the complex plane. T indicates that the closed string vertices must be ordered among themselves and with respect to the open string ones according to the increasing modulus of the variables x and z; instead the ordering of the open string vertices is fixed by the ϑ functions.

Clearly the amplitude (2) is explicitly factorizable in a multiperipheral configuration where all the intermediate resonances are open string states. Moreover we show in I that it is factorizable in all the channels which should resonate according to the dual rules, and all the poles are associated with open or closed string resonances (ordinary or SV states, respectively).

‡1 $\bar{z}$ is the complex conjugate of z.

‡2 Actually the space of the physical SV states of momentum q is the direct product of two spaces of physical states of the open string belonging to the same level and with momentum $q/2$. The vertex (3) is obtained from the usual SV vertex [given, e.g., in (6)] by identifying the two sets of oscillators appearing in it.

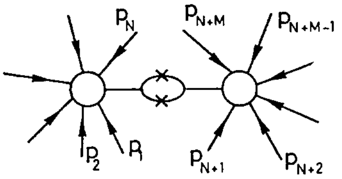

Fig. 2a.

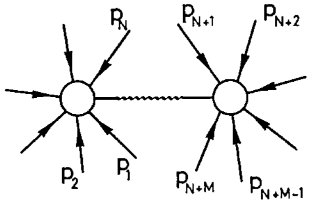

Fig. 2b.

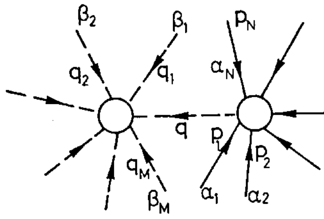

Fig. 3.

The link between our formalism and the dual loop theory is given by the non-planar orientable graph of fig. 2a which, at the critical value of dimension can be factorized by means of the states of the dual Pomeron sector (fig. 2b). The analogue of the graph of fig. 2b can be calculated with our method using the propagator of the SV states and the transition amplitude from an off-mass shell SV state to N on-mass shell Reggeons. As shown in I, both these quantities are obtained factorizing the mixed amplitude $A(N\mathbf{R}, M\mathbf{P})$ (eq. (2)) in the channel pictured in fig. 3.

One gets:

$$A(N\mathbf{R}, M\mathbf{P}) = \sum_{\lambda,\mu} {}_b\langle 0|{}_c\langle 0|\mathcal{A}(1,2,\ldots,M)|\lambda, q/2\rangle_b|\mu, q/2\rangle_c$$

$$\times \int_\Gamma \frac{\mathrm{d}^2 z}{|z|^2} \langle\lambda, q/2|z^{-L_0-1}|\lambda, q/2\rangle\langle\lambda, q/2|\mathcal{B}(1,2,\ldots,N)|\mu, -q/2\rangle\langle\mu, -q/2|\bar{z}^{-L_0-1}|\mu, -q/2\rangle\,, \tag{4}$$

where:

(i) the amplitude

$$ {}_b\langle 0|{}_c\langle 0|\mathcal{A}(1,2,\ldots,M)|\lambda, q/2\rangle_b|\mu, q/2\rangle_c$$

$$= \int \prod_{l=1}^{M-1} \frac{\mathrm{d}^2 z_i}{|z_i|^2}\, {}_b\langle 0|{}_c\langle 0|T[\mathcal{W}^{\beta_1}_{bc}(z_1, \bar{z}_1; q_1)\ldots\mathcal{W}^{\beta_M}_{bc}(1, 1; q_M)]\,|\lambda, q/2\rangle_b|\mu, q/2\rangle_c \tag{5}$$

is the $(M+1)$ SV state amplitude (with the state of momentum q off-mass shell); in (5) the integration is extended over the whole complex plane and

$$\mathcal{W}^{\beta}_{bc}(z, \bar{z}; q) = \mathcal{V}^{\alpha}_{b}(z, q/2)\mathcal{V}^{\bar{\alpha}}_{c}(\bar{z}, q/2) \tag{6}$$

is the usual SV vertex;

(ii) the quantity

$$\int_\Gamma \frac{\mathrm{d}^2 z}{|z|^2} \langle\lambda, q/2|z^{-L_0-1}|\lambda, q/2\rangle\langle\mu, -q/2|\bar{z}^{-L_0-1}|\mu, -q/2\rangle$$

$$\equiv \int_\Gamma \frac{\mathrm{d}^2 z}{|z|^2}\, {}_b\langle\lambda, q/2|{}_c\langle\mu, q/2|z^{-L_{0b}-1}\bar{z}^{-L_{0c}-1}|\lambda, q/2\rangle_b|\mu, q/2\rangle_c\,, \tag{7}$$

where the integration is extended inside the unitary circle in the complex plane of z, (7) is the propagator of the SV states [‡3];

‡3 Let us notice that the propagator (7) forces the Reggeon states, $|\lambda, q/2\rangle$ and $|\mu, q/2\rangle$ to belong to the same eigenvalue of L_0; hence their direct product is a SV state. Moreover, due to the projective invariance properties of $\mathcal{A}(1, 2, \ldots, M)$ the only states $|\mu, q/2\rangle$ that contribute to the sum in (4) are the physical ones.

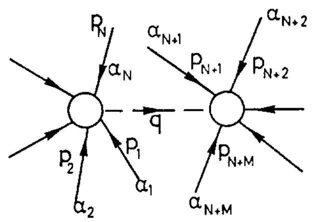

Fig. 4.

(iii) the amplitude

$$\langle\lambda, q/2|\mathcal{B}(1,2,...,N)|\mu, -q/2\rangle = \mathrm{e}^{\mathrm{i}\pi(q^2/2)} \int_0^{2\pi} \prod_{i=2}^{N} \mathrm{d}\sigma_i \; \vartheta(\sigma_i - \sigma_{i-1})$$

$$\times \langle\lambda, q/2|\mathcal{V}_{\alpha_1}(1;p_1)\,\mathcal{V}_{\alpha_2}(\mathrm{e}^{\mathrm{i}\sigma_2};p_2)\cdots\mathcal{V}_{\alpha_N}(\mathrm{e}^{\mathrm{i}\sigma_N};p_N)|\mu; -q/2\rangle \tag{8}$$

is the amplitude that connects the off-mass shell SV state of momentum q with N external Reggeons [‡4].

By sewing together two of these amplitudes B by means of the SV propagator (7) one can write the following expression for the many Reggeon → SV state → many Reggeon amplitude depicted in fig. 4

$$\mathcal{B}(N\mathbf{R}\to\mathbf{P}\to M\mathbf{R}) = \sum_{\lambda,\mu}\int\frac{\mathrm{d}^2z}{|z|^2}\int_0^{2\pi}\prod_{i=2}^{N}\mathrm{d}\sigma_i\,\vartheta(\sigma_i-\sigma_{i-1})\int_0^{2\pi}\prod_{j=2}^{M}\mathrm{d}\sigma_{N+j}$$

$$\times\,\vartheta(\sigma_{N+j}-\sigma_{N+j-1})\,\mathrm{e}^{\mathrm{i}\pi q^2}\langle\lambda, q/2|z^{-L_0-1}\mathcal{V}_{\alpha_1}(1;p_1)\,\mathcal{V}_{\alpha_2}(\mathrm{e}^{\mathrm{i}\sigma_2};p_2)\cdots\mathcal{V}_{\alpha_N}(\mathrm{e}^{\mathrm{i}\sigma_N};p_N)P|\mu, -q/2\rangle$$

$$\times\,\langle\mu, -q/2|\bar{z}^{-L_0-1}\mathcal{V}_{\alpha_{N+1}}(1;p_{N+1})\,\mathcal{V}_{\alpha_{N+2}}(\mathrm{e}^{\mathrm{i}\sigma_{N+2}};p_{N+2})\cdots\mathcal{V}_{\alpha_{N+M}}(\mathrm{e}^{\mathrm{i}\sigma_{N+M}};p_{N+M})|\lambda, q/2\rangle\,. \tag{9}$$

In this expression we have introduced the projection operator P on the physical Reggeon states because, as the factorization (4) shows, the off-mass shell states $|\lambda, q/2\rangle$ and $|\mu, -q/2\rangle$ must be physical.

After use of the transformation property of the vertices

$$z^{-L_0}\,\mathcal{V}_\alpha(x;p)\,z^{L_0} = \mathcal{V}_\alpha\left(\frac{x}{z};p\right) \quad \text{with} \quad z = r\,\mathrm{e}^{-\mathrm{i}\sigma_1} \tag{10}$$

and the change of variables $\sigma_i + \sigma_1 \to \sigma_i$ ($i = 2, 3, ..., N$) the expression (9) becomes

$$\mathcal{B}(N\mathbf{R}\to\mathbf{P}\to M\mathbf{R}) = \mathrm{e}^{\mathrm{i}\pi q^2}\sum_{\lambda,\mu}\int\mathrm{d}V\langle\lambda, q/2|\mathcal{V}_{\alpha_1}\left(\frac{\mathrm{e}^{\mathrm{i}\sigma_1}}{r};p_1\right)\mathcal{V}_{\alpha_2}\left(\frac{\mathrm{e}^{\mathrm{i}\sigma_2}}{r};p_2\right)$$

$$\cdots\mathcal{V}_{\alpha_N}\left(\frac{\mathrm{e}^{\mathrm{i}\sigma_N}}{r};p_N\right)r^{-2L_0-2}P|\mu, -q/2\rangle\langle\mu, -q/2|\mathcal{V}_{\alpha_{N+1}}(1;p_{N+1})\,\mathcal{V}_{\alpha_{N+2}}(\mathrm{e}^{\mathrm{i}\sigma_{N+2}};p_{N+2})$$

$$\cdots\mathcal{V}_{\alpha_{N+M}}(\mathrm{e}^{\mathrm{i}\sigma_{N+M}};p_{N+M})|\lambda, q/2\rangle \tag{11}$$

where the integration domain is given by

‡4 In I it is shown that when the states $|\lambda, q/2\rangle$ and $|\mu, -q/2\rangle$ are on their mass shell, the amplitude (8) becomes the mixed amplitude (2) for N Reggeon 1SV state. The proof is performed by writing $\langle\lambda, q/2|$ as

$$\lim_{z\to 0}\langle 0|(\mathcal{V}/z)(z;-q/2) \quad \text{and} \quad |\mu, -q/2\rangle = \lim_{z\to 0}(\mathcal{V}/z)(1/\bar{z};-q/2)|0\rangle\,,$$

and then sending the unitary circle into the real axis by means of the projective transformation $z\to z' = -\mathrm{i}(z+1)/(z-1)$.

$$\int \mathrm{d}V = \int_0^1 \frac{\mathrm{d}r}{r} \int_0^{2\pi} \mathrm{d}\sigma_1 \int_{\sigma_1}^{\sigma_1+2\pi} \prod_{i=2}^{N} \mathrm{d}\sigma_i \,\vartheta(\sigma_i-\sigma_{i-1}) \int_0^{2\pi} \prod_{j=2}^{M} \mathrm{d}\sigma_{N+j}\,\vartheta(\sigma_{N+j}-\sigma_{N+j-1})\,, \tag{12}$$

and corresponds to the unitary circle for the variables of the vertices $N+1, N+2, ..., N+M$ and to a larger circle (of radius $1/r$ with r integrated between 0 and 1) for the variables of the vertices $1, 2, ..., N$.

The completeness of the states $|\lambda\rangle$ and $|\mu\rangle$ allows to write the sum over $|\lambda\rangle$ and $|\mu\rangle$ as a trace in the harmonic oscillator space without zero mode:

$$\mathcal{B}(N\mathbf{R}\to\mathbf{P}\to M\mathbf{R}) = \mathrm{e}^{\mathrm{i}\pi q^2} \int \mathrm{d}V\, r^{-(q^2/2)-2}\, \mathrm{Tr}\left[{}_0\langle q/2|P\mathcal{V}_{\alpha_1}\left(\frac{\mathrm{e}^{\mathrm{i}\sigma_1}}{r};p_1\right)\cdots\mathcal{V}_{\alpha_N}\left(\frac{\mathrm{e}^{\mathrm{i}\sigma_N}}{r};p_N\right) r^{2R}|-q/2\rangle_0\right.$$

$$\times\ {}_0\langle -q/2|\mathcal{V}_{\alpha_{N+1}}(\mathrm{e}^{\mathrm{i}\sigma_{N+1}};p_{N+1})\cdots\mathcal{V}_{\alpha_{N+M}}(\mathrm{e}^{\mathrm{i}\sigma_{N+M}};p_{N+M})|q/2\rangle_0 \tag{13}$$

where the vectors $|\pm q/2\rangle_0\,({}_0\langle\mp q/2|)$ represents an incoming (outgoing) state of momentum $\pm q/2$ in the space of the zero model only and $L_0 = -(p_0^2/2) - R$.

The trace appearing in (13) is formally that of the planar loop; then the projection operator P is equivalent (at the critical value of dimension) to the factor

$$f(r^2)^2 = \prod_{n=1}^{\infty} (1-r^{2n})^2\,. \tag{14}$$

Now one can easily recognize that (13) gives exactly the same amplitude ‡5 of the graph of fig. 2b at the critical value of the space-time dimension (see, e.g., refs. [5] and [6]). It is quite amusing that expression (13) is obtained in the dual loop theory *after* the Jacobi transformation in the graph of fig. 2a; however, this fact is not surprising because our integration variables have been chosen from the very beginning in such a way as to make evident the Pomeron poles. In our formalism the amplitude (13) can be written in a self-consistent way also for a number of dimensions less than the critical one ‡6; however, if $d \neq 26$ it is different from the expression obtained in the loop theory; it seems interesting to investigate the meaning of that amplitude in such a case.

Our procedure for constructing the twisted loop diagram shows that the Pomeron is a factorizable pole and that the corresponding decay amplitude of a Pomeron into N Reggeons is given by the expression (8), which, on the mass-shell of the Pomeron, coincides with the 1SV state–N Reggeon amplitude as given by (2). It would be interesting to study more closely the relationship between our procedure of factorization and the one used in refs. [5] and [6].

More generally, it is immediate to prove that (2) is actually the M Pomeron–N Reggeon amplitude (when all the external particles are on their mass shell). In fact, factorizing the one-Pomeron decay amplitude one gets the vertex ‡7 of an on-mass shell Pomeron between the two off-mass shell physical Reggeons (fig. 5):

$$\langle\lambda, -p_1|\mathcal{W}_\beta(q)|\mu, p_2\rangle = \langle\lambda, -p_1|\int_0^\pi \mathrm{d}\sigma\, \mathcal{V}_\alpha(\mathrm{e}^{\mathrm{i}\sigma};q/2)\mathcal{V}_{\bar\alpha}(\mathrm{e}^{-\mathrm{i}\sigma};q/2)|\mu, p_2\rangle\,. \tag{15}$$

‡5 Due to different conventions about the zero mode, the quantity

$$\exp\left\{\gamma_0^2\left(\sum_{i=1}^{N} p_i\right)^2\right\}{}_0\langle 0|\mathcal{V}(p_1)\mathcal{V}(p_2)\cdots\mathcal{V}(p_N)|0\rangle_0$$

given in ref. [6] is equivalent to our ${}_0\langle q/2|\mathcal{V}(p_1)\mathcal{V}(p_2)\cdots\mathcal{V}(p_N)|-q/2\rangle_0$ with $q = \sum_{i=1}^N p_i$.

‡6 The only difference is that the projection operator is no longer $f(r^2)^2$, due to the presence of the Brower states [14].

‡7 As shown in I, the vertex (15) can be further factorized in a Pomeron–Reggeon transition vertex and in a three-Reggeon vertex; hence it may happen that the expression (15) diverges because q^2 is just on the pole of a Reggeon; in such a case, it is understood that the residue must be taken.

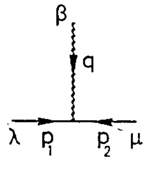

Fig. 5.

These vertices can be sewed together and with Reggeon vertices (by means of Reggeon propagators attached to off-mass shell Reggeon legs) to form a tree [‡8] representing an M Pomeron–N Reggeon transition amplitude; the amplitude so built coincides with the M SV state–N Reggeon amplitude. Moreover, the unified model amplitude (2) factorizes in the SV amplitude (see I and also eq. (4)); hence the N on-mass shell Pomeron amplitude coincides with the SV amplitude.

We can then conclude that if from the loop theory one can extract in a consistent way Pomeron–Reggeon amplitudes, the spectrum and the interaction of the Pomerons coincide with the ones of the SV states.

Let us stress that our results are not the complete many-loop dual theory [‡9]. We have only formulated the theory (complete at the lowest order [‡10] in g – i.e., at the tree level) of the interaction of the particles of the Pomeron sector among themselves and with Reggeons; these results could also be obtained, in principle, by considering the dual Reggeon graphs containing only non-planar orientable loops and taking their residua when all the Pomerons are on-mass shell.

Because in all the treatment of this work (and of I), only the projective properties of the vertices $\mathcal{V}$ and $\mathcal{W}$ have been used, the extension of our results to the Neveu–Schwarz model ought to be straightforward.

We acknowledge useful discussions with M. Ademollo, D. Amati, E. Del Giudice, S. Fubini, E. Galzenati, R. Musto, F. Nicodemi and D. Olive. We thank D. Olive for a critical reading of the manuscript.

‡8 If the tree is ended by physical states there is no trouble with spurious states, due to the good projective transformation properties of the $\mathcal{V}$'s and the $\mathcal{W}$'s (see Appendix A of I).

‡9 The amplitudes we have written in this work (and in I) can be topologically characterized according to the number of borders of the world surface of the interacting strings. The interaction amplitude among Pomerons only (the SV amplitude) do not involve open strings and hence corresponds to a surface without borders; the Reggeon amplitude (the conventional model) and the mixed Pomeron–Reggeon amplitude (given in I and written in eq. (2)) correspond to surfaces with one border; the one-loop amplitude of fig. 4 (and the analogous with some external Pomerons, that we can easily write) corresponds to a surface with two borders. It is not immediate to write in a closed form amplitudes with a larger number of borders.

‡10 The three-Reggeon coupling constant g determines uniquely also the coupling constants g_{P} (three-Pomeron vertex), g_{PR} (Pomeron–Reggeon transition) and g_{PRR} (Pomeron–Reggeon–Reggeon vertex). In fact from the dual identities

and from the identity of fig. 2a and fig. 2b, one gets (with $\alpha'_{\mathrm{R}} = 1$): $g_{\mathrm{PR}} \simeq g; g_{\mathrm{PRR}} = g_{\mathrm{P}} \simeq g^2$.

References

[1] For a general review of these models, see, e.g.:
G. Veneziano, Lecture Notes at the Erice Summer School (1970);
V. Alessandrini, D. Amati, M. Le Bellac and D. Olive, Phys. Reports 1 (1971) 269;

P. Di Vecchia and S. Fubini, Lecture Notes at the Erice Summer School (1972);
J.H. Schwarz, Phys. Reports 8C (1973) 270.
[2] D.J. Gross, A. Neveu, J. Scherk and J.H. Schwarz, Phys. Rev. D2 (1970) 697;
C.S. Hsue, B. Sakita and M.A. Virasoro, Phys. Rev. D2 (1970) 2857;
G. Frye and L. Susskind, Phys. Lett. 34B (1970) 589.
[3] C. Lovelace, Phys. Lett. 34B (1970) 500.
[4] L. Brink and D. Oliver, Nucl. Phys. B58 (1973) 237.
[5] E. Cremmer and J. Scherk, Nucl. Phys. B50 (1972) 222.
[6] L. Clavelli and J.A. Shapiro, Rutgers University Preprint (1973).
[7] D. Oliver and J. Scherk, Phys. Lett. 44B (1973) 296.
[8] M.A. Virasoro, Phys. Rev. 177 (1969) 2309;
J.A. Shapiro, Phys. Lett. 33B (1970) 361;
E. Del Giudice and P. Di Vecchia, Nuovo Cimento 5A (1971) 90;
M. Yoshimura, Phys. Lett. 34B (1971) 79.
[9] J.H. Schwarz, Nucl. Phys. B46 (1972) 61;
A. Neveu, Princeton University Preprint (1972).
[10] M. Ademollo, A. D'Adda, R. D'Auria, E. Napolitano, P. Di Vecchia, F. Gliozzi and S. Sciuto, CERN Preprint TH.1832 (1974).
[11] Y. Nambu, Proc. Intern. Conf. on Symmetries and quark models, Wayne State University (1969);
H. Nielsen, XV Intern. Conf. on Higher energy physics, Kiev (1970);
L. Susskind, Nuovo Cimento 69 (1970) 457;
L.N. Chang and J. Mansouri, Phys. Rev. D5 (1972) 2535.
O. Hara, Progr. Theor. Phys. 46 (1971) 1549;
T. Goto, Progr. Theor. Phys. 46 (1971) 1560;
J. Mansouri and Y. Nambu, Phys. Lett. 39B (1972) 357;
P. Goddard, J. Goldstone, C. Rebbi and C. Thorn, Nucl. Phys. 56B (1973) 109.
[12] M. Ademollo et al., CERN Preprint TH.1702 (1973).
[13] P. Campagna, S. Fubini, E. Napolitano and S. Sciuto, Nuovo Cimento 2A (1971) 911.
[14] R. Brower and C. Thorn, Nucl. Phys. B31 (1971) 163.

NARROW BARYONIUM STATES IN QCD

H.G. DOSCH[1] and M.G. SCHMIDT
CERN, Geneva, Switzerland

Received 18 March 1977

The unconventional states of $qq\bar{q}\bar{q}$, $q\bar{q}$ and pure gluon type, appearing in $B\bar{B}$ dual diagrams with nonplanar baryons are discussed, treating their interpolating fields in a confinement approach to QCD due to Migdal. The mass spectrum is given to lowest order and the quantum numbers are discussed. It is argued that some of the resonances should have narrow width and hence could be identified with the narrow resonances in $p\bar{p}$ scattering.

The observation of narrow ($\Gamma \sim 3$–20 MeV) resonances in $B\bar{B}$ scattering [1] has renewed the interest in unconventional meson states. It is an attractive idea that the binding of such states is closely related to that of the baryons [2]. Baryons are expected to be non-planar objects in space time in the (non Abelian) quark-gluon gauge theory of strong interactions (QCD). The three quarks of a baryon are argued to be confined by three strings – realized by gauge gluons – which are coupled together in a central region antisymmetrically in the colour indices. The $1/N_c$ topological expansion [3] ($N_c = 3$ in QCD) breaks down in that central space-time tube as elaborated by Rossi and Veneziano in ref. [4]).

Dual diagrams first introduced as a convenient means to handle group theory, obtain a dynamical interpretation in the string picture. In $B\bar{B}$ scattering with triple string baryons there are then two types [4] of duality diagrams instead of one conventional diagram (the latter one leads to inconsistencies, as is well known) (fig. 1). In graphs 1a and 1b there appear unconventional meson states of type $qq\bar{q}\bar{q}$ and $q\bar{q}$; graph 1c contains a pure glue state.

In this note we present estimates for the mass spectra and quantum numbers of these three new types of states as well as some considerations about their decay properties. This is done by constructing gauge invariant local field operators interpolating these states and treating these operators in an infrared regularization procedure recently proposed by Migdal [5].

The essential idea of this approach is to extract in a unique way a set of particle poles from vacuum expectation values of time-ordered products of gauge invariant local field operators calculated in QCD perturbation theory (in g^2). Confinement, not present in finite order perturbation theory, is enforced by a Padé

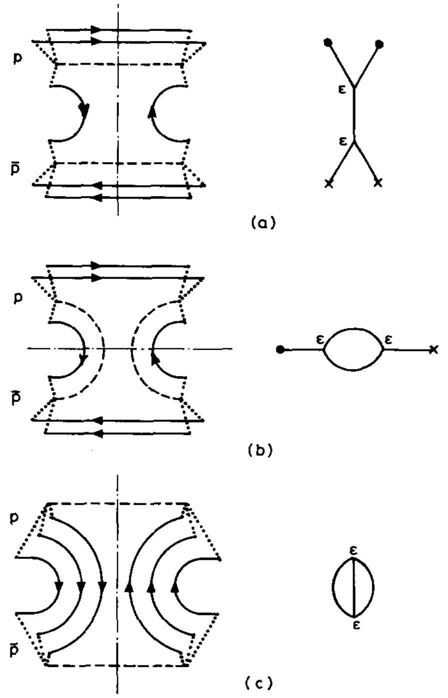

Fig. 1. Dual diagrams for $B\bar{B}$ scattering and string states corresponding to the dot-lined cross-section [M_4^2, M_2^2, M_0^2, respectively in the notation of ref. [4]]. The solid lines in the dual diagram represent quarks, the dashed ones represent nonplanarity lines.

[1] On leave of absence from: Institut f. Theoretische Physik, Universität Heidelberg, Germany.

Table 1

(Γ_1, Γ_2)	SU_3 flavour	$J^P; C_n$	$\Gamma_{M1}\Gamma_{M2}$
(γ^5, γ^5)	$1 \oplus 8$	$1^{\pm}; -$	$(\gamma_5, \gamma_5), (1, \gamma_5), (1, 1), (\gamma^\mu, \gamma^\mu), (\gamma^5\gamma^\mu, \gamma^5\gamma^\mu)$ $(\gamma^5, \gamma^\mu), (1, \gamma^\mu), (\gamma^5, \gamma^5\gamma^\mu), (1, \gamma^5\gamma^\mu)$
$(\gamma^5, \gamma^\mu) + (\gamma^\mu, \gamma^5)$	$8 \oplus (10 + \overline{10})$	$0, 1, 2^{\pm}; +$	$(\gamma^5, \gamma^\mu), (1, \gamma^\mu)$ $(\gamma^5, \gamma^5), (1, \gamma^5), (1, 1), (\gamma^\mu, \gamma^\mu), (\gamma^5\gamma^\mu, \gamma^5\gamma^\mu)$
$(\gamma^5, \gamma^\mu) - (\gamma^\mu, \gamma^5)$	$8 \oplus (10 - \overline{10})$	$0, 1, 2^{\pm}, -$	$(\gamma^5, \gamma^5\gamma^\mu), (1, \gamma^5\gamma^\mu)$ $(\gamma^5, \gamma^5), (1, \gamma^5), (1, 1), (\gamma^\mu, \gamma^\mu), (\gamma^5\gamma^\mu, \gamma^5\gamma^\mu)$
(γ^μ, γ^μ)	$1 \oplus 8 \oplus 27$	$0, 1, 2, 3^{\pm}, -$	as for $(\Gamma_1, \Gamma_2) = (\gamma^5, \gamma^5)$

First column: $\Gamma^{(1)}$ and $\Gamma^{(2)}$ of interpolating fields of type $\phi_1^{(0)}$ (see eqs. (4) and (5)), which are argued to lead to the lowest masses of the $\bar{q}\bar{q}qq$ system.
Second column: SU_3 flavour classification, spin, parity and charge conjugation of the neutral member. Note the parity doubling due to both parities of $F_{\mu\nu}$.
Third column: Matrices Γ_{M1}, Γ_{M2} for which the three-point function $\langle T\,\phi_1^{(0)}\phi_{M1}\phi_{M2}\rangle$ vanishes up to g^2; $\phi_M(x) = N\bar{\psi}(x)\bar{\psi}\Gamma_{Mi}\psi(x)$. For pseudoscalar, scalar, vector and axial vector fields we have $\Gamma_{Mi} = \gamma_5, 1, \gamma^\mu$ and $\gamma^5\gamma^\mu$, respectively.

approximation in the Mandelstam variables, generalized to tensor functions around a point Λ in the deep Euclidean region where asymptotic freedom justifies perturbation theory. The Padé approximants of order (M, N) turn out to have a unique limit for $M, N, \Lambda \to \infty$ if $(MN/\Lambda^2) = R^2$ is kept fixed in a fixed order of perturbation theory. R (a kind of "bag radius") is supposed to be pushed to infinity in higher orders in g^2 if the parameters (R, g^2) are fixed by two experimental masses.

In zeroth order the QCD structure does not enter explicitly, but only as a justification of the method starting from asymptotic freedom. The mass spectrum appearing in the two-point functions of local gauge invariant operators of dimension d is in this approach given by the zeros of the Bessel function

$$J_{d-2}(2RM) = 0. \tag{1}$$

The direct influence of the gluon interaction will be discussed later. The parameter R fitted by Migdal [5] to the meson spectra (in particular the vector-meson trajectories), also gives satisfactory results for the baryon spectra [6] and will be used here to estimate the spectra of the unconventional states.

Examples of local field operators corresponding to the states M_4^2 and M_2^2 of figs. 1a and 1b are:

$$\phi_1(x) = N(\bar{\psi}_{a\kappa}(x)\bar{\psi}_{b\lambda}(x)\overleftrightarrow{\mathcal{D}}_{\mu_1 c}{}^{d_1} \ldots \overleftrightarrow{\mathcal{D}}_{\mu_n d_n}{}^{c'} \times \psi_{\kappa'}^{a'}(x)\psi_{\lambda'}^{b'}(x))\epsilon^{abc}\epsilon_{a'b'c'}\Gamma_{\kappa\lambda;\,\kappa'\lambda'}, \tag{2a}$$

$$\phi_2(x) = N(\bar{\psi}_{a,\kappa}(x)\overleftrightarrow{\mathcal{D}}_{\mu_1 b}{}^{d_1} \ldots \overleftrightarrow{\mathcal{D}}_{\mu_e d_e}{}^{b'}\mathcal{D}_{\mu_{e+1} c}{}^{d_{e+1}} \ldots \ldots \mathcal{D}_{\mu_n d_n}{}^{c'}\psi_{\kappa'}^{a'}(x))\epsilon^{abc}\epsilon_{a'b'c'}\Gamma_{\kappa\kappa'}. \tag{2b}$$

Pure gluon operators have been discussed in ref. [5]. Here κ, λ denote spinor and flavour indices,

$$\mathcal{D}_{\mu c}{}^{c'} = \frac{\partial}{\partial x^\mu}\delta_c{}^{c'} + \mathrm{i}g/2\, A_\mu \lambda_c{}^{c'}, \tag{3}$$

is the covariant derivative.

N indicates normal product and normalization factors. ψ is the quark and A_μ the gauge gluon field. In ϕ_1 and ϕ_2 there is also the possibility to attach covariant derivatives to the spinors before contracting with ϵ (corresponding to string pieces directly connected to the quarks).

A great manifold of the states of type ϕ_1 and ϕ_2 is coupled to zeroth order in g (i.e., by overlap) to the conventional meson states[‡1]. The operators of lowest dimensionality of type ϕ_1 not coupled to zeroth order

[‡1] These states are not supposed to be narrow. Those of type ϕ_1 – starting from

$$N\bar{\psi}_{a\kappa}(x)\bar{\psi}_{b\lambda}(x)\psi_{\kappa'}{}^{a'}(x)\psi_{\lambda'}{}^{b'}(x)\epsilon^{abc}\epsilon_{a'b'c}$$

could be used in order to explain the broad bumps in the T, U region, similar to ref. [2]. Their lowest dimension is $d = 6$ (with maximal spin 2), and hence the T and U region would be reached by the third and fourth recurrence, respectively.

to conventional states[‡2] are

$$\phi_1{}^0(x) = N(\bar{\psi}_{a\kappa}(x)\,\bar{\psi}_{b\lambda}(x)\,F_{\mu\nu}(x)_c{}^{c'} \times \psi_{\kappa'}{}^{a'}(x)\,\psi_{\lambda'}{}^{b'}(x))\,\epsilon^{abc}\epsilon_{a'b'c'}\Gamma_{\kappa\lambda;\kappa'\lambda'}, \tag{4a}$$

and of type ϕ_2

$$\phi_2{}^0(x) = N(\bar{\psi}_{a\kappa}(x)F_{\mu\nu}(x)_b{}^{b'}F_{\rho\sigma}(x)_c{}^{c'} \times \psi_{a'\kappa'}(x))\,\epsilon^{abc}\epsilon_{a'b'c'}\Gamma_{\kappa;\kappa'}. \tag{4b}$$

The gluon field tensors $F_{\mu\nu}$ arise from the antisymmetrization of covariant derivatives (3). For the spinor part of $\Gamma_{\kappa\lambda;\kappa'\lambda'}$ we choose the form (without loss in generality)

$$\Gamma_{\kappa\lambda;\kappa'\lambda'} = \Gamma_{\kappa\lambda}{}^{(1)}C \times C^{\mathrm{T}}\Gamma_{\kappa'\lambda'}{}^{(2)} \tag{5}$$

with the 16 Dirac matrices Γ. The most prominent s wave couplings correspond to $\Gamma^{(i)} = \gamma_5, \gamma_\mu$ (see the table 1).

The simplest pure gluon operator with ϵ–ϵ structure is given by

$$\phi_3{}^0 = F_{\mu\nu}(x)_a{}^{a'}F_{\mu'\nu'}(x)_b{}^{b'}F_{\mu''\nu''}(x)_c{}^{c'}\epsilon_{a'b'c'}\epsilon^{abc}. \tag{4c}$$

With massless quarks, all the states of the same type (4), according to eq. (1) have to 0th order the same mass, determined by the dimensions of $\phi_1^{(0)}$, $\phi_2^{(0)}$ and $\phi_3^{(0)}$, $d_1 = 8, d_2 = 7$ and $d_3 = 6$. The first non-trivial zero of the "Bessel function" yields the masses

$$M_1{}^0 = 1990\,\mathrm{MeV},\ M_2{}^0 = 1760\,\mathrm{MeV},\ M_3{}^0 = 1520\,\mathrm{MeV}. \tag{6}$$

Here we have used $R = 2.500\ \mathrm{GeV}^{-1}$, fitted in ref. [5] in order to give the correct ρ mass (for comparison: the lowest nucleon mass (N, Δ) with this value of R is 1100 MeV, the N–Δ splitting coming out correctly with the gluon corrections). The zeroth order trajectories are given in fig. 2.

The influence of gluon interaction up to order g^2 – for normal mesons [5] and baryons [6] simply to be taken into account by adding in eq. (1) anomalous dimensions of the operators – is more complicated in the case considered here. There are transitions between operators of types and (1) and (2) to order g and also decays into conventional mesons to that order not suppressed in an $1/N_c$ expansion. We hence give only some plausible arguments on the effects of gluon exchange.

‡2 They are, however, coupled to daughters of highly excited planar meson states with $F_{\mu\nu}$ coupling. We do not consider these as conventional.

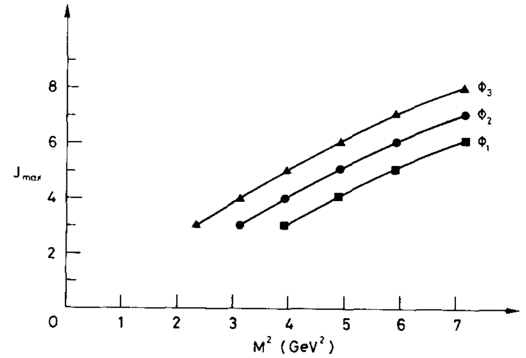

Fig. 2. Trajectories with maximal spin ($J_{\max}$) for unconventional meson states: $qq\bar{q}\bar{q}\,(\phi_1)$, $q\bar{q}\,(\phi_2)$, pure glue (ϕ_3).

(1) The combined self-interaction of the fermions and gluons will decrease d and hence the mass. The anomalous dimension (in Feynman gauge) of the gluon is $\gamma_v = -13/3\ g^2/8\pi^2$; of the fermion $\gamma_F = 2/3\ g^2/8\pi^2$; $g^2/8\pi^2 = 0.31$ fitted in ref. [5] to the ρ trajectory.

(2) Gluon exchange inside the $qq(\bar{q}\bar{q})$ system decreases the dimension most for $\Gamma_4^{(i)} = \gamma^5$, less for γ^μ. This leads to a splitting between a pseudoscalar and vector diquark system of about 100 MeV.

Mass corrections to the quarks make s wave (γ_5, γ_i) diquarks lighter than p wave ($1, \gamma_5\gamma_i$) diquarks. Hence the states listed in table 1 should be the lightest states of type $qq\bar{q}\bar{q}$ (with an increase in mass from above to below).

Since in states of types ϕ_2 and ϕ_3, two and three gluons, respectively, are present, the mass of these states will be lowered considerably due to the large negative anomalous dimension of the gluon.

We now present some arguments on the decay width of these states. In order to calculate these widths in accordance with the regularization scheme of ref. [5] one had to apply the Padé procedure to the N point functions $\langle T\phi_i, \phi_{M1} \dots \phi_{Mn}\rangle$ governing the decay. Here we argue that the three-point functions of some of the fields of type $\phi_1{}^0$ and interpolating fields of the most prominent mesons vanish up to order g^2. This is due to a cancellation of the contribution of the (divergent) diagram 3a with that of b. In the last column of table 1 we indicate the three-point functions which vanish up to order g^2 due to this cancellation

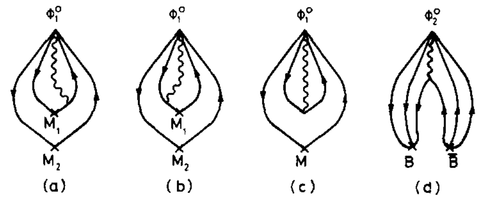

Fig. 3. Diagrams for the n point function of the field $\phi_1^{(0)}$ with (a), (b) two (conventional) meson fields $(M_{(1)}, M_{(2)})$; (c) one meson field; (d) two baryon fields.

or trace identities. Furthermore, by the same argument the 5, 7, ..., point functions of the operators listed in the table with scalar or pseudoscalar fields vanish up to order g^2, thus forbidding to this order, e.g., 4π, 6π ..., decay.

The two point function of $\phi_i^{(0)}$ with conventional meson fields (diagram 3c) vanishes up to order g^2 because of symmetric integration.

The decay (and production) of states corresponding to ϕ_1 in channels with a baryon-antibaryon pair is allowed to order g and hence should compete with mesonic decay modes in spite of the smaller phase space.

By ordering according to g we have assumed this effective coupling constant to be still small, since the soft gluons are taken care of already in the zeroth order calculation of this procedure [5]. Note that the numerical value of R used here is adapted to a calculation up to g^2.

The decay and production amplitude of states corresponding to ϕ_2 and ϕ_3 is of order g^2 and g^3, respectively. In our approach based on low order perturbation theory we do not see the suppression of purely mesonic channels as compared to baryonic ones as proposed in ref. [4].

It is tempting to attribute the observed narrow resonances in the 1900 MeV region to $\phi_1^{(0)}$ type states since – following the above arguments – these are coupled stronger to $B\bar{B}$ than ϕ_2 and ϕ_3 type states and since their mass is also in the range predicted (e.g., eq. (6)). If one also wants to associate the 1795 NN bound state with the $\phi_1^{(0)}$ type one would be urged to identify this state with one of the (γ_5, γ_5) species and the 1935 MeV states with the (γ^μ, γ^μ) species since they both have decay channels suppressed in a similar way. There are enough candidates to have several states in the 1935 MeV region. An analysis of quantum numbers of the states and of their decay channels of course would make an identification according to table 1 much more stringent.

There are also further states of predicted narrow width of ϕ_2 and ϕ_3 type with masses below the $p\bar{p}$ threshold. Altogether there is a vast number of new states which wait for an experimental check. The pure glue state is predicted to have the lowest mass of the baryonium ($\epsilon\epsilon$ type) states. It is supposed to couple weakly only as a resonance in $B\bar{B}$, but this does not imply a weak coupling as a "Regge" trajectory in $B\bar{B}$ scattering according to common ideas about the Zweig rule; and hence the proposal [4] that this type gives the leading Regge trajectory dual to leading three-meson (jet) production is not contradicted.

In our discussion of the lowest baryonium states no arguments about highly excited states on leading straight trajectories corresponding to stretched strings enter. On the contrary, the quarks and gluons seem to sit together as close as possible. Narrow-width effects seem to arise – not from a long straight string but from "string nodes" $F_{\mu\nu}$.

Therefore a determination of the angular momenta would be especially sensitive to the ideas presented here: all the resonances could have small angular momentum (see table 1) without losing their narrow width.

We would like to thank D. Amati, J. Ellis, G. Rossi and G. Veneziano for interesting discussions and comments on the manuscript. One of us (M.G. Schmidt) would like to thank A.A. Migdal for enlightening conversations about his paper.

References

[1] A.S. Carrol et al., Phys. Rev. Lett. 32 (1974) 247;
V. Chaloupka et al., Phys. Lett. 61B (1976) 487;
W. Brückner et al., CERN preprint (1976).

[2] C. Rosenzweig, Phys. Rev. Lett. B6 (1976) 679;
G.F. Chew, preprint LBL-5391.

[3] G. 't Hooft, Nuclear Phys. B72 (1974) 461;
G. Veneziano, Nuclear Phys. B117 (1976) 519.

[4] G.C. Rossi and G. Veneziano, CERN preprint, TH 2287;
M. Imadin, S. Otsuki and F. Toyoda, Prog. Theor. Phys. 55 (1976) 551; 57 (1977) 517.

[5] A.A. Migdal, Chernogolovka preprint (1976).

[6] H.G. Dosch and M.G. Schmidt, in preparation.

INCORPORATION OF BARYONS INTO THE TOPOLOGICAL EXPANSION★

F.J. CAPRA[1]

Lawrence Berkeley Laboratory, University of California, Berkeley, California 94720, USA

Received 16 February 1977

Veneziano's topological expansion is extended to duality diagrams involving mesons and baryons.

Veneziano [1] has proposed a unitarization scheme for planar dual models, known as the topological expansion, which is based on the parameter $1/N$, where N is the number of flavors in the model, and is related to the topology of duality diagrams in such a way that each order of the expansion contains diagrams with the same topological structure. In this scheme, planar diagrams are defined as diagrams that can be drawn on a plane without any quark lines crossing each other. Higher-order diagrams can be drawn in the same way on closed surfaces of increasing genus, or number of handles. All meson diagrams can be associated with oriented bordered surfaces embedded in these closed surfaces, and can be classified by the number of their boundaries b (lines to which the external mesons are attached) and the genus h of the embedding surface [2,3]. In this note, we extend Veneziano's scheme, which was formulated only for mesons, to include diagrams involving mesons and baryons. This treatment is a variation of a scheme proposed by Stapp [4] but is a closer to the conventional representation of baryons in dual diagrams. It also differs from Stapp's treatment in the way it deals with baryon loops.

Baryons have to be represented by three quark lines going in the same direction in a symmetric way, so that none of them occupies a special position. This can be done by drawing the quark lines on a cylinder, or sphere. Thus we shall represent a baryon as shown in fig. 1, where dotted quark lines are understood to run on the back of the cylinder. The cylinder axis has a definite direction and represents the flow of baryon number. We shall call it the baryon axis.

★ Participating guest: Lawrence Berkeley Laboratory.

[1] This work was done under the auspices of the Division of Physical Research of the Energy Research and Development Administration.

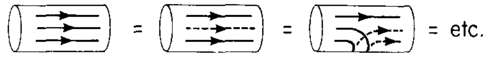

Fig. 1. Quark lines of a baryon embedded in a cylinder.

The cylinder or sphere, then, is the minimal embedding surface suitable for diagrams involving baryons. All such diagrams which can be drawn on a sphere shall be called planar. Mesons can be connected with any of the three quark lines making up a baryon, e.g., as shown in fig. 2.

In order to classify duality diagrams according to their topological structure, we have to associate them with oriented surfaces. Such an association is not obvious for diagrams involving baryons because of the fact that the three quark lines making up a baryon run in the same direction. Stapp [4] has proposed the image of a baryon as an arrow with three feathers attached to it, each of them representing an oriented surface, and he has given a prescription of how to "cap" these three strips so that they form a single oriented surface. Drawing the three quark lines on a sphere, we do not need Stapp's arrow image and capping prescription but simply close the quark lines on themselves to obtain the same oriented surface. This is shown in fig. 3 where the shaded part of the sphere is the oriented bordered surface associated with the baryon. We shall interpret the closed quark lines of a baryon in such a way that only the parts running in the direction of the baryon axis carry flavor. The lines running against the baryon axis do not carry flavor and shall be called dead lines. They serve merely to identify the topology of the diagram and do not seem to play any further role. In

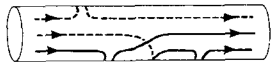

Fig. 2. Mesons coupled to different baryon quark lines.

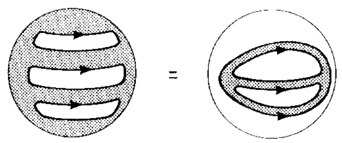

Fig. 3. Two equivalent representations of the oriented bordered surface (shaded) associated with a baryon.

fact, we shall never need to draw dead lines explicitly when we study duality diagrams.

Associating baryons with oriented bordered surfaces in this way, we see that each quark line in a baryon is part of a separate boundary component which can be linked to the boundary components of other baryons through meson connections. It will be interesting to assume that the boundary components of a baryon cannot be linked to each other. In such a theory, the three quark lines in a baryon have separate identities, not connected with their flavors. This new concept of quark-line identity, which can be best illustrated graphically by using colors but should not be confused with the color concept of quantum chromodynamics, promises to have interesting physical consequences. Details will be given in a forthcoming paper.

The number of handles of a meson diagram can be written

$$2h = \tfrac{1}{2}(v - n_{\mathrm{M}}) - k + 2, \tag{1}$$

where v is the number of vertices, n_{M} the number of external mesons, and k the number of boundary components ("boundaries" and "windows") of the bordered surface. Associating baryons with oriented bordered surfaces in the way outlined above, we see that each baryon axis becomes associated with two "vertices". The generalization of eq. (1) to diagrams including baryons thus can be written

$$2h = \tfrac{1}{2}(v - n_{\mathrm{M}}) + B - k + 2, \tag{2}$$

where v is the number of (meson-meson and meson-baryon) vertices and B is the number of baryon axes.

Diagrams containing baryon loops need special consideration because the quark lines in a baryon loop are closed lines and thus have no ends which can be connected through a dead line. Our procedure for associating a baryon with a single oriented surface is thus not immediately applicable to baryon loops. However, the quark lines of external baryons really do not have any ends either because each diagram should be considered as part of a larger process to which it is connected by its external lines. The association of baryons with oriented surfaces, although extremely useful, is therefore somewhat artificial. It does not seem any more artificial to associate a baryon loop with an oriented surface in a similar way by cutting through the three quark lines anywhere around the loop and closing each quark line on itself through a dead line as before. Since we shall never need to draw dead quark lines, we shall never have to exhibit the cut through a baryon loop either.

With this understanding, eq. (2) is applicable also to diagrams containing baryon loops. The number of handles of a diagram containing one baryon loop and an arbitrary number of external mesons is given by

$$2h = 3 - k. \tag{3}$$

Diagrams with $k = 3$ are planar, but diagrams with $k = 1$ seem to have one handle. The diagram shown in fig. 4, for example, can indeed be embedded in a torus. However, diagrams of this kind are forbidden by our assumption that the boundary components of a baryon cannot be interconnected. In a theory with separate quark-line identities, therefore, all baryon loops are planar.

In the $1/N$ expansion, the order of a particular diagram is obtained by counting powers of the coupling constant g. In the meson case, a contribution to the n-point function exhibiting b boundaries (boundary components with external mesons attached to them) and w windows (boundary components with no external lines attached to them) depends on g and N in the following way [1]

$$A_n \sim g^{n-2}\,(g^2)^{b+2h-1}(g^2N)^w. \tag{4}$$

The extension of eq. (4) to diagrams with n_{M} external mesons and n_{b} external baryons reads

$$A_n \sim g^{n_{\mathrm{M}}-n_{\mathrm{B}}-2}\,(g^2)^{b+2h-1-l_{\mathrm{B}}}\,(g^2N)^w \tag{5}$$

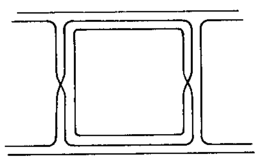

Fig. 4. A forbidden diagram interconnecting the boundary components of a baryon loop.

where l_B is the number of baryon loops. Baryon loops will be enhanced by a factor N with respect to meson loops because of the extra quark line in the loop. This enhancement can be suppressed by suppressing the factor $(g^2)^{-l_B}$ in eq. (5). Although such a suppression of baryon loops is desirable for defining a planar bootstrap similar to the meson case, we see at present no physical reason for it.

I am indebted to Professor G.F. Chew and to Dr. H.P. Stapp for stimulating discussions.

References

[1] G. Veneziano, Nucl. Phys. B74 (1974) 365; Phys. Lett. 52B (1974) 220.
[2] K. Ciafaloni, G. Marchesini and G. Veneziano, Nucl. Phys. B98 (1975) 472, 493.
[3] F.J. Capra, Lawrence Berkeley Laboratory Preprint LBL-4295 (1975).
[4] H.P. Stapp, Lawrence Berkeley Laboratory Preprint LBL-6118 (1977).

EXPERIMENTAL COMPARISON OF J/ψ PRODUCTION BY $\pi^{\pm}$, $K^{\pm}$, p AND $\bar{p}$ BEAMS AT 39.5 GeV/c

M.J. CORDEN, J.D. DOWELL, D. EASTWOOD, J. GARVEY, R.J. HOMER, M. JOBES, I.R. KENYON, T. McMAHON, R.J. VALLANCE, P.M. WATKINS, J.A. WILSON
Birmingham University, Birmingham, UK

J. GAGO[1], M. JUNG[2], P. SONDEREGGER, D. TREILLE, P.L. WOODWORTH
CERN, European Organization for Nuclear Research, Geneva, Switzerland

V. ECKARDT, J. FENT, K. PRETZL, P. SEYBOTH, J. SEYERLEIN
Max Planck Institut für Physik und Astrophysik, München, Germany

D. PERRIN
University of Neuchâtel, Neuchâtel, Switzerland

B. CHAURAND, G. De ROSNY, L. FLURI, A. ROMANA, R. SALMERON, A. WIJANGCO
Ecole Polytechnique, Palaiseau, France

and

K.C.T.O. SUMOROK
Rutherford Laboratory, Oxfordshire, UK

Received 20 April 1977

Measurements have been made of relative production cross sections of the J/ψ by $\pi^{\pm}$, $K^{\pm}$, p and $\bar{p}$ at 39.5 GeV/c incident on copper. J/ψ production rates from π^-, K^- and $\bar{p}$ are similar. The J/ψ relative particle/anti-particle production cross sections for $x > 0$ are $\sigma(\pi^+)/\sigma(\pi^-) = (0.87 \pm 0.14)$, $\sigma(K^+)/\sigma(K^-) = (0.85 \pm 0.5)$ and $\sigma(p)/\sigma(\bar{p}) = (0.15 \pm 0.08)$. The small p/$\bar{p}$ cross section ratio disagrees with models of J/ψ production by gluon amalgamation.

There has been considerable speculation as to the production mechanism of the J/ψ(3100) in hadronic interactions [1–4]. Large differences should exist between the proton and anti-proton induced cross sections if valence quark annihilation contributes significantly to J/ψ production. Clear differences have been observed between J/ψ production with pion and proton beams both in cross sections and in the distributions of the produced J/ψ in the Feynman x variable [5–9].

The aim of the experiment reported here was to measure J/ψ production by $\pi^{\pm}$, $K^{\pm}$, p and $\bar{p}$ beam particles in the same large acceptance apparatus. The production of the J/ψ decaying into $\mu^+\mu^-$ was measured at 39.5 GeV/c using both negative and positive unseparated beams from the CERN SPS incident on a copper target located in the Omega spectrometer [10]. Production of J/ψ was observed with all six beam particles ($\pi^{\pm}$, $K^{\pm}$, p and $\bar{p}$) and relative cross sections have been obtained for J/ψ production for $x > 0$ using the Feynman x variable $x = 2P_L^*/\sqrt{s}$ where p_L^* is the centre of mass longitudinal momentum of the muon pair, and $\sqrt{s}$ is the centre of mass energy.

The apparatus, shown schematically in fig. 1, was designed to detect muon pairs with high efficiency for $x > 0$. Three threshold Cerenkov counters were used to identify incident beam particles. Scintillation counters S1–S4 defined the incident beam with V2 and V4

[1] On leave from the I.S.T., University of Lisbon, Lisbon, Portugal.
[2] On leave from Bonn University, Bonn, Germany.

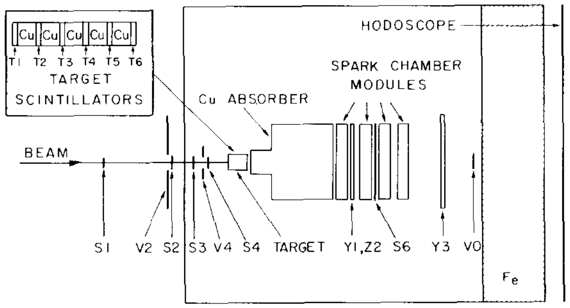

Fig. 1. Schematic layout of the apparatus.

providing protection against beam tails and halo muons. The target consisted of five 4 cm thick copper slabs interleaved with scintillation counters T1–T6. Pulse height information was recorded from all Cerenkov, beam and target counters. A 1.46 m thick copper absorber immediately after the target reduced the hadron flux by a factor of thirty. Particles emerging from the absorber were detected with a four-element scintillation counter hodoscope, S6, 1.5 m wide and 1.0 m high. A small counter, V0, was used to veto beam muons. There were three planes of multiwire proportional chambers (Y1, Z2 and Y3 with vertical, horizontal and vertical wires respectively) which were used to provide a particle multiplicity requirement and to reduce $\mu^+\mu^-$ pairs of masses below 1.4 GeV/c^2. Particle trajectories were recorded with a TV readout of forty optical spark chamber gaps, in a region of 1.7 T average magnetic induction. Particles leaving the chamber system passed into the 1.25 m thick iron return yoke of the magnet which acted as a second hadron absorber before a final counter hodoscope of sixty elements covering an area 6 m wide and 3.8 m high.

The spark chambers were triggered when the following conditions were satisfied:

(a) a single incident beam hadron (defined by $S1 \cdot S2 \cdot S3 \cdot S4 \cdot \overline{V0} \cdot \overline{V2} \cdot \overline{V4}$) was present with no other beam particle within ±20 nsec;

(b) the final counter of the target (T6) had a pulse height greater than 1.3 times that of an average single particle;

(c) a signal was present from S6 (this was used in strobing the multiwire chambers);

(d) signals were present from two non-adjacent elements in the final hodoscope situated downstream of the magnet return yoke;

(e) there was a multiplicity of two or three in the multiwire planes Y1 and Z2;

(f) for incident pions only, and if the multiplicity was two, triggers from low mass muon pairs were effectively reduced by requiring either a vertical separation between hits in multiwire chamber Z2 larger than 30 cm, or an appropriate correlation between the horizontal separations (ΔY1, ΔY3) of hits in multiwire planes Y1 and Y3.

In a twenty day run 445, 000 triggers were recorded with negative beam and 201, 000 with positive beam. The beam intensity was limited to 3×10^6 in an effective spill of 300 ms. The trigger rate was 10 per burst. Beam fractions were 93.9% π^-, 3.4% K^-, 2.7% $\bar{p}$; and 72.2% π^+, 3.7% K^+ and 24.1% p. The total amounts of gated negative and positive beam were 4.0×10^{10} and 1.4×10^{10} respectively.

All triggers were processed through a modified version of the offline pattern recognition and geometric reconstruction program ROMEO [11]. The single spark resolution was 500 μm in space and the efficiency for reconstructing muon tracks exceeded 95%. In order to locate the vertex of the interaction to within a target element, the program used the pulse heights from counters T1 to T6. The resulting distribution of interactions through the target was consistent with the known cross sections in copper. Each track reconstructed in the spark chambers was extrapolated back to the appropriate target element centre plane taking into account the energy losses.

The track was discarded if its displacement from the beam axis was inconsistent with multiple scattering errors. The correlation between mean angular and position displacements arising from multiple scattering was used to reduce the average errors on the angles of the extrapolated tracks. This procedure reduced the error on the muon pair effective mass by a factor of 1.6 and yielded a J/ψ width consistent with the Monte Carlo estimate of 0.35 GeV/c^2.

The negative and positive beam data yielded 2009 and 418 events respectively containing a $\mu^+\mu^-$ pair with effective mass above 1.6 GeV/c^2 and satisfying the following criteria:

(a) both tracks come from a common vertex as described earlier and have associated hits in the final hodoscope;

(b) the momentum of each muon was less than 30 GeV/c and the sum of the two momenta did not ex-

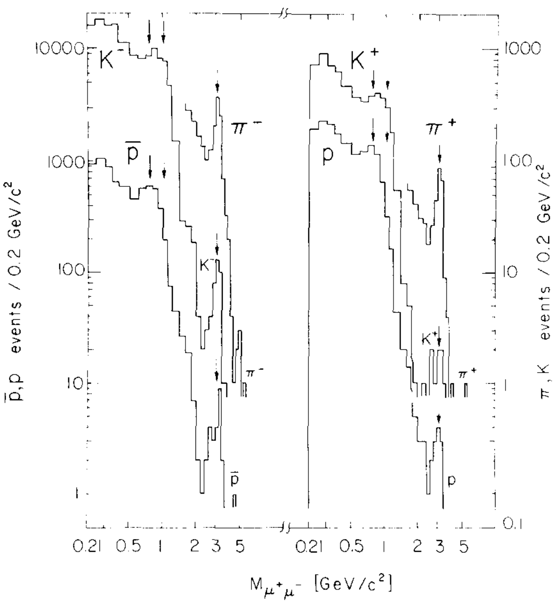

Fig. 2. Observed $\mu^+\mu^-$ effective mass spectra from $\pi^\pm$, $K^\pm$, p and $\bar{p}$ beams. The $\pi^\pm$ data are depressed at low masses by the trigger and are shown above 1.6 GeV/c^2 only. Arrows denote the masses of the ρ, ϕ and ψ mesons. For ease of display, different scales are used for nucleon and meson induced events.

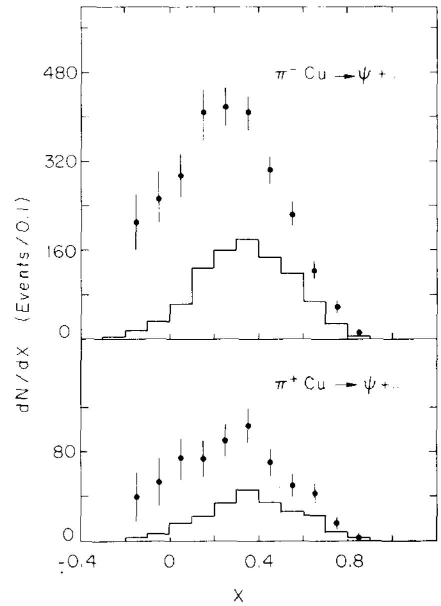

Fig. 3. dN/dx distributions for $\mu^+\mu^-$ pairs of effective mass $2.7 < M\mu\mu < 3.5$ GeV/c^2 (a) for π^- beam (b) for π^+ beam. The histograms show the raw data. The points, with statistical errors only, represent the data corrected for acceptance.

ceed the beam momentum within measurement errors;

(c) the reconstructed track length in the spark chambers was greater than 20 cm for each track.

The $\mu^+\mu^-$ mass spectra produced by π^- and π^+ beams shown in fig. 2 exhibit clear J/ψ signals with masses 3.12 and 3.15 GeV/c^2 and FWHM's 0.43 GeV/c^2 and 0.36 GeV/c^2 respectively. We can put an upper limit on ψ' production and decay to $\mu^+\mu^-$ of 4% of the J/ψ rate and we ignore it hereafter. With the above criteria there are 8 and 2 like sign muon pairs in the mass range 2.7–3.5 GeV/c^2 for negative and positive beam, roughly 1% of the respective J/ψ signals. In figs. 3(a) and (b) we display the dN/dx distribution of $\mu^+\mu^-$ events in the J/ψ region ($2.7 < M\mu\mu < 3.5$ GeV/c^2) for π^- and π^+ beams respectively. The data points are corrected for acceptance assuming that J/ψ production is unpolarized. Fig. 4 shows the distributions of dN/dp_T^2 for $x > 0$ and the same mass range. These are well fitted by the form $Ae^{-Bp_T^2}$ where $B = (1.3 \pm 0.1)$ and (1.5 ± 0.2) (GeV/c)$^{-2}$ for π^- and π^+ induced J/ψ's respectively. In a previous experiment with a π^- beam at 43 GeV/c [8], a similar slope B of

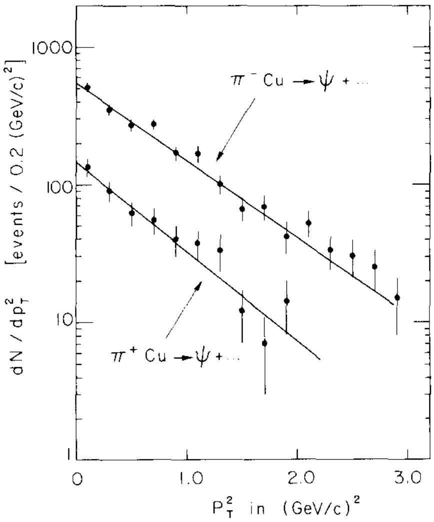

Fig. 4. dN/dp_T^2 distributions of $\mu^+\mu^-$ pairs of effective mass $2.7 < M\mu\mu < 3.5$ GeV/c^2 and $x > 0$ for π^- and π^+ incident beam after correction for acceptance. The fits are of the form $Ae^{-Bp_T^2}$ in the range $0 < p_T^2 < 2.0$ (GeV/c)^2.

Table 1 (as explained in the text).

		π^-	π^+	K^-	K^+	$\bar{p}$	p
(a) Number of events in J/ψ region for $x > 0$		700 ± 42	179 ± 16	30	7	22	10
Number of events in J/ψ region for $x > 0$ weighted for acceptance		1850 ± 140	434 ± 44	73	24	65	29
Number of events in J/ψ region for $0.4 > x > 0$		471 ± 30	108 ± 14	19	6	19	7
Number of events in J/ψ region for $0.4 > x > 0$ weighted for acceptance		1322 ± 106	297 ± 33	50	22	58	24
(b) J/ψ signal $x > 0$	Method 1			73 ± 13	24 ± 9	65 ± 14	29 ± 9
	Method 2			58 ± 16	17 ± 11	53 ± 16	27 ± 10
(c) J/ψ cross section relative to that for π^- beam for $x > 0$	Method 1	1	0.87 ± 0.14	1.1 ± 0.2	1.0 ± 0.4	1.1 ± 0.2	0.16 ± 0.05
	Method 2			0.9 ± 0.2	0.7 ± 0.5	0.9 ± 0.3	0.14 ± 0.05
(d) Particle/antiparticle ratio for J/ψ for $x > 0$	Method 1	0.87 ± 0.14		0.9 ± 0.4		0.15 ± 0.06	
	Method 2			0.8 ± 0.5		0.16 ± 0.08	

$(1.7 \pm 0.4)\ (\mathrm{GeV}/c)^{-2}$ was found, while substantially lower values have been obtained with pion beams at higher energies [12].

The mass distributions for $\mu^+\mu^-$ pairs produced by K^-, K^+, $\bar{p}$ and p are also shown in fig. 2. All exhibit clear enhancements at the J/ψ mass. Strong signals from $\rho/\omega \to \mu\mu$ and, for $K^\pm$ beams only, shoulders from $\phi \to \mu\mu$ signals can also be seen. Every event appearing in fig. 2 with muon pair mass above 2.4 GeV/c^2 has been examined carefully for any inconsistencies in the data such as disagreement between Cerenkov pulse height information and discriminator responses.

Table 1a shows the number of events with $x > 0$ (and for the restricted range $0 < x < 0.4$) unweighted and weighted for acceptance in the range $2.7 < M\mu\mu < 3.5$ GeV/c^2 produced by each minority beam particle. The numbers for $\pi^\pm$ for $x > 0$ were extracted from Gaussian plus background fits to their unweighted and weighted mass spectra. We have estimated the number of J/ψ produced by each minority beam particle for $x > 0$ in two ways. The first method assumes that all events with $2.7 < M\mu\mu < 3.5$ GeV/c^2 are J/ψ and gives an upper limit; the second method assumes a linear background under the J/ψ using the sidebands $2.3 < M\mu\mu < 2.7$ GeV/c^2 and $3.5 < M\mu\mu < 3.9$ GeV/c^2 and yields a lower limit. The signals obtained from the weighted data by each method for $x > 0$ are shown in table 1b. The errors quoted are statistical only. In order to convert these numbers to relative cross sections we have used the integrated beam fluxes and compositions quoted above and a ±10% relative normalisation error. Table 1c shows the cross sections for J/ψ production relative to that for π^- beam after allowing for a small difference in absorption length in copper for each incident particle. Finally, table 1d shows the same result expressed as particle/anti-particle ratios. If the mass dependence of the background above 2.3 GeV/c^2 were widely different between particles and antiparticles the quoted errors would increase.

We obtain an estimate for the absolute cross section for π^- induced J/ψ production with $x > 0$ of 910 ± 190 nb/copper nucleus. Assuming a linear A dependence this corresponds to 14 ± 3 nb/nucleon. This is consistent with the value obtained by Antipov et al. [8].

To summarise, we have found that for J/ψ production on copper at 39.5 GeV/c beam momentum for $x > 0$:

$$\sigma(\pi^-) : \sigma(K^-) : \sigma(\bar{p}) = 1 : 1.0 \pm 0.3 : 1.0 \pm 0.3 .$$

Rough equality between these cross sections is expected in quark annihilation models [1, 2]. The particle/antiparticle ratios are again for $x > 0$:

$\sigma(\pi^+)/\sigma(\pi^-) = 0.87 \pm 0.14$,

$\sigma(K^+)/\sigma(K^-) = 0.85 \pm 0.50$, and

$\sigma(p)/\sigma(\bar{p}) = 0.15 \pm 0.08$.

This first measurement of the $p/\bar{p}$ ratio is particularly interesting as it is predicted to be widely different in different models. In the quark annihilation model of Donnachie and Landshoff [1] the $\bar{p}$ induced production of J/ψ is enhanced over the p induced production at our relatively low beam momentum by the large valence quark contribution. Our ratios are consistent with their predictions. Fritzsch [3] in a similar calculation which neglects the contribution of charmed quarks in the sea obtains a very small $p/\bar{p}$ ratio for small x. Ellis, Einhorn and Quigg [4] have discussed the J/ψ production ratios for hadrons and their antiparticles arising from gluon amalgamation and predict each ratio to be unity. This is in clear disagreement with our $p/\bar{p}$ ratio.

We thank the SPS crew for their extra efforts at the beginning of the machine operation, the EA and EP mechanics groups, and the staff of the Omega Spectrometer. We thank also Dornach Metallwerk AG of Dornach, Switzerland, for lending us the copper for the absorber.

References

[1] A. Donnachie and P.V. Landshoff, Nucl. Phys. B112 (1976) 233, also private communication.
[2] D. Sivers, Nucl. Phys. B106 (1976) 95, also private communication.
[3] H. Fritzsch, Calt 68-582 (Jan. 1977).
[4] S.D. Ellis, M.B. Einhorn and C. Quigg, Phys. Rev. Lett. 36 (1976) 1263.
[5] K.J. Anderson et al., Phys. Rev. Lett. 36 (1976) 237.
[6] K.J. Anderson et al., Production of the J(3.1) and $\psi'(3.7)$ by 225 GeV π^+, π^- and protons, submitted to the Tbilisi Conference, 1976.
[7] G.J. Blanar et al., Phys. Rev. Lett. 35 (1975) 346.
[8] Yu.M. Antipov et al., Dimuon production by 43 GeV/c negative particles, Tbilisi-Moscow preprint.
[9] Yu.M. Antipov et al., Phys. Lett. 60B (1976) 309.
[10] O. Gildemeister, Intern. Conf. on Instrumentation for high energy physics, Frascati, 1973.
[11] F. Bourgeois, H. Grote and J.-C. Lassalle, Pattern recognition methods for omega and SFM spark chamber experiments, CERN/DD/DH/70-1;
H. Grote, M. Hansroul, J.-C. Lassalle and P. Zanella, Identification of digitized particle trajectories, International Computing Symposium, 1973 (North-Holland, 1974).
[12] D. Hitlin, SLAC-PUB-1869 (1977).

THE CROSS-SECTION FOR J/ψ PRODUCTION IN PROTON-PROTON COLLISIONS AT CENTRE-OF-MASS ENERGIES BETWEEN 23 AND 63 GeV

J.H. COBB, S. IWATA[1], R.B. PALMER, D.C. RAHM, I. STUMER
Brookhaven National Laboratory[2], Upton, New York, USA

C.W. FABJAN, I. MANNELLI[3], K. NAKAMURA[4], A. NAPPI[3], W. STRUCZINSKI[5], W.J. WILLIS
CERN, Geneva, Switzerland

M. GOLDBERG, N. HORWITZ, G.C. MONETI
Syracuse University[6], Syracuse, New York, USA

and

C. KOURKOUMELIS, A.J. LANKFORD, P. REHAK[7]
Yale University, New Haven, Connecticut, USA

Received 7 February 1977

The cross-section for J/ψ production in proton-proton collisions has been measured as a function of centre-of-mass energy at the CERN Intersecting Storage Rings by observing its decay into electron-positron pairs. This cross-section is found to rise by a factor of about six over the full centre-of-mass energy range from $\sqrt{s} = 23$ to $\sqrt{s} = 63$ GeV. Electrons resulting from this decay were identified by the use of liquid argon calorimeters and lithium foil transition radiators. Measurements of the energies of the electrons were obtained from the liquid argon calorimeters.

We have measured the cross-section times branching ratio for the production of the J/ψ and its decay into electron-positron pairs over the full range of centre-of-mass energies available at the ISR and find that it rises by a factor of about six between $\sqrt{s} = 23$ and $\sqrt{s} = 63$ GeV.

The apparatus used is shown in fig. 1. The J/ψ was observed by its decay into electron-positron pairs. The energies [‡1] of the two electrons were measured in the segmented lead-liquid argon calorimeters [1] which also provided discrimination against hadron background. Additional electron-hadron discrimination was obtained by detecting, in xenon-filled proportional wire chambers [2], the transition radiation photons generated by the passage of the electrons through thin lithium foils. Cylindrical proportional wire chambers situated just outside the ISR vacuum chambers were used in order to reject electron pairs originating from photon conversions within the apparatus. Ionization-loss measurements made with two planes of scintillation counter hodoscopes allowed the elimination of Dalitz pairs, electron pairs originating from photon conversions in the vacuum chamber wall, and slow, heavily ionizing particles.

Two triggers were used concurrently to select events of interest. One, the "high-high" trigger, required that, in at least two of the four models [‡2] of the experiment, there appeared sufficiently energetic

[1] Permanent address: Nagoya University, Nagoya, Japan.
[2] Research under the auspices of ERDA.
[3] On leave of absence from the University of Pisa and INFN Sezione di Pisa, Italy.
[4] Permanent address: University of Tokyo, Tokyo, Japan.
[5] Now at: Phys. Inst. T.H. Aachen, Aachen, Germany.
[6] Work supported by the National Science Foundation.
[7] Now at: Brookhaven National Laboratory, Upton, NY, USA.
[‡1] The energy scale is linear, and the scale is established such that the masses of the π^0 and η are correct.

[‡2] At times some modules were not active. Subseuqnet calculations of geometric efficiencies have taken this into account.

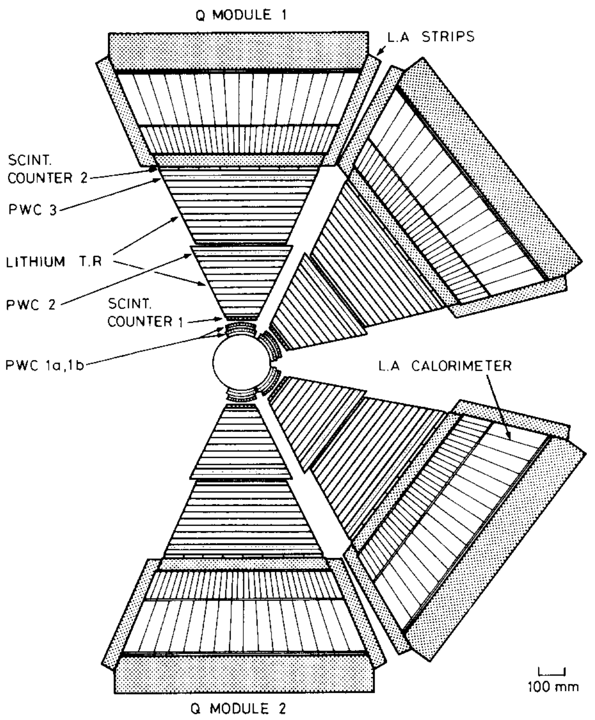

Fig. 1. Vertical section of the apparatus transverse to the proton beams.

electromagnetic showers defined by simultaneous thresholds on the energy deposited in localized regions of the first 3.5 and the next 3 radiation lengths of the lead plate-liquid argon ion chambers. These thresholds were determined by the requirement that the trigger rate be acceptably low and, as a consequence, were such that the J/ψ was not recorded with full efficiency. The other trigger, "double-correlation", had considerably lower energy thresholds but required that a charged track was detected in the scintillation counter hodoscopes and second xenon chamber in spatial coincidence with the electromagnetic shower in the calorimeter. For the data reported herein these geometrical constraints were, however, such that again the J/ψ events were not recorded with maximum efficiency. The causes of inefficiences were quite different for the two triggers, but since the trigger conditions were recorded it was known for each event which trigger condition had been satisfied. Hence it was possible to use each trigger to determine the efficiency of the other. The combined trigger efficiency was about 50% at the J/ψ mass rising to 90% at high masses.

The segmentation of the liquid argon detectors into 20 mm wide strips running in three different directions allowed an unambiguous reconstruction of showers to be made. Four additional space points were measured for each charged track, two in the cylindrical proportional chambers and two in the xenon chambers. All of these used charge-division read-out to give the coordinate in the direction parallel to the beams.

Background to the true two-electron signal arises from hadrons interacting in the calorimeter, hadron tracks overlapping in the calorimeter with the electromagnetic showers of photons, and electrons originating from low-mass electron pairs. The trigger requirements and the calorimeter shower reconstruction procedure required that the longitudinal and radial distributions of deposited energy were characteristic of an electromagnetic shower and thus substantially reduced these backgrounds. In addition, the following requirements were imposed before a track was accepted as being an electron:

(a) that the pulse height measured in the scintillator hodoscopes was less than 1.6 times that of a minimum ionizing particle;

(b) that the transition radiation signal observed in the xenon chambers exceeded a threshold value (which was chosen such as to have an acceptance for electrons independent of their energy);

(c) that, when associated with an electron candidate, no other shower gave an effective mass consistent with that of the π^0, and

(d) that the electromagnetic shower lay in a certain, slightly restricted, fiducial volume of the calorimeter.

The selection of these requirements for background rejection was guided by exposures of a complete detector module to test beams of known particles, which also allowed the electron detection efficiency to be determined. It was subsequently found that when any of the above requirements was released the J/ψ signal could still be observed and thereby it was possible to estimate the efficiency of each one using the actual data sample. The results of these two estimations were in satisfactory agreement. The greatest loss of real events was caused by the restriction on the scintillation counter pulse height but it was the most essential for eliminating background.

The efficiency of our reconstruction procedure was

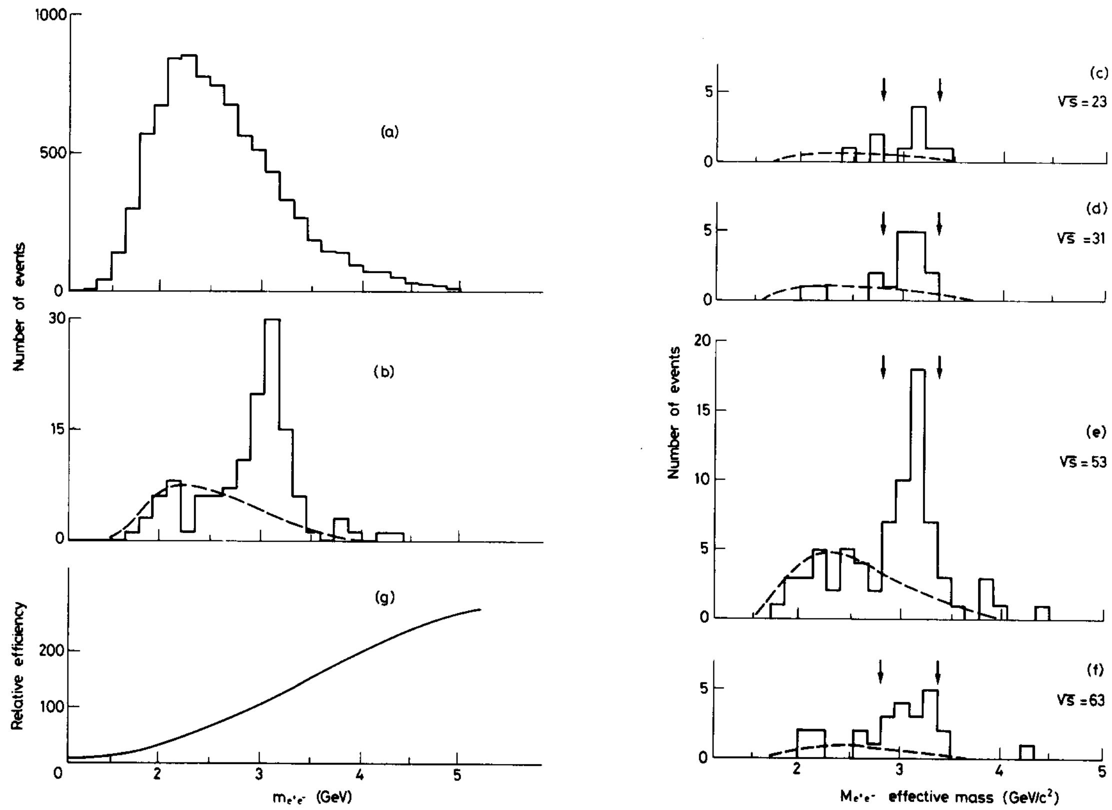

Fig. 2. Distribution of effective masses of double electron candidates: (a) All. (b) After applying the requirements described in the text, then (c) to (f) separated according to $\sqrt{s}$. (g) relative efficiency of the apparatus as a function of m_{ee}.

determined from a study of cosmic-ray muons and from inspection of event displays.

Fig. 2a shows the distribution of the effective masses of pairs of electron candidates without the application of any of the above requirements (a, b, c, d). There is no sign of a J/ψ peak. Figs. 2b to 2f show the mass distributions after these requirements have been made, for the total sample and for the samples at each centre-of-mass energy. There are clear J/ψ peaks with relatively iittle background. The observed r.m.s. width of the J/ψ, 7.4%, is equal to that expected from test beam calibration of the calorimeter. Two methods were employed to study the background. One method was based on the assumption that, with the above cuts, the single electron candidates were almost entirely composed of background (which we found to be true by comparison with the known single electron rates). Pairs of unrelated single electrons were combined to give a simulated electron pair mass spectrum. The other method was to use the shape of the distribution shown in fig. 2a and to normalize it to the low mass region of the final mass spectrum shown in fig. 2b. The results of these calculations agreed to within 20% implying that the background arises predominantly from uncorrelated pairs of misidentified particles. The second method was used for the background subtraction for the J/ψ cross-section.

The geometric and trigger acceptance of the apparatus for the J/ψ as a function of transverse momentum, p_T, and rapidity, y, was evaluated by means of a Monte Carlo program, assuming an isotropic decay. Comparing the distribution of observed events with the results of this calculation we find that the y-distribution is consistent with a constant value in the range $-0.65 \leqslant y \leqslant +65$. Then, assuming this distribution to be flat, the acceptance was integrated over y and used to correct the data as a function of p_T. It was found that $\langle p_T \rangle = 0.94 \pm 0.18$ GeV/c and that the data could

Table 1
Numbers of events, integrated luminosities and J/ψ cross-section divided according to $\sqrt{s}$.

$\sqrt{s}$ (GeV)	23	31	53	63
L (10^{36} cm^{-2})	0.8	1.4	2.1	0.4
Number of events	6	13	42	15
$B \times \frac{d\sigma}{dy}\Big\|_{y=0}$ (10^{-33} cm^2)	5.9	8.4	16.6	31.9
Statistical error (10^{-33} cm^2)	±2.4	±2.3	±2.6	±8.2
Absolute error (10^{-33} cm^2)	±3.9	±5.0	±9.2	±18.8

be described by the form:

$$\frac{d\sigma}{dp_T^2} \propto e^{-bp_T}, \tag{1}$$

with $b = 2.1 \pm 0.4$.

The final acceptance calculation was performed using this distribution and the result is shown in fig.2g as a function of electron pair effective mass. The numbers of events between 2.75 and 3.45 GeV/c^2 were taken as the raw J/ψ signals and are given in table 1, together with the integrated luminosities and cross-sections derived after background subtraction ‡3. In addition to the statistical error, which is sufficient for comparing the cross-sections at the different centre-of-mass energies – because the over-all efficiency should be substantially independent of $\sqrt{s}$ – there is a scale error of a factor of about two which should be borne in mind when comparing these results with those of other experiments.

Fig. 3 shows our results with the statistical errors only (the scale error being shown on the figure) together with a compilation of previous results [3] ‡4. The over-all agreement, in particular with the rather well determined values at Fermilab energies, is satisfactory. This newly demonstrated rise of the J/ψ production cross-section, which amounts to a factor of $5.41^{+5.0}_{-1.8}$ over the range of $\sqrt{s}$ covered by our experiment, agrees with the predictions of various theoretical models, in particular with that of the quark-antiquark fusion model of Donnachie and Landshoff [4], and in this framework provides a useful check of the quark distribution within the proton.

‡3 If a value of $b = 1.6$ is used for the P_T distribution assumed [eq. (1)] then all cross-sections are increased by 12%.

‡4 Another experiment has been done at $\sqrt{s} = 52$ GeV, but with $y = 1.6$, by E. Nagy et al. The results is $B_{\mu\mu}(d\sigma/dy) = (7.2 \pm 2.4) \times 10^{-33}$ cm^2.

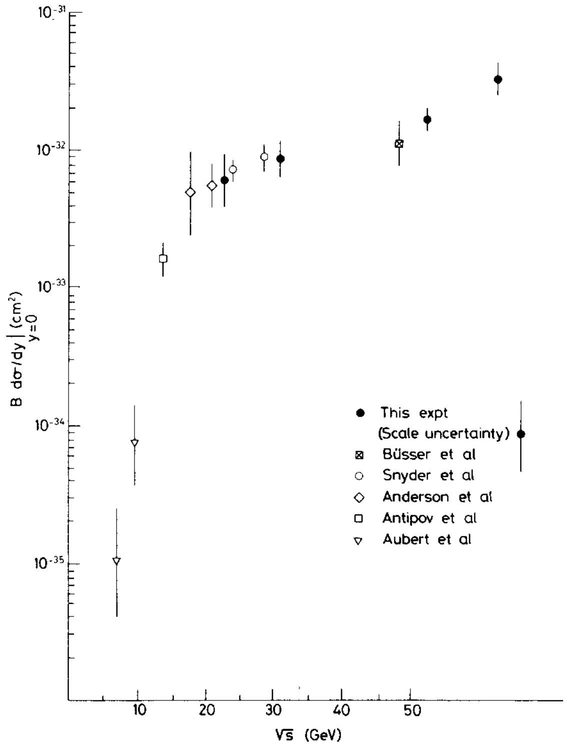

Fig. 3. $B(J/\psi \to e^+e^-) \times (d\sigma/dy|_{y=0})$ as a function of $\sqrt{s}$ compared with the results compiled in ref. [3].

[1] W.J. Willis and V. Radeka, Nucl. Instrum. Meth. 120 (1975) 221.
[2] J. Fisher et al., Nucl. Instrum. Meth. 136 (1976) 19; J.H. Cobb et al., Transition radiators for electron identification at the CERN ISR, to be published in Nucl. Instrum. Meth. (1977).
[3] B.C. Brown et al., Study of J/ψ and ψ′ production in proton-nucleus collisions with electron and muon pairs, FNAL preprint (1977). See also: J.J. Aubert et al., Phys. Rev. Lett. 33 (1974) 1404; Yu.M. Antipov et al., Phys. Lett. 60B (1976) 309; K.J. Anderson et al., Phys. Rev. Lett. 36 (1976) 237; H.D. Snyder et al., Phys. Rev. Lett. 36 (1976) 1415; F.W. Büsser et al., Phys. Lett. 56B (1975) 482.
[4] A. Donnachie and P.V. Landshoff, Nucl. Phys. B112 (1976) 233.